SAND2015-10037R

Application of Generic Disposal System Models

Fuel Cycle Research & Development

Prepared for
U.S. Department of Energy
Used Fuel Disposition

P.E. Mariner, W.P. Gardner,
G.E. Hammond, S.D. Sevougian,
E.R. Stein
Sandia National Laboratories

September 22, 2015

FCRD-UFD-2015-000126
SAND2015-xxxxxx

Sandia National Laboratories is a multi-program laboratory managed and operated by Sandia Corporation, a wholly owned subsidiary of Lockheed Martin Corporation, for the U.S. Department of Energy's National Nuclear Security Administration under contract DE-AC04-94AL85000.

ACKNOWLEDGEMENTS

The authors greatly appreciate the contributions of the WIPP program and the associated managers and technical staff of Sandia Orgs. 06931 and 06932 toward the testing of PFLOTRAN capabilities as well as the impetus to add additional capabilities. This includes Chris Camphouse, Christi Leigh, Todd Zeitler, and Sungtae Kim, with a special thanks to HeeHo Park. Also, Kris Kuhlman of Sandia Org. 06224 provided valuable advice and insights, as did Peter Lichtner of OFM Research, the original developer of PFLOTRAN.

EXECUTIVE SUMMARY

The Used Fuel Disposition Campaign (UFDC) of the U.S. Department of Energy (DOE) Office of Nuclear Energy (NE), Office of Fuel Cycle Technology (OFCT) is conducting research and development (R&D) on geologic disposal of used nuclear fuel (UNF) and high level nuclear waste (HLW). Two of the high priorities for UFDC disposal R&D are design concept development and disposal system modeling (DOE 2011, Table 6). These priorities are directly addressed in the Generic Disposal Systems Analysis (GDSA) work package of the UFDC. GDSA is tasked with developing a disposal system modeling and analysis capability for evaluating disposal system performance for nuclear waste for a range of disposal options (e.g., salt, granite, clay, and deep borehole disposal).

This report describes specific GDSA activities in fiscal year 2015 (FY2015) toward the development of the enhanced disposal system modeling and analysis capability for geologic disposal of nuclear waste. The GDSA framework employs the PFLOTRAN thermal-hydrologic-chemical multi-physics code (Hammond et al. 2011a) and the Dakota uncertainty sampling and propagation code (Adams et al. 2013a; Adams et al. 2013b). Each code is designed for massively-parallel processing in a high-performance computing (HPC) environment. Multi-physics representations in PFLOTRAN are used to simulate various coupled processes including heat flow, fluid flow, waste dissolution, radionuclide release, radionuclide decay and ingrowth, precipitation and dissolution of secondary phases, and radionuclide transport through the engineered barriers and natural geologic barriers to a well location in an overlying or underlying aquifer. Dakota is used to generate sets of representative realizations and to analyze parameter sensitivity.

In FY2015, advances in the GDSA modeling capability included among other advances the addition of two source term dissolution models. One model, the Fuel Matrix Degradation Model, developed largely at Argonne National Laboratory, was directly coupled to the PFLOTRAN waste package process model. A second dissolution model, a HLW glass dissolution model, was built inside the PFLOTRAN waste package process model. It calculates the dissolution rate using a simple expression and accounts for changing isotopic composition over time. Additional models developed or revised for the GDSA performance assessment (PA) capability this year include a new conceptual model for the effective simulation of canister corrosion, a revised approach for simulating isotope decay and partitioning, and a new mathematical model for simulating solid solution reactions.

A significant effort was made in FY2015 to integrate GDSA PA model development with UFDC work completed or underway in other work packages and at other laboratories. The GDSA group requested formal input from the other work packages on process models and data that could be coupled or integrated with the GDSA PA model. Requested input for proposed process models included descriptions of purpose, importance, addressed features, events, and processes (FEPs), coupled parameters, implementation, and readiness. A total of 18 process model templates were received. These templates were used by management to plan work scopes for FY2016 work packages and to help prioritize GDSA integration of proposed process models over the next several years.

New generic reference case applications were developed in FY2015, and the previously developed reference case for a generic UNF repository in bedded salt was expanded. The two new generic reference cases include a new salt repository reference case for defense HLW and a new clay repository reference case for UNF. Initially, the FY2014 salt repository reference case for UNF was enlarged from a thin three-dimensional vertical slice of the repository to a full three-dimensional simulation involving multiple drifts. This enlarged domain was duplicated to create the new salt reference case for defense HLW glass. Glass dissolution and radionuclide release were simulated in the defense repository reference case using the new HLW glass source dissolution model. The template of the enlarged domain was also used to build

the new reference case for a generic UNF repository in clay. The new clay reference case was based on the repository design defined for the argillite reference case in Jove Colon et al. (2014).

A variety of results for the three reference cases are presented in this report, including deterministic and probabilistic results for isothermal and thermal salt UNF simulations, deterministic results for a thermal salt HLW simulation, deterministic and probabilistic results for isothermal clay UNF simulations, and deterministic results for a thermal clay UNF simulation. Also presented are the results of a preliminary grid refinement exercise and comparisons of the present multi-drift pair salt simulations to previous single-drift pair salt simulations.

Order of magnitude differences between predicted radionuclide concentrations in thermal and isothermal simulations for both the salt and the clay UNF repositories imply that multi-physics mechanistic modeling will produce a different prediction than a modeling method that relies on simplifications or abstractions of a system. Future model integration work will help to determine an efficient balance between the mechanistic modeling necessary for realism and the simplifications necessary to produce a tractable system. Parameter sensitivity analyses like those presented in this report can help guide model development and integration, data acquisition, and site selection.

Similarly large differences between single-drift pair and multi-drift pair model predictions along with differences in prediction sensitivity to input parameters imply that accurate representation of a system is necessary both for accurate prediction and for accurate understanding of system behavior, and that repository design may influence radionuclide release. To assess the influence of repository design (with the eventual goal of optimizing it) on radionuclide releases, larger repositories of varying layout will be simulated in the future. When a site is chosen, simulation of potential repository designs should be a part of the planning process.

The preliminary grid refinement exercise demonstrated a quantifiable effect of grid refinement on first arrival times. As GDSA modeling capabilities are expanded and refined and input parameter values updated and improved, assessing the effects of grid spacing choices will be necessary to maintain confidence in model results. The large number of simulations involved in the salt and clay probabilistic runs afforded an opportunity to refine solver tolerances in order to minimize numerical artifacts. Optimization of solver tolerances for large probabilistic simulations is an area of ongoing research.

Progress in the development of the GDSA framework continues to affirm that HPC-capable codes can be used to simulate important multi-physics couplings directly in a total system performance assessment of a geologic repository. The generic repository applications modeled to date indicate that the developing capability can simulate complex coupled processes in a multi-kilometer domain while simultaneously simulating the coupled behavior of meter-scale features, including every waste package within the domain.

This report fulfills the Generic Disposal System Analysis Work Package Level 2 Milestone – *Application of Generic Disposal System Models* (M2FT-15SN0808011).

CONTENTS

Page

FIGURES

Page

TABLES

Page

ACRONYMS

CFM	Continuum Fracture Model
CFR	Code of Federal Regulations
DOE	U.S. Department of Energy
DPC	dual-purpose canister
DRZ	disturbed rock zone
EBS	engineered barrier system
EDZ	excavation disturbed zone
EF	early failure
FEP	feature, event, and process
FMDM	Fuel Matrix Degradation Model
FY	fiscal year
GC	general corrosion
GDSA	generic disposal system analysis
GWd	gigawatt-day
HDF5	hierarchical data format, version 5
HLW	high-level radioactive waste
HPC	high-performance computing
HS	Hanford Site
IAEA	International Atomic Energy Agency
INL	Idaho National Laboratory
LANL	Los Alamos National Laboratory
LBNL	Lawrence Berkeley National Laboratory
LC	localized corrosion
LHS	latin hypercube sampling
LOE	level of effort
MIC	microbiologically-influenced corrosion
MPI	message passing interface
MTHM	metric tons heavy metal
N/A	not applicable
NBS	natural barrier system
NE	Office of Nuclear Energy
NEA	Nuclear Energy Agency
NWPA	Nuclear Waste Policy Act
OFCT	Office of Fuel Cycle Technology
OoR	(age) out-of-reactor
ORNL	Oak Ridge National Laboratory

ACRONYMS (CONT.)

PA	performance assessment
PETSc	Portable Extensible Toolkit for Scientific Computation
PMC	process model coupler
PWR	pressurized water reactor
QA	quality assurance
R&D	research and development
RBSN	Rigid-Body-Spring-Network
RN	radionuclide
SCC	stress corrosion cracking
SNF	spent nuclear fuel
SNL	Sandia National Laboratories
SRS	Savannah River Site
TBD	to be determined
THC	thermal-hydrologic-chemical
THM	thermal-hydrologic-mechanical
THMC	thermal-hydrologic-mechanical-chemical
TRL	technology readiness level
TSPA	total system performance assessment
UFDC	Used Fuel Disposition Campaign
UNF	used nuclear fuel
WF	waste form
WHO	World Health Association
WIPP	Waste Isolation Pilot Plant
WP	waste package
1D, 2D, 3D	one-, two-, and three-dimensional

Page intentionally blank

1. INTRODUCTION

The Used Fuel Disposition Campaign (UFDC) of the U.S. Department of Energy (DOE) Office of Nuclear Energy (NE), Office of Fuel Cycle Technology (OFCT) is conducting research and development (R&D) on geologic disposal of used nuclear fuel (UNF) and high level nuclear waste (HLW). Two of the highest priorities for UFDC disposal R&D are design concept development and disposal system modeling (DOE 2011, Table 6). These priorities are directly addressed in the Generic Disposal Systems Analysis (GDSA) work package of the UFDC. GDSA is tasked with developing a disposal system modeling and analysis capability for evaluating disposal system performance for nuclear waste in geologic media. This developing capability is called the GDSA model framework or the GDSA capability in this report.

Quantitative risk assessment has greatly advanced since the 1970s when it was first applied to nuclear waste disposal (Meachem et al. 2011). In the 1990s, a set of flow and transport codes was developed to probabilistically assess post-closure safety of the Waste Isolation Pilot Plant (WIPP), a deep geologic repository for transuranic waste in southeastern New Mexico. In 2008, GoldSim, a commercial Monte Carlo simulation software, provided the primary assessment framework for the proposed Yucca Mountain repository for UNF and HLW in Nevada. In that assessment, GoldSim was used to couple subsystem codes and model abstractions, perform various calculations, sample parameter distributions, and provide total system realizations. With the start of the UFDC, as DOE's focus turned to other repository concepts, GoldSim continued to provide the primary assessment framework (Freeze et al. 2013a). In 2013, however, GDSA transitioned to a framework based on PFLOTRAN and Dakota, a framework that GDSA continues to use and develop today. PFLOTRAN is a reactive flow and transport model for describing surface and subsurface processes (Hammond et al. 2011a; Lichtner and Hammond 2012), and Dakota is an uncertainty quantification and sensitivity analysis code (Adams et al. 2013a; Adams et al. 2013b). These codes were chosen to provide the primary GDSA framework because they are open source, massively parallel, and together have the potential to simulate a total integrated geologic repository system and its surroundings probabilistically and in three dimensions.

This report describes GDSA accomplishments for fiscal year 2015 (FY2015). Recent prior development and accomplishments are documented in Freeze et al. (2013b), Sevougian et al. (2013; 2014), Clayton et al. (2011), Freeze and Vaughn (2012), and Vaughn et al. (2013).

The overall objective of the GDSA work package is to develop a disposal system modeling and analysis capability that supports the prioritization of disposal research R&D and the evaluation of disposal system performance, including uncertainty, for a range of disposal options (e.g., salt, argillite, crystalline, deep borehole). The objective is to develop a GDSA capability that will:

- integrate updated conceptual models of subsystem processes and couplings developed under other DR work packages;
- evaluate disposal research R&D priorities;
- leverage existing computational capabilities (e.g., meshing, visualization, high-performance computing (HPC)) where appropriate; and
- use an open source environment.

Three major tasks were identified for FY2015 in pursuit of this objective:

- Integrate source term, decay, and solubility modeling capabilities for isotopes within the system model architecture;
- Integrate updated subsystem conceptual models into the system model architecture; and

- Develop and perform simulations of selected repository reference cases to evaluate the importance of various system components and configurations (e.g., waste form, dual-purpose canisters (DPCs), engineered barrier system (EBS) features, host rock features) and to inform R&D planning.

This report addresses the GDSA Work Package Level 2 Milestone – Generic Disposal System Modeling Report (M2FT-15SN0808011). It incorporates information from the following supporting Milestones: M4FT-15AN0806016 (Jerden et al. 2015a); M3FT-15AN0806014 (Jerden et al. 2015b); M2FT-14SN0806051 (Jove Colon et al. 2014); M3FT-14SN0808032 (Sevougian et al. 2014); M4FT-15AN0806012 (Jerden et al. 2014); M2FT-14SN0808033 (Freeze et al. 2013b); M2FT-13SN0806062 (Sassani et al. 2013); and M3FT-13SN0808062 (Freeze et al. 2013c).

Section 1.1 describes the range of UFDC disposal options. Section 2 discusses the GDSA performance assessment (PA) vision and summarizes the conceptual model framework and the PFLOTRAN-based computational framework of the GDSA modeling capability. Section 3 reports progress on process model integration, including integration activities with other disposal research work packages, newly added process model capabilities, and a description of code enhancements for external process model coupling. Section 4 provides generic demonstration problems in bedded salt for a commercial repository and a defense repository and an additional demonstration problem for a commercial repository in argillite. Deterministic and probabilistic results for these generic applications are provided. Section 5 provides a summary and conclusions.

1.1 Disposal Options

Disposal options for UNF and HLW include "open" modes, where extended ventilation can remove heat for many years after underground waste emplacement, and "enclosed" modes, where waste emplacement is in direct or close contact with natural or engineered materials (e.g., buffer or backfill). For the various geologic media and waste disposal concepts, specific disposal options include (Hardin et al. 2012):

- **Salt (enclosed)** – A repository in bedded salt in which individual, carbon steel waste packages are placed on the floor in drifts or alcoves, and immediately covered (backfilled) with run-of-mine salt. All repository openings are backfilled at closure, and shafts are sealed (Hardin et al. 2012, Section 1.4.5.2).
- **Granite/Crystalline (enclosed)** - A repository in crystalline rock (e.g., granite). Vertical borehole emplacement is used with a copper waste package (e.g., Swedish KBS-3 concept), with a clay buffer installed at emplacement. Access and service drifts are backfilled with low-permeability clay-based swelling backfill at closure. Access shafts are sealed at closure (Hardin et al. 2012, Section 1.4.5.1).
- **Clay/Shale (enclosed)** – Waste is emplaced in blind, steel-lined horizontal borings constructed from horizontal access drifts. UNF is emplaced in carbon steel packages with a clay buffer. HLW glass is emplaced in stainless steel pour canisters, within a steel liner. Access and service drifts are backfilled with low permeability clay-based backfill at closure. Access shafts and ramps are sealed at closure (Hardin et al. 2012, Section 1.4.5.3). Another option for clay/shale is in-drift emplacement of waste packages with multiple engineered buffer layers (Section 4.3).
- **Deep Borehole (enclosed)** – Ongoing studies are assessing the feasibility of drilling large-diameter holes to 5 km in low-permeability crystalline basement rock. Waste packages would contain single UNF assemblies, or reduced quantities of HLW glass, and would be stacked in the lower 2 km of each hole. The upper section would be sealed (Brady et al. 2009; Arnold et al. 2011).

- **Shale Unbackfilled (open)** – A repository in a clay/shale environment constructed such that ventilation is maintained for at least 50 to 100 years after waste emplacement and before the repository is closed. At repository closure, the access and service drifts (shafts) are backfilled, but not the disposal drift segments where waste packages are emplaced (Hardin et al. 2012, Section 1.5.1).
- **Sedimentary Backfilled (open)** – A repository in unsaturated soft rock constructed such that ventilation is maintained for at least 50 to 100 years after waste emplacement and before the repository is closed. The waste emplacement, access, and service drifts are backfilled at the time of repository closure (Hardin et al., Section 1.5.2).
- **Hard Rock, Unsaturated (open)** – A repository in competent, indurated rock (e.g., igneous or metamorphic) using in-drift emplacement and forced ventilation for 50 to 100 years after waste emplacement. The hydrologic setting is unsaturated, so the emplacement drifts are not backfilled at closure, but other engineered barriers may be installed such as corrosion resistant metallic barriers to water movement (DOE 2008).

2. GDSA PERFORMANCE ASSESSMENT

A performance assessment (PA) for underground disposal of nuclear waste requires a comprehensive analysis of features, events, and processes (FEPs) that could potentially affect the release of radionuclides from emplaced waste packages and the transport of released radionuclides to the biosphere. A central component of a PA is the computational framework. Section 2.1 discusses the GDSA long-term vision for the computational framework. The present computational framework and conceptual model framework are summarized in Section 2.2.

2.1 GDSA PA Vision

A new potential geologic repository may not be sited for two decades (DOE 2013). With continued advances in general computational capabilities during that time, GDSA PA software will need to keep up. The long-term mission for the GDSA effort is therefore to develop a geologic repository modeling capability that can adapt to, and take advantage of, future advances in computational software and hardware. An additional long-term mission is to create and maintain a suite of generic repository reference case applications for demonstrating and testing the evolving GDSA software and for evaluating the effects of model features, events, processes, and input parameters on total system performance.

In consideration of this vision for GDSA, two open source, HPC codes will serve as the core of the modeling capability: PFLOTRAN and Dakota. PFLOTRAN is a massively-parallel thermal-hydrologic-chemical (THC) flow and transport code, and Dakota is a versatile probabilistic code (Section 2.2.2). The PFLOTRAN code will be developed over time by GDSA to accommodate new geologic disposal process models and capabilities through additional code development or coupling with external process models. The HPC capabilities of PFLOTRAN and Dakota will allow for ever higher fidelity in GDSA total system performance assessments as more powerful HPC resources become available.

As the GDSA model framework evolves, the GDSA group will continue to generate and refine three-dimensional models of generic disposal repository concepts complete with surrounding geospheres and connected biospheres. Sensitivity analyses will be performed on these models to distinguish the importance of features, processes, and parameters on model results. These analyses will help to prioritize future disposal R&D. The resulting reference case models will also be useful as starting points when the time comes to apply the GDSA capability to selected sites.

2.2 GDSA PA Framework

A PA model is an important component of a comprehensive PA for a nuclear waste repository. In a comprehensive PA all plausible scenarios and processes that may affect repository performance are addressed. FEPs and scenarios are evaluated and screened. Potentially pertinent FEPs are identified for simulation in the PA model. Probabilistic simulations are performed, and results are evaluated against performance metrics. Uncertainty and sensitivity analyses may also be performed to inform prioritization of additional research and model development. An overview of PA methodology and terminology is presented in Sevougian et al. (2014, Section 2) and Meachem et al. (2011, Section 1).

The PA model framework consists of a conceptual model framework and a computational framework. The conceptual model framework (Section 2.2.1) is the assemblage of FEPs and their interactions pertinent to repository system performance. The computational framework (Section 2.2.2) is the integration of software codes and mathematical models for quantitatively simulating the conceptual model and probabilistically assessing repository performance.

2.2.1 Conceptual Model Framework

A conceptual model framework requires a coherent representation of all pertinent FEPs. Figure 2-1 schematically illustrates a generic conceptual model framework for a repository system. This figure sequentially identifies the various media through which radionuclides must travel to reach the biosphere. To calculate a dose to a receptor in the biosphere from a nominal scenario, radionuclides released from the waste form must pass through the repository engineered barrier system (EBS) and the surrounding natural barrier system (NBS).

The features of a conceptual model are the physical components of the EBS and NBS. Primary features include radionuclide inventories, waste forms, waste packages, buffer materials, seals, drifts, shafts, host rock, surrounding stratigraphy, groundwater, fractures, aquifers, wells, springs, soil, etc. For implementation in a PA model, the conceptual model framework provides information regarding repository layout, e.g., the sizes and locations of waste packages, drifts, buffer/backfill, shafts, and seals. In addition, the conceptual model provides information beyond the repository to describe the dimensions, properties, and locations of important features in the surrounding geosphere and accessible biosphere.

There are two general concepts for deep geologic disposal of nuclear waste: mined repository disposal and deep borehole disposal. These concepts have markedly different EBS and NBS features. For a mined repository, waste is generally placed along horizontal drifts at a depth of several hundred meters. Concepts for mined repository disposal have been developed for several host rock types including salt, argillite, crystalline, and sedimentary (Section 1.1). For deep borehole disposal concepts, the host rock is crystalline and the waste is emplaced vertically at depths of approximately 3,000 to 5,000 meters (Arnold et al. 2011). Waste packages, buffer/backfill, seals, orientation, host rock, depth, and extent are important differentiating features of these disposal concepts.

Important processes and events in the conceptual model are those that could significantly affect the movement of radionuclides in the EBS and NBS. Such processes and events include waste package corrosion, waste form dissolution, radionuclide release, radioactive decay, heat transfer, aqueous transport, advection, diffusion, sorption, aqueous chemical reactions, precipitation, buffer chemical reactions, gas generation, colloidal transport, earthquakes, inadvertent human intrusion of the repository, etc. A FEPs database like the one developed and described in Freeze et al. (2011) can be used to help identify a full set of potentially important FEPs for a specific conceptual repository model. Many of the FEPs in a FEPs database may be included in the PA model. In a comprehensive PA, excluded FEPs (i.e., FEPs not included in the PA model) must be addressed in separate analyses and arguments.

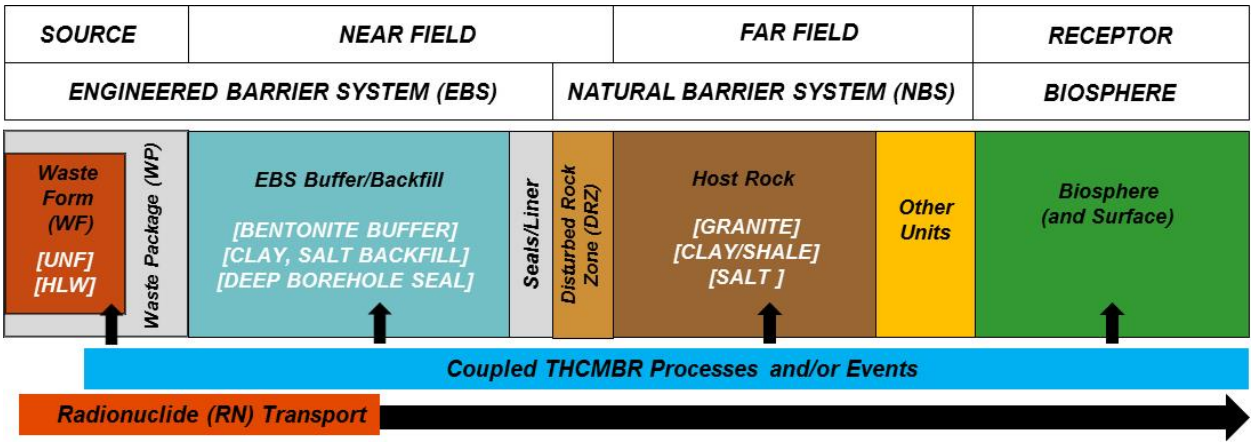

Figure 2-1. Schematic diagram of the conceptual model framework of a generic geologic disposal system.

2.2.2 Computational Framework

PA model simulations require a large number of realizations and an enormous number of calculations. For this reason, the GDSA PA computational framework is designed for massively-parallel processing in a high-performance computing (HPC) environment. The GDSA computational framework consists of the following components:

- Input parameter database
- Software for sampling, sensitivity analysis, and uncertainty quantification (Dakota)
- Petascale reactive multiphase flow and transport code (PFLOTRAN), working in concert with coupled process model codes (e.g., FMDM)
- Computational support software and scripts for meshing, processing, and visualizing results (e.g., CUBIT, Python, ParaView, VisIt).

The flow of data and calculations through these components is illustrated in Figure 2-2. In a probabilistic simulation, Dakota generates stochastic input for each GDSA PA realization based on parameter uncertainty distributions defined in the input set. The sampled inputs are used by PFLOTRAN and its coupled process models to simulate source term release, EBS evolution, flow and transport through the EBS and NBS, and uptake in the biosphere. After the simulation, various software packages may be used to reduce and illustrate the output calculations of parameters and performance metrics. Dakota may also be used to evaluate the effects of parameter uncertainty on specific outputs.

Dakota and PFLOTRAN are the core simulation codes of the GDSA PA computational framework. These components are described in more detail in Sections 2.2.2.1 and 2.2.2.2.

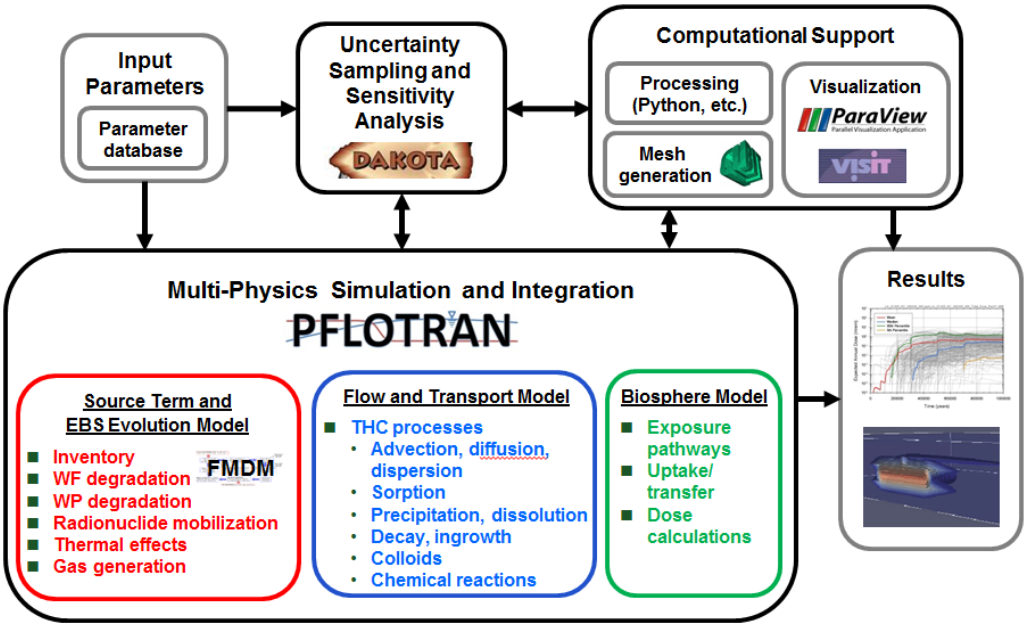

Figure 2-2. GDSA PA computational framework.

2.2.2.1 Dakota

The Dakota software toolkit is open source software developed and supported at Sandia National Laboratories (Adams et al. 2013a; Adams et al. 2013b). GDSA modeling uses Dakota as the interface between input parameters and PFLOTRAN. Dakota is also used to analyze the effects of uncertainty in GDSA parameter values on repository performance.

Dakota can be used to manage uncertainty quantification, sensitivity analyses, optimization, and calibration. Specific Dakota capabilities important to GDSA include (Figure 2-3):

- Generic interface to simulations
- Mixed deterministic / probabilistic analysis
- Uncertainty quantification with sampling and epistemic methods
- Supports scalable parallel computations on clusters.

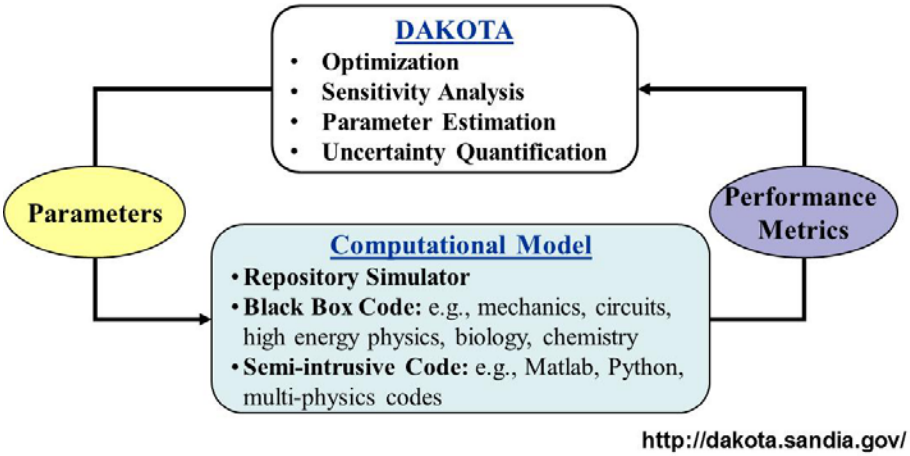

Figure 2-3. Dakota software workflow and capabilities.

2.2.2.2 PFLOTRAN

PFLOTRAN (Hammond et al. 2011a; Lichtner and Hammond 2012) is an open source, reactive multi-phase flow and transport simulator designed to leverage massively-parallel high-performance computing to simulate subsurface earth system processes. PFLOTRAN has been employed on petascale leadership-class DOE computing resources (e.g., Jaguar [at Oak Ridge National Laboratory (ORNL)] and Franklin/Hopper [at Lawrence Berkeley National Laboratory (LBNL)]) to simulate THC processes at the Nevada Test Site (Mills et al. 2007), multi-phase CO_2-H_2O for carbon sequestration (Lu and Lichtner 2007), CO_2 leakage within shallow aquifers (Navarre-Sitchler et al. 2013), and uranium fate and transport at the Hanford 300 Area (Hammond et al. 2007; Hammond et al. 2008; Hammond and Lichtner 2010; Hammond et al. 2011b; Lichtner and Hammond 2012; Chen et al. 2012; Chen et al. 2013).

PFLOTRAN solves the non-linear partial differential equations describing non-isothermal multi-phase flow, reactive transport, and geomechanics in porous media. Parallelization is achieved through domain decomposition using the Portable Extensible Toolkit for Scientific Computation (PETSc) (Balay et al. 2013). PETSc provides a flexible interface to data structures and solvers that facilitate the use of parallel computing. PFLOTRAN is written in Fortran 2003/2008 and leverages state of the art Fortran programming (i.e. Fortran classes, pointers to procedures, etc.) to support its object-oriented design. The code provides "factories" within which the developer can integrate a custom set of process models and time integrators for simulating surface and subsurface multi-physics processes. PFLOTRAN employs a single, unified framework for simulating multi-physics processes on both structured and unstructured grid discretizations (i.e. there is no duplication of the code that calculates multi-physics process model functionals in support of structured and unstructured discretizations). The code requires a small, select set of third-party libraries (e.g., MPI, PETSc, BLAS/LAPACK, HDF5, Metis/Parmetis). Both the unified structured/unstructured framework and the limited number of third-party libraries greatly facilitate usability for the end user.

Specific PFLOTRAN capabilities for the simulation of generic disposal systems include:

- Multi-physics
  - Multi-phase flow
  - Multi-component transport
  - Biogeochemical processes
  - Thermal and heat transfer processes

- High-Performance Computing (HPC)
  - Built on PETSc – parallel solver library
  - Massively Parallel
  - Structured and Unstructured Grids
  - Scalable from Laptop to Supercomputer
- Modular design based on object-oriented Fortran 2003/2008 for easy integration of new capabilities

Flow and transport processes simulated by PFLOTRAN are illustrated schematically in Figure 2-4 for the near field and in Figure 2-5 for the far field. These figures also illustrate where process model feeds or abstractions may be used to represent some of the more complex multi-physics couplings in specific disposal concepts.

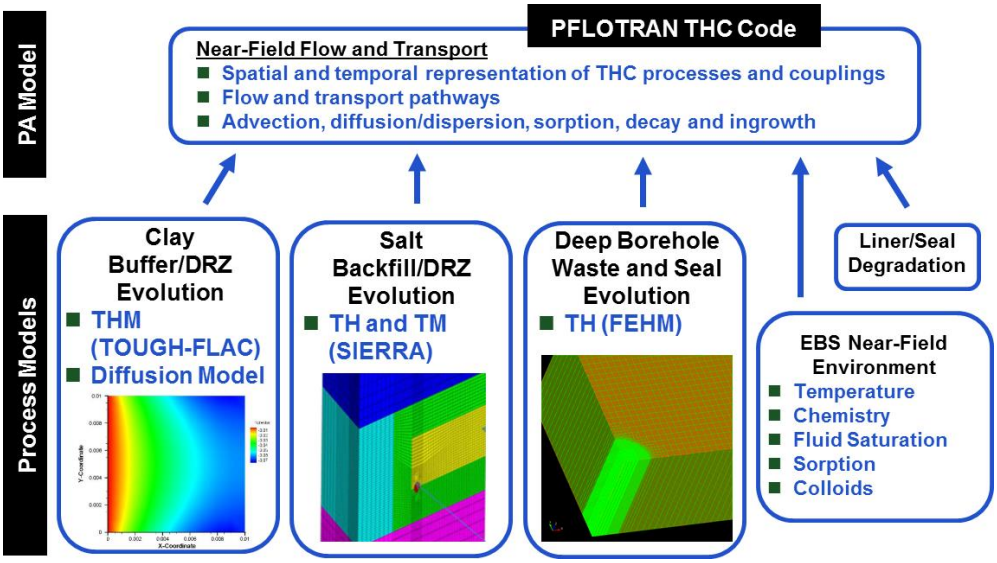

Figure 2-4. Implementation of PFLOTRAN for near-field flow and transport.

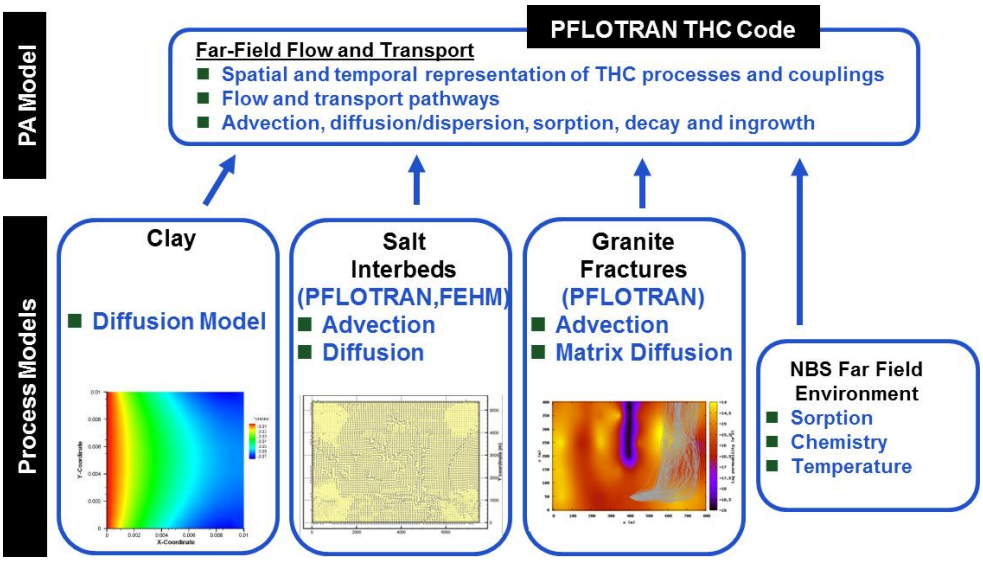

Figure 2-5. Implementation of PFLOTRAN for far-field flow and transport.

3. GDSA Process Model Development

The coupling of process models provides powerful capabilities for analyzing sensitivities and reducing uncertainty in PA applications. This approach of using detailed models directly in a PA is a continuation of the successful modeling approach adopted for PAs of the WIPP (Rechard 1995; 2002; Rechard and Tierney 2005) and differs from the modeling approach adopted for past PAs for disposal of UNF and HLW in volcanic tuff (Rechard and Stockman 2014). Section 3.1 describes the activities performed by GDSA this year to identify process models for coupling to the GDSA computational framework. Section 3.2 discusses two waste form dissolution models added to the GDSA model framework this year and additional process models that were conceptualized or further advanced. Section 3.3 explains the restructuring of PFLOTRAN this year to improve process model coupling and describes how the Fuel Matrix Degradation Model was coupled to PFLOTRAN.

3.1 Process Model Integration

Figure 3-1 shows a schematic timeline for the evolution of U.S. repository performance assessment with two key points indicated: the present time (2015) and the beginning of the repository licensing phase in 2042 (DOE 2013). Throughout this nearly 30-year timeframe, it is expected that conceptual models, numerical models, computer hardware, and computer software will all evolve significantly. This evolution demands that the GDSA architecture be flexible enough to accommodate the associated advances, which is the motivation behind developing the GDSA framework for the most advanced hardware architecture currently available, i.e., an HPC parallel computational environment. It is similarly the motivation for developing GDSA software in an open-source format. During the evolution from generic to site-specific performance assessment, as indicated in Figure 3-1, the GDSA model framework has three primary, ongoing functions:

1. Support safety case development during all phases of the waste disposal system lifecycle
2. Evaluate potential disposal concepts and sites in various host rock media, and later the chosen site to be licensed
3. Help prioritize *generic* R&D activities (later, *site-specific*)

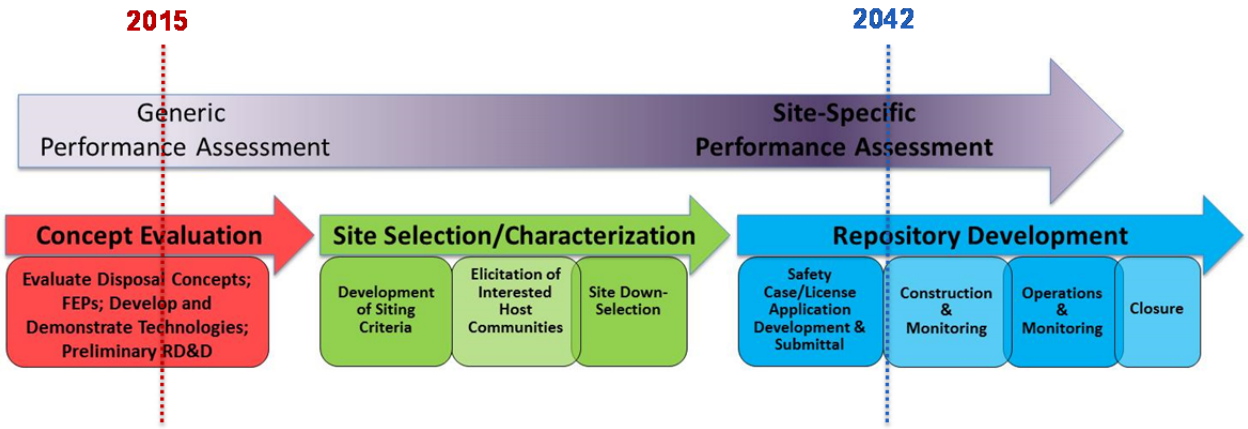

Figure 3-1. Evolution of performance assessment through various phases of repository development.

Regarding Function #1, increased confidence and transparency in the repository safety case may be fostered by two important features of a performance assessment model: (1) less reliance on assumptions and simplifications ("abstractions"); and (2) realistic spatial resolution of features and processes,

including direct representation of all emplaced waste packages. Advances in hardware and software will facilitate both of these goals, i.e., the goals of greater process resolution and greater spatial-temporal resolution. However, because it is an evolutionary process, varying degrees of simplification will be necessary for some time but less than in the past for the commercial spent nuclear fuel (SNF) repository program. The discussion here focuses on how to keep simplification to a minimum and to directly model the underlying conservation equations, if possible.

To ensure an efficient representation of processes in the system performance assessment, given evolving hardware and software constraints, an ongoing dialog is necessary between PA scientists who focus on an efficient total system model, and domain scientists who concentrate on a detailed representation of a specific domain and associated process(es). This "integration" dialog requires an ongoing initiative to maintain its force. To that end, a more focused integration effort has been established this fiscal year (FY2016) with the following goals:

1. Determine how to couple each process model with the PA model (e.g., directly coupled, used to develop a reduced-order model, or used only for FEPs screening), with a goal of having a more mechanistic PA model.
2. Articulate which processes and models are needed by PA/GDSA but are not currently being developed as part of UFD R&D activities (i.e., "missing" models)—thus ensuring that the long-term plan for the GDSA performance assessment model/software includes integration of all the key FEPs that influence biosphere dose for any of the four primary generic disposal system concepts: mined repositories in argillite, crystalline, or salt host rock, or a deep borehole disposal system in crystalline basement rock.
3. Develop the GDSA model framework to an extent that it can provide guidance and direction for other R&D activities (including experimental work) that support some model or aspect of a model that is coupled to PA or some model or activity that underpins the safety case—as informed by R&D priorities in the 2011 UFD R&D Roadmap (DOE 2011).

With regard to the first goal of integrating process models more "mechanistically" in the GDSA Framework, two points may be emphasized: (1) reduced-order (i.e., reduction in the number of processes, if one is much more dominant; or simplification of the constitutive model for a given process) or reduced-dimension models are to be preferred over response surfaces, and (2) mechanistic models within the PA are important if coupled-process effects are expected to have a strong influence on dose at the biosphere. As described below (see Table 3-2), a response-surface representation of a process model may still be appropriate within the PA model at this time if (1) a reduced-order model adversely affects the fidelity of the represented process, (2) direct coupling exceeds current hardware capabilities for running a total system model, or (3) the represented process occurs and is finished at very early times in the system performance period and therefore may be represented more simply as an effect on initial conditions for long-term simulations.

The current integration effort has been realized in large part through the use of Model Integration Templates. A blank Model Integration Template, designed by GDSA researchers, is shown in Table 3-1. This template was sent to UFD domain scientists with the idea that filling out each of these questions would help focus process model development in a way that it is more integrated as part of a total system representation. A total of more than twenty Model Integration Templates were completed (see Appendix A), including four by GDSA modelers (for missing processes/submodels), which were then distilled into a Model Integration Table to be used for prioritization of process model integration with GDSA. The initial Model Integration Table (not shown here), and the underlying Model Integration Templates (in Appendix A), were examined to determine what further information might be required in order to establish a priority ranking and integration schedule. Based on this, ten process models were chosen for further information gathering by GDSA. This was accomplished during a "lightning round"

session at the 2015 Annual UFD Working Group Meeting, held June 9-11 in Las Vegas, Nevada. Ten lightning talks (i.e., limited to five minutes each) were given by process modelers for each of the ten chosen models, with two objectives for each talk: (1) why the given process model is important to PA, and (2) how it can be coupled to GDSA in the next year or two.

Table 3-1. Model integration template.

1. Name of Model:
2. Principal Investigator(s) and Affiliation:
3. Brief Model Description: • Describe the processes and/or events considered in the model, as well as the applicable feature (e.g., waste form, DRZ, etc.), i.e., include a description of the FEP or FEPs addressed by this model.
4. R&D Issue(s) and Safety Case Objectives Addressed by This Model: • How will the modeled FEP(s) affect repository performance (especially biosphere dose) in a meaningful way? • Why is it important from a regulatory perspective? • Describe the current "state of the art" knowledge regarding the issue(s) addressed and why this particular model advances the state of the art in an important way.
5. Proposed method for coupling this model to the PA model[1] • Direct coupling or abstraction? • Time scale of transient modeled processes (10 years, 100 years…. 1,000,000 years?). • Degree of abstraction: reduced dimensionality; simplified representation; response surface. • Key environmental inputs required from the PA model (and its coupled submodels) and key outputs delivered by this model. • Are there other models you are aware of that are not being developed, which are needed for your model or for PA?
6. Real time integration horizon: estimate how long before the proposed model is ready for integration with PA and how long the integration activities might take? • Are there intermediate steps or degrees of coupling with PA, e.g., can you couple a certain version of your model in an expedited fashion and then go to the next more detailed version—please describe how

Information from the lightning-round session was then used by GDSA scientists, with assistance from the Crystalline and Argillite work package managers, to update the initial Model Integration Table with priority rankings to specify the timeframe for integration of each process model with GDSA (near term, medium term, far term) as well as the order in which to implement them, i.e., first, second, third, etc. The updated Model Integration Table is reproduced here as Table 3-2. It includes five categories of models to be integrated with GDSA:

1. Process models to be implemented collaboratively (between GDSA and other work packages),
2. Process models to be implemented by GDSA,
3. Missing models with perhaps the most potential impact on GDSA efficacy,
4. Other process models with a longer integration time frame,
5. Other GDSA process models with a longer integration timeframe.

There are three main evaluation columns in Table 3-2:

- Column 5: Current Level of Readiness/Technical Maturity, i.e., how soon could we integrate?

- Column 6: Level of Effort for Integration with PA/PFLOTRAN, i.e., how long will it take once we start?
- Column 7: Integration Time Frame ("Priority Order and Urgency"), i.e., how soon should we integrate?

The urgency ratings for Column 7 are "N = near term," "M = medium term," and "F = far term." The individual urgency rating given to each process model in this column represent a judgment call by GDSA scientists regarding how important each of these models are to total system performance. The priority ranking (1, 2, 3, 4, 5) indicates the order in which the process models will be coupled to the GDSA/PFLOTRAN Framework, with all "N" models coupled first, regardless of their priority ranking, followed by the "M" models, and then the "F" models.

A helpful visual representation of process model/GDSA integration is presented in Figure 3-2 for Crystalline process models and experiments. It is a variant on the well-known PA pyramid concept (SNL 2008, Fig. ES-6), but it amplifies on the usual pyramid concept by showing connections or links between process models and lab experiments.

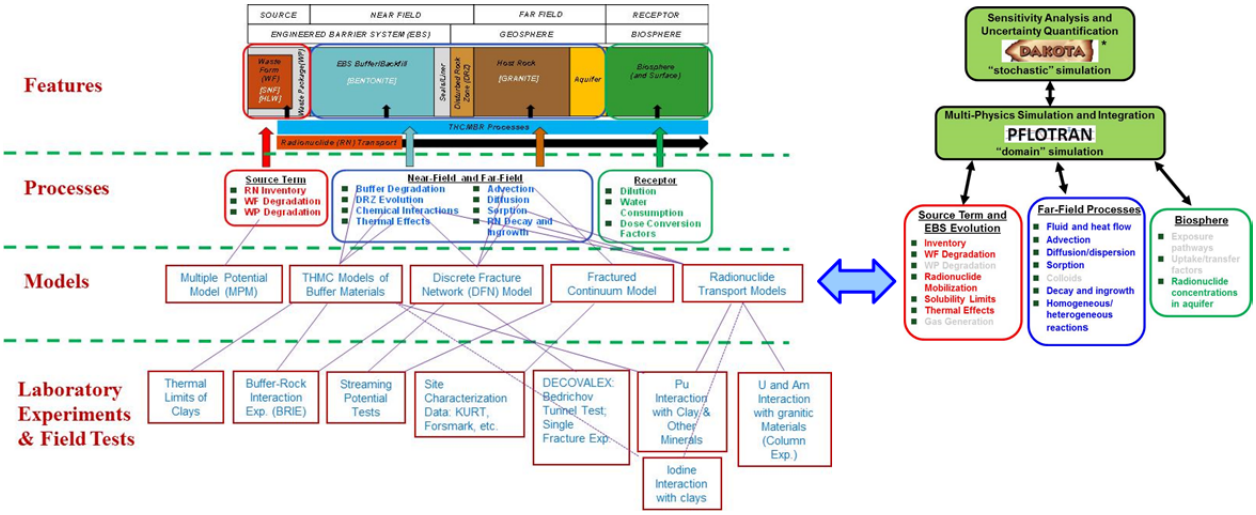

Figure 3-2. Crystalline workscope pyramid and integration with GDSA.

Subsequent to the GDSA/process model integration session and the associated update of the Model Integration Table, a further integration meeting was held with DOE staff in Las Vegas, Nevada on August 6, 2015. This produced the following action items for FY2016 to further the integration effort (refer to Table 3-2):

1. Deliverables for various planning packages (for the salt, clay, granite, and deep borehole concepts) will include text proposing how specific process models are to be used to support PA and the safety case, based on the opinion of the responsible PI for each process model. This applies to both near-term integration models and far-term integration models.
2. An integration meeting between the UFD Campaign and the Waste Forms Campaign will be convened to integrate the HLW degradation model being developed in the latter campaign with GDSA/PFLOTRAN.

3. An integration meeting between WIPP researchers (under DOE-EM) and GDSA researchers (under DOE-NE) will be convened to begin collaborative work on a nesting capability for PFLOTRAN (see Table 3-2).
4. A meeting will be convened to integrate work being done on discrete fracture modeling (DFNWorks) and a multi-continuum/dual-continuum capability in PFLOTRAN, including the use of a possible reduced-order Continuum Fracture Model (CFM). This is important for FY2016 because GDSA researchers plan to develop a crystalline/granite reference case in FY2016.

Table 3-2. Model integration table.

Process Model	Code	Process(es)	Personnel	Current Level of Readiness/ Technical Maturity How soon could we?	Level of Effort (LOE) for Integration with PA/PFLOTRAN How long once we start? L = 1 month M = 6 months H = 1 year or more	Integration Time Frame ("Priority Order/ and Urgency") How soon should we? Urgency categories: N = Near term M = Medium term F = Far term	NOTES (Green is generally preferable)
						↓ PA ranking ↓	
Process Models to be Implemented Collaboratively (between GDSA and other work packages):							
FMDM	FMDM	Mixed potential model of used fuel matrix degradation	J. Jerden, R. Wittman ANL	**Ongoing**	**M**	**1, N**	• Direct implementation in PFLOTRAN already complete and now at the testing stage. Additional development and more efficient coding suggested • Primary FEP score[1] = 4.01
Colloid-Facilitated Transport Model (see GDSA below)	RELAP	Colloid filtration and adsorption	P. Reimus LANL	**6-12 months?**	**L - M**	**1, N**	• **Direct implementation in PFLOTRAN suggested, with perhaps some simplification**. • TRL (technical readiness level) not indicated • LOE indicated as L-M. • FEP 2.2.09.60 score = 3.29
Radionuclide transport as pseudocolloids	N/A	Desorption rate of radionuclides from pseudocolloids	J. Begg, P. Zhao, C. Joseph, M. Zavarin LLNL	**6-12 months?**	**L - M**	**1, N** **(Combine with LANL model)**	• Abstraction suggested (half-life model). **1st order "decay" model could be directly implemented** • TRL = indicates it is ready now • LOE not indicated; simple model said to be ready currently but to be improved upon over the next 3 years (add redox) • Highest relevant FEP score probably 3.29
HLW WF degradation	N/A	Glass waste degradation	Ebert ANL	**? 6 months ?**		**1, N**	**Needed for Defense Waste Repository**
Non-Darcy Flow Model	TOUGH2	Flow in low permeability media, specifically in	Y. Wang, L. Zheng LBNL	**Now**	**L**	**2, M**	• **Direct implementation in PFLOTRAN suggested**. • TRL = now

Table 3-2. Model integration table.

Process Model	Code	Process(es)	Personnel	Current Level of Readiness/ Technical Maturity How soon could we?	Level of Effort (LOE) for Integration with PA/PFLOTRAN How long once we start? L = 1 month M = 6 months H = 1 year or more	Integration Time Frame ("Priority Order/ and Urgency") How soon should we? Urgency categories: N = Near term M = Medium term F = Far term	NOTES (Green is generally preferable)
		compacted clay					• LOE not given • Primary FEP score = 2.58
Discrete Fracture Model Network (DFN) Model	DFN mesh + FEHM (DFNWorks)	Fluid flow & transport in fracture networks	H. Viswanathan LANL	**Now**	**L**	**2, M** **(initial work to be done by LANL in PFLOTRAN)**	• Abstraction suggested (upscaled parameters or "emulator", **or use of Sandia CFM).** • TRL = not indicated • LOE= not indicated. • Primary FEPs score = 3.74, 3.74, 3.65, 3.65, 3.65
Coupled THC processes in Salt	FEHM	Coupled thermal-hydrologic-chemical processes in a salt repository	P. Stauffer LANL	**Now**	**M**	**2, M** **(initial work to be done by LANL in PFLOTRAN)**	• **Direct implementation in PFLOTRAN suggested over a long time period,** with abstraction "emulator" mentioned. • TRL = several years of development • LOE of H+ (years). • Many high-priority FEPs listed.
Waste Canister Corrosion Model	FMDM-like	Mixed potential reaction/diffusion model	J. Jerden, C. Jove Colon ANL, SNL	**1 year?**	**M - H**	**3, M**	• **Direct implementation in PFLOTRAN suggested, similar to SNF degradation** • FEP 2.1.03.02 score = 4.34
Process Models to be Implemented by GDSA:							
Decay in Precipitate Phase	PFLOTRAN	Decay/ingrowth of radionuclides in mineral phases and release of decay products	Mariner, Hammond SNL	**Now**	**M**	**1, N**	• Direct coupling in PFLOTRAN. • LOE indicated as L-M. • Highest FEP score probably 4.86
Waste Form Radioactive Decay Model	PFLOTRAN	Decay and ingrowth of isotopes within WF over time	Mariner, Hammond SNL	**Now**	**M**	**1, N**	

Table 3-2. Model integration table.

Process Model	Code	Process(es)	Personnel	Current Level of Readiness/ Technical Maturity How soon could we?	Level of Effort (LOE) for Integration with PA/PFLOTRAN How long once we start? L = 1 month M = 6 months H = 1 year or more	Integration Time Frame ("Priority Order/ and Urgency") How soon should we? Urgency categories: N = Near term M = Medium term F = Far term	NOTES (Green is generally preferable)
Effective Solubility Model for Isotopes	PFLOTRAN	Precipitation and dissolution of isotopes	Mariner, Hammond SNL	**Now**	**M**	**1, N**	• Direct coupling in PFLOTRAN. • LOE indicated as L-M. • Highest FEP score probably 4.86
WP Degradation Model (non-mechanistic)	PFLOTRAN	Degradation of WP outer barrier over time, including GC, SCC, LC, and EF	Mariner, Hammond SNL	**Now**	**M**	**2, N**	• Direct coupling in PFLOTRAN (sampled rates) • LOE indicated as "several weeks" • Highest FEP score = 4.34
Dual or multi continuum	PFLOTRAN	Transport processes (matrix diffusion) in the near and far field	G. Hammond SNL	**Now**	**M - H**	**3, N**	Ready now
Solution Density	PFLOTRAN	Density dependence on salinity and temperature	Hammond SNL	**Now**	**M–**	**3, N**	Temperature dependence is already implemented
Pitzer Activity Model	PFLOTRAN	Speciation and solubility	G. Hammond, P. Lichtner SNL	**Now**	**L- M**	**4, N**	Ready now
Models with Perhaps the Most Impact on GDSA Efficacy							
Nested EBS, near-field, far-field models	PFLOTRAN	Nesting of gridded domains with process models of varying sophistication	G. Hammond SNL	**1 to 2 years?**	**M - H**	**5, M**	• **Direct implementation in PFLOTRAN** • TRL = several years off • LOE = probably 6 months to a year • FEP not explicitly scored, but "disposal system modeling" rated as "high" priority as a "cross-cutting" issue.
Disruptive events	PFLOTRAN	PA processes initiated or dependent upon various external events, such as human intrusion and seismicity. Also	Mariner, Sevougian, Hammond, et al. SNL et al.	**To be determined (TBD)**	**H+**	**F**	Requires conceptual model(s) for various repository concepts

Table 3-2. Model integration table.

Process Model	Code	Process(es)	Personnel	Current Level of Readiness/ Technical Maturity How soon could we?	Level of Effort (LOE) for Integration with PA/PFLOTRAN How long once we start? L = 1 month M = 6 months H = 1 year or more	Integration Time Frame ("Priority Order/ and Urgency") How soon should we? Urgency categories: N = Near term M = Medium term F = Far term	NOTES (Green is generally preferable)
		includes effect of early WP failures					
Other Process Models with a Longer Integration Time Frame:							
Flow properties of reconsolidated and damaged salt	N/A	Rock characteristic curves (Pc and rel perm vs. Sw) for salt	K. Kuhlman, C. Howard, T. Dewers SNL	**TBD**	**L**	**F**	• Direct coupling—data input for characteristic curves • LOE is "rapid" • Highest relevant FEP score = 2.80
Rigid-Body-Spring-Network (RBSN)	TOUGH2-RBSN	Discrete Fracture Network (DFN) with THM (argillite/clay)	K. Kim, J. Houseworth, J. Rutqvist, J. Birkholzer LBNL	**Far out!**	**M - H**	**M - F**	• Abstraction suggested (fracture property response surface). A coupled version of RBSN requires dynamic input (T, p, σ). • TRL = not indicated explicitly • LOE indicated as a "few months". • Primary FEP score = 2.58
THMC processes in EBS	TOUGHREACT-FLAC3D	THMC (includes clay illitization)	J. Rutqvist, L. Zheng LBNL	**M, C indicated to need "work"**	**TBD**	**M - F**	• Response surface suggested (permeability, porosity, cation exchange capacity, swelling stress). • TRL = M, chemical processes still under development • LOE not given • Primary FEP score = 3.50
THM model of buffer materials (unsaturated)	BBM+TOUGHREACT+FLAC	Coupled thermal-hydrological-mechanical processes in compacted clays	J. Rutqvist, J. Birkholzer LBNL	**Now for 2-D** **Several years for 3-D**	**H**	**M - F**	• Response surface suggested (permeability and porosity fields) • TRL = not given but indicates several years for 3D, but perhaps "now" for 2D • LOE not given; but underlying process model will be ported to HPC in a few years.

Table 3-2. Model integration table.

Process Model	Code	Process(es)	Personnel	Current Level of Readiness/ Technical Maturity How soon could we?	Level of Effort (LOE) for Integration with PA/PFLOTRAN How long once we start? L = 1 month M = 6 months H = 1 year or more	Integration Time Frame ("Priority Order/ and Urgency") How soon should we? Urgency categories: N = Near term M = Medium term F = Far term	NOTES (Green is generally preferable)
							• Primary FEP score = 3.50
Salt Coupled THM processes	TOUGH-FLAC	Coupled thermal-hydrological-mechanical processes in salt EBS and EDZ	J. Rutqvist, L. Martin, J. Birkholzer LBNL	**Now for 2-D** **Several years for 3-D**	**H**	**M - F**	• Response surface suggested (permeability and porosity fields) • TRL = not given but indicates several years for 3D, but perhaps "now" for 2D • LOE not given; but says the underlying process model will be ported to HPC in a few years. • Primary FEP score = 2.58
Two-Part Hooke's Model (saturated)	TPHM-FLAC3D	Clay deformation	L. Zheng, J. Houseworth LBNL	**TBD**	**TBD**	**M - F**	• Abstraction suggested (permeability, porosity, stress). • LOE not really given—hinted to be perhaps an "H". • Primary FEP score = 2.58
Poisson-Boltzmann Nernst-Plank (PBNP) Radionuclide Diffusion Model	CrunchEDL, PHREEQC(?)	1-D reactive diffusion in compacted clay	C. Steefel LBNL	**TBD**	**M**	**M - F**	• Combined response surface (electric potential field) and directly coupling (diffusion constitutive model). • Indicates M+ for LOE ("few months"). • Primary FEPs score = 3.55, 3.06
Kinetic Multiple Site Sorption-Desorption Model	Unnamed code	Radionuclide sorption-desorption in granitic materials	P. Reimus LANL	**TBD**	**L**	**N - M**	• Direct implementation in PFLOTRAN suggested, but some abstraction is necessary (as well as parameterization of the abstraction). • LOE hinted to be probably M-H. • Primary FEP scores = 3.06, 2.40, 2.40
Colloid Stability Model (see GDSA below)	No code yet	Intrinsic Pu colloid stability in both the near and the far fields, as a function of T	P. Zhao, M. Zavarin LLNL	**TBD**	**M - H**	**F**	• Abstraction suggested but not discussed. Seems to be direct implementation of intrinsic Pu colloid "dissolution" rate in PFLOTRAN. • LOE not listed but probably M; time

Table 3-2. Model integration table.

Process Model	Code	Process(es)	Personnel	Current Level of Readiness/ Technical Maturity How soon could we?	Level of Effort (LOE) for Integration with PA/PFLOTRAN How long once we start? L = 1 month M = 6 months H = 1 year or more	Integration Time Frame ("Priority Order/ and Urgency") How soon should we? Urgency categories: N = Near term M = Medium term F = Far term	NOTES (Green is generally preferable)
							frame for readiness not given • Many loosely related FEPs listed; probably highest rated relevant FEP (2.2.09.59) score =3.29
Diffusion of actinides through bentonite	N/A	Speciation, sorption, diffusion;	C. Joseph, M. Zavarin LLNL	**TBD**	**L – M ?**	**F**	• Direct implementation in PFLOTRAN suggested (but not clear if this is a model or just a data-gathering experiment for Fick's Law). Data gathering time frame up to 6 years. • LOE probably L-M. • Primary FEP score = 4.86, 3.06, etc.
Thermodynamic and sorption database(s)	N/A	Thermodynamic, surface complexation/ion-exchange databases	M. Zavarin, C. Joseph, C. Duffin, T. Wolery LLNL	**TBD**	**TBD**	**F**	• Abstraction suggested but not clear; seems like direct implementation • LOE TBD, but readiness requires 3 years of database development • Highest FEP score probably 3.55
Other GDSA Process Models with a Longer Integration Timeframe:							
Solid Solution Model	PFLOTRAN	Precipitation and dissolution of solid solutions	Lichtner SNL	**TBD**	**H**	**M**	
Biosphere Model	TBD	Biosphere pathway model	?	?	**L**	**F**	Site-specific Requires conceptual model(s)

[1] FEP scores are from the UFD R&D Roadmap (DOE 2011). Higher scores indicate higher importance.

3.2 GDSA Process Model Development

GDSA made significant progress in FY2015 in process model development and coupling. The Fuel Matrix Degradation Model (FMDM), developed primarily at Argonne National Laboratories, was coupled to PFLOTRAN. As discussed in Section 3.3, this was a major effort. Section 3.2.1 describes the FMDM and provides a demonstration of the coupling. Section 3.2.2 presents a new source dissolution model for HLW glass dissolution that was developed and implemented by GDSA for the defense repository application presented in Section 4.2. Section 3.2.3 describes the newly added source composition and source heat flux capability for tracking the evolving mass fractions of radionuclides in the waste form and the changing heat flux source term. Section 3.2.4 presents a conceptualization of a canister degradation model for future implementation in the GDSA model framework. Section 3.2.5 discusses progress made in the implementation of radionuclide decay in the precipitate phase and isotope equilibrium partitioning. Section 3.2.6 summarizes GDSA development of a new state-of-the-art solid solutions model.

3.2.1 Fuel Matrix Degradation Model

A major advance for the GDSA modeling capability this year is the addition of the Fuel Matrix Degradation Model (FMDM), version 2.3. The FMDM was developed at Argonne National Laboratory for the Used Fuel Disposition Campaign and is documented in detail in Jerden et al. (2015a). This model calculates the aqueous dissolution rate for used fuel owing to the interfacial corrosion potential from anodic and cathodic half reactions. Processes and inputs accounted for in the FMDM include:

- generation of radiolytic oxidants,
- catalyzed oxidation of hydrogen gas,
- precipitation of secondary phases,
- complexation of uranyl bicarbonate,
- oxidation of ferrous iron,
- temperature variations, and
- diffusion of chemical species at the interface.

Figure 3-3 shows the coupling required between the waste package process model of the PFLOTRAN code (shown as the Generic Disposal System Model) and the FMDM. The FMDM requires as input: temperature, fuel burnup, dose rate at the fuel surface, and aqueous concentrations of H_2, O_2, CO_3^{2-}, and Fe^{2+}. In addition, the FMDM needs the concentrations of the following species, calculated by the FMDM at the previous time step: UO_2^{2+}, $UO_2(CO_3)_2^{2-}$, UO_2(aq), U(IV)(s), U(VI)(s), H_2, O_2, H_2O_2 , CO_3^{2-}, and Fe^{2+}. These concentrations are recalculated at each time step by the FMDM and must be stored by the PFLOTRAN code for the next time step. In return, the FMDM calculates the fuel dissolution rate in $M/L^2/T$ (mass per area per time), from which PFLOTRAN calculates the reduction in the mass of used fuel in the cell and the corresponding release rates of each radionuclide.

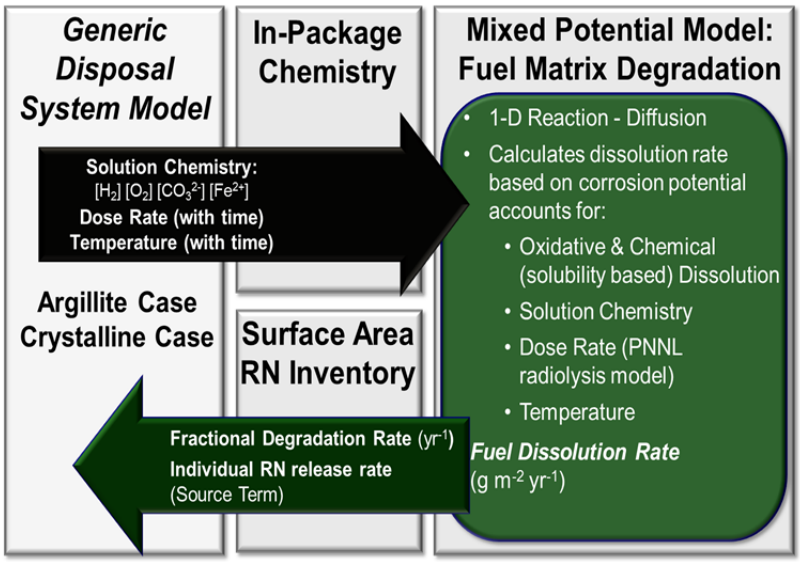

Figure 3-3. Schematic diagram showing the flow of information between the FMDM and PFLOTRAN (taken from Jerden et al., 2015b).

Coupling the FMDM with PFLOTRAN required thoughtful planning and a restructuring of PFLOTRAN factories. To complete the coupling, several mechanisms were implemented within the waste package process model of PFLOTRAN:

- a mechanism for applying the FMDM individually to different waste form cells and only to waste form cells,
- a mechanism for storing calculations by the FMDM for each waste form cell for use in subsequent calls to the FMDM,
- a mechanism for tracking the mass of used fuel in each waste form cell, and
- a mechanism for calculating individual radionuclide release rates from the returned used fuel dissolution rate.

Refactoring was needed to improve workflow not only for the FMDM but also for other process models to be coupled in the future. Section 3.3 discusses the refactoring in more detail.

To test the coupled FMDM, a demonstration was performed on 4 rows of 13 used fuel cells in a 101 × 101 × 21 m grid at 1 m resolution (~214,000 grid cells). The conditions were:

- 100 years at 1 yr time step (10^{-6} yr initial time step),
- 5 m spacing between used fuel cells within a row,
- 20 m spacing between rows,
- 0.001 M O_2(aq), HCO_3^-, H_2(aq), Fe^{2+},
- 55-65 yr burnup (random),
- 0.8-1 m^2 reactive surface area (random),
- 1 m/yr (x direction), 0.14 m/yr (y direction) pore water velocity.

The results of the demonstration are shown in Figure 3-4. At 0.1 yr, tracer concentrations are low but differ among used fuel cells due to the random assignments of burnup and reactive surface area. The time

is too short at 0.1 yr to observe much transport away from the used fuel. At 100 yr, concentrations are much higher and significant advection and dispersion is observed due to the gradual flow of water past the used fuel.

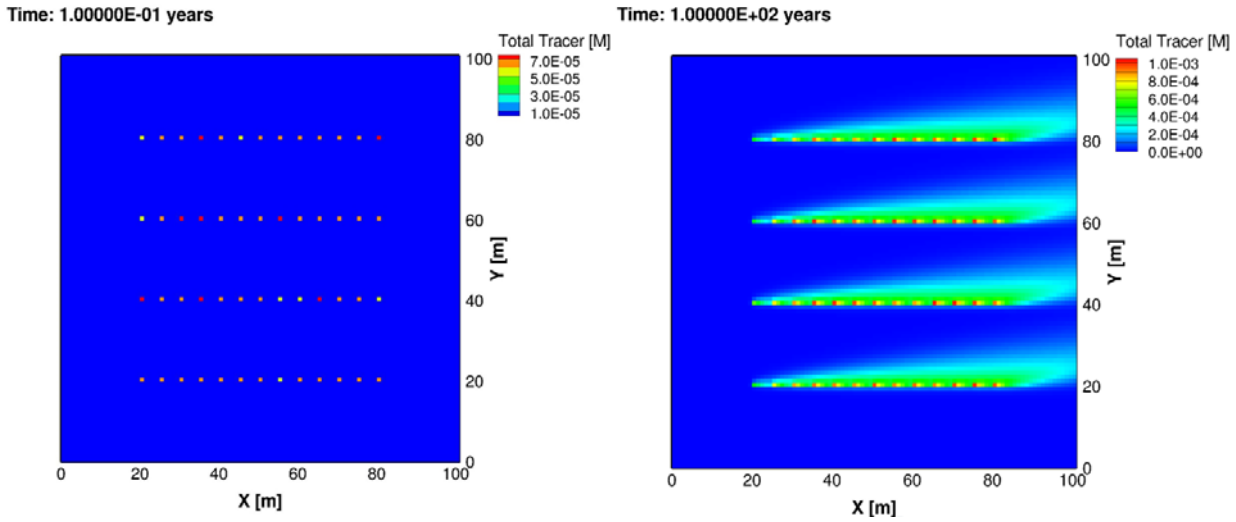

Figure 3-4. PFLOTRAN-FMDM coupling demonstration for an array of 52 used fuel cells in a saturated porous medium.

While PFLOTRAN-FMDM coupling is successfully established, it is not yet complete and optimized. Optimization is needed to speed up FMDM simulation. FMDM run time has a major impact on the overall run time of a repository simulation when there are a large number of waste packages. It is likely that the FMDM code can be sped up with more efficient solving techniques. Effective ways to reduce the number of calls to the FMDM in a simulation are also likely. In addition, the PFLOTRAN post-processing of the FMDM output is not complete. Converting the used fuel degradation rate into release rates for specific radionuclides needs to be finalized. This may be accomplished using the strategy developed for glass dissolution, as described in the next section.

3.2.2 Source Dissolution Model

The development of the source dissolution model within the PFLOTRAN waste package process model is another important accomplishment this year. This model manages the dissolution of a solid source and the release of its components over time. It was successfully used to simulate the dissolution of HLW glass in the defense waste repository application presented in Section 4.2.

The objective of the source dissolution model is to provide flexibility in defining source term compositions and source term mass fluxes. The source material for this model may be a waste form and/or other material (e.g., steel). The initial mass of the source material and the mass fractions of the released components are defined in the input. Source term compositions that change over time, such as the isotope mass fractions in nuclear waste, are accommodated (Section 3.2.3).

The dissolution/degradation rate for the source dissolution model may come from an independent process model (e.g., FMDM), a user-defined rate equation (or set of equations), or sampled distributions. Currently, the model is developed for coupling the FMDM and for incorporating a user-defined rate equation. In the current state of the PFLOTRAN waste package process model, user-defined rate expressions must be written into the PFLOTRAN code. This hardwiring could be replaced in the future with a means to define (or choose) rate equations in the input file.

Figure 3-5 shows the general implementation of the source dissolution model. The rate model is selected by the user and returns the dissolution rate in units of $M/L^2/T$. In the current model, this rate is converted to a fractional dissolution rate as described below. Additional rate models other than fractional dissolution may be added as needed. The fractional dissolution rate is used to calculate the mass remaining. This mass is recorded and used to calculate the mass dissolved during the time step. From this and the component mass fractions, component release rates are calculated.

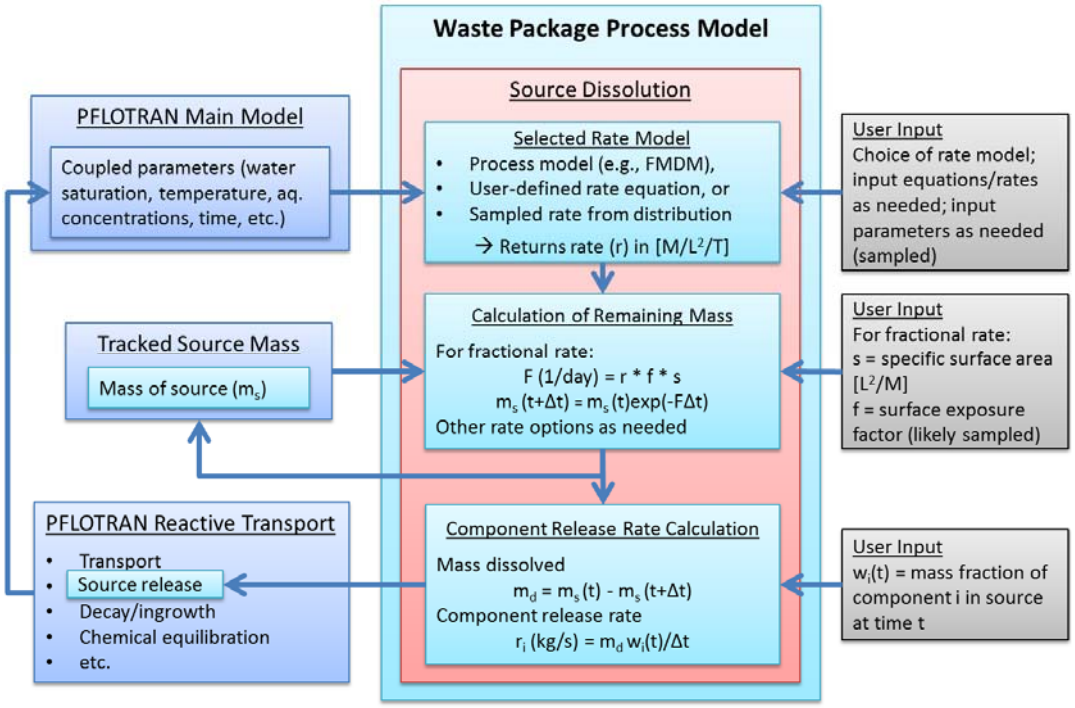

Figure 3-5. General workflow of the source dissolution model of the PFLOTRAN waste package process model.

The source dissolution model is demonstrated in Section 4.1 for HLW glass. In the demonstration, the following user-defined rate equation is used:

$$r(T) = 560e^{\frac{-7397}{T(t,\bar{x})}} \quad (1)$$

This equation is the long-term HLW glass dissolution rate formula provided in Kienzler et al. (2012, p. 17). In this equation, the dissolution rate $r(T)$ is in units of kg/m^2/day, and temperature $T(t,\bar{x})$ is in Kelvin and varies in time t and space $\bar{x}$. The dissolution rate is converted to a fractional dissolution rate F (day^{-1}) using the geometric specific surface area of the solid s (m^2/kg) and a surface exposure factor f:

$$F = r(T)fs \quad (2)$$

For a HLW glass log, s is the cylindrical area divided by the mass. The exposure factor f accounts for additional specific surface area from fractures and roughness. This factor may differ from cell to cell. It could also vary in time if so defined by the user in the rate equation.

Component release in the source dissolution model assumes congruent dissolution of the mass fractions in the source. For nuclear waste, isotopes are the components released from the source. As radionuclides decay and ingrow, the source's isotopic composition changes over time. Thus, prior to repository

simulation, a lookup table of isotope mass fractions over time is prepared so that the model can interpolate the appropriate fractions for the current time step (Section 3.2.3).

The model was tested in the defense repository simulation (Section 4.1). It performed as designed, exhibiting decreasing rates of glass dissolution as affected by temperature, appropriate reductions in mass of glass remaining, and increasing aqueous concentrations of ^{129}I (Figure 3-6). For ^{129}I, the mass fraction remains nearly constant over one million years (see Figure 3-7) because of the long half-life of ^{129}I and negligible ingrowth of ^{129}I in the glass. An important feature yet to be added to the model is the instantaneous fractional release of radionuclides upon waste package breach.

The user-defined dissolution rate capability of the source dissolution model is expected to be useful for many general applications. However, it is likely not capable of mechanistically addressing multiple interrelated processes. For the more complicated dissolution models, separate codes may be developed and coupled to the source dissolution model. For HLW glass dissolution, a mechanistic model is being developed at Argonne (Ebert et al. 2015). It requires a set of chemical feedbacks that will eventually necessitate PFLOTRAN simulation of bulk water chemistry (as will be the case for a fully implemented FMDM). Such models are welcome and encouraged and will add to the collection of available source term models.

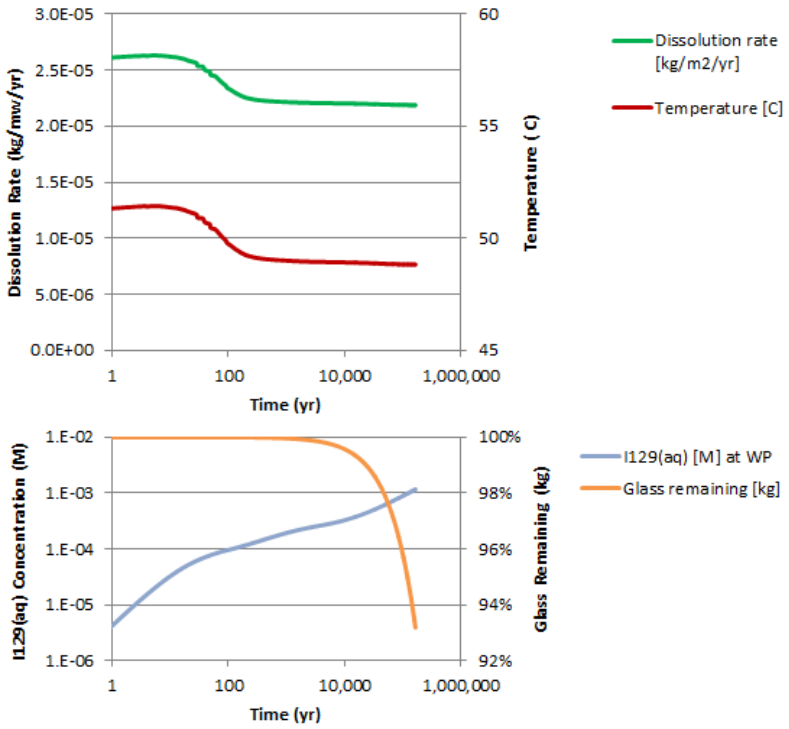

Figure 3-6. Glass dissolution rates and resulting ^{129}I (aq) concentrations calculated for a waste package in the defense repository simulation.

3.2.3 Source Composition and Source Heat Flux

The composition and heat flux of nuclear waste are key inputs in repository simulations. The heat flux is needed to calculate the temperature in the EBS and beyond. The composition is needed to calculate the release rates of radionuclides. Complicating these source terms is the fact that they change significantly over the duration of the safety assessment period.

Prior to GDSA model simulation, changing source composition and heat flux are calculated in a pre-processor. For example, for the defense HLW glass simulation in Section 4.2, a Microsoft Excel file was used to calculate the effects of radioactive decay in Hanford HLW glass on source term heat flux and composition. These calculations are used to prepare tables of heat flux and isotope mass fractions as a function of time so that the source dissolution model of the PFLOTRAN waste package process model can interpolate and apply accurate source terms at each time step. Figure 3-7 shows the mass fractions of selected radionuclides calculated by the pre-processor for Hanford HLW glass.

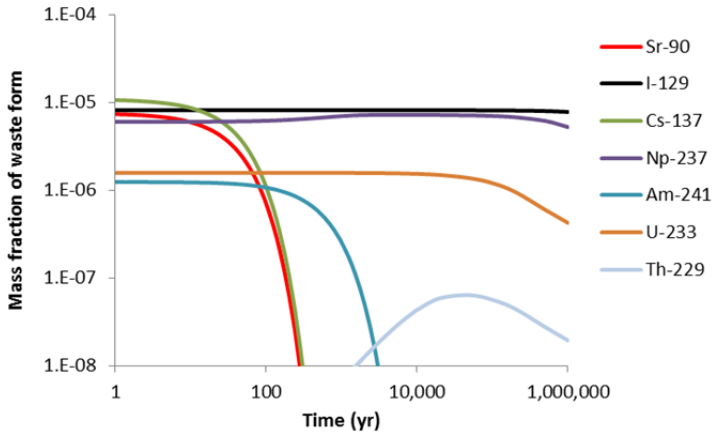

Figure 3-7. Selected isotopes plotted as mass fractions of waste form mass in Hanford HLW glass over time.

3.2.4 Canister Degradation Model

Waste package canisters may degrade by multiple mechanisms. Mechanisms include general corrosion, stress corrosion cracking (SCC), pitting corrosion, microbiologically-influenced corrosion (MIC), rock fall, etc. Which process dominates at a given time in a simulation depends on local conditions and degradation rates. A canister degradation model will need to account for all important degradation processes and how they affect the timing of waste package breach, canister barrier performance after breach, local groundwater conditions, and precipitation of secondary minerals.

This year a conceptual model was advanced for simulating the degradation of a waste package canister in the GDSA model framework. Canister degradation is planned for implementation as an additional process model within the PFLOTRAN waste package process model. Much like the source dissolution model (Section 3.2.2), the canister degradation model will be designed for use with external canister degradation models or simpler built-in models that can either be selected or defined by the user. Initially, simple models will be programmed into the PFLOTRAN code.

Figure 3-8 shows the conceptual work flow. For the initial implementation, the conceptual model focuses on (1) the timing of canister breach and (2) the performance of the canister after breach. In this conceptual model, the status of the canister is defined by two abstract terms, canister vitality (V) and canister performance (P). Canister vitality is a normalized measure of remaining time before canister breach, and canister performance is a normalized measure of the physical ability of the canister to contain the source. Initially, both terms have a value of 1. Before canister breach, while corrosion reduces the time remaining before canister breach, the canister vitality decreases. When it reaches zero, the canister is breached and canister performance begins to decrease.

In GDSA modeling to date, a single waste package and its contents are given a single grid block. Until nested gridding is implemented and related scaling challenges are overcome, higher resolution for the

waste package is not practical with a structured grid. GDSA modeling will likely continue with structured gridding (meshes defined by orthogonal planes) until more time can be invested in meshing (either through unstructured grids or block grid refinement).

With a single cell representing a waste package, the effects of canister degradation must somehow be represented by properties of the cell. Prior to breach of the canister, no water enters the waste package cell, none of the waste form dissolves, and no waste form components are released to surrounding cells. The ability of water, gas, and species to move between the waste package cell and surrounding cells is initially planned to be controlled by adjusting the permeability and tortuosity of the waste form cell. Thus, prior to breach, both the permeability and tortuosity of the waste form cell are set at zero. Zero permeability prevents advection, and zero tortuosity prevents diffusion (Tortuosity in PFLOTRAN is the square of the ratio of the linear distance to the particle path.). After breach, as canister performance diminishes, the permeability and tortuosity of the waste form cell is increased until canister performance is negligible and permeability and tortuosity are representative of the waste package cell with a fully degraded canister.

Adjusting the permeability and tortuosity of waste form cells to simulate canister performance is not ideal. A better approach would be to include differential equations to simulate transport across waste package barriers. Alternatively, for the conceptual approach developed here, creating a mesh to define the waste package canister separate from the waste form would allow the permeability and tortuosity of the canister cells to be adjusted instead of the permeability and tortuosity of the waste package cells.

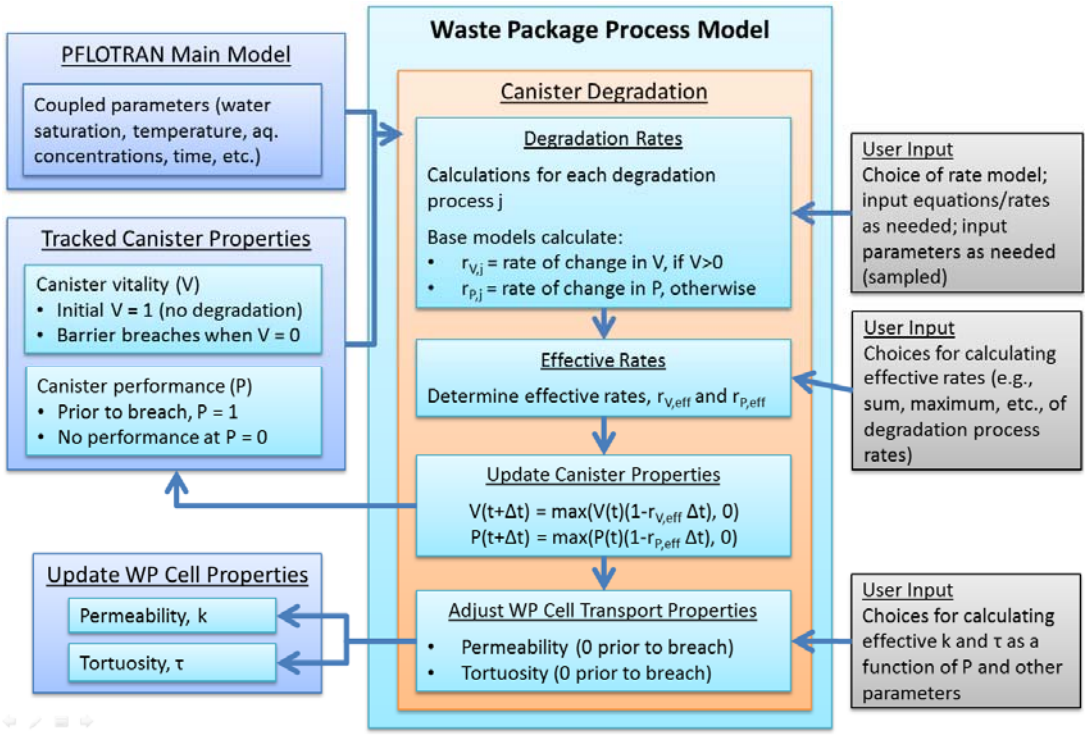

Figure 3-8. Conceptual workflow planned for the canister degradation model of the PFLOTRAN waste package process model.

Aside from changes in the physical barrier, canister corrosion alters the local chemical and physical environment by consuming reactants and generating products. Corrosion not only produces secondary mineral precipitation but also, if rapid relative to the migration of nearby aqueous and gas species, affects

local aqueous and gas composition. Many of these effects provide important feedbacks that may alter corrosion rates. In addition, the accumulation of precipitated secondary phases may affect radionuclide transport by providing a substrate for sorption. Corrosion could also release radionuclides generated by neutron activation. These effects will need to be considered in future development of the model.

3.2.5 Isotope Decay and Partitioning

Key processes that affect concentrations of an isotope in the GDSA reference cases are illustrated in Figure 3-9. Nearly all of these processes can be simulated using the main PFLOTRAN code. The exception is that PFLOTRAN does not simulate radioactive decay in the precipitate phase except through the creation of a "reaction sandbox" module (Lichtner et al. 2015). PFLOTRAN also does not automatically account for the effects of isotope fractions on isotope precipitation due to elemental aqueous solubility. Because these processes are important to PA modeling, it is necessary to include them in the GDSA model framework.

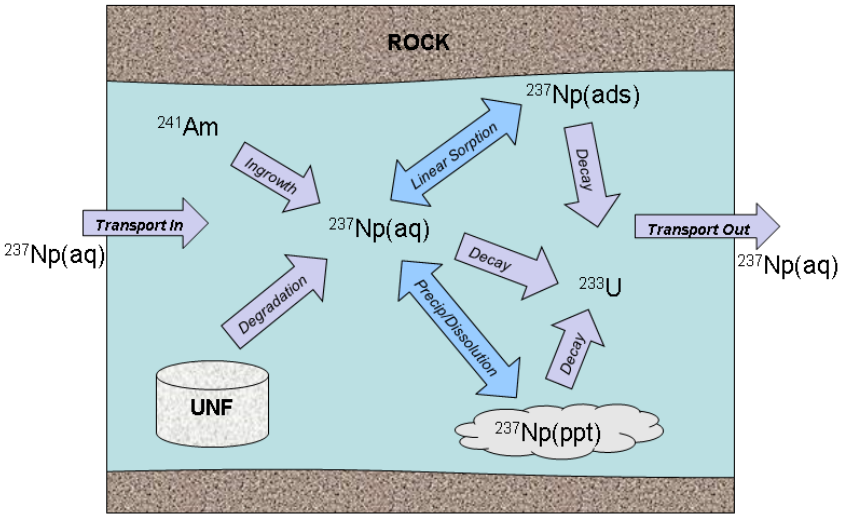

Figure 3-9. Schematic diagram of processes affecting ^{237}Np concentrations in aqueous, adsorbed, and precipitate phases.

Decay in the precipitate phase and equilibrium isotope partitioning could potentially be included in the GDSA model framework by building them into, or coupling them with, the PFLOTRAN chemical speciation model. Doing so would require a significant effort. Particularly problematic is the decay of radionuclides in precipitated minerals in the reactive transport solver.

In the current GDSA model framework, decay and ingrowth in the aqueous and sorbed phases is performed using the PFLOTRAN chemical speciation model. Thus, decay and ingrowth is included in the reactive transport calculations. Because the model cannot handle decay in the precipitate and because the addition of this capability to the PFLOTRAN chemical speciation model is not readily achievable at this time, a different approach to decay and ingrowth for all phases is envisioned. This alternative model would operate separately from the PFLOTRAN chemical speciation model and separately from the reactive transport calculations.

In the envisioned approach, decay and partitioning processes would be conducted in sequence. First, the net overall decay rate of the isotope is calculated. This rate is the sum of the decay and ingrowth rates of the total concentration of the isotope in the cell. A new total concentration of the isotope is calculated from this rate. Next, the bulk isotope concentrations of each element are summed to calculate the total elemental concentrations in the cell and the overall isotope mole fractions for the element. With this

information, equilibrium isotope partitioning is performed across all phases (e.g., aqueous, sorbed, precipitate, and other phases as needed, such as gas and colloids). The concentrations of each element are partitioned among the phases using a simple set of explicit calculations. These calculations require no iteration. With the newly calculated elemental concentrations in each phase, isotope distributions within each phase are set to the same distribution as the bulk isotope distribution determined after the decay and ingrowth step. Distributing isotopes in this way maximizes entropy and ensures that important isotopes are not disproportionally trapped within a precipitate phase.

Implementation of the proposed decay and equilibrium partitioning models is discussed in detail in Sevougian et al. (2014, Section 2.2.2.1.2). At the time of that report it was thought that the decay step could be executed within the reactive transport step by including the net decay rates in the Jacobian. However, accounting for decay in the precipitate phase is a major obstacle. In the coming year, the implementation of these models outside the reactive transport step will be further pursued.

It is important to note that the proposed equilibrium partitioning model is a conditional model that requires the user to define distribution coefficients and elemental solubility limits. The model is expected to be highly useful in much of the GDSA modeling of generic repository reference cases and for applications where conditions are sufficiently stable. However, when reactions occur that cause conditions to change (e.g., pH), a full reactive transport calculation using a chemical speciation model is needed. Reactive transport can be simulated using the PFLOTRAN chemical speciation model but only for elements. A chemical speciation model that includes (or is compatible with) isotope decay, ingrowth, and precipitation would be highly useful for investigating the effects of changing conditions on isotope concentrations and isotope partitioning. Developing this capability for such applications is likely to be challenging but should be explored and pursued.

3.2.6 Solid Solutions

A new mathematical model for simulating solid solutions was developed by Dr. Peter Lichtner of OFM Southwest Research for future incorporation into PFLOTRAN (Lichtner 2015). A solid solution is a homogeneous crystalline phase in which different atoms or molecules may partially substitute for original atoms and molecules within the crystalline phase. Solid solutions in nuclear waste disposal include spent nuclear fuel, mixed oxide fuel, altered layers of vitrified nuclear waste, cement, $(Ra, Ba)SO_4$, steel, corrosion products, and clays (Bruno et al. 2007).

A solid solutions model is needed to expand options for increasingly mechanistic models of waste form dissolution, material degradation, and transport and fate of radionuclides. The current version of the model assumes ideal solid solutions where reactions with an aqueous solution are treated kinetically using a transition state rate law for the overall reaction and a pseudo-kinetic rate law for exchange reactions (Lichtner 2015). A demonstration for a binary solid solution, analogous to an ideal $(Ra, Ba)SO_4$ system, is developed in *Mathematica* and presented in Lichtner (2015). Future work is needed to extend the model to non-ideal solid solutions and to incorporate order-disorder phenomena (Lichtner and Carey 2006; Sack and Lichtner 2009).

3.3 Process Model Coupling

PFLOTRAN was refactored this year to improve the coupling of process models. Section 3.3.1 describes the new coupling infrastructure, and Section 3.3.2 describes the coupling of the FMDM.

3.3.1 PFLOTRAN Process Model Coupling Infrastructure

Historically, PFLOTRAN has utilized a workflow similar to many other simulators for modeling reactive multiphase flow and multicomponent transport in the subsurface. Figure 3-10 illustrates this workflow where the code is first initialized, then enters a time stepping loop where flow and reactive transport are

repeatedly solved until the end of the simulation, after which the code is finalized (shut down). This approach works well for a fixed set of processes specific to traditional flow and transport. However, such a workflow is somewhat rigid and difficult to extend without a significant refactoring (restructuring) of the code to accommodate new processes and numerical methods.

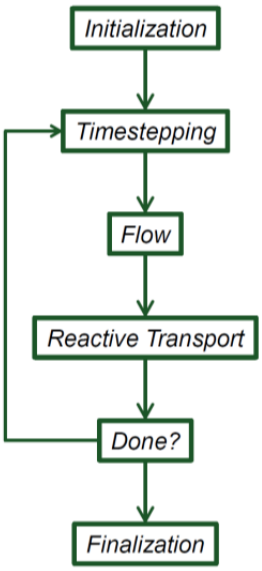

Figure 3-10. Traditional workflow for subsurface flow and transport.

In 2013, PFLOTRAN was refactored into a more modular simulation framework with the use of modern Fortran (i.e. Fortran 2003/2008 capability). Modern Fortran classes provide encapsulation, inheritance and polymorphism through classes common to other object-oriented programming languages (e.g. C++, Java, etc.). They afford the programmer increased flexibility in developing an extensible simulation framework. PFLOTRAN's original workflow can be generalized into three steps: initialization, execution, and finalization as shown in Figure 3-11.

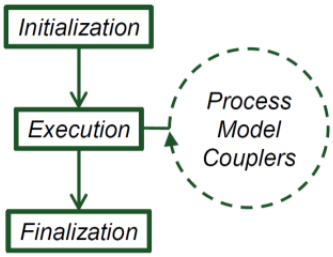

Figure 3-11. Generalized PFLOTRAN workflow that better enables customization.

The function of the initialization and finalization steps in the generalized workflow is similar to that of the original workflow, except factories (code that constructs and destroys data structures, linkages, etc.) can be developed to customize the simulation framework to the individual needs of the modeler. In other words, the factory sets up and initializes a unique set of process models chosen by the user at the beginning and dismantles these process models at the end.

Within the execution step, any number of process models can be coupled and run at identical or dissimilar time scales. The "Process Model Coupler" or PMC class enables this flexibility. As illustrated in Figure 3-12, the PMC is a Fortran class that encapsulates a process model (in this case, multiphase flow), providing numerical methods (time integrators and solvers) for solution, and establishes connectivity between process models. Each PMC has two pointers to other process models, one to a peer and the other to a child. The child PMC is continually playing catch up with the parent PMC. In other words, after each parent PMC time step, the child PMC immediately takes as many time steps as necessary to catch up with the parent, whether the child's time step be lock-step (identical duration) or smaller. The child's time step cannot be larger than the parent. Necessary information (e.g. state and secondary variables) is transferred to the child immediately prior to the child's step and transferred back immediately after the child catches the parent. The peer PMC, on the other hand, can take any number of time steps of any size and synchronizes with the original PMC at select points in time (synchronization points). In between the synchronization points, the peers are unrestricted by each other and information is only transferred between peers at the synchronization point. In the context of synchronization and the parent-child relationship, the time at the end of the parent PMC's time step becomes the synchronization point for the child PMC.

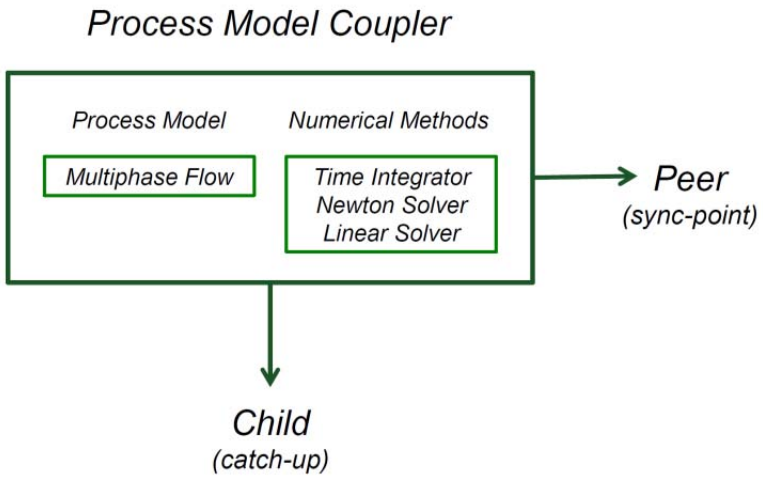

Figure 3-12. The PFLOTRAN Process Model Coupler or PMC. This data structure enables the linkage of process models to (1) the numerical methods employed for solution and (2) other process models.

PFLOTRAN's PMCs can be nested in sophisticated trees or graphs to accommodate any number of processes coupled across varying time scales. Figure 3-13 demonstrates the nesting of six PMCs where PMC A is the parent (and master, meaning it governs all time stepping) with PMCs B, M and Y as its children. PMC A's time step becomes the synchronization point for all three of these children. PMC B and Y also have independent children, C and Z, respectively.

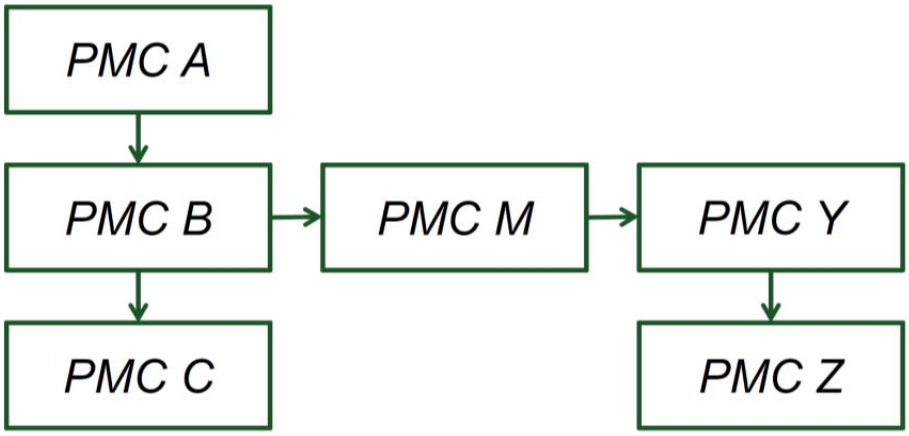

Figure 3-13. An example hierarchy of Process Model Couplers within a graph.

Substituting this graph of PMCs in PFLOTRAN modular workflow (i.e. Figure 3-11), a custom workflow is established for six-PMC simulation as shown in Figure 3-14. Note that in comparison to the traditional workflow in Figure 3-10, a single time stepping loop no longer applies to all process models. Instead, each process model coupler has its own time stepping loop that steps until a synchronization point (time) is reached. A custom factory is built for this simulation that creates the respective PMCs (including underlying data structures, process models, solvers, time integrators, etc.), establishes the hierarchical connectivity, and initializes the PMCs prior to execution and destroys them at shutdown. Often, the developer can create a custom factory as an extension of an existing factory through well-planned code reuse.

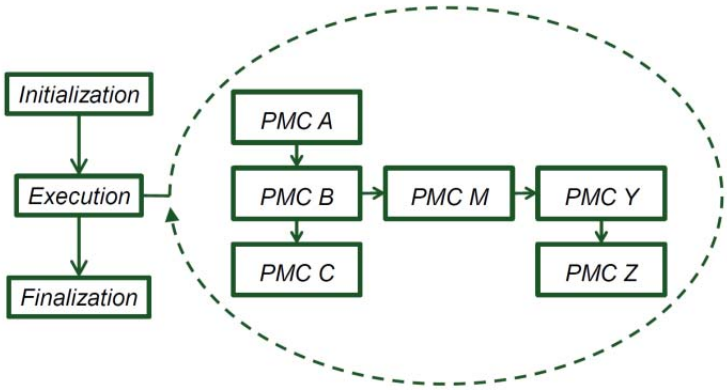

Figure 3-14. An example hierarchy of PMCs embedded within the module workflow.

3.3.2 PFLOTRAN-FMDM Coupling

PFLOTRAN's generalized workflow is demonstrated through the coupling of the Fuel Matrix Degradation Model (FMDM) to PFLOTRAN. The FMDM (Jerden et al. 2015a) calculates the diffusive flux of radionuclide emanating from a nuclear waste form. This flux serves as a source term within PFLOTRAN's reactive transport calculation for each waste form designated in the input file. Parameters read from the input file such as the waste form's specific surface area and burnup and state variables

including temperature and species concentrations are passed from PFLOTRAN to FMDM. The FMDM is executed at a point in time after which a flux of radionuclide is returned to PFLOTRAN, introduced into the transport equation through a source term. Figure 3-3 provides a schematic of the FMDM workflow.

These steps are repeated for each waste form in the conceptual model. The PFLOTRAN-FMDM workflow is shown in Figure 3-15.

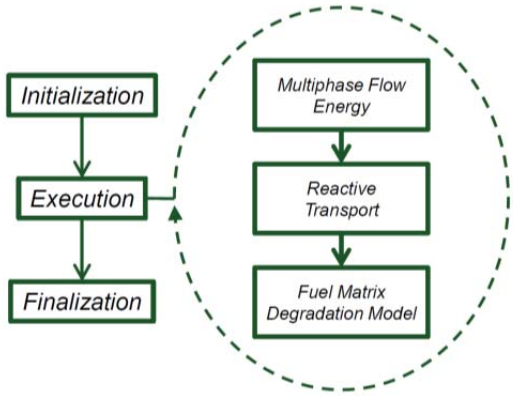

Figure 3-15. The PFLOTRAN-FMDM workflow with a custom tree of PMCs.

The FMDM process model within PFLOTRAN is actually a wrapper routine that calls a single external subroutine developed by Jerden et al. (2015a). Pseudocode for FMDM process model (within the FMDM PMC) is presented in Figure 3-16. During PFLOTRAN's initialization stage, the FMDM block is read from the PFLOTRAN input file and data structures are created and initialized. The execution state consists of solving each waste form (through a call to subroutine AMP_Step()) and updating the corresponding PFLOTRAN source term for each time step. At the end of the simulation, the FMDM PMC and underlying data structures are destroyed. Details regarding the FMDM conceptual model and algorithmic design (e.g. code executed within the call to AMP_Step()) are provided by Jerden et al. (2015a).

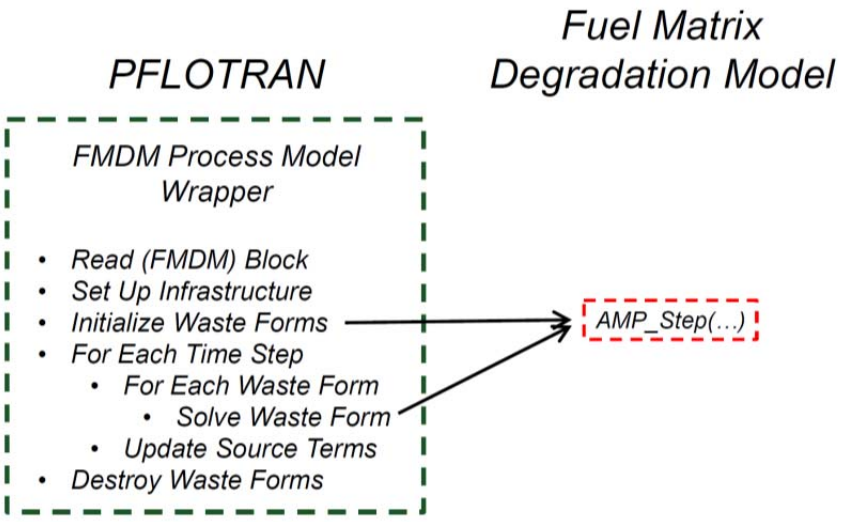

Figure 3-16. Pseudocode for the FMDM process model in PFLOTRAN.

4. GENERIC REPOSITORY APPLICATIONS

4.1 Salt Reference Case for UNF

The salt reference case for geologic isolation of UNF has been developed, refined, and documented over the past two years (Freeze et al. 2013b; Sevougian et al. 2013; 2014). The conceptual model remains the same, a mined repository for isolation of UNF in bedded salt (Figure 4-1), but the numerical implementation has been updated from a single-drift pair model domain to a multi-drift pair model domain. In addition, the single-drift pair model domain has been used in a preliminary assessment of the effect of grid spacing on numerical dispersion.

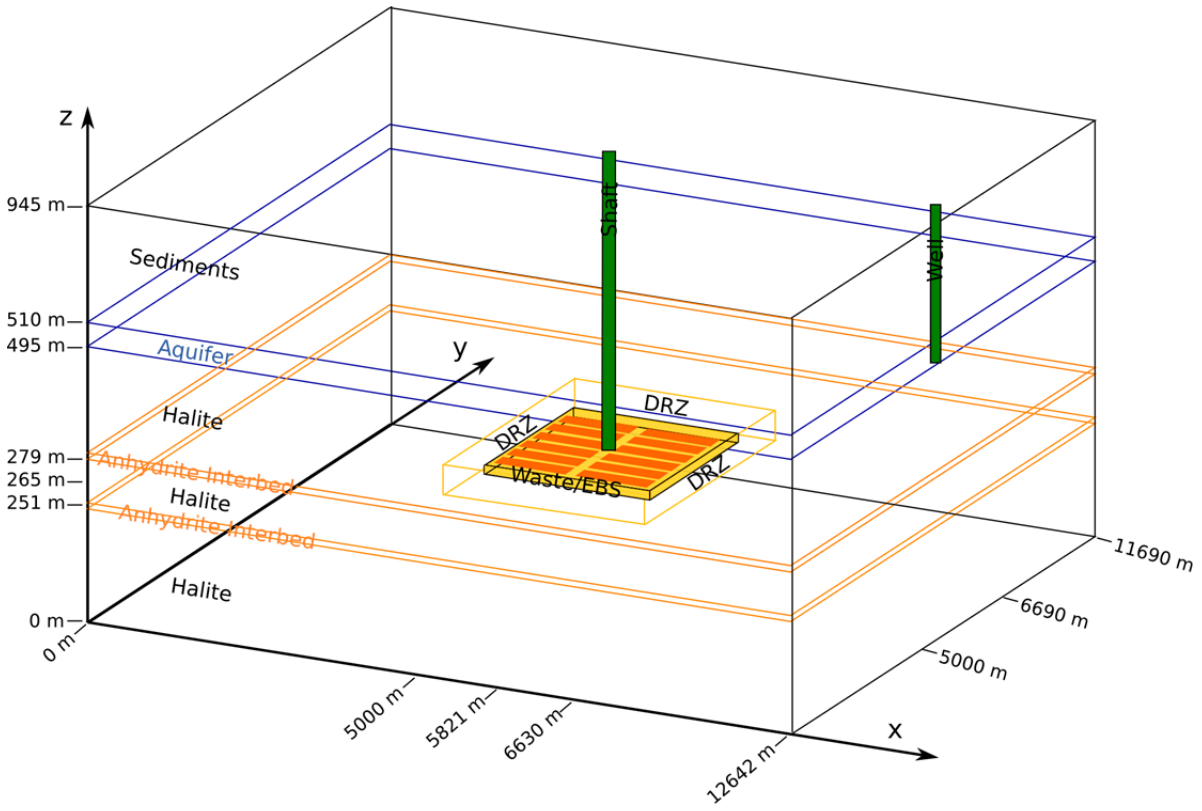

Figure 4-1. General view of repository layout and stratigraphy (modified from Freeze et al. 2013b).

4.1.1 Waste Inventory

The salt reference case waste inventory remains the same as that used by Sevougian et al. (2014) and described in full by Freeze et al. (2013b). The repository capacity is 70,000 MTHM (the maximum allowed by the Nuclear Waste Policy Act of 1983 and about half of the total commercial UNF inventory predicted by 2055 in the "no replacement scenario" (Carter et al. 2013). For simplicity, we assume that the entire inventory consists of PWR UNF assemblies, each containing 0.435 MTHM. Radionuclide inventories (Table 4-1) and decay heat versus time curves (Figure 4-2) are taken from Carter et al. (2013) and assume an initial enrichment of 4.73 wt% ^{235}U and 60 GWd/MTHM burn-up. The salt reference case assumes 50-year out-of-reactor (OoR) storage prior to geologic waste isolation. Because the average burn-up of UNF under the "no replacement scenario" is predicted to be only 54 GWd/MTHM (Carter et al. 2013), the assumption of 60 GWd/MTHM results in a conservatively high heat load.

Table 4-1. UNF inventory of selected radionuclides for the salt reference case.

Isotope	Waste inventory mass[1] (g/MTHM)	Molecular weight[2] (g/mol)	Mass fraction[2] (g/g UNF)	Moles per gram UNF (mol/g UNF)
^{238}U	9.10×10^{5}	238.05	6.32×10^{-1}	2.66×10^{-3}
^{237}Np	1.24×10^{3}	237.05	8.61×10^{-4}	3.63×10^{-6}
^{241}Am	1.25×10^{3}	241.06	8.68×10^{-4}	3.60×10^{-6}
^{242}Pu	8.17×10^{2}	242.06	5.68×10^{-4}	2.34×10^{-6}
^{129}I	3.13×10^{2}	129.00	2.17×10^{-4}	1.69×10^{-6}
^{234}U	3.06×10^{2}	234.04	2.13×10^{-4}	9.08×10^{-7}
^{230}Th	2.28×10^{-2}	230.03	1.58×10^{-8}	6.89×10^{-11}
^{233}U	1.40×10^{-2}	233.04	9.73×10^{-9}	4.17×10^{-11}
^{229}Th	6.37×10^{-6}	229.03	4.43×10^{-12}	1.93×10^{-14}
^{226}Ra	3.18×10^{-6}	226.03	2.21×10^{-12}	9.77×10^{-15}

[1] from Carter et al. (2013, Table C-1)
[2] from Sevougian et al. (2013, Table 1)

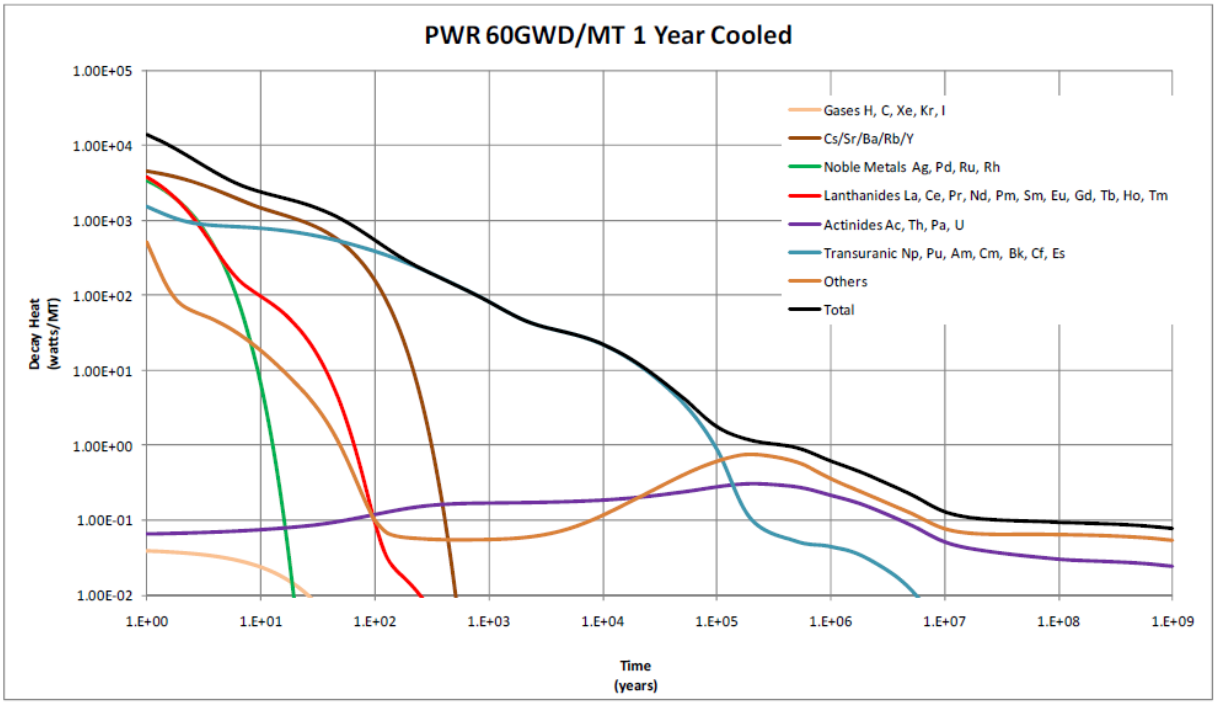

Figure 4-2. Heat decay curve for PWR UNF (60 GWd/MT burnup) from Carter et al. (2013).

4.1.2 Natural Barrier System

The natural barrier system comprises the bedded salt (halite) hosting the repository, the disturbed rock zone (DRZ) surrounding the repository, and the stratigraphic section above and below the repository horizon, including: additional bedded halite; two thin anhydrite interbeds; an aquifer overlying the halite; and generic overburden sediments at the top of the section (Figure 4-1). Parameterization of these materials draws upon the well-characterized Permian Basin bedded salt and associated stratigraphic

section in the location of WIPP as well as bedded salt locations elsewhere in the United States (Freeze et al. 2013b; Sevougian et al. 2013; 2014). Material properties for the deterministic case are given in Table 4-2. Likely ranges of values and corresponding probabilistic distributions are discussed in Freeze et al. (2013b) and Sevougian et al. (2013; 2014) and summarized in Sections 4.1.2.1 through 4.1.2.5.

Table 4-2. NBS deterministic parameters for the salt reference case (taken from Sevougian et al. 2013).

Model Region	Permeability (m^2)	Porosity	Tortuosity [1]	Effective Diffusion Coefficient [2] (m^2/s)	Longitudinal Dispersivity (m) [10]	Saturated Thermal Conductivity [4,9] (W/m/K)	Heat Capacity [5] (J/kg/K)	Grain Density [7] (kg/m^3)
DRZ	1.12×10^{-16}	0.0129	0.23	6.82×10^{-12}	1.0	4.9	927	2170.0
Halite	3.16×10^{-23}	0.0182	0.01	4.19×10^{-13}	50.0	4.9	927	2170.0
Interbed (anhydrite)	1.26×10^{-19}	0.011	0.22	5.57×10^{-12}	50.0	4.9	927	2960.0
Aquifer [6]	1.00×10^{-13}	0.150	0.53	1.83×10^{-10}	50.0	1.5	959	2820.0 [8]
Sediments [6]	1.00×10^{-15}	0.20	0.58	2.67×10^{-10}	50.0	1.5	927	2700.0

[1] Tortuosity = $[\text{porosity}]^{(1/3)}$, except for halite
[2] Effective diffusion coefficient = (free water diffusion coefficient) × (tortuosity) × (water-saturated porosity)
[3] from Freeze and Cherry (1979), Tables 2.2 and 2.4
[4] Hardin et al. 2012, Tables D-1, D-2, and D-5 (based on Clayton and Gable 2009, Fluor 1985, and Fluor 1986)
[5] Hardin et al. 2012, Table D-3 (based on Clayton and Gable 2009, Fluor 1985, and Fluor 1986)
[6] Hardin et al. 2012, Tables D-1, D-3, and D-5 (based on alluvium from Smyth et al. 1979 and Wollenburg et al. 1982)
[7] Crain's Petrophysical Handbook and PetroWiki (online)
[8] Fox 2008, Table 26 (Culebra dolomite)
[9] Saturation function = Brooks-Corey for all units; however, all material regions are fully saturated, i.e., $S_w = 1$
[10] Transverse dispersivity = 0

4.1.2.1 Disturbed Rock Zone (DRZ)

The DRZ is defined as the volume of the host rock (halite) that experiences durable (but not necessarily permanent) changes due to the presence of the repository – for instance changes in porosity, permeability, or thermal conductivity due to expansion during excavation, or changes in saturation, chemistry, or thermal properties due to the presence of waste. The extent of the DRZ is assumed to be 3 drift diameters (about 12 meters) on all sides of the repository. On the basis of parameters used to characterize WIPP, the reference case DRZ porosity is assumed to be 0.0129 and the log permeability (m^2) distribution is assumed to be uniform over a range of -19.4 to -12.5, with a mean of -15.95 (1.12×10^{-16} m^2, the value used in deterministic simulations) (Fox 2008; Freeze et al. 2013b; Sevougian et al. 2013; 2014).

4.1.2.2 Repository Horizon (Halite)

The repository horizon is assumed to be a 495-m-thick bedded halite formation of >50% purity, interrupted by anhydrite impurities (Section 4.1.2.3). Material properties, thickness, and depth to top (450 m) of the modeled halite are consistent with properties of five major U.S. bedded salt formations (Freeze et al. 2013b; Sevougian et al. 2012; 2013; 2014). On the basis of parameters used to characterize the WIPP, the reference case halite porosity is assumed to have a cumulative distribution (simplified to uniform) with a minimum of 0.001, median of 0.01, and maximum of 0.0519 (Fox 2008; Freeze et al. 2013b; Sevougian et al. 2013; 2014). The mean value of 0.0182 is used in deterministic simulations. Log halite permeability (m^2) is assumed to vary over a uniform distribution of -24 to -21 (Fox 2008; Freeze et al. 2013b; Sevougian et al. 2013; 2014). Reference case simulations set the log of halite permeability equal to the mean of this range: -22.5 (permeability = 3.16×10^{-23} m^2).

4.1.2.3 Anhydrite Interbeds

Interbeds consisting of non-halite stringers (such as anhydrite, clay, or polyhalite) with thicknesses on the order of centimeters to meters are commonly observed throughout the major U.S. bedded salt deposits. These interbeds are more permeable than the surrounding halite and may become fractured as a result of repository excavation, and therefore serve as potential pathways for radionuclide transport. The reference case assumes 1-m-thick anhydrite interbeds located immediately above and below the DRZ. On the basis of parameters used to characterize WIPP, anhydrite porosity is assumed to be 0.011 and log permeability (m^2) is assumed to have a Student-t distribution (simplified to uniform) over a range of -21.0 to -17.1 with a mean of -18.9 (permeability = 1.26×10^{-19} m^2, the value used in deterministic simulations) (Fox 2008; Freeze et al. 2013b; Sevougian et al. 2013; 2014).

4.1.2.4 Aquifer

The salt reference case assumes a 15-m thick aquifer overlies the halite host rock and provides a potential pathway to the receptor location in the biosphere, conceptualized as a withdrawal well at the 5-km withdrawal boundary. A receptor well is the first reference biosphere of the International Atomic Energy Association (IAEA) (IAEA 2003) and is the route of exposure in the GDSA reference cases. Aquifer properties are consistent with those of dolomite aquifers such as the Culebra dolomite overlying the WIPP. In deterministic simulations, aquifer porosity and log permeability (m^2) are modeled on those of the Culebra (0.15 and -13, respectively; Fox 2008; Freeze et al. 2013b; Sevougian et al. 2013; 2014). In probabilistic simulations, aquifer permeability is sampled (using a log uniform distribution) over the upper end of likely values for dolomite formations (log permeability (m^2) from -14.0 to -12.0; Freeze and Cherry 1979).

4.1.2.5 Overburden Sediments

The salt reference case assumes a 435-m-thick overburden of generic sediment. Material properties including porosity (0.2) and permeability (10^{-15} m^2) are appropriate for an unconsolidated, silty deposit (Freeze and Cherry 1979).

4.1.3 Engineered Barrier System

The engineered barrier system (EBS) comprises the waste form, waste package, backfill (drift and hallway), and shaft seal. Material properties are unchanged from the latest iteration of the salt reference case (Sevougian et al. 2014). Parameter values used in deterministic simulations are listed in Table 4-3. Likely ranges of values and probabilistic distributions are discussed by Freeze et al. (2013b) and Sevougian et al. (2013; 2014) and summarized in Sections 4.1.3.1 through 4.1.3.4. Section 4.1.3.5 reviews repository layout.

Table 4-3. EBS deterministic parameters for the bedded salt reference case (taken from Sevougian et al. 2013).

Model Region	Permeability (m^2)	Porosity	Tortuosity[1]	Effective Diffusion Coefficient[2] (m^2/s)	Longitudinal Dispersivity (m)[3]	Saturated Thermal Conductivity[4,7] (W/m/K)	Heat Capacity[5] (J/kg/K)	Grain Density[6] (kg/m^3)
Waste Package	1.00×10^{-13}	0.300	1.00	6.90×10^{-10}	0.5	16.7	466	5000.0
Backfill	1.00×10^{-18}	0.113	0.48	1.24×10^{-10}	0.2	2.5	927	2170.0
Shaft (sealed)	1.58×10^{-20}	0.113	0.48	1.24×10^{-10}	20.0	2.5	927	2170.0

[1] Tortuosity = $[\text{porosity}]^{(1/3)}$, except for waste package
[2] Effective diffusion coefficient = (free water diffusion coefficient) × (tortuosity) × (porosity) × (saturation), where the free water diffusion coefficient = 2.3×10^{-9} m^2/s (Cook and Herczeg 2000)

[3] Transverse dispersivity = 0
[4] Hardin et al. 2012, Tables D-1, D-2, and D-5 (based on Clayton and Gable 2009, Fluor 1985, and Fluor 1986)
[5] Hardin et al. 2012, Table D-3 (based on Clayton and Gable 2009, Fluor 1985, and Fluor 1986)
[6] Crain's Petrophysical Handbook and PetroWiki (online)
[7] Saturation function = Brooks-Corey for all units; however, all material regions are fully saturated, i.e., $S_w = 1$

4.1.3.1 Waste Form

The salt reference case assumes that the waste form is PWR UNF with a burnup of 60 GWd/MTHM and initial enrichment of 4.73 wt% ^{235}U, aged 50 yr OoR. Each PWR assembly is assumed to contain 0.435 MTHM and 1.44×10^6 g/MTHM of radionuclides, with initial mass fractions as listed in Table 4-1. The waste form releases radionuclides in two fractions: an instant-release fraction from radionuclides located in the fuel and cladding gap and grain boundaries, and a slow-release fraction due to UO_2 matrix degradation. The salt reference case assumes an instant-release fraction of 0.025 for ^{129}I and zero for all other radionuclides tracked in model simulations. The rate of release of the slow-release fraction (all radionuclides) depends upon the rate of waste form degradation and radionuclide mass fractions in the waste form (Table 4-1). Fractional degradation rate of the waste form is defined on the basis of fuel corrosion rates in various synthetic groundwaters (Kienzler et al. 2012). The probabilistic distributions in Table 4-4 are assumed to be log-uniform.

Table 4-4. UNF degradation rate constants[1] (taken from Sevougian et al. 2014).

Case	λ (s^{-1})	λ (d^{-1})	λ (yr^{-1})	Time for 50% Degradation (yrs)	Time for 99% Degradation (yrs)
Deterministic	1.1574×10^{-11}	10^{-6}	3.6525×10^{-4}	~ 1,900	~ 12,500
Probabilistic – Lower	1.1574×10^{-13}	10^{-8}	3.6525×10^{-6}	~ 190,000	~ 1,250,000
Probabilistic – Upper	1.1574×10^{-10}	10^{-5}	3.6525×10^{-3}	~ 190	~ 1,250

[1] from Kienzler et al. (2012, Figures 18 and 19)

4.1.3.2 Waste Package

The waste package is assumed to consist of a stainless steel canister containing 12 PWR UNF assemblies (5.22 MTHM) and a carbon steel overpack (Freeze et al. 2013b; Sevougian et al. 2013; 2014). The waste package is 5 meters in length and has a diameter of 1.29 m, consistent with the 12-PWR waste package described by Hardin et al. (2012). Until a waste package failure model is developed, the salt reference case assumes instantaneous waste package failure. See Freeze et al. (2013b) for development of waste package model parameters (material properties). Probabilistic simulations sample on waste package porosity using a uniform uncertain distribution from 0.05 to 0.5.

4.1.3.3 Backfill (Drifts and Hallway)

In the salt reference case, waste packages are emplaced on the drift floor and covered with crushed salt backfill, and the access hallway and 5 meters of each drift adjacent to the hallway are sealed with crushed salt backfill (Freeze et al. 2013b; Sevougian et al. 2013; 2014). Backfill is expected to consolidate as drifts and access hallways close due to creep of the salt host rock, but the extent to which it will consolidate is uncertain. Experiments related to the WIPP shaft seal indicate that consolidation is enhanced by the addition of 1 wt % water (Hansen et al. 2012), which might not be used in backfill. Therefore the conservative assumption is made that crushed salt backfill properties will be similar to those of the crushed salt component of the WIPP shaft seal at early times (0 to 200 yr). Log permeability (m^2) is set equal to the mean (-18.0) of the distribution reported by Fox (2008). In probabilistic simulations, porosity is sampled using a uniform uncertain distribution over the range 0.01 to 0.20.

4.1.3.4 Shaft Seal

It is assumed that the shaft seal will be similar to the WIPP multi-component barrier of clay, asphalt, concrete, and crushed salt (James and Stein 2002), but because the crushed salt layers will provide the limiting permeability, material properties of the salt reference case shaft seal are assigned on the basis of the crushed salt component, which is expected to consolidate to a state close to that of intact halite within 200 years (DOE 2009, Section PA-2.1.3). Log permeability is set equal to the mean (-19.8) of the distribution reported by Fox (2008) for the WIPP shaft seal crushed salt component at late times (200 – 10,000 yr). In probabilistic simulations, porosity is sampled using a uniform uncertain distribution over the range 0.01 to 0.20.

4.1.3.5 Repository Layout

The repository is located at a depth of 680 m below the ground surface, and in the middle of the 495-m-thick bedded salt formation. Pairs of disposal drifts lie at right angles to a central access hallway. Drift centers are separated by 20 m. Waste packages are emplaced horizontally, lengthwise within the drifts with a spacing of 10 m center-to-center (5-m spacing, end-to-end). Repository access is via vertical shafts, which intersect the central access hallway. Repository dimensions are listed in Table 4-5.

Table 4-5. Dimensions for the salt reference case repository layout (taken from Sevougian et al. 2014).

Parameters	Value
Waste Package (WP)	
WP length (m)	5.00
WP outer diameter (m)	1.29
WP center-to-center spacing in-drift (m)	10.0
Inventory per 12-PWR WP (MTHM)	5.225
Approx. number of WPs for 70,000 MTHM	13,397.4
Emplacement Drift	
Drift height (m)	4.0
Drift width (m)	6.0
Drift center-to-center spacing (m)	20.0
Pillar width (m)	14.0
Number of WPs per drift	80
Drift seal length (m)	10.0
Drift length, including seals (m)	805.0
Central access hallway height (m)	4.0
Central access hallway width (m)	8.0
Approx. number of drifts needed for 70,000 MTHM	167.5
Repository	
Number of drift pairs (rounded up)	84
Repository length (m)	1,618.0
Repository width (m)	1,666.0
Repository Depth (m)	680.0
Total length of all drifts (m)	135,240

4.1.4 Thermal and Chemical Environment

Temperature, fluid saturation, and porewater composition influence waste degradation rate, and solubility and transport of dissolved radionuclides. Though porewater composition will be site-dependent,

porewater in a bedded halite formation is expected to be concentrated brine. Michigan Basin Devonian brine composition (Table 4-6) is taken to be representative of porewater composition in bedded halite (Sevougian et al. 2012; 2013; 2014).

Table 4-6. Reference brine composition

Characteristic	Reference Values[1]
$[Na^+]$	12,400 - 103,000 mg/l
$[Mg^{2+}]$	3,540 - 14,600 mg/l
$[K^+]$	440 - 19,300 mg/l
$[Ca^2]^+$	7,390 - 107,000 mg/l
$[SO_4^{2-}]$	0 - 1,130 mg/l
$[Cl^-]$	120,000 - 251,000 mg/l
pH	3.5 - 6.2
Specific Gravity	1.136 - 1.295
Density (kg/m^3)	1220.0[2]

[1] from Wilson and Long (1993) as summarized in Sevougian et al. (2013, Table 3-2)
[2] from Fox (2008, Table 29)

4.1.4.1 Diffusion and Dispersion

Molecular diffusion is expected to be a dominant form of radionuclide transport in the low-permeability host halite. The salt reference case assumes a single porewater diffusion coefficient (D_{pw}) for all species equal to 2.3×10^{-9} m^2/s (Cook and Herczeg 2000). Effective diffusion coefficients (D_e) (Table 4-2 and Table 4-3) are material-dependent and calculated as $D_e = \tau\phi s D_{pw}$ where τ is tortuosity, ϕ is porosity, and s is saturation.

In higher-permeability strata (i.e., anhydrite interbeds and aquifer), fluid advection becomes a significant means of radionuclide transport and mechanical dispersion (the spreading of a solute due to variations in groundwater velocity) overwhelms diffusion. Radionuclide flux due to mechanical dispersion depends on linear fluid velocities and is proportional to material-dependent dispersivities (Table 4-2 and Table 4-3).

4.1.4.2 Solubility

The maximum concentration of a radioisotope in solution depends upon the solubility of the corresponding element and (ignoring the possibility of isotope fractionation during precipitation and dissolution reactions) the isotope fraction. Element solubility limits are a function of element properties and porewater (brine) properties, such as redox conditions, pH, and brine composition and temperature. Element solubilities appropriate for the concentrated brine expected in a bedded salt formation are taken from Clayton et al. (2011) and converted to conditional radioisotope solubilities by assuming that isotope ratios remain constant among waste form, aqueous phase, and secondary mineral phases (Table 4-7). An improved model for calculating the effects of element solubility on radionuclide concentrations based on changing isotopic distributions is in development (Section 3.2.5).

Table 4-7. Solubility limits for salt reference case elements and isotopes

Isotope	Element solubility limit[a]	Isotope ratio[b]	Isotope conditional solubility limit
	(mol/L)	(mol isotope / mol element)	(mol/L)
^{233}U	1.12×10^{-7}	1.52×10^{-8}	1.70×10^{-15}
^{237}Np	1.51×10^{-9}	1.00	1.51×10^{-9}
^{241}Am	5.85×10^{-7}	0.82	4.8×10^{-7}
^{129}I	unlimited	0.77	unlimited
^{229}Th	4.00×10^{-3}	2.19×10^{-4}	assumed unlimited

[a] from Clayton et al. (2011, Table 3.1-4)

[b] calculated from 30 yr OoR, 60 GWd/MTHM inventory in Carter et al. (2013, Table C-1)

4.1.4.3 Sorption

Radionuclides can be sorbed onto engineered and natural surfaces. Many different models for the complex surface chemistry reactions included in sorption have been developed with varying levels of sophistication. The salt reference case assumes the simplest model: linear sorption characterized by the distribution coefficient K_d. The salt reference case uses K_d values for radionuclude sorption in anhydrite interbeds of a bedded salt formation (Table 4-8; Clayton et al. 2011), and applies these values to the entire model domain. Though uncertainty distributions are given for multiple radionuclides, at this time, probabilistic simulations sample on K_d^I and K_d^{Np} only.

Table 4-8. K_d values for the salt reference case.

Element	Uncertainty Distribution (ml/g)	Deterministic Value (ml/g)[1]
U	Uniform Min: 0.2; Max: 1.0	0.6
Np	Uniform Min: 1.0; Max: 10.0	5.5
Am	Uniform Min: 25; Max: 100	62.5
I	Uniform Min: 9.28×10^{-7}; Max: 7.84×10^{-3}	0.0
Th	Uniform Min: 100; Max: 1000	550.0

[1] from Clayton et al. (2011, Table 3.1-7) except for iodine.

4.1.4.4 Temperature

Temperature in the repository depends on the background geothermal gradient (Section 4.1.5.1) and on the heat pulse generated by radioactive decay of the waste. Though diffusion, solubility, and sorption are all expected to be temperature-dependent, at this time they are not modeled as such.

4.1.5 Developing the Salt Reference Case Models

4.1.5.1 Conceptual Model

The salt reference case conceptual model includes all of the components and processes described in Sections 4.1.1 through 4.1.4. It imagines a regional setting with no topographic relief, horizontal bedding, a geothermal gradient of ~8°C/km (as measured near the WIPP; Mansure and Reiter 1977), and a regional head gradient west to east of -0.0013 (m/m), similar to the gradient observed in the Culebra dolomite near the WIPP site (Hart et al. 2009). The stratigraphic section is described in Section 4.1.2. The repository is

placed in the middle of the halite layer, 680 m below the surface, and 5 kilometers from a hypothetical withdrawal well, at which location radionuclide concentrations are monitored in the overlying aquifer.

Only the undisturbed scenario is considered. At repository closure (the start of the numerical simulation), the repository is assumed to be saturated with formation porewater and waste packages are assumed to have failed, resulting in an initial radionuclide concentration within each waste package calculated on the basis of initial radionuclide inventory (Section 4.1.1), initial release fraction (Section 4.1.3.1), and saturated porosity of the waste package (Table 4-3). Additional radionuclides are released as the waste form degrades (Section 4.1.3.1). Each waste package is conceptualized as a transient heat source. Energy output decreases with time and can be calculated at any time from the values in Figure 4-2 and the inventory of heavy metal in the waste package (Table 4-5). Processes include advective and conductive heat transport, advective, diffusive, and dispersive solute transport, waste form degradation, precipitation and dissolution according to radionuclide solubility limits, sorption, and radioactive decay and ingrowth (in the aqueous phase).

4.1.5.2 Numerical Implementation

Numerical simulations of fluid flow and reactive transport for the salt reference case were performed using PFLOTRAN and 3D, structured grids with variable spacing. A set of grids similar to the single-drift pair grid used to model past iterations of the salt reference case (Freeze et al. 2013b; Sevougian et al. 2013; 2014) was used to assess the effect of grid spacing on numerical dispersion (Section 4.1.6.1). For the first time, a larger grid was used to simulate a multi-drift pair repository. Deterministic and probabilistic simulations of the multi-drift repository were run isothermally (without a heat source, in PFLOTRAN Richards mode) and thermally (with a repository heat source and a regional temperature gradient, in PFLOTRAN general mode) (Section 4.1.6.2). In all simulations, regional fluid flow due to an east-west pressure gradient was established with boundary conditions.

4.1.5.3 Model Domain

Single-drift pair: The single-drift pair model domain (shaded region in Figure 4-3) used to assess the effect of grid spacing on numerical dispersion is identical to that used in previous iterations of the salt reference case (Freeze et al. 2013b; Sevougian et al. 2013; 2014); it is 12,642 m in length (x), 20 m in width (y), and 945 m in height (z). In the y direction, this domain includes a single drift (widthwise) and a shaft sandwiched between half-widths of EDZ halite pillars. With reflection boundary conditions applied at the front and back of the model domain (y = 0 and 20 m), this domain corresponds to an infinite number of drift pairs each with its own shaft.

Multi-drift pair: The multi-drift pair model domain (shaded region in Figure 4-4) is the same in length (x) and height (z) as the single-drift pair domain, and is 5100 m in width (y). The additional width accommodates 5 drift pairs at the front of the model domain and 5000 m of undisturbed host rock extending to the back of the model domain. With a reflection boundary condition applied at the front of the domain, this domain simulates a repository of 10 drift pairs. Figure 4-5 shows an x-z slice through the repository at the y-midpoint of the first drift. Figure 4-6 shows an x-y slice at the z-midpoint of the repository.

4.1.5.4 Grid Spacing

In both model domains, grid spacing is finest in the repository, where it is on the order of 1 m and dependent upon the dimensions of the various EBS components and the DRZ. Each waste package is a single grid cell, 5 by 1.29 by 1.014 m (resulting in a volume equal to that of the cylindrical waste package described in Section 4.1.3.2).

Single-drift pair domain (grid refinement exercise): Grid spacing increases in the x direction with distance from the repository. It decreases in the x direction as the east withdrawal boundary is approached, providing a precise location at which to monitor radionuclide concentrations, and then increases to the end of the model domain. Grid spacing varies in the z direction in order to accommodate the repository, DRZ, interbeds, and aquifers. Grid spacing in the y direction is entirely dependent upon near field dimensions. Five single-drift pair grids were generated for the grid refinement study. Exact cell counts for each grid are listed in Section 4.1.6.1 in Table 4-9.

Multi-drift pair domain: Grid spacing is similar to that in the single-drift pair domain, except that it increases in the y direction with distance from the repository. One multi-drift pair grid was generated with a cell count of 387 in x, 39 in y, 71 in z, and 1,071,603 cells in the entire model domain.

4.1.5.5 Initial Conditions

Isothermal simulations: Initial conditions specified are fluid pressure and radionuclide concentrations. Initial pressure throughout the model domain produces a hydrostatic gradient in the vertical direction and a head gradient of -0.0013 (m/m) from west (left) to east (right). Simulations track 5 radionuclides: ^{241}Am, ^{237}Np, ^{233}U, ^{229}Th, and ^{129}I. Initial radionuclide concentrations in all cells except the waste package cells are 10^{-20} mol/L, an approximation of 0 mol/L on a log basis. In the waste package cells, initial concentrations of ^{241}Am, ^{237}Np, ^{233}U, and ^{229}Th are set to 10^{-20} mol/L and initial concentrations of ^{129}I are 7.27×10^{-4} mol/L to account for the instant release of ^{129}I from the waste form.

Thermal simulations: In addition to initial fluid pressure and radionuclide concentrations, initial temperature is specified. Initial pressure and temperature are consistent with a head gradient of -0.0013 (m/m) from west (left) to east (right), and a geothermal gradient of ~8°C/km, achieved by applying a constant temperature of 20°C at the top of the model domain and constant temperature of 28°C at the base of the model domain. Initial radionuclide concentrations are identical to those in the isothermal simulations.

4.1.5.6 Boundary Conditions

Isothermal simulations: Boundary conditions must be set for the six faces of the model domain. The following applies to both single-drift pair and multi-drift pair isothermal simulations. The west (left) and east (right) are held at initial pressures in order to maintain the west to east head gradient throughout the simulation time. Radionuclide concentrations at these faces are held such that any fluid entering the model domain contains 10^{-20} mol/L of each radionuclide, while fluid exiting the model domain is allowed to carry with it ambient concentrations. Diffusive flux is disallowed at the outlet boundary by specifying a zero concentration gradient. Top, bottom, front, and back faces of the domain are no-flow boundaries (pressure and concentration gradients of zero). No-flow boundaries at the front and back of the single-drift pair model domain create reflection planes and result in effectively simulating an infinite number of drift pairs. The no-flow boundary at the front of the multi-drift model domain similarly creates a reflection plane (doubling the size of the repository to 10 drift pairs), but does not have the same effect at the back of the model domain, because the domain is large enough that radionuclide transport does not reach the back of the domain.

Thermal simulations: Boundary conditions for the six faces of the model domain are set as follows: The west (left), east (right), top, and bottom faces are held at initial pressures and temperatures. The front and back faces are no-flow boundaries (neither fluid nor heat). As in the isothermal case, where fluid enters the model domain, it enters with all radionuclide concentrations set to 10^{-20} mol/L, and where it exits the model domain, it exits carrying ambient concentrations. For the present work, thermal simulations were run in the multi-drift pair domain only; see Freeze et al. (2013b) and Sevougian et al. (2013; 2014) for a complete discussion of previous single-drift pair simulations (thermal and isothermal).

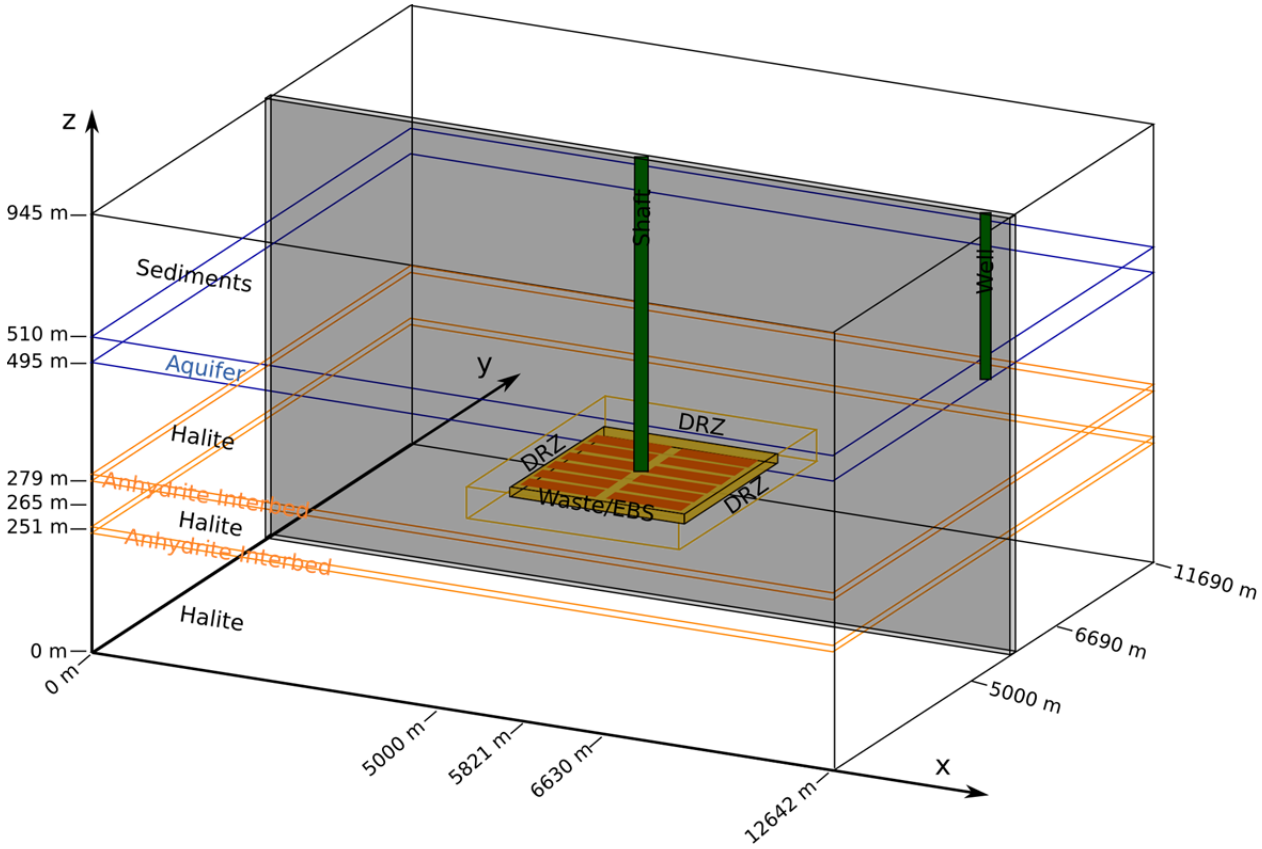

Figure 4-3. Salt reference case conceptual model. Shaded area corresponds to the single-drift pair domain.

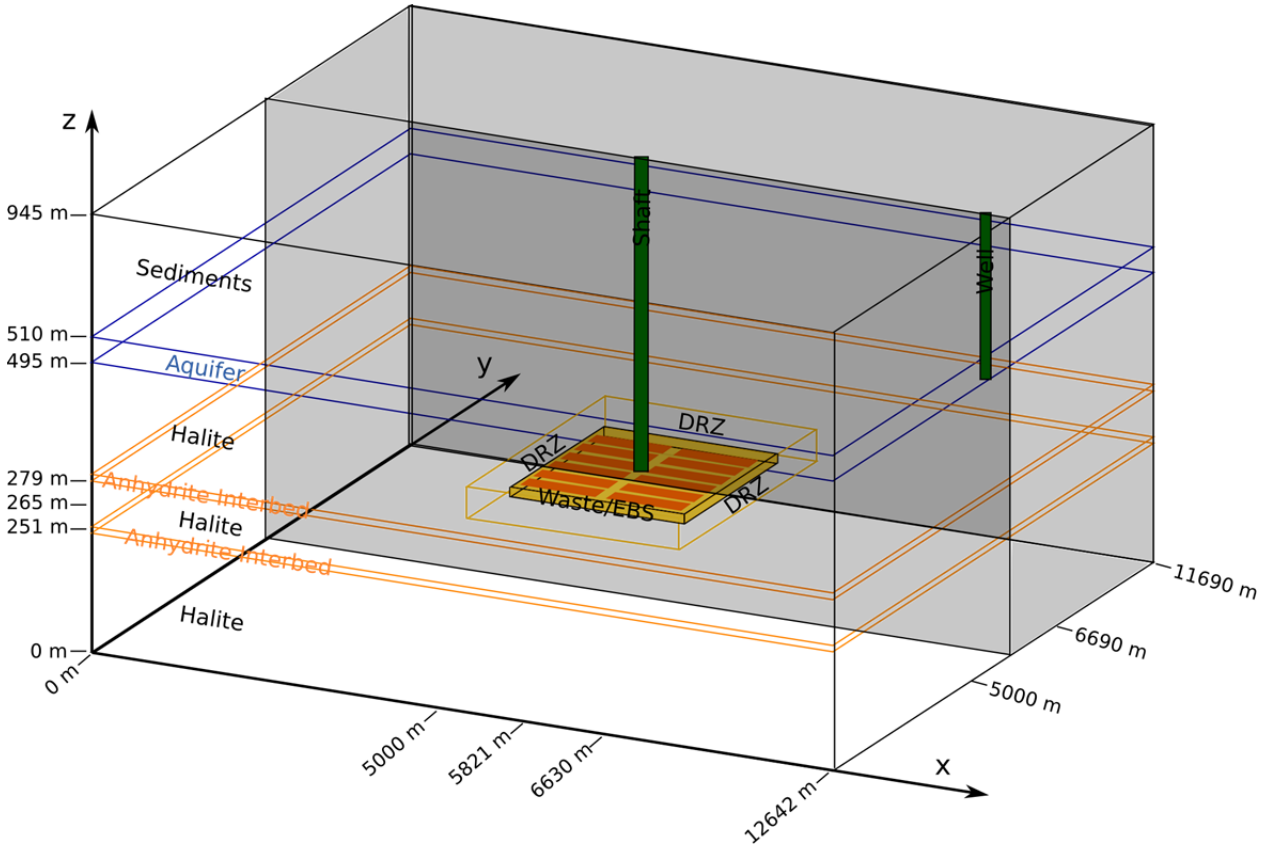

Figure 4-4. Salt reference case conceptual model. Shaded area corresponds to multi-drift pair domain.

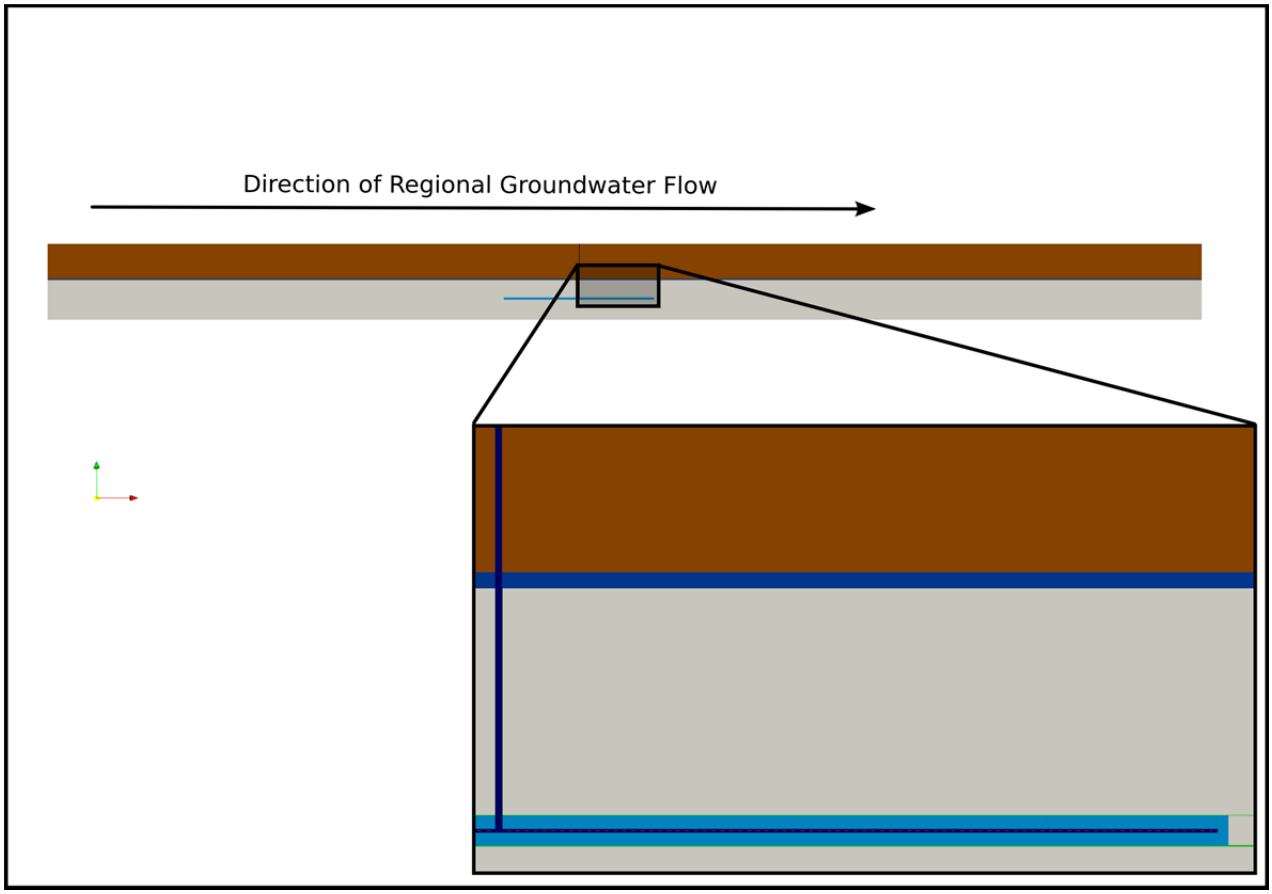

Figure 4-5. X-Z slice of reference case model at the Y midpoint of the first drift pair in the repository. Halite is shown in grey, dark brown is sediments, aquifer is shown in royal blue, light blue is the DRZ, the anhydrite beds are shown in green and backfill is shown in dark blue.

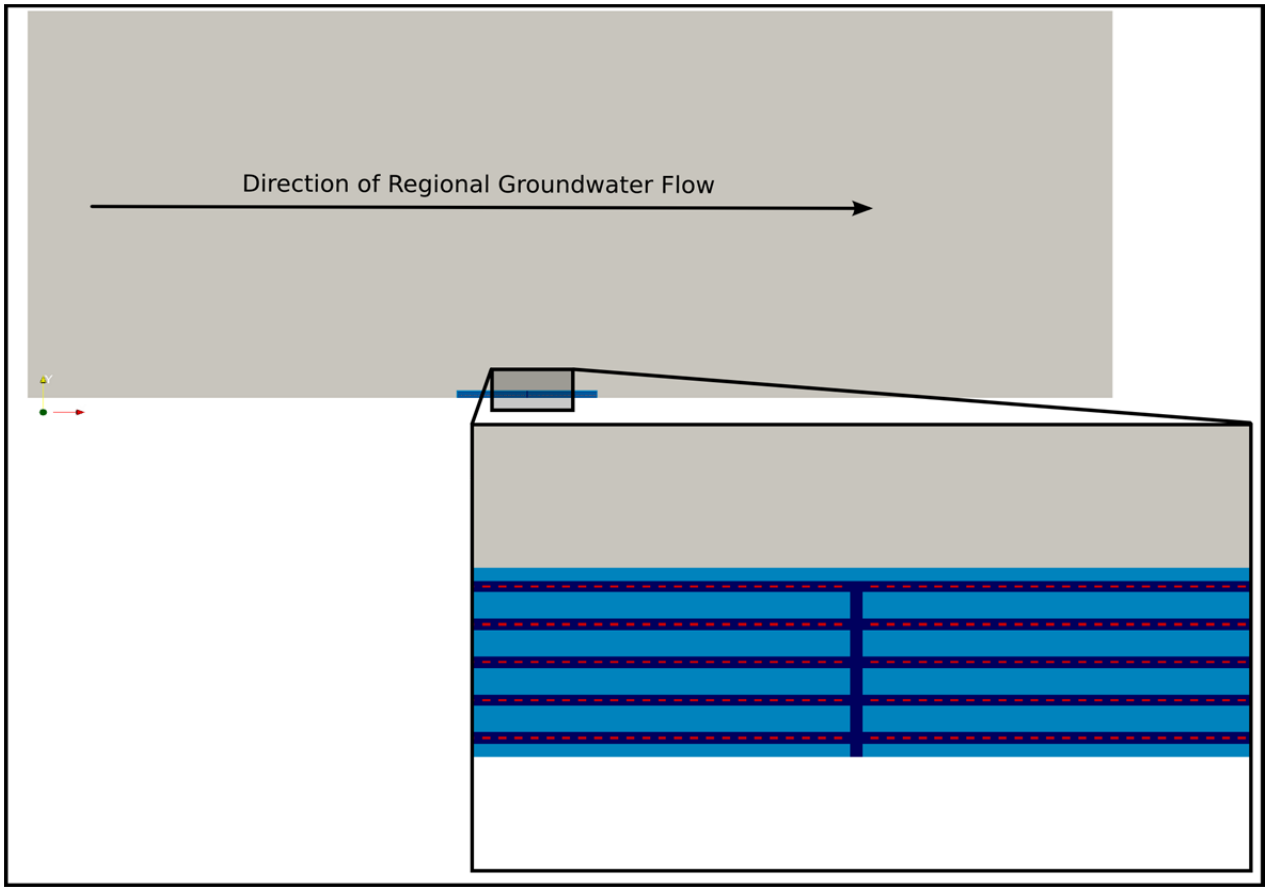

Figure 4-6. X-Y slice of the for the salt reference case model. Halite is grey, DRZ is light blue, backfill is dark blue and waste packages are shown in red.

4.1.5.7 Waste Package Source Terms

Heat source: Each waste package is modeled as a transient heat source. The energy (watts per waste package) entering the model domain is updated periodically according to values in a lookup table. The initial value is that for PWR UNF 50 yr OoR (calculated from the total decay heat at 50 years plotted in Figure 4-2). Time steps are synced with lookup table times, and between specified times, the energy input is linearly interpolated.

Radionuclide source: The degrading waste form is modeled as a far-from-equilibrium mineral, dissolving according to a zero-order rate law as an approximation of the fractional degradation rate given in Section 4.1.3.1. Each waste package cell is assigned an initial volume fraction of waste-form mineral of 0.105 (Freeze et al. 2013b), which amounts to 0.69 m^3. The waste-form mineral has a dissolution rate constant of 4.8×10^{-8} $mol/m^2/s$ and an assumed specific surface area of 9.5 m^2/m^3. Using a molar volume of 9.1 cm^3/mol (based on $UO_2(s)$), and the mineral volume fraction of 0.105 from above, this degradation rate will completely dissolve the waste form mineral in 7,600 years. This decay time is in the range of the distributions in Table 4-4.

4.1.5.8 Solubility Limits

Radionuclide solubility limits currently are set by defining fictitious solid phases (one for each solubility-controlled radionuclide) with conditional solubilities (in terms of total aqueous concentration) equal to those in Table 4-7. The defined solid phases are assumed to precipitate and dissolve at rates fast enough to maintain equilibrium between the solid and aqueous phases. An improved model for calculating the effects of element solubility on radionuclide concentrations based on changing isotopic distributions is in development (Section 3.2.5).

4.1.6 Salt Reference Case Results

Included below are results of a grid refinement study (single-drift pair domain, isothermal deterministic simulations), and for the first time model predictions from multi-drift pair simulations (isothermal and thermal, deterministic and probabilistic). Results are discussed in terms of ^{129}I concentration because its long half-life, unlimited solubility, and lack of sorption result in nearly conservative behavior. After comparing multi-drift pair thermal and isothermal results, we briefly compare multi-drift pair results to previously reported (Sevougian et al. 2014) single-drift pair results. These comparisons indicate that employing mechanistic modeling and accurately representing the repository system will be important to accurate performance assessment of future repositories. The current models are limited by their generic nature, and should not be interpreted in terms of repository performance in a bedded salt formation, but as we continue to add and refine modeling capabilities, generic modeling efforts and associated sensitivity studies will contribute to prioritization of experimental efforts and site-specific data acquisition, optimization of repository layout and design, and improvement of modeling techniques themselves including balancing mechanistic and reduced-order modeling approaches for best effect.

4.1.6.1 Single-Drift Pair Domain (Grid Refinement)

The grid refinement exercise compared ^{129}I breakthrough curves at the well observation location, a point in the aquifer overlying the bedded halite at a distance of 5 kilometers from the repository. Breakthrough curves (Figure 7) were compared among 5 single-drift pair grids (Table 4-9): a grid whose x and z discretization correspond to the that in the multi-drift pair grid; a grid with modest refinement in the x, y, and z directions; a grid in which the number of cells in the x direction was approximately double that in the multi-drift pair grid; a grid in which the number of cells in the z direction was nearly double that in the multi-drift pair grid; and a grid in which the number of cells in both the x and z directions was doubled. In all simulations, the initial background concentration of ^{129}I was set to 10^{-20} mol/L (an approximation of 0 mol/L on a log scale), and ^{129}I reaches the well observation location on the order of 10^4 years. The grid with the finest discretization increased the first arrival time of ^{129}I (the first time at which $[^{129}I] > 10^{-20}$ mol/L) by approximately 50% relative to the coarsest grid.

Table 4-9. Number of cells in grid and time of ^{129}I first arrival.

Simulation	Cells in x	Cells in y	Cells in z	Total cells	^{129}I first arrival time (yr)
Original	387	5	71	137385	13812
Modest refinement	414	9	87	324162	15500
Double X	839	9	87	656937	17000
Double Z	414	9	147	547722	18000
Double X and Z	839	9	147	1109997	21000

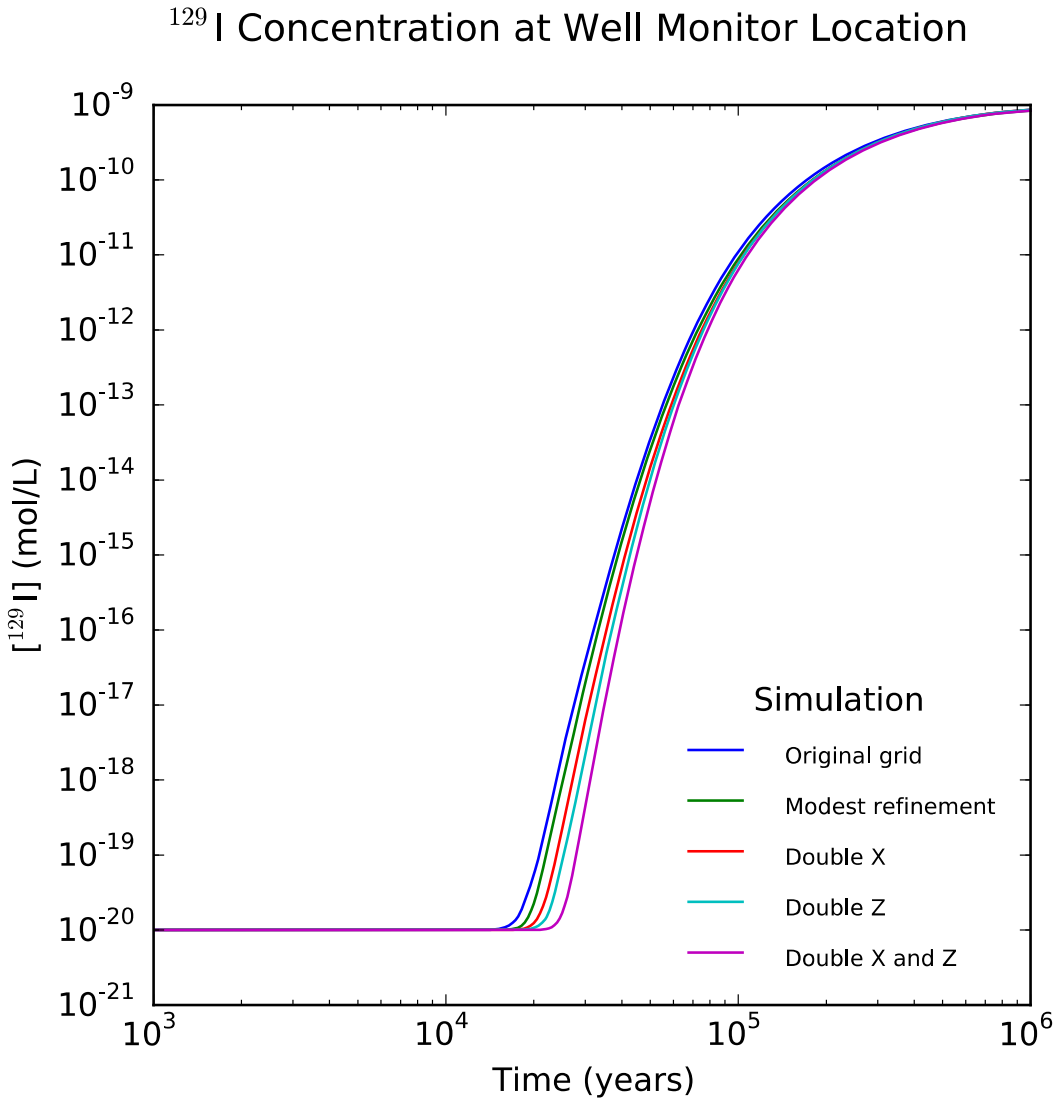

Figure 4-7. ^{129}I concentration as a function of time at the well observation location (^{129}I breakthrough curves).

4.1.6.2 Multi-Drift Pair Domain

Deterministic Isothermal Results

Concentrations of ^{129}I at various times in the multi-drift pair deterministic isothermal simulation are shown in Figure 4-8 through Figure 4-13. Initially (Figure 4-8), ^{129}I is confined to the waste packages. At 1000 years (Figure 4-9), ^{129}I has begun to exit the repository via two means: diffusion up the relatively high-porosity shaft and advection in the relatively high-permeability anhydrite interbeds. By 30,000 years (Figure 4-11), ^{129}I has diffused into the aquifer, where advective transport due to regional flow creates a low-concentration plume. Over time, the plume spreads laterally and vertically due to diffusion. By 100,000 years (Figure 4-12), ^{129}I has diffused into the overlying sediments above the aquifer (and to a lesser extent downward into the low-porosity halite). By 10^6 years the ^{129}I plume has spread to the top of the domain in the vertical direction as well as laterally in the y-direction away from the repository (Figure 4-13). It should be noted that for the purpose of discussion, very small concentrations of ^{129}I are contoured. At 10^6 years, the maximum concentration contour at the well observation location (x = 11,600

m) is 10^{-12} mol/L, approximately two orders of magnitude less than the limit set for ^{129}I in drinking water by the World Health Association (WHO 2011).

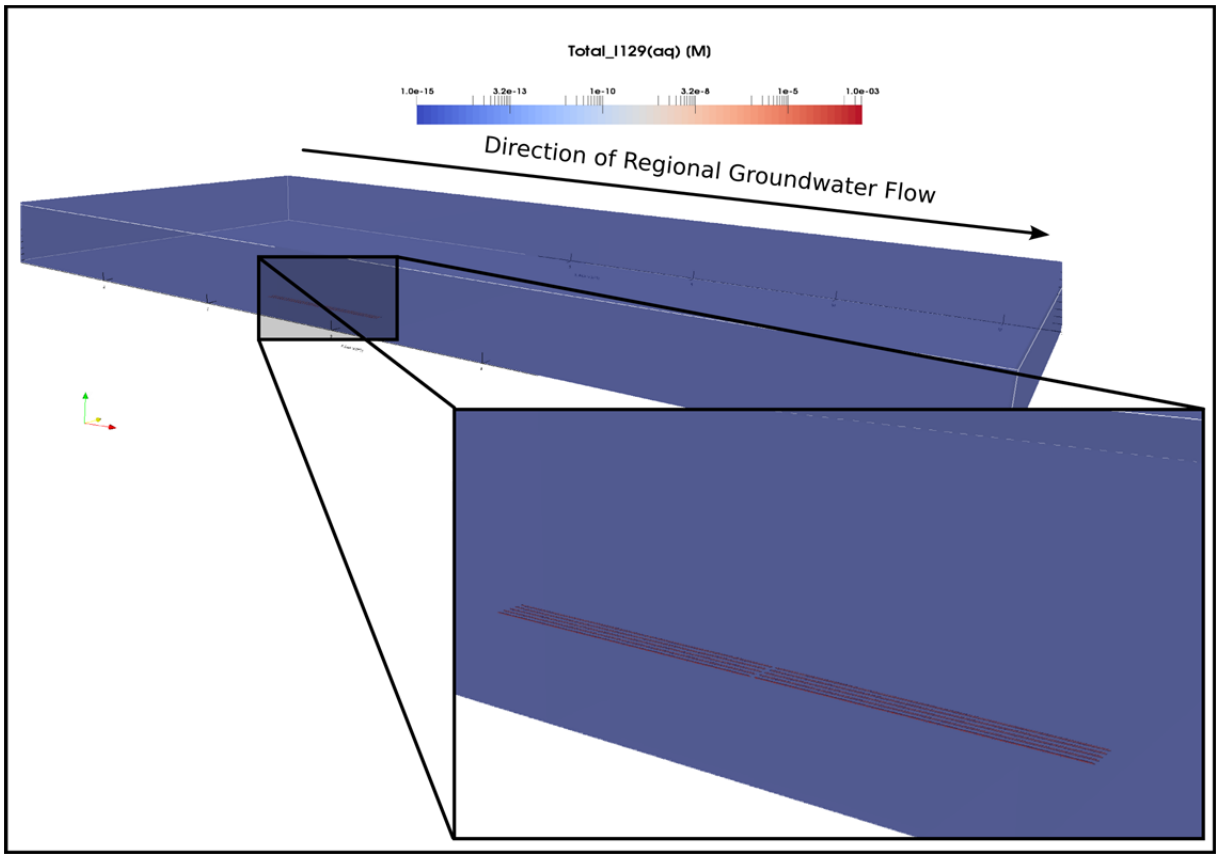

Figure 4-8. ^{129}I concentration contours for the salt deterministic isothermal simulation at 0 yr. Initially ^{129}I is confined to the waste packages, each of which is outlined by the ^{129}I concentration contour. Positive x-direction is to the right and the direction of regional groundwater is shown.

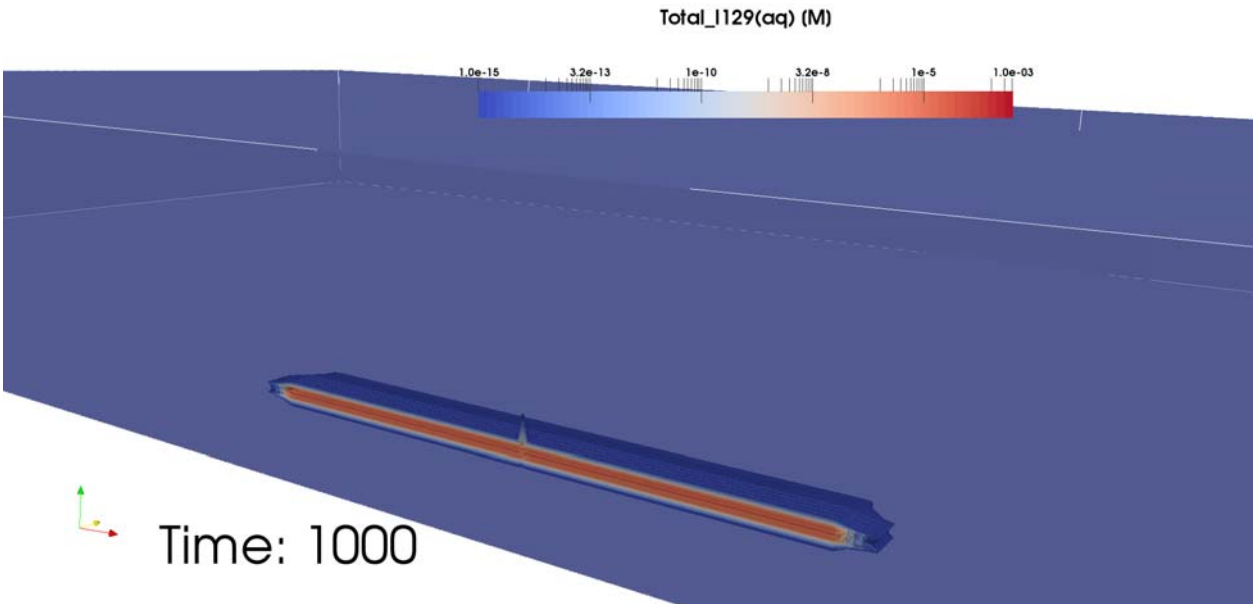

Figure 4-9. ^{129}I concentration contours for the salt deterministic isothermal simulation at 1000 yr. Preferential diffusion up the shaft and into the anhydrite interbeds can be seen.

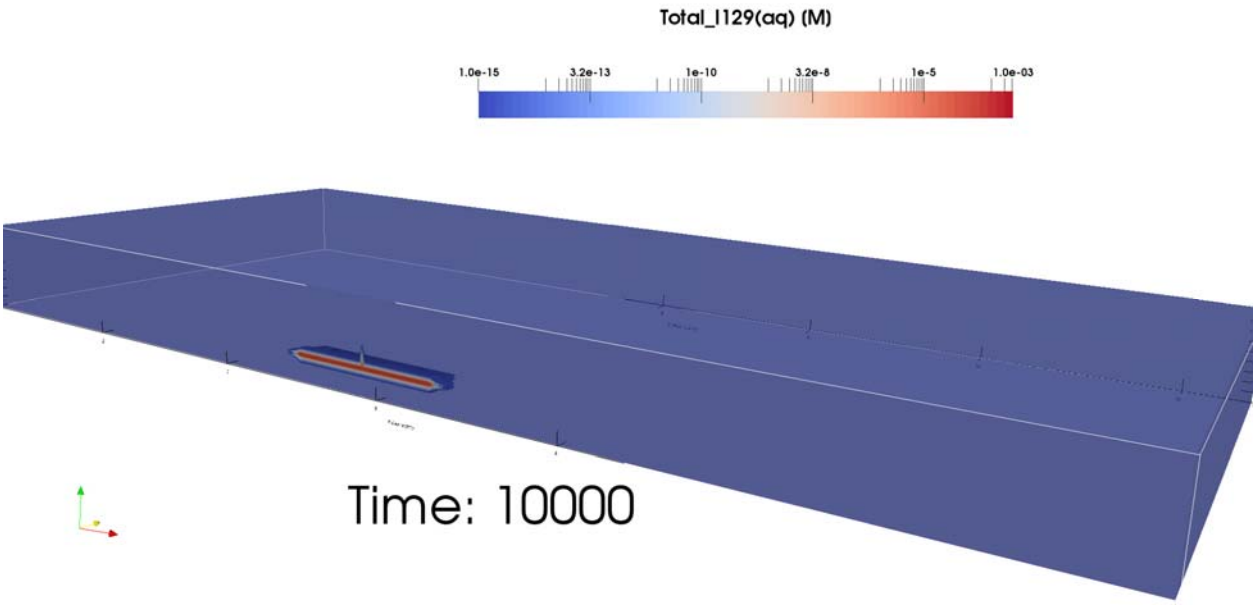

Figure 4-10. ^{129}I concentration contours for the salt deterministic isothermal simulation at 10,000 yr.

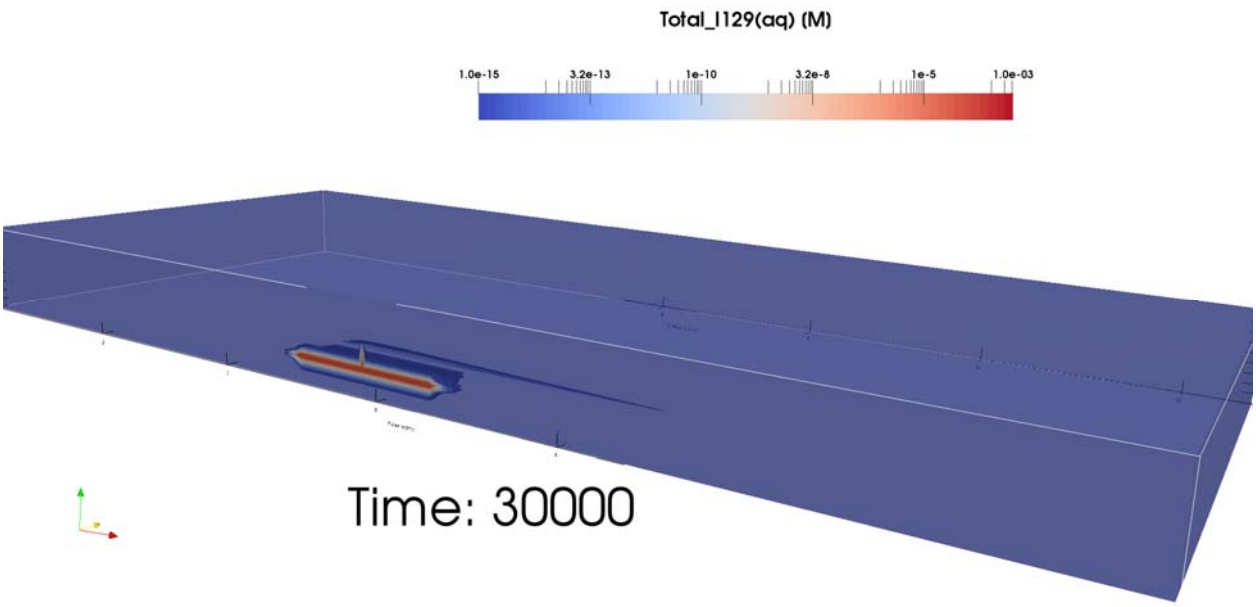

Figure 4-11. ^{129}I concentration contours for the salt deterministic isothermal simulation at 30,000 yr. ^{129}I has diffused up the shaft and into the aquifer. Advection in the aquifer begins.

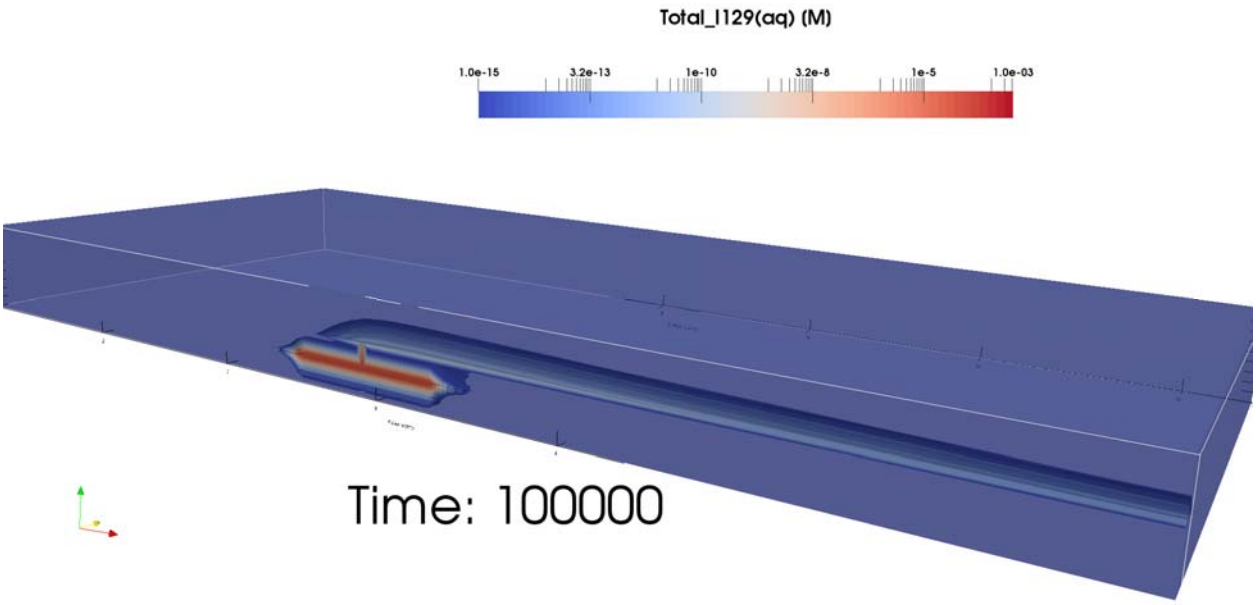

Figure 4-12. ^{129}I concentration contours for the salt deterministic isothermal simulation at 100,000 yr. Diffusion from aquifer into overlying sediments is occurring.

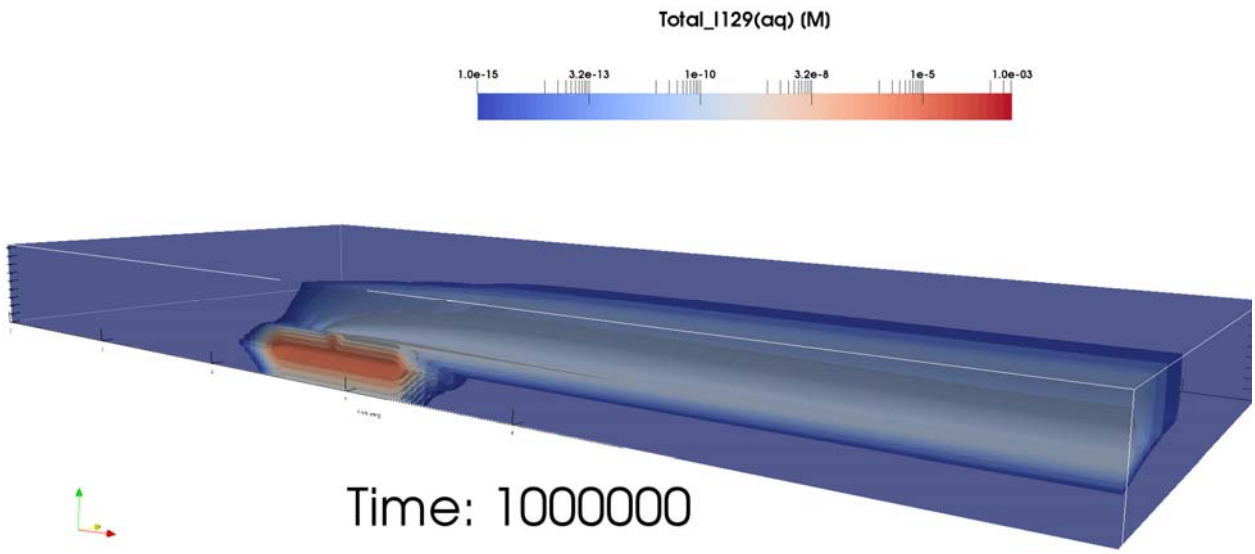

Figure 4-13. ^{129}I concentration contours for the salt deterministic isothermal simulation at 10^6 yr. Lateral diffusion (in the y direction) away from the repository is apparent.

Deterministic Thermal Results

Temperature and fluid flow fields at various times for the multi-drift pair deterministic thermal simulation are shown in Figure 4-14 through Figure 4-20. By 10 years (Figure 4-15), the rising temperatures in the repository are driving fluid flow out of the repository. Maximum temperatures are achieved around 100 years (Figure 4-16); the repository remains warmer than background at 1000 years (Figure 4-17), and fluid flow out of the repository is still occurring. By 10,000 years repository temperatures have returned to near background, and the thermal influence on the flow field is beginning to diminish (Figure 4-18).

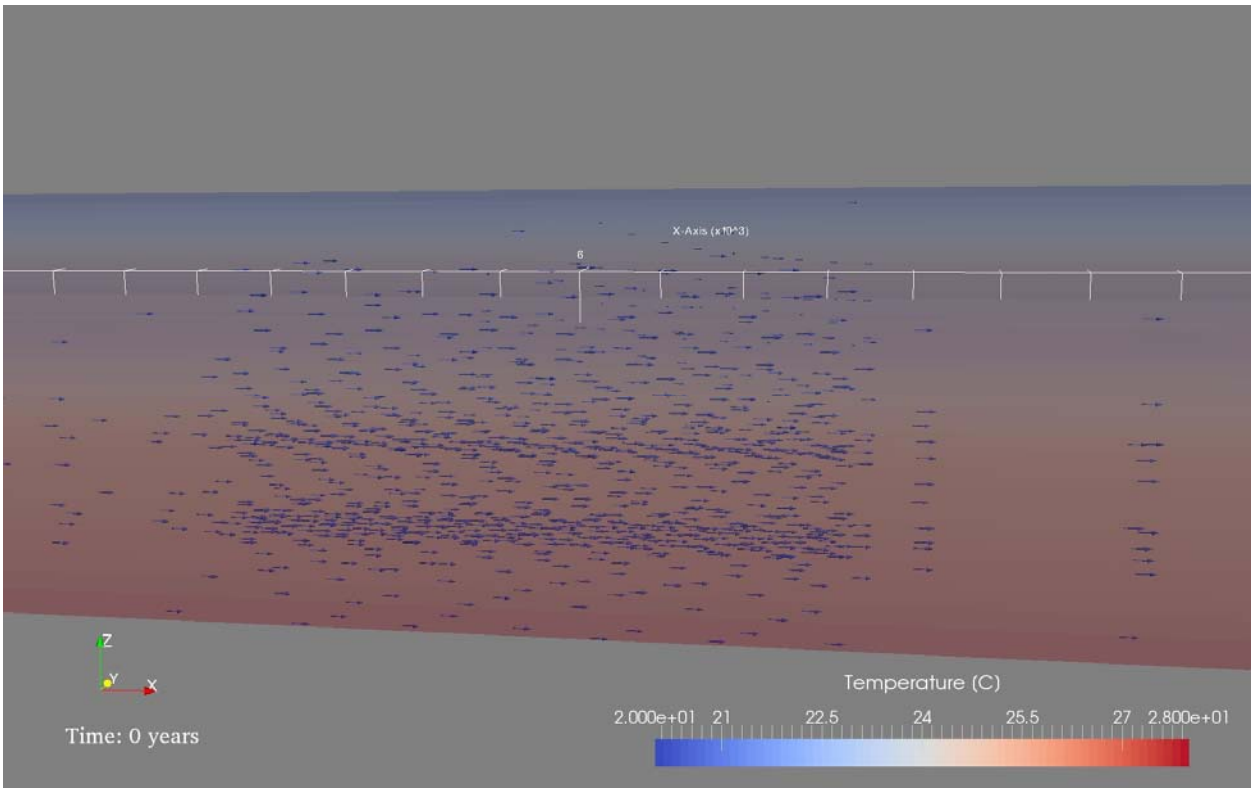

Figure 4-14. Background geothermal temperature gradient and regional flow field at 0 yr for the salt thermal deterministic simulation. The 3D model domain (truncated in the x direction) is transparent and colored by temperature. Blue arrows indicate the direction of the regional flow field established by applying a head gradient of -0.0013 m/m from west (left) to east (right). Notice that the maximum temperature on the color scale of 28°C in this figure is less than the maximum of 150°C in the figures that follow.

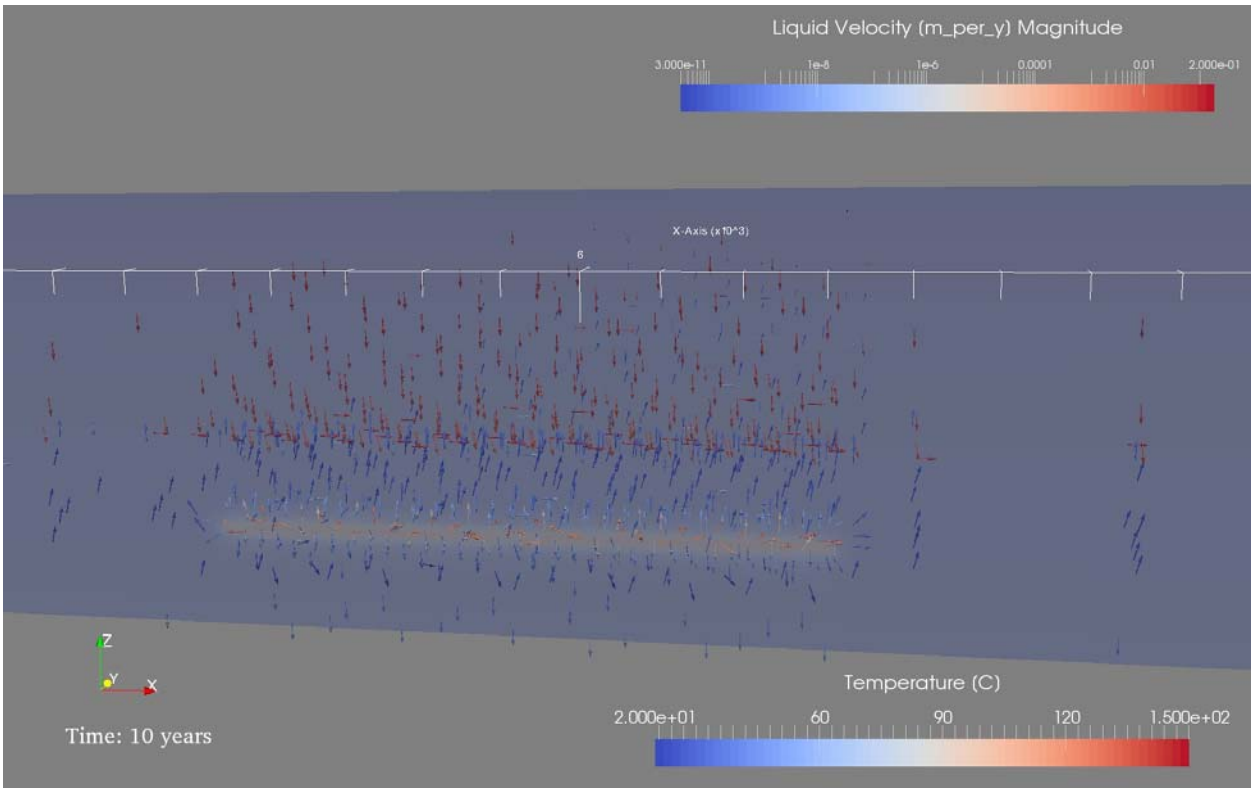

Figure 4-15. Near field temperature and fluid flow field for the salt deterministic thermal simulation at 10 yr. Fluid flow vectors are colored by flow velocity and the model domain is colored by temperature. The location of the repository can be seen by its elevated temperatures, which are high enough to drive fluid flow out of the repository.

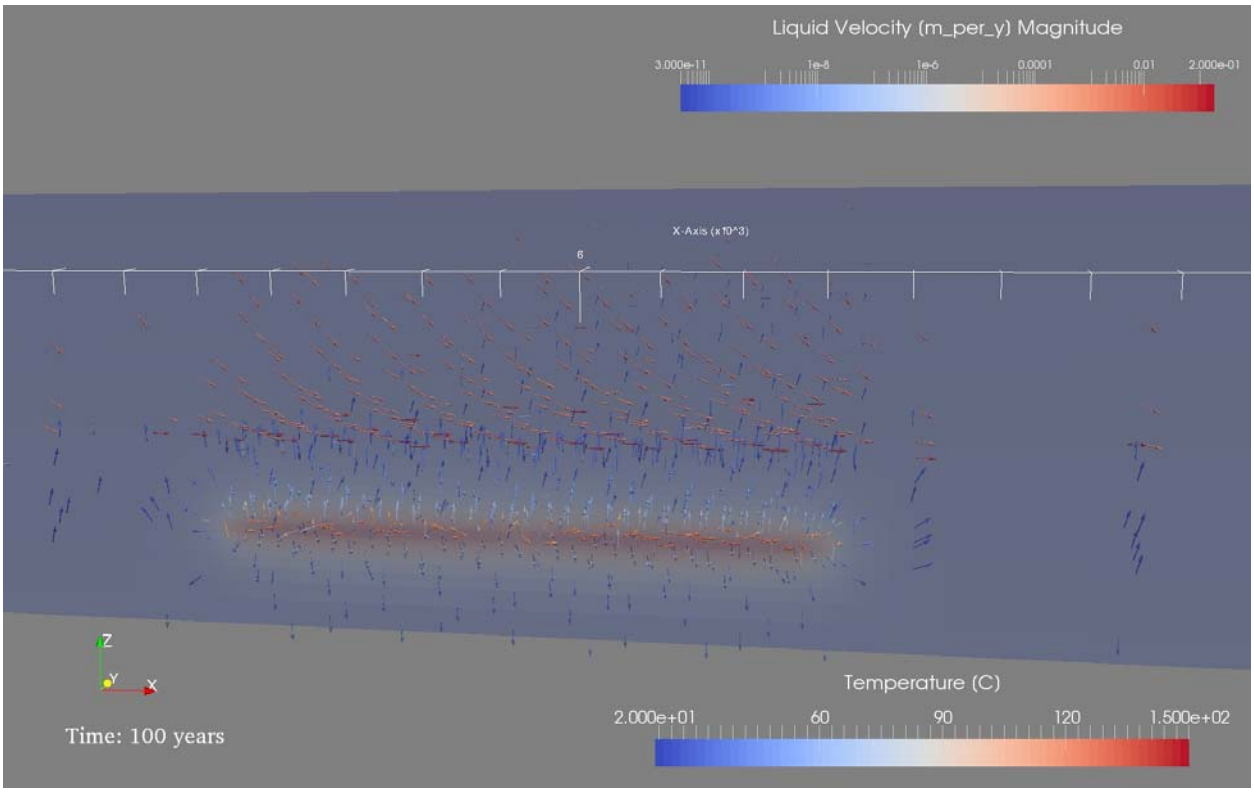

Figure 4-16. Near field temperature and fluid flow field for the salt deterministic thermal simulation at 100 yr. Fluid flow vectors are colored by flow velocity and the model domain is colored by temperature. Repository temperatures are peaking and the associated increase in fluid pressure drives fluid flow out of the repository.

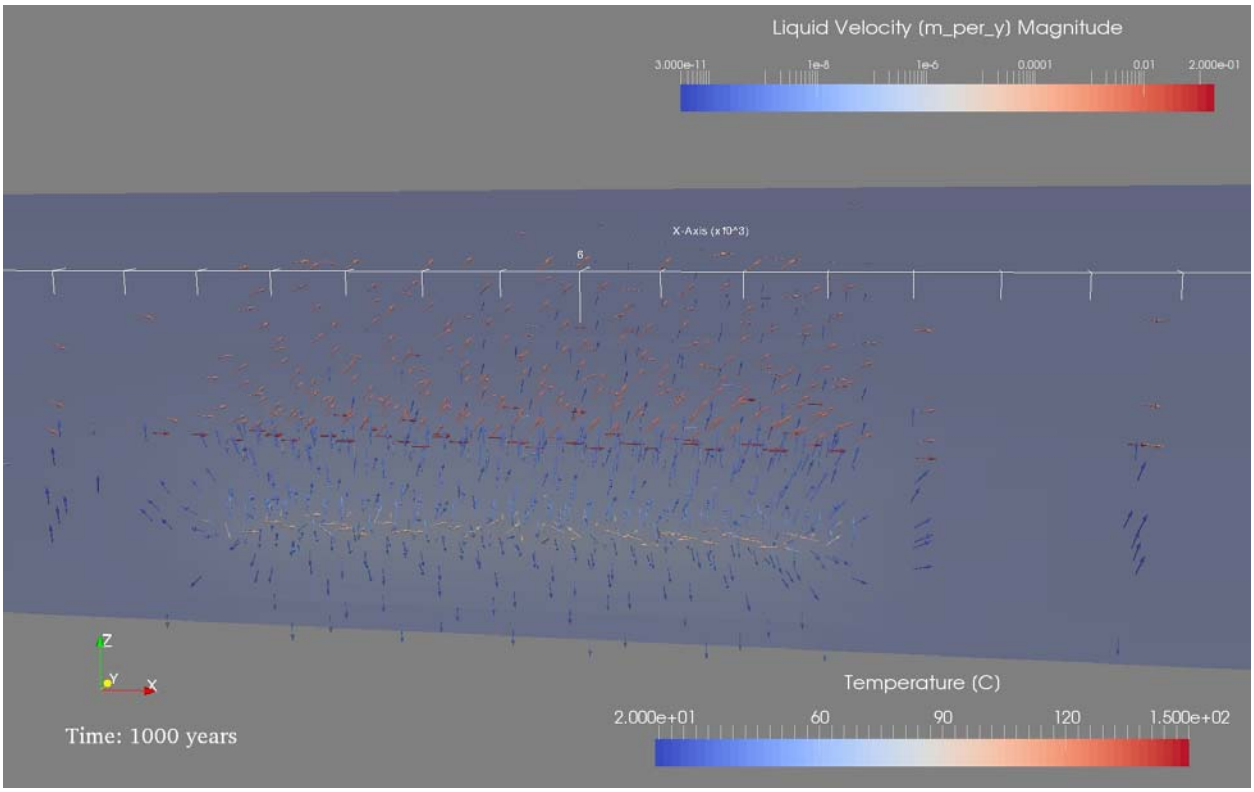

Figure 4-17. Near field temperature and fluid flow field for the salt deterministic thermal simulation at 1000 yr. Fluid flow vectors are colored by flow velocity and the model domain is colored by temperature. The repository is cooling, but fluid flow is still out of the repository.

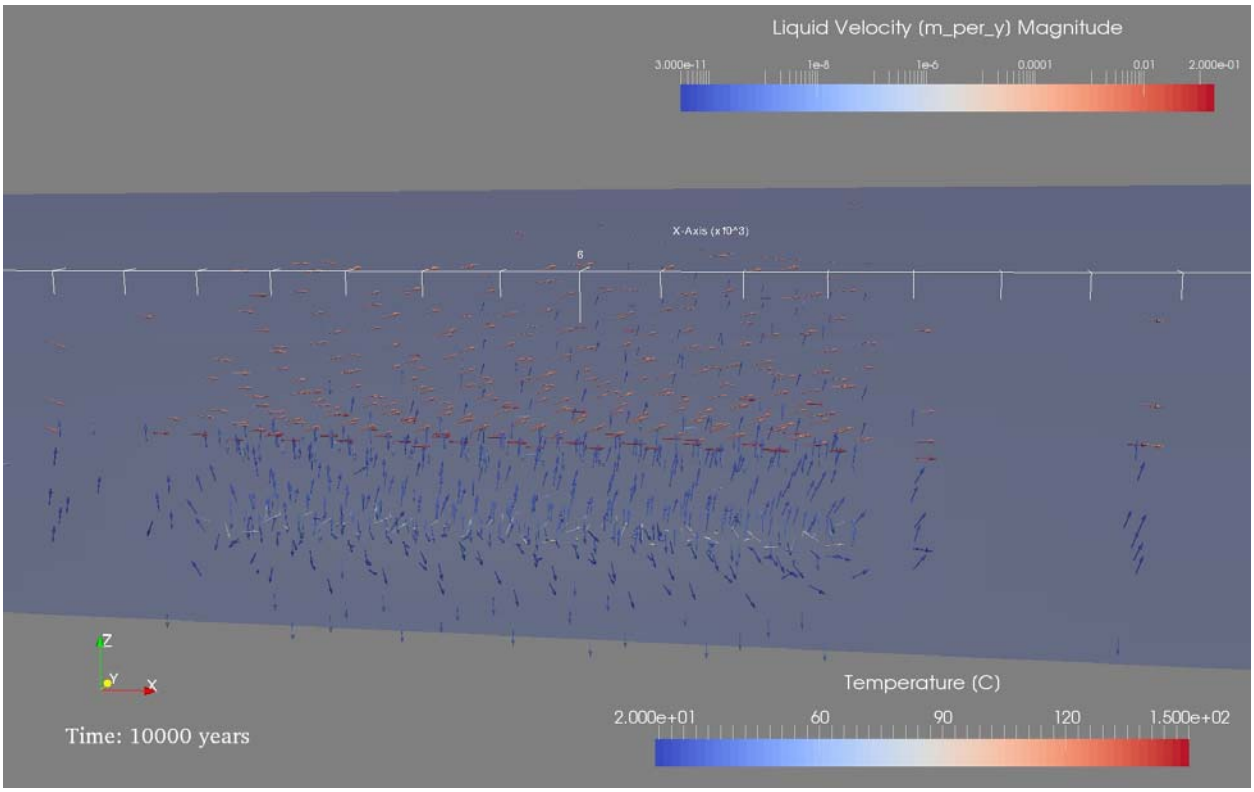

Figure 4-18. Near field temperature and fluid flow field for the salt deterministic thermal simulation at 10,000 yr. Fluid flow vectors are colored by flow velocity and the model domain is colored by temperature.

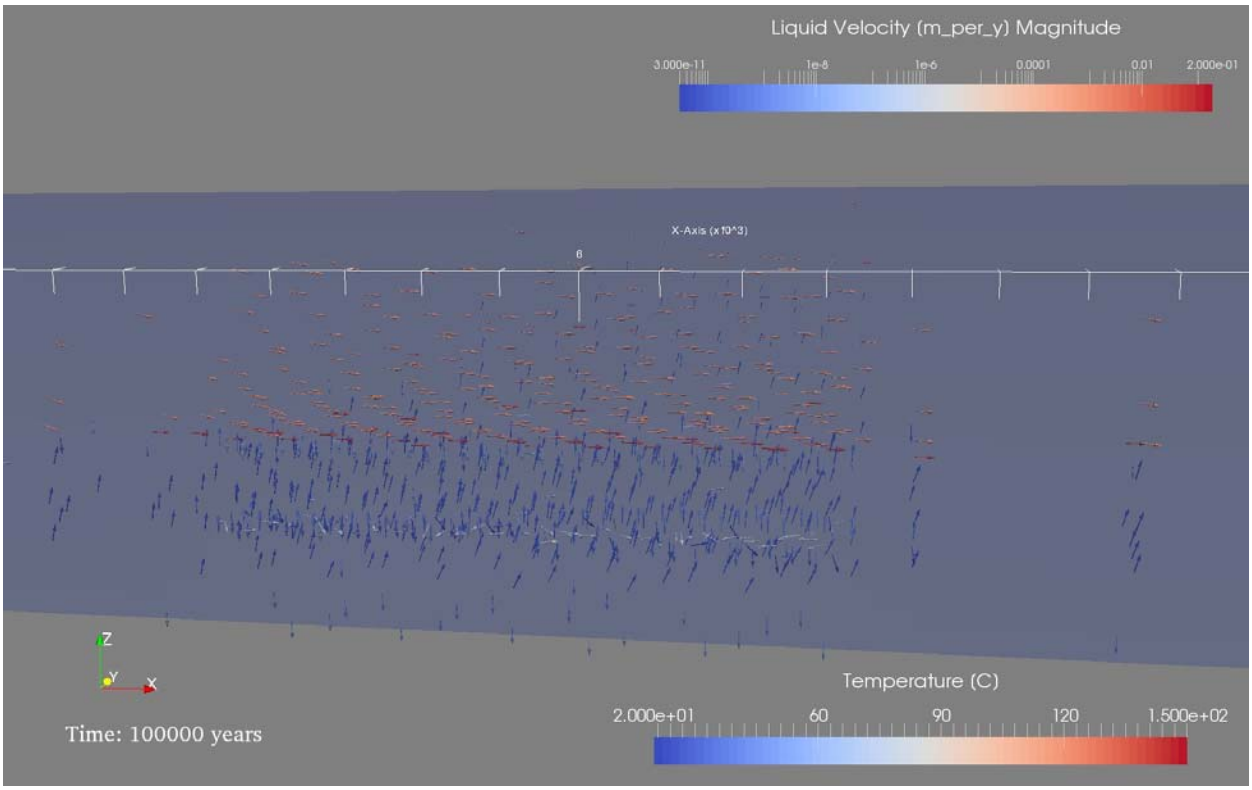

Figure 4-19. Near field temperature and fluid flow field for the salt deterministic thermal simulation at 100,000 yr. Fluid flow vectors are colored by flow velocity and the model domain is colored by temperature.

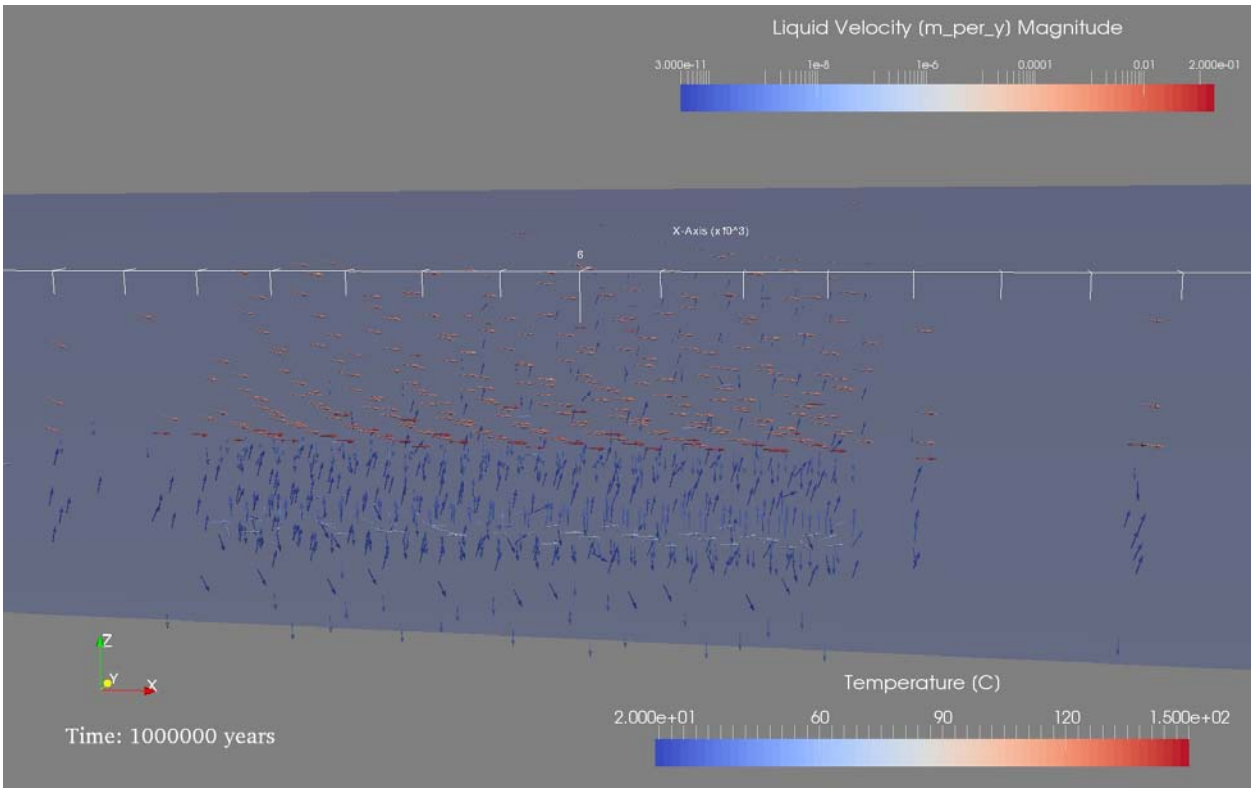

Figure 4-20. Near field temperature and fluid flow field for the salt deterministic thermal simulation at 10^6 yr. Fluid flow vectors are colored by flow velocity and the model domain is colored by temperature.

The spatial distribution of ^{129}I at times up to 10^6 years is shown in Figure 4-21 through Figure 4-24. By 1000 years (Figure 4-21), ^{129}I has diffused into the shaft and entered the anhydrite interbeds. At 30,000 years (Figure 4-22), ^{129}I at the level of 10^{-15} mol/L has reached the aquifer. By 10^6 years, the maximum ^{129}I concentration contour at the well observation location (x = 11,600 m) is 10^{-13} mol/L, one order of magnitude less than predicted in the same location by the isothermal simulation.

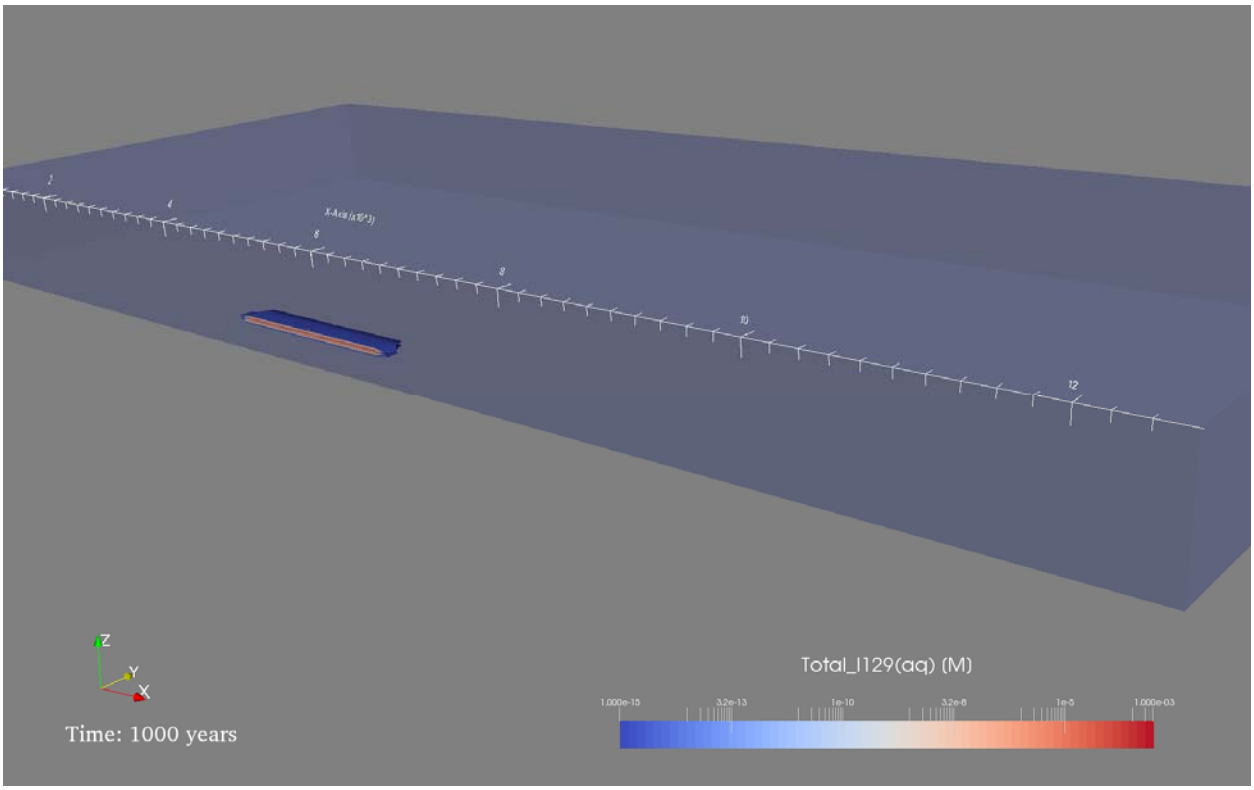

Figure 4-21. ^{129}I concentration for the salt deterministic thermal simulation at 1000 years. Contours of ^{129}I concentration and the 3D model domain are colored by ^{129}I concentration.

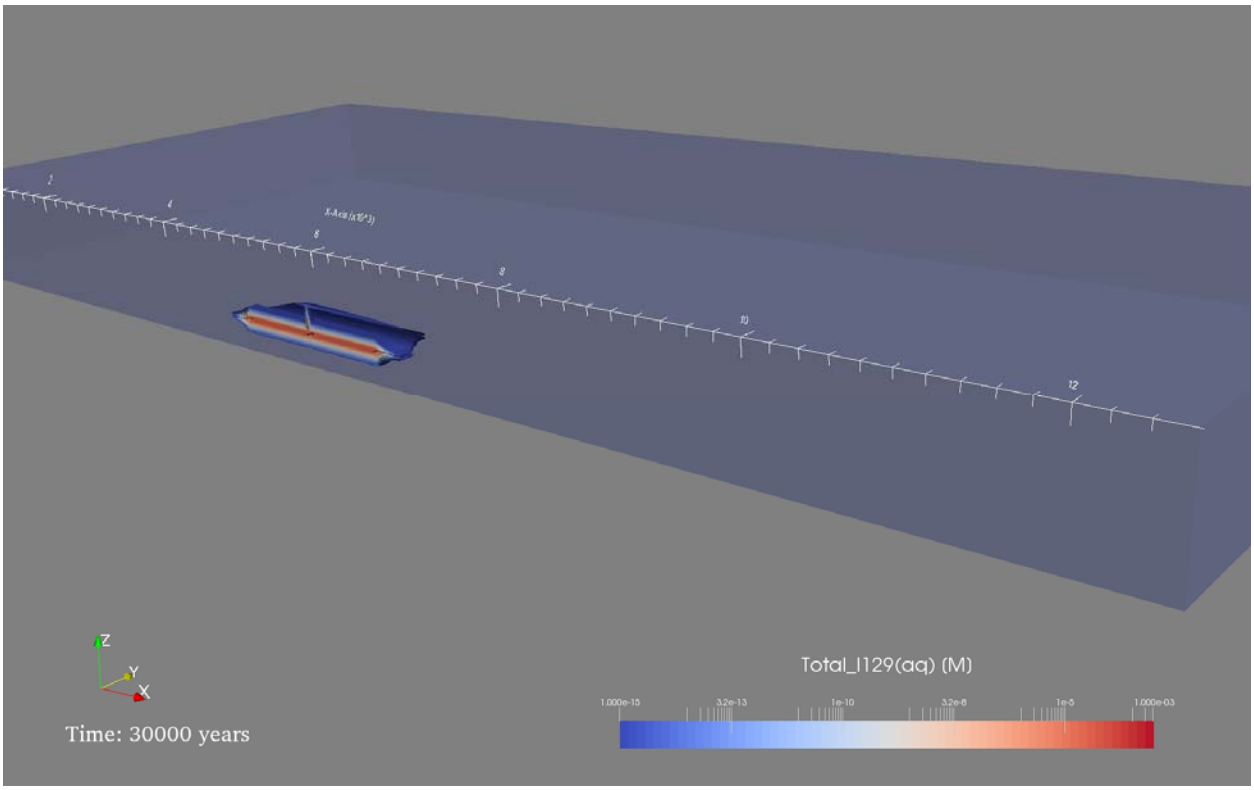

Figure 4-22. ^{129}I concentration for the salt deterministic thermal simulation at 30,000 years. Contours of ^{129}I concentration and the 3D model domain are colored by the ^{129}I concentration.

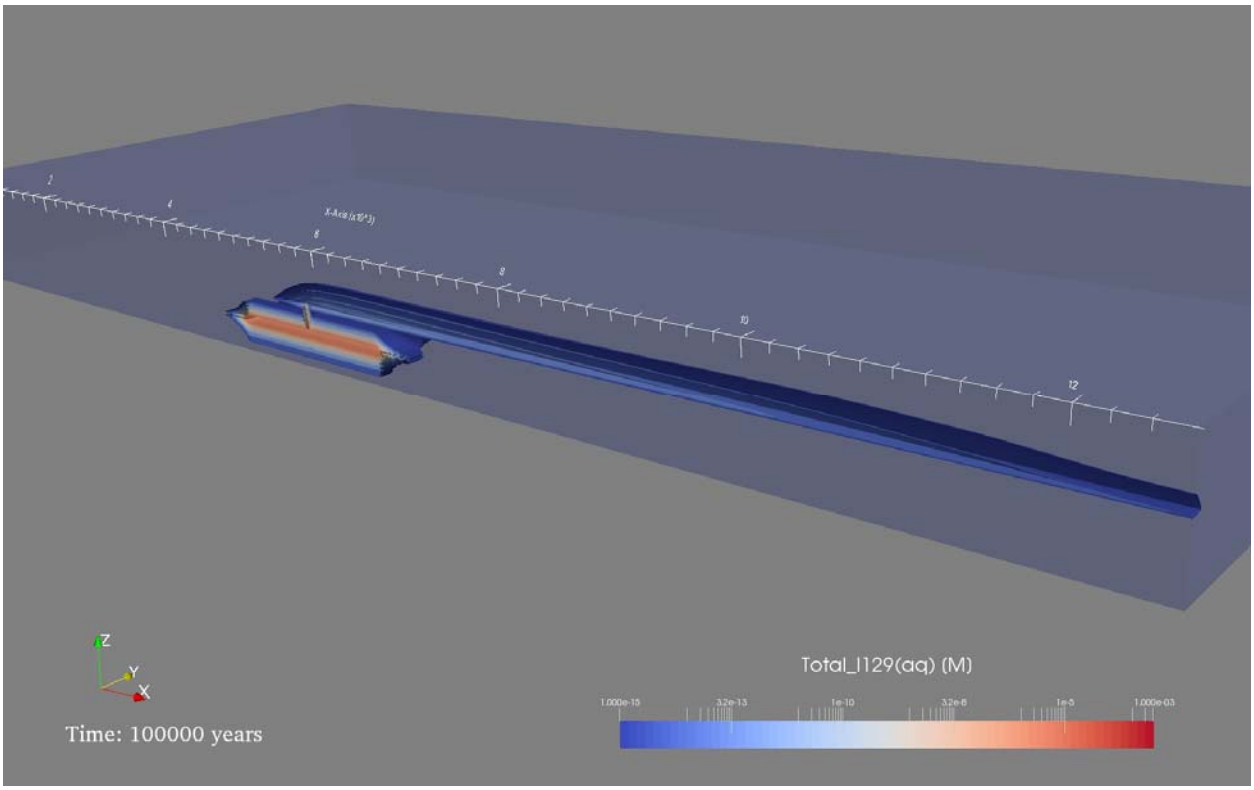

Figure 4-23. ^{129}I concentration for the salt deterministic thermal simulation at 100,000 years. Contours of ^{129}I concentration and the 3D model domain are colored by the ^{129}I concentration.

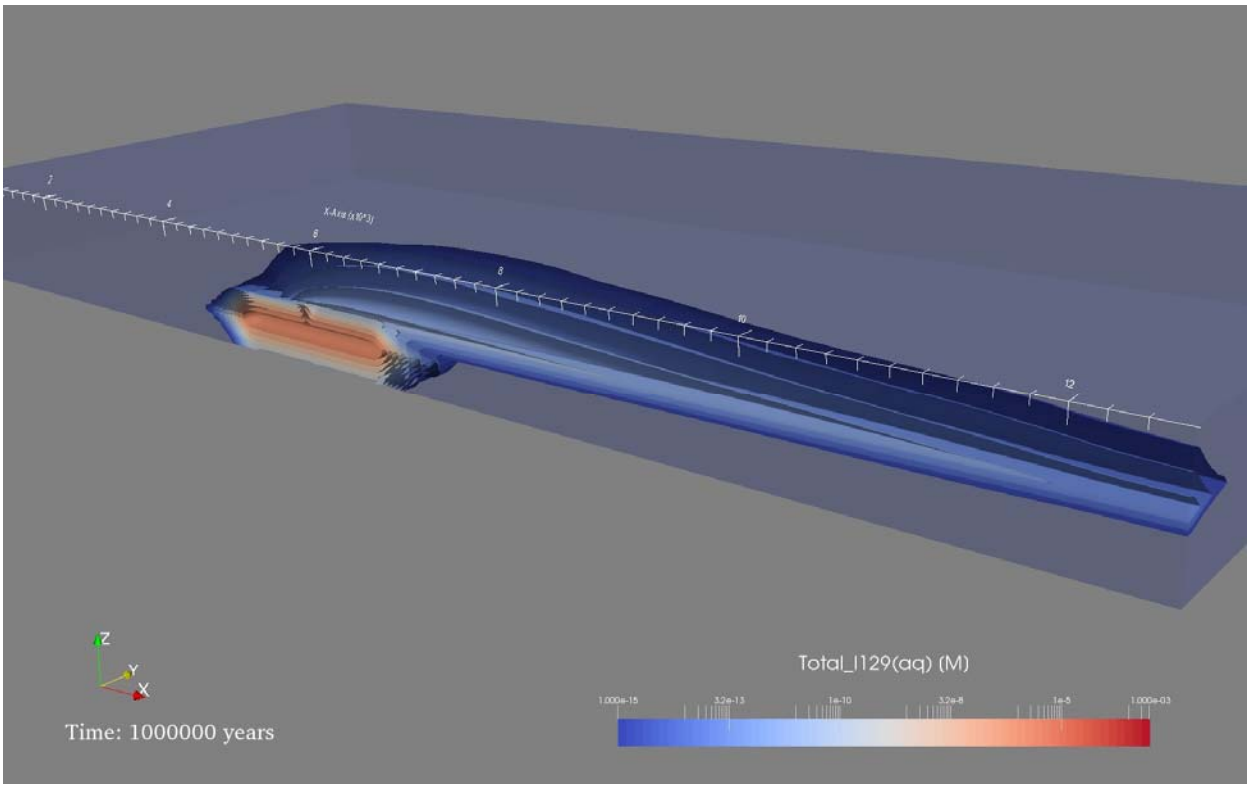

Figure 4-24. ^{129}I concentration for the salt deterministic thermal simulation at 10^6 years. Contours of ^{129}I concentration and the 3D model domain are colored by the ^{129}I concentration.

Probabilistic Results

Probabilistic simulations were carried out to perform a rough sensitivity analysis on the salt reference case and to demonstrate the PA capability to perform probabilistic assessment and sensitivity analysis on a large multi-drift pair model domain. Selected parameters were sampled using the Dakota uncertainty quantification and sampling software system (Section 2.2.2.1). Sampled parameters and their distributions are described in Sections 4.1.1 through 4.1.4 and summarized in Table 4-10. Radionuclide breakthrough (^{129}I) was monitored in 10 locations, all of which lie on the midline of the first drift pair (y = 10 m; Figure 4-25).

Table 4-10. Salt repository reference case probabilistic properties (taken from Sevougian et al. 2014).

Model Parameter	Deterministic Value	Probability Range	Distribution Type
Waste form degradation rate constant (mol/m^2/s)	4.8×10^{-8}	$1.00 \times 10^{-10} – 1.00 \times 10^{-7}$	Log uniform
^{129}I K_d^P (ml/g)	0.0	$9.28 \times 10^{-7} – 7.84 \times 10^{-3}$	Log uniform
^{237}Np K_d^P (ml/g)	5.5	1.0 – 10.0	Log uniform
Waste Package Porosity	0.30	0.05 – 0.50	Uniform
Backfill Porosity	0.113	0.010 – 0.200	Uniform
Shaft Porosity	0.113	0.010 – 0.200	Uniform
DRZ Porosity	0.0129	0.0010 – 0.1000	Uniform
Halite Porosity	0.0182	0.0010 – 0.0519	Uniform[1]
Anhydrite Interbed Permeability (m^2)	1.26×10^{-19}	$1.00 \times 10^{-21} – 1.00 \times 10^{-17}$	Log uniform[2]
Aquifer Permeability (m^2)	1.00×10^{-13}	$1.00 \times 10^{-14} – 1.00 \times 10^{-12}$	Log uniform

[1]The uniform distribution is a simplification of the cumulative distribution reported in Freeze et al. (2013b, Section 3.2.3.2)
[2]The log uniform distribution is a simplification of the Student-t distribution reported in Freeze et al. (2013b, Section 3.2.3.3)

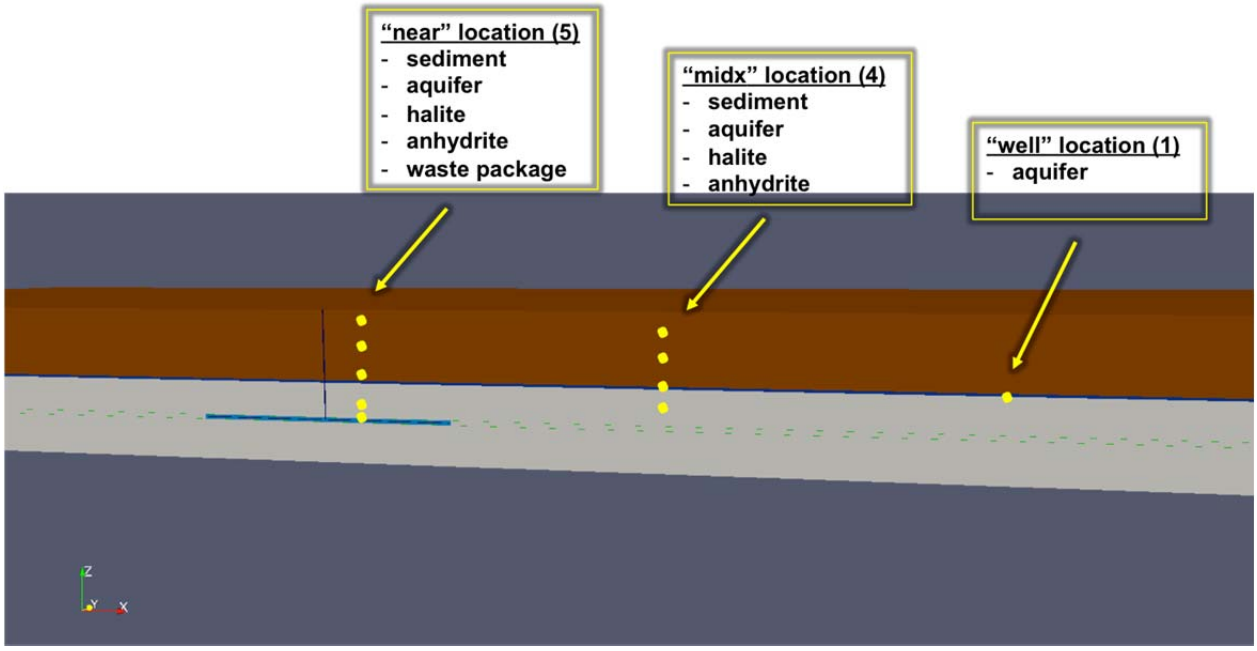

Figure 4-25. Locations of observation points for sensitivity analysis of probabilistic simulations.

Isothermal Probabilistic Results

The ^{129}I breakthrough curves at the locations shown in Figure 4-25 are given in Figure 4-26 through Figure 4-30 for the salt isothermal probabilistic simulations. The anhydrite "near" location experiences early arrival times (~100 years) and maximum concentrations between 10^{-7} and 10^{-5} mol/L (Figure 4-26a). Concentrations at the halite "near" location continually climb, reaching maximum concentrations between 10^{-8} and 10^{-7} mol/L by the end of the simulation (Figure 4-26b). At the aquifer "near" location, concentrations continue to climb throughout the million-year simulation generally staying between 10^{-12} to 10^{-10} mol/L, while at the sediment "near" location the ranges are from 10^{-13} to 10^{-10} mol/L (Figure 4-27). Similar behavior but slightly lower concentrations are seen at the aquifer and sediment "midx"

locations (Figure 4-29), and again at the well observation location (Figure 4-30), where maximum concentrations range from 10^{-13} to 10^{-11} mol/L. The anhydrite and halite 'midx' locations (Figure 4-28) experienced the lowest maximum concentrations, 10^{-19} to 10^{-16} mol/L and 10^{-17} to 10^{-14} mol/L, respectively, among all observation points.

Apparent numerical artifacts can be seen early in the breakthrough curves at observation points in the aquifer and the sediments (Figure 4-27, Figure 4-29, and Figure 4-30). In subsequent deterministic simulations, tighter solver tolerances have been used to remove such artifacts, but these probabilistic simulations were not rerun with the tighter solver tolerances in order to conserve computing resources. Because the early behavior does not affect maximum concentrations at later times, the observed artifacts do not affect current sensitivity analyses. Optimization of solver tolerances for large probabilistic simulations is an area of ongoing research.

Spearman rank correlation coefficients, which identify non-linear (monotonic) relationships between parameters and responses, are used to investigate sensitivity of the maximum ^{129}I concentration at each observation point to the parameters in Table 4-10. The rank correlation coefficients for all observation points are shown in Figure 4-31 through Figure 4-35; values vary with location. At the anhydrite and halite "near" locations, where diffusion directly out of the repository provides the shortest transport path, the ^{129}I concentration has a strong positive correlation with waste dissolution rate (Figure 4-30). At the aquifer and sediments "near" locations, where preferential diffusion up the shaft provides the most efficient transport path, ^{129}I concentration has a strong positive correlation with shaft porosity (Figure 4-32). At these locations, it is negatively correlated with aquifer permeability because a more permeable aquifer causes higher groundwater velocities resulting in greater dilution of ^{129}I in the aquifer. At the aquifer and sediments "midx" locations (Figure 4-34), ^{129}I concentration is similarly correlated with shaft porosity and aquifer permeability, but at the well observation location (Figure 4-35), a negative correlation with halite porosity is observed, likely due to increased diffusion of ^{129}I into the halite with increased diffusion coefficient.

a)

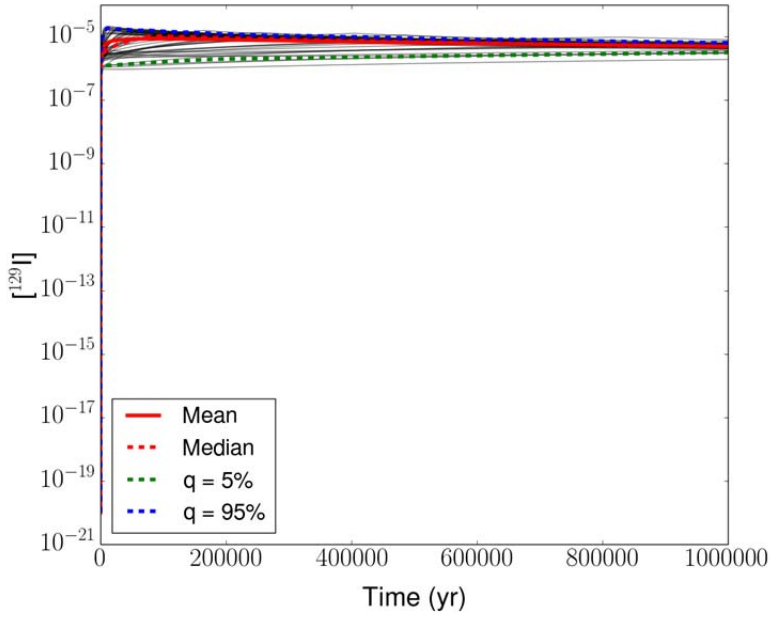

b)

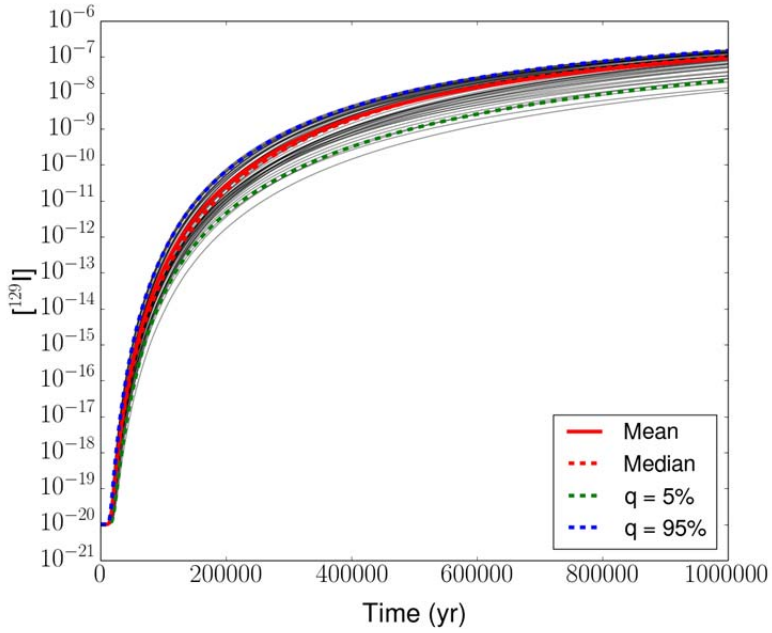

Figure 4-26. Horsetail plot of ^{129}I dissolved concentration for the probabilistic isothermal simulation at:
a) "Anhydrite Near": x = 6212 m, y = 10 m, z = 279.5 m
b) "Halite Near": x = 6212 m, y = 10 m, z = 375 m

a)

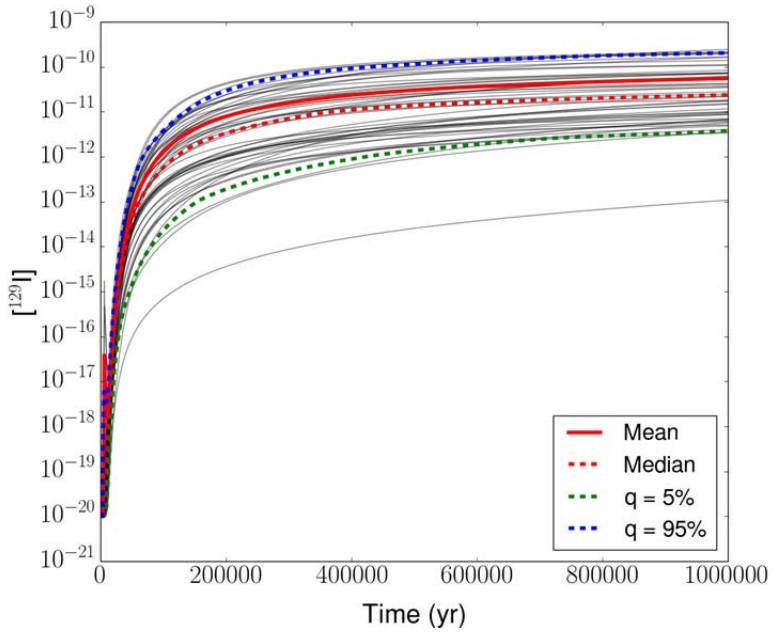

b)

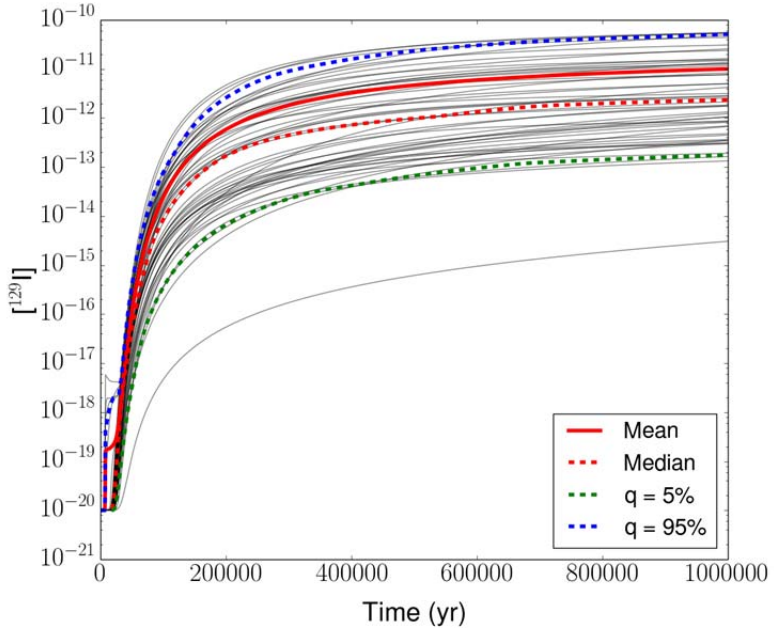

Figure 4-27. Horsetail plot of ^{129}I dissolved concentration for the probabilistic isothermal simulation at:

a) "Aquifer Near": x = 6212 m, y = 10 m, z = 502.5 m

b) "Sediments Near": x = 6212 m, y = 10 m, z = 600 m

a)

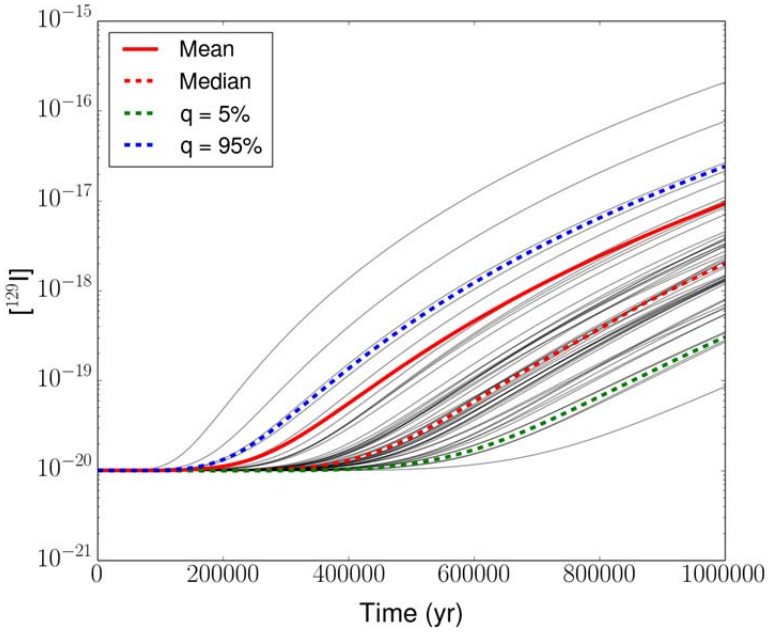

b)

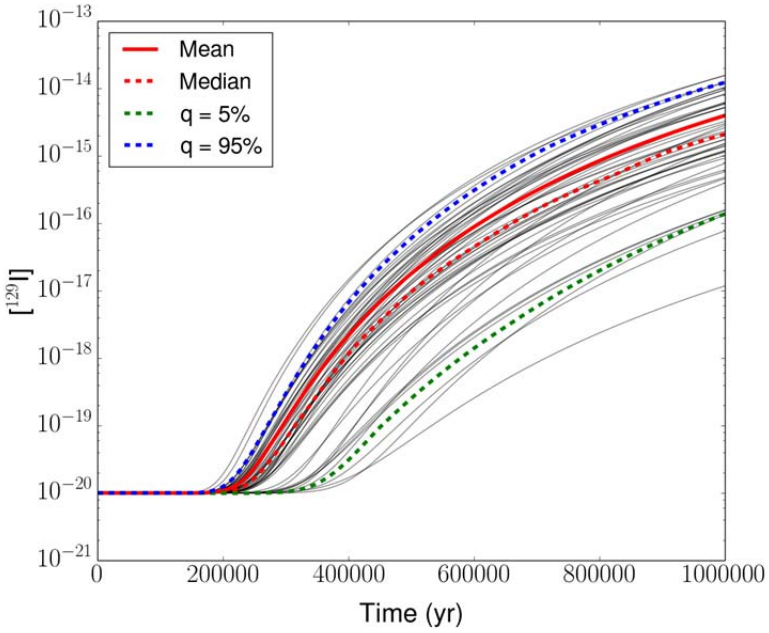

Figure 4-28. Horsetail plot of ^{129}I concentration for the probabilistic isothermal at:

a) "Anhydrite Mid-x": x = 7500 m, y = 10 m, z = 279.5 m

b) "Halite Mid-x": x = 7500 m, y = 10 m, z = 375 m

a)

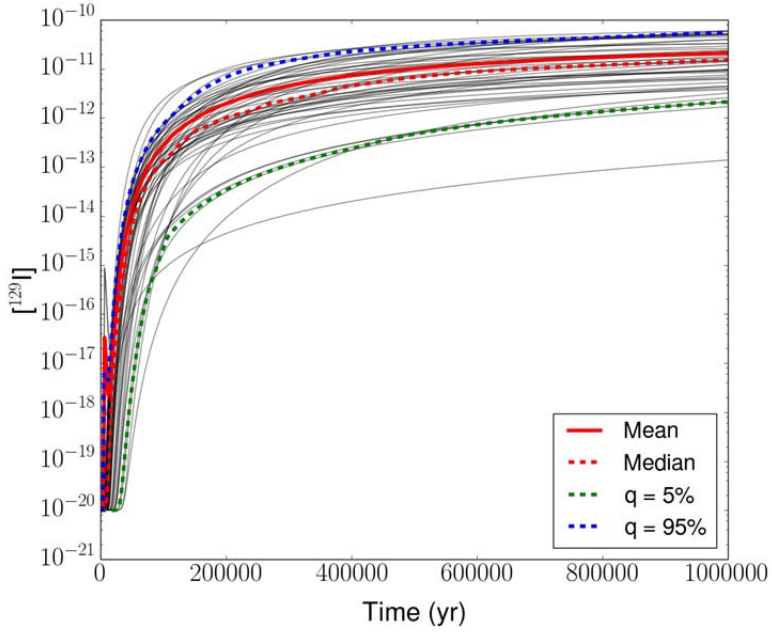

b)

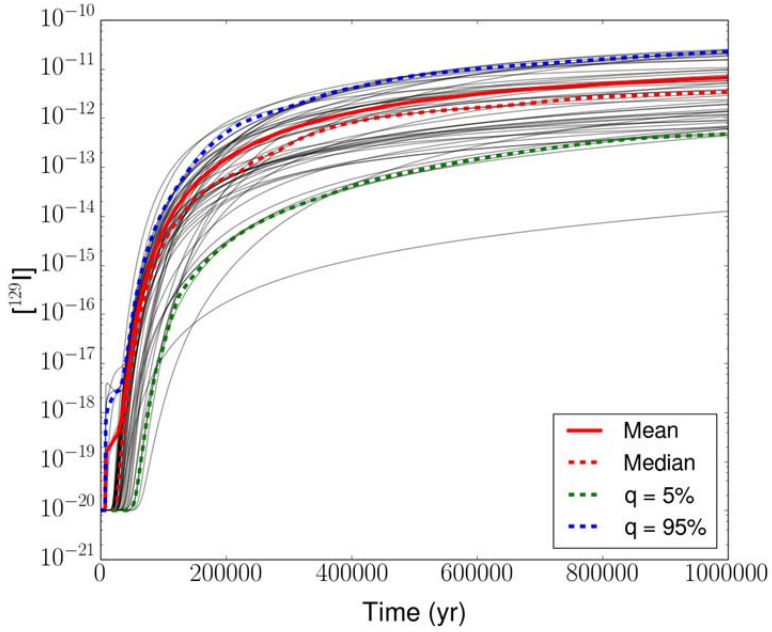

Figure 4-29. Horsetail plot of ^{129}I concentration for probabilistic isothermal generic salt repository at:

a) "Aquifer Mid-x": x = 7500 m, y = 10 m, z = 502.5 m

b) "Sediments Mid-x": x = 7500 m, y = 10 m, z = 600 m

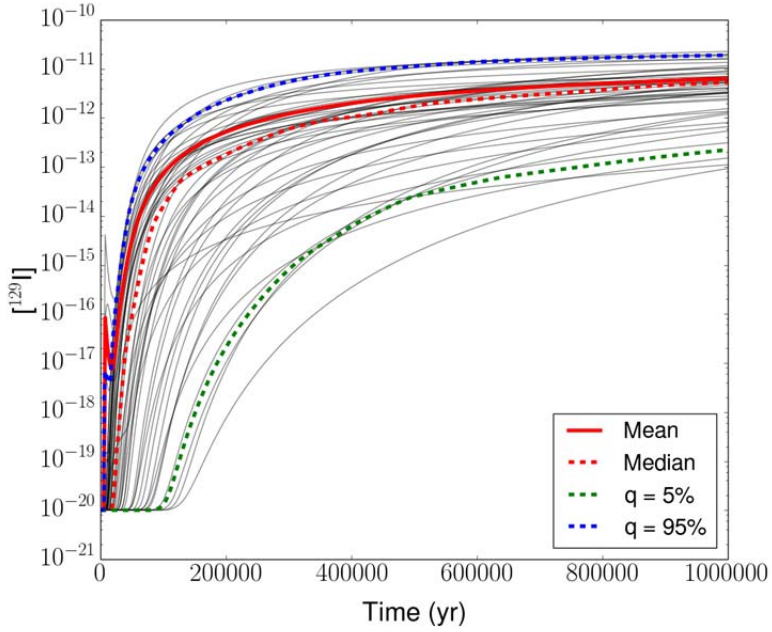

Figure 4-30. Horsetail plot of ^{129}I concentration for probabilistic isothermal generic salt repository at aquifer monitor well location x = 11,600 m, y = 10 m, z = 502.5 m.

a)

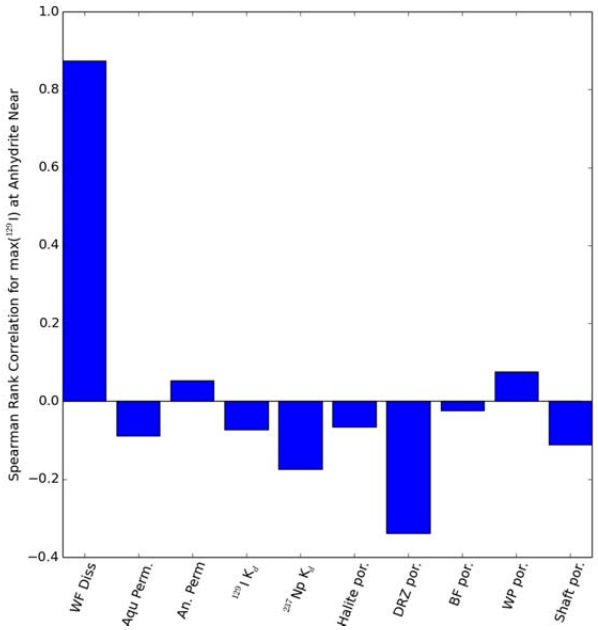

b)

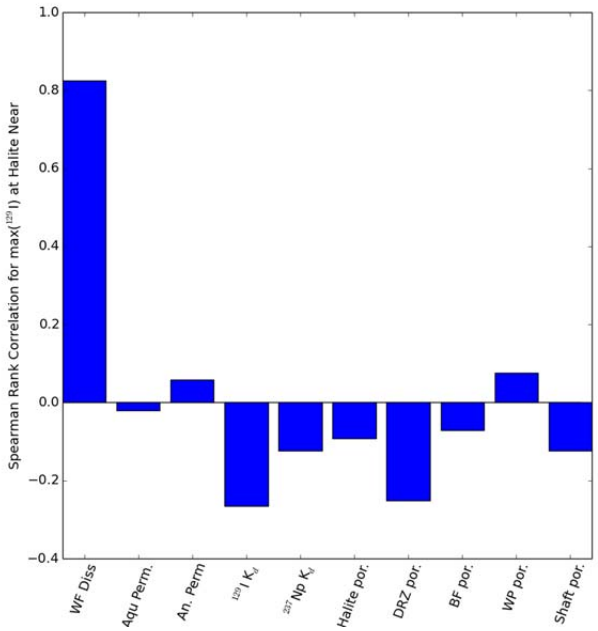

Figure 4-31. Rank correlation coefficients for maximum observed ^{129}I concentration versus sampled parameters probabilistic isothermal simulation at:

- **a) "Anhydrite Near": x = 6212 m, y = 10 m, z = 279.5 m**
- **b) "Halite Near": x = 6212 m, y = 10 m, z = 375 m**

a)

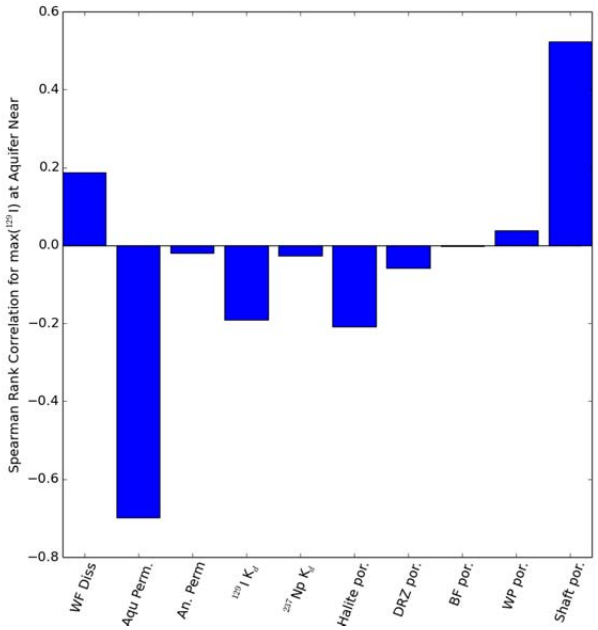

b)

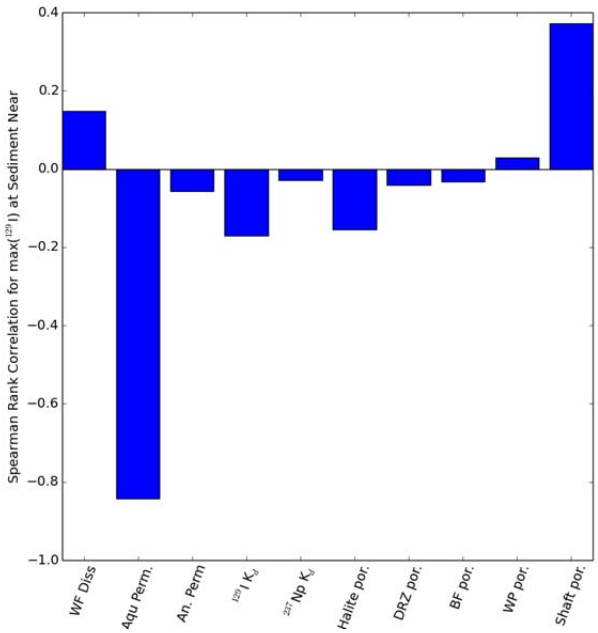

Figure 4-32. Rank correlation coefficients for maximum observed ^{129}I concentration versus sampled parameters probabilistic isothermal simulation at:

a) "Aquifer Near": x = 6212 m, y = 10 m, z = 502.5 m

b) "Sediments Near": x = 6212 m, y = 10 m, z = 600 m

a)

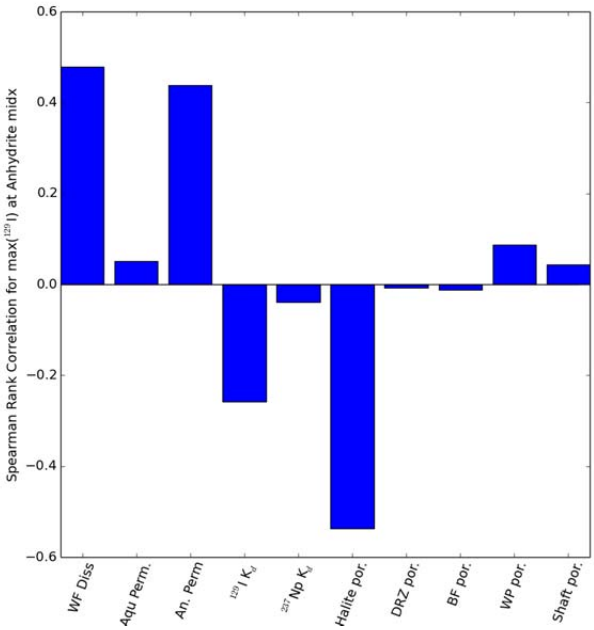

b)

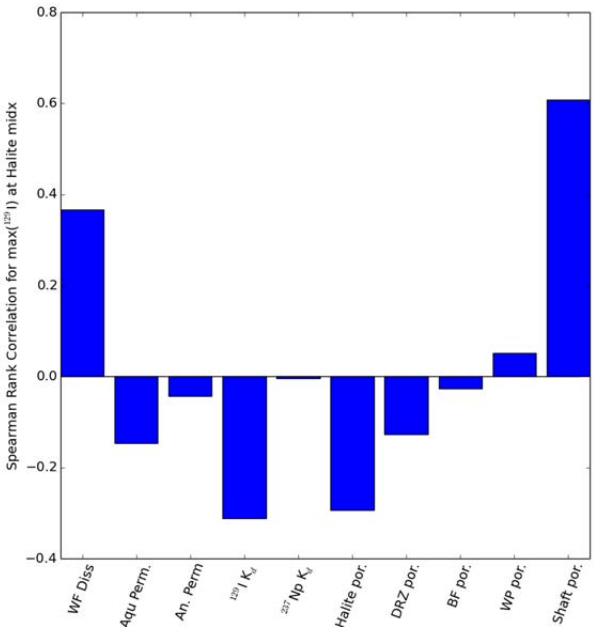

Figure 4-33. Rank correlation coefficients for maximum observed ^{129}I concentration versus sampled parameters probabilistic isothermal simulation at:

a) "Anhydrite Mid-x": x = 7500 m, y = 10 m, z = 279.5 m

b) "Halite Mid-x": x = 7500 m, y = 10 m, z = 375 m

a)

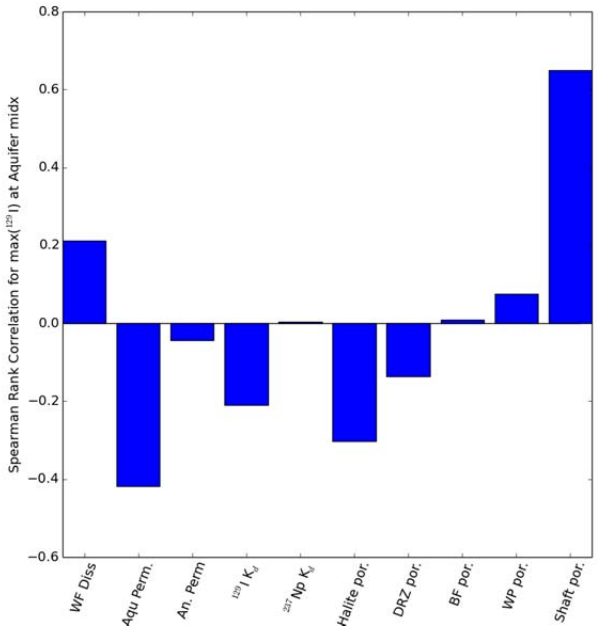

b)

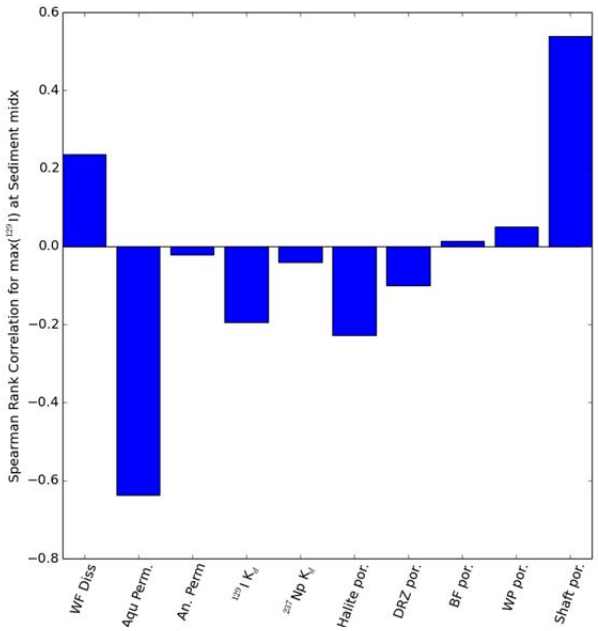

Figure 4-34. Rank correlation coefficients for maximum observed ^{129}I concentration versus sampled parameters probabilistic isothermal simulation at:

a) "Aquifer Mid-x": x = 7500 m, y = 10 m, z = 502.5 m

b) "Sediments Mid-x": x = 7500 m, y = 10 m, z = 600 m

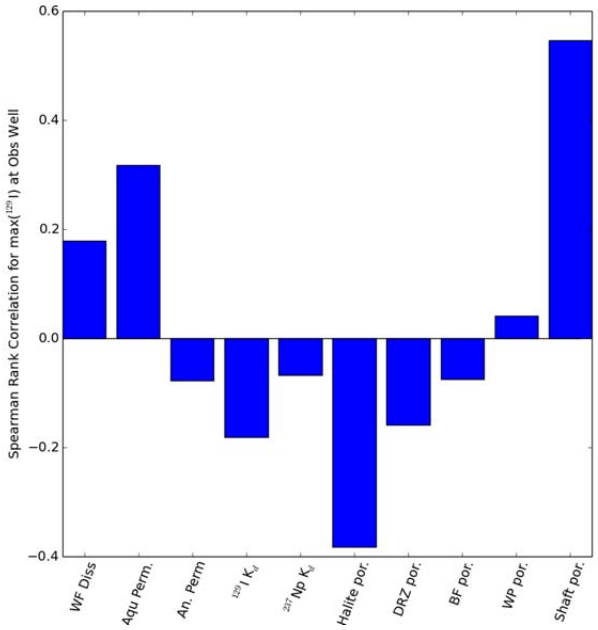

Figure 4-35. Rank correlation coefficients for maximum observed ^{129}I concentration versus sampled parameters probabilistic isothermal simulation at the aquifer monitor well location: x = 11,600 m, y = 10 m, z = 502.5 m

Thermal Probabilistic Results

Shapes of the ^{129}I breakthrough curves (Figure 4-36 through Figure 4-40) and maximum concentrations predicted by the salt thermal probabilistic simulations are similar to those predicted by the isothermal probabilistic simulations. As in the isothermal simulations, the anhydrite "near" location experiences early arrival times (~100 years) and maximum concentrations between 10^{-7} and 10^{-5} mol/L (Figure 4-36a). Concentrations at the halite "near" location continually climb, reaching maximum concentrations between 10^{-8} and 10^{-7} mol/L by the end of the simulation (Figure 4-36b). At the aquifer "near" location, concentrations continue to climb throughout the million-year simulation generally staying between 10^{-12} to 10^{-10} mol/L, while at the sediment "near" location the ranges are from 10^{-13} to 10^{-10} mol/L (Figure 4-37). Similar behavior but slightly lower concentrations are seen at the aquifer and sediment "midx" locations (Figure 4-39), and again at the well observation location (Figure 4-40), where maximum concentrations are for the most part between 10^{-13} to 10^{-11} mol/L. The anhydrite and halite 'midx' locations (Figure 4-38) experienced the lowest maximum concentrations, 10^{-19} to 10^{-16} mol/L and 10^{-16} to 10^{-14} mol/L, respectively.

Spearman rank correlation coefficients (correlating maximum ^{129}I concentration at each observation point to the parameters in Table 4-10) are shown in Figure 4-41 through Figure 4-45. As in the isothermal simulations, values vary with location. At the anhydrite and halite "near" locations, the ^{129}I concentration has a strong positive correlation with waste dissolution rate (Figure 4-41). At the aquifer and sediments "near" locations, ^{129}I concentration is positively correlated with waste form dissolution rate and shaft porosity and negatively correlated with aquifer permeability (Figure 4-42). At the aquifer and sediments "midx" locations (Figure 4-44), the correlation with shaft porosity is stronger and with waste form dissolution rate weaker; at the well observation location (Figure 4-45), a strong positive correlation with shaft porosity is observed.

a)

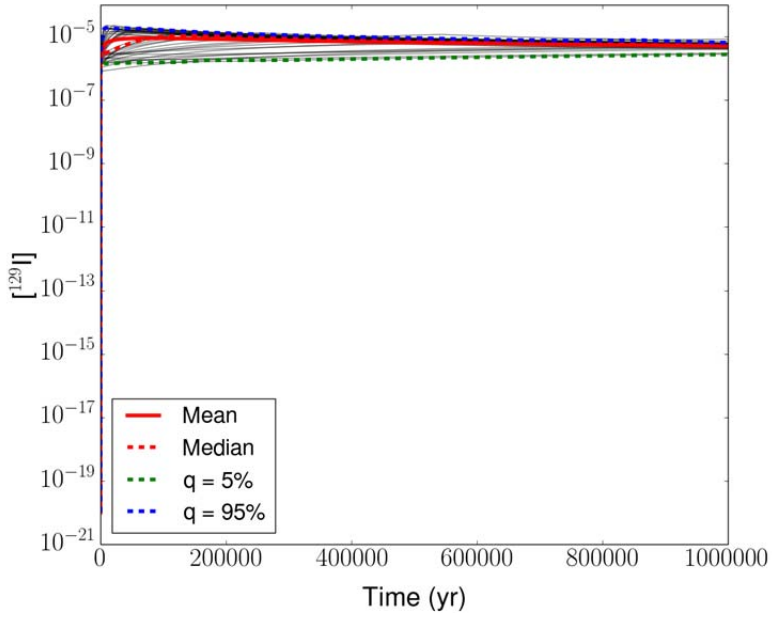

b)

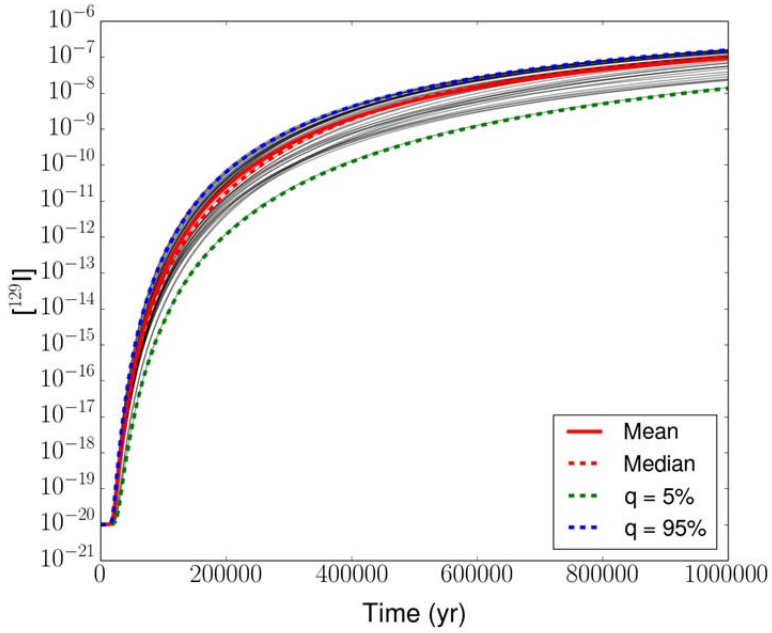

Figure 4-36. Horsetail plot of ^{129}I dissolved concentration for the probabilistic thermal simulation at:
a) "Anhydrite Near": x = 6212 m, y = 10 m, z = 279.5 m
b) "Halite Near": x = 6212 m, y = 10 m, z = 375 m

a)

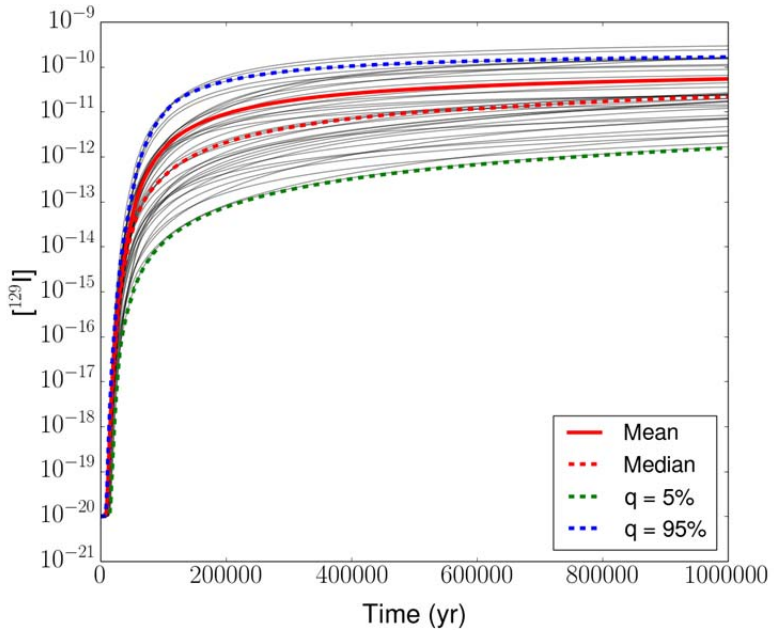

b)

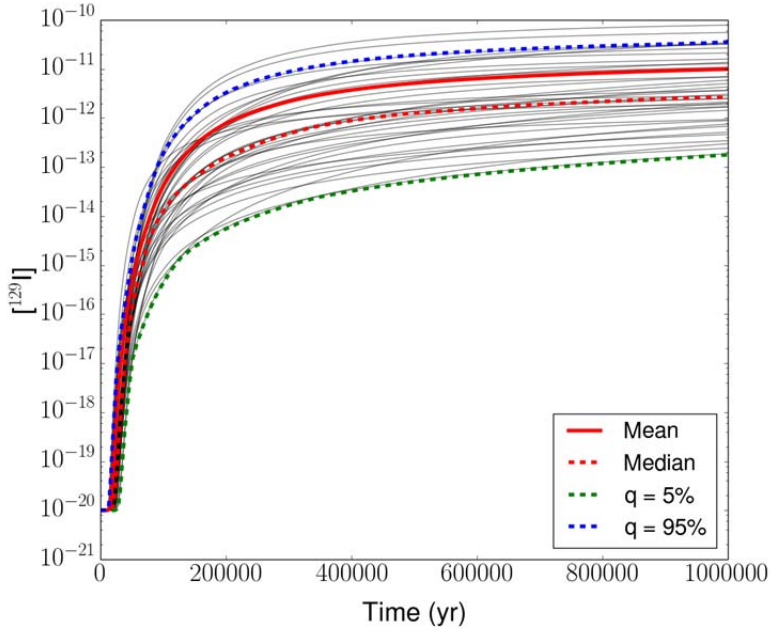

Figure 4-37. Horsetail plot of ^{129}I dissolved concentration for the probabilistic thermal simulation at:

a) "Aquifer Near": x = 6212 m, y = 10 m, z = 502.5 m

b) "Sediments Near": x = 6212 m, y = 10 m, z = 600 m

a)

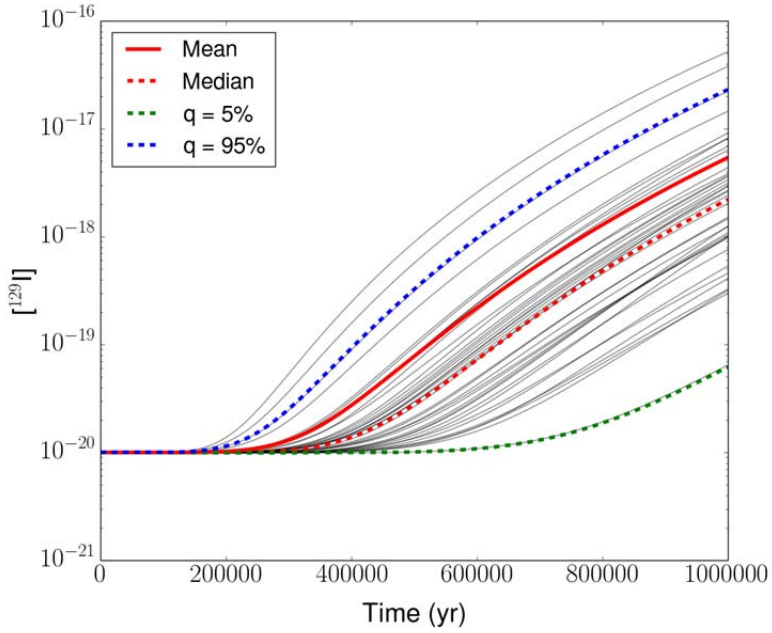

b)

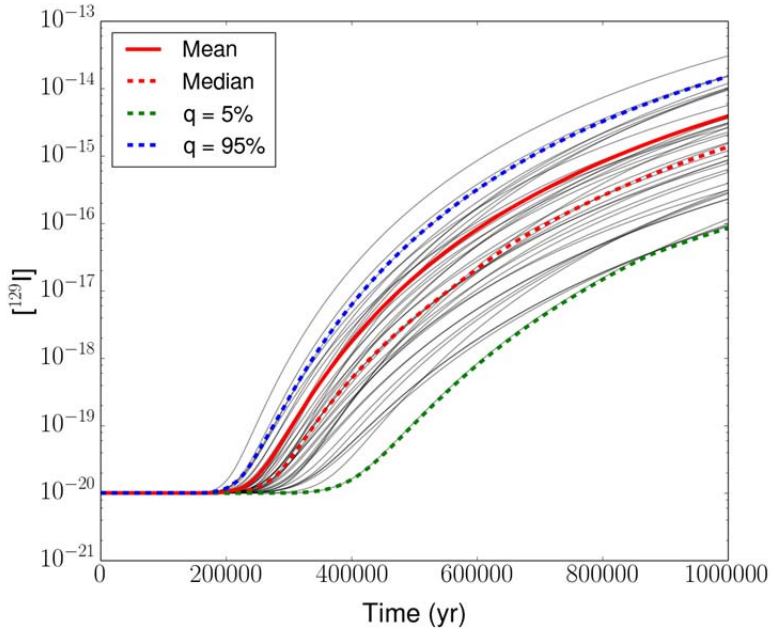

Figure 4-38. Horsetail plot of ^{129}I concentration for the probabilistic thermal at:

a) "Anhydrite Mid-x": x = 7500 m, y = 10 m, z = 279.5 m

b) "Halite Mid-x": x = 7500 m, y = 10 m, z = 375 m

a)

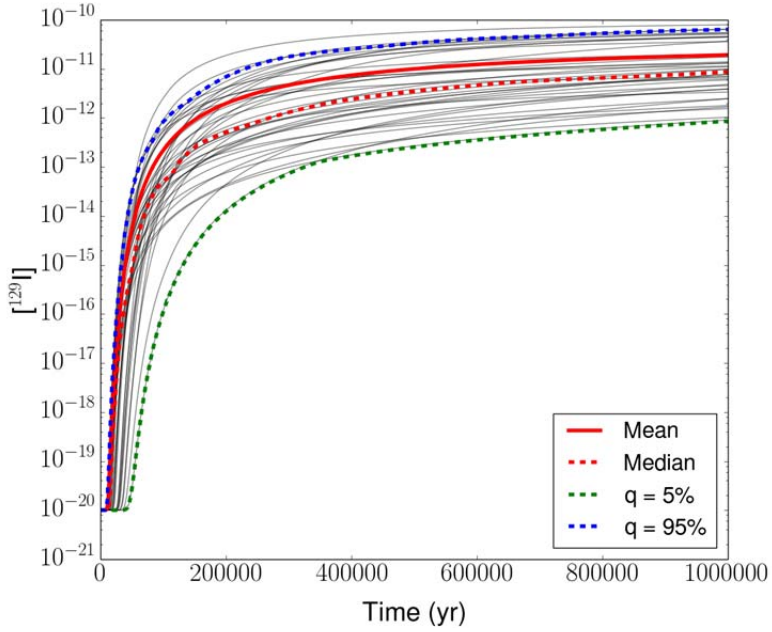

b)

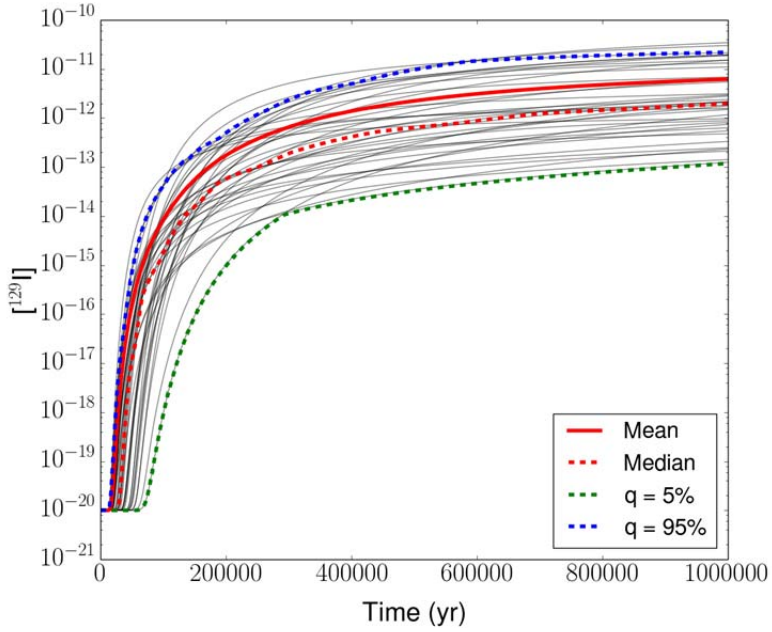

Figure 4-39. Horsetail plot of ^{129}I concentration for probabilistic thermal generic salt repository at:

a) "Aquifer Mid-x": x = 7500 m, y = 10 m, z = 502.5 m

b) "Sediments Mid-x": x = 7500 m, y = 10 m, z = 600 m

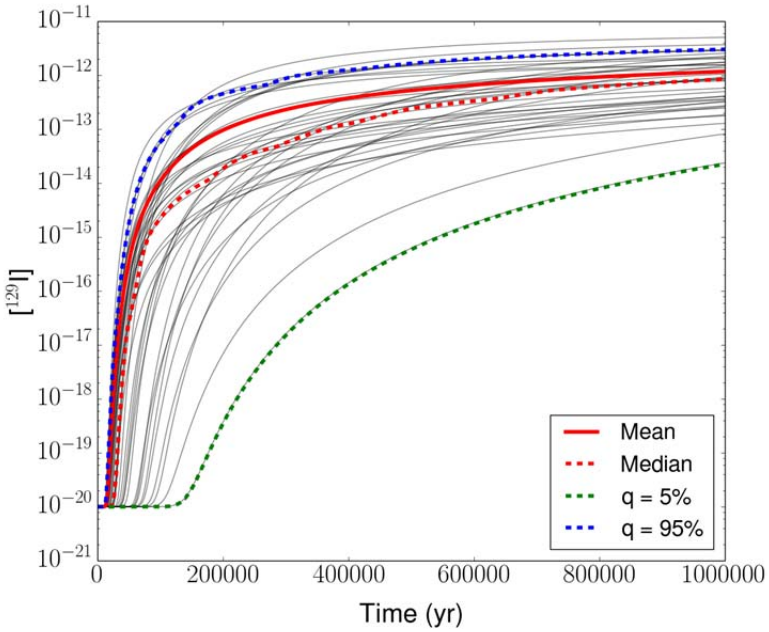

Figure 4-40. Horsetail plot of ^{129}I concentration for probabilistic thermal generic salt repository at aquifer monitor well location x = 11,600 m, y = 10 m, z = 502.5 m.

a)

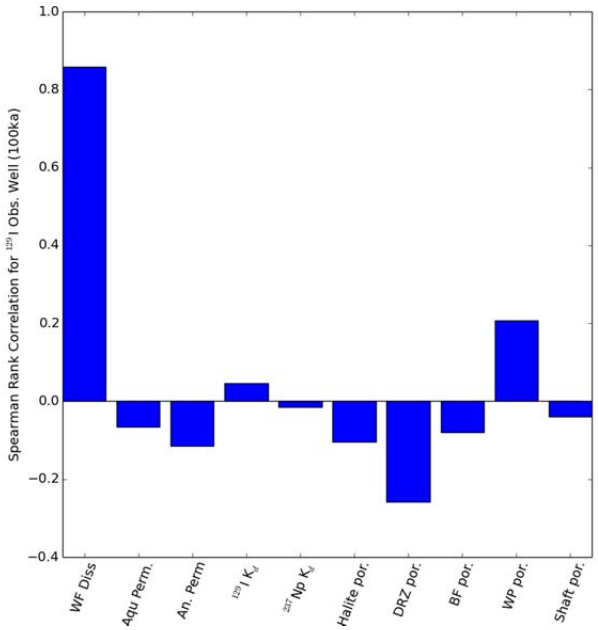

b)

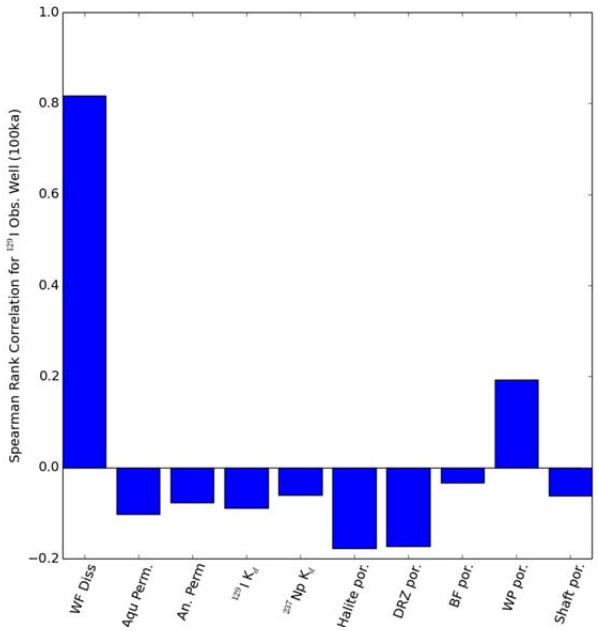

Figure 4-41. Rank correlation coefficients for ^{129}I concentration versus sampled parameters probabilistic thermal simulation at:

a) "Anhydrite Near": x = 6212 m, y = 10 m, z = 279.5 m

b) "Halite Near": x = 6212 m, y = 10 m, z = 375 m

a)

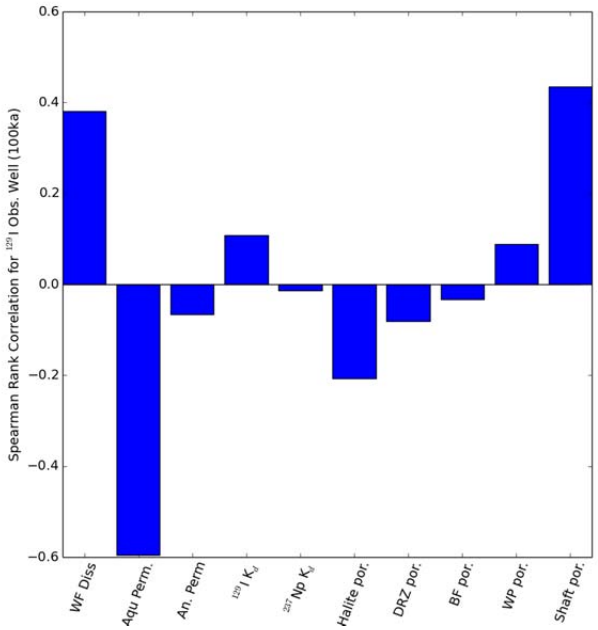

b)

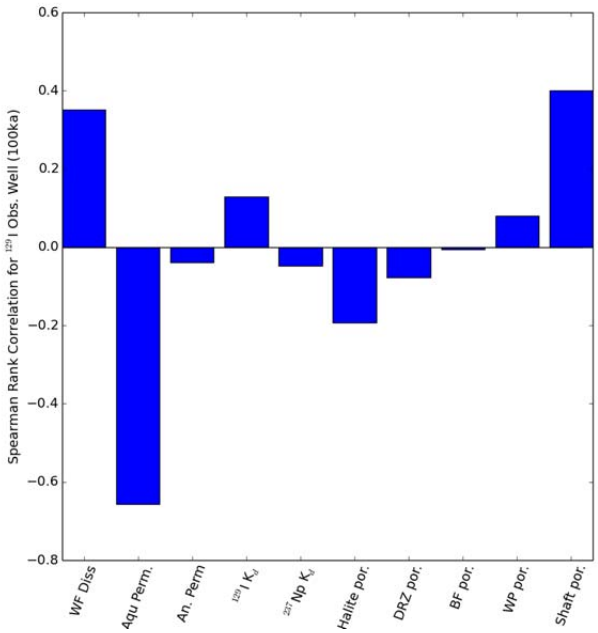

Figure 4-42. Rank correlation coefficients for ^{129}I concentration versus sampled parameters probabilistic thermal simulation at:

a) "Aquifer Near": x = 6212 m, y = 10 m, z = 502.5 m

b) "Sediments Near": x = 6212 m, y = 10 m, z = 600 m

a)

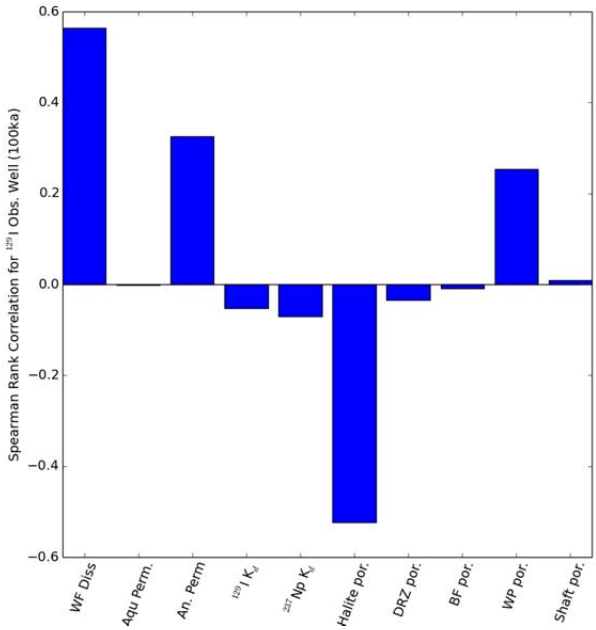

b)

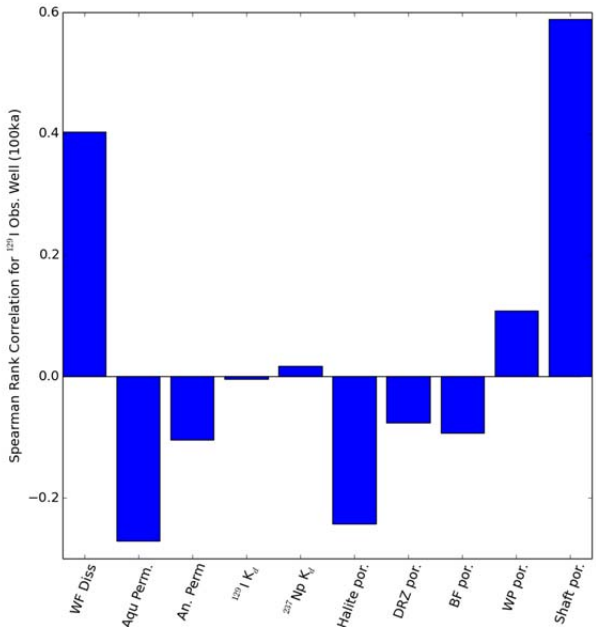

Figure 4-43. Rank correlation coefficients for ^{129}I concentration versus sampled parameters probabilistic thermal simulation at:

a) "Anhydrite Mid-x": x = 7500 m, y = 10 m, z = 279.5 m

b) "Halite Mid-x": x = 7500 m, y = 10 m, z = 375 m

a)

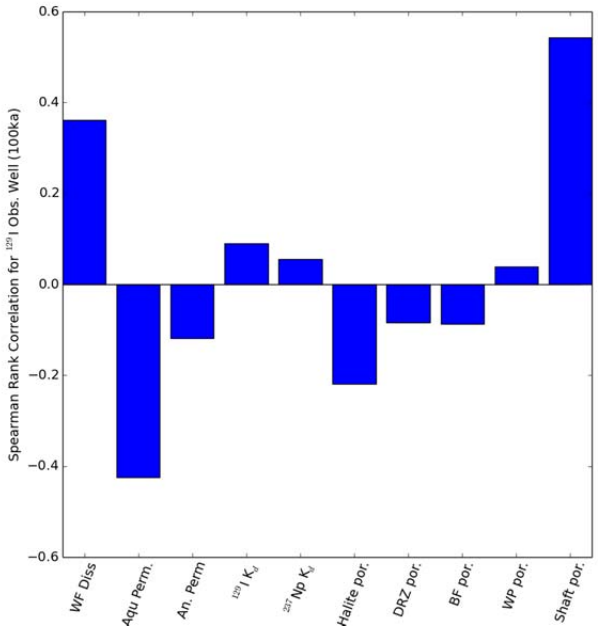

b)

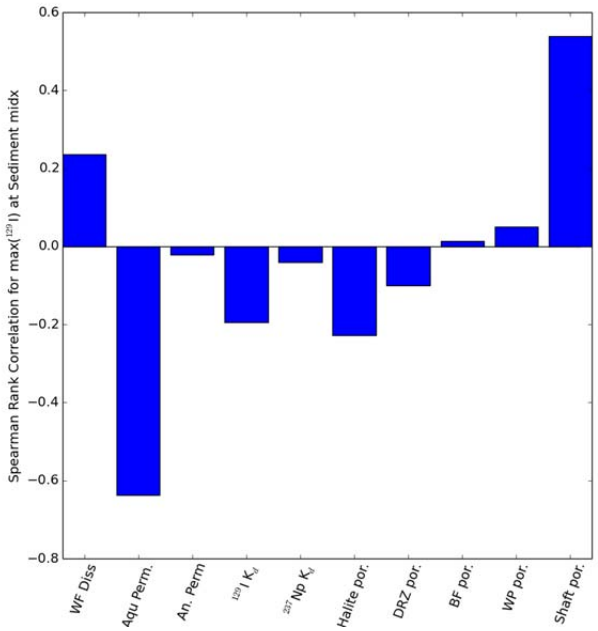

Figure 4-44. Rank correlation coefficients for ^{129}I concentration versus sampled parameters probabilistic thermal simulation at:

a) "Aquifer Mid-x": x = 7500 m, y = 10 m, z = 502.5 m

b) "Sediments Mid-x": x = 7500 m, y = 10 m, z = 600 m

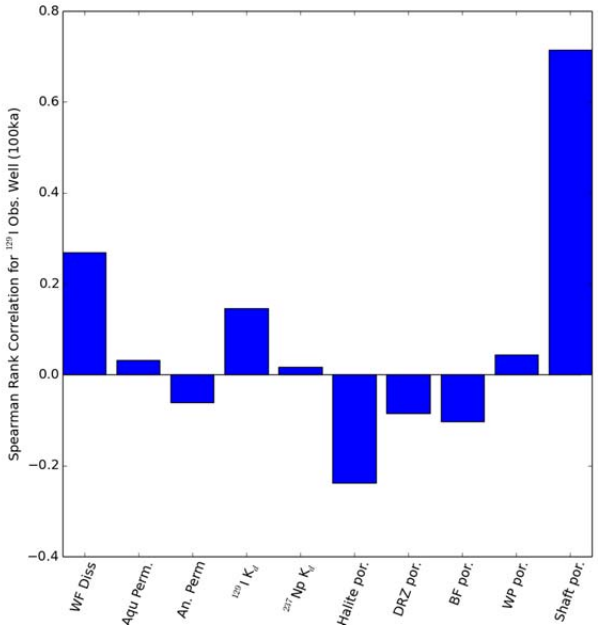

Figure 4-45. Rank correlation coefficients for ^{129}I concentration versus sampled parameters probabilistic thermal simulation at the aquifer monitor well location: x = 11,600 m, y = 10 m, z = 502.5 m

Comparison of Multi-Drift Pair Isothermal and Thermal Simulations

The effect of mechanistically modeling coupled heat and fluid flow on predicted radionuclide transport can be investigated by comparing the results of the salt isothermal and thermal simulations. Thermal probabilistic simulations predict maximum ^{129}I concentrations at the well observation location (Figure 4-46) several times less than those predicted by the probabilistic isothermal simulations. A larger reduction in maximum predicted concentration (about one order of magnitude) is observed in comparing the thermal deterministic simulation to the isothermal deterministic simulation (compare Figure 4-13 and Figure 4-24).

Rank correlation coefficients for thermal and isothermal probabilistic simulations are compared in Figure 4-47. In the thermal simulations, ^{129}I concentration is most strongly correlated with shaft porosity. In the isothermal simulations, shaft porosity (positively correlated) and halite porosity (negatively correlated) have an almost equal influence on maximum ^{129}I concentration.

Differences between thermal and isothermal simulations imply that multi-physics mechanistic modeling will produce a different prediction than a modeling method that relies on simplifications or abstractions of a system. Should thermal or more highly mechanistic models produce results that are similar to those of simplified models, they are useful nevertheless in validating the simplified models (e.g., Rechard 1995). Future modeling work will help to determine an efficient balance between the mechanistic modeling necessary for realism and the simplifications necessary to produce a tractable system. Continued sensitivity analyses can help guide data acquisition and site selection.

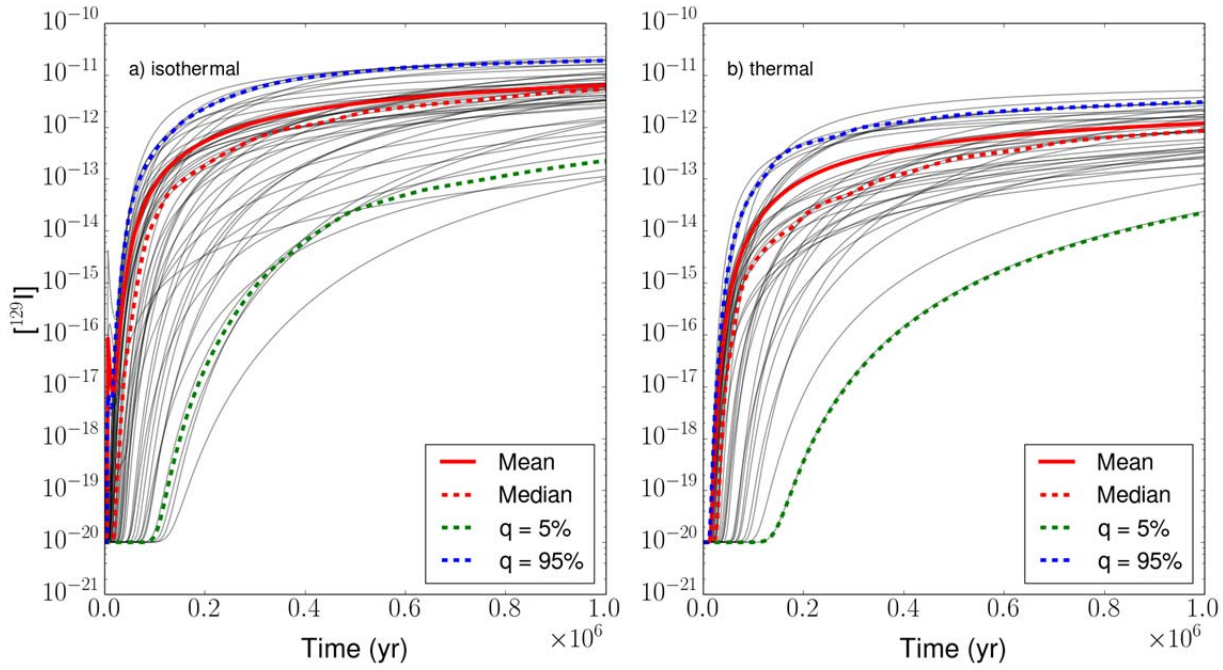

Figure 4-46. Comparison of probabilistic breakthrough curves at the well observation location for the a) isothermal and b) thermal multi-drift pair simulations.

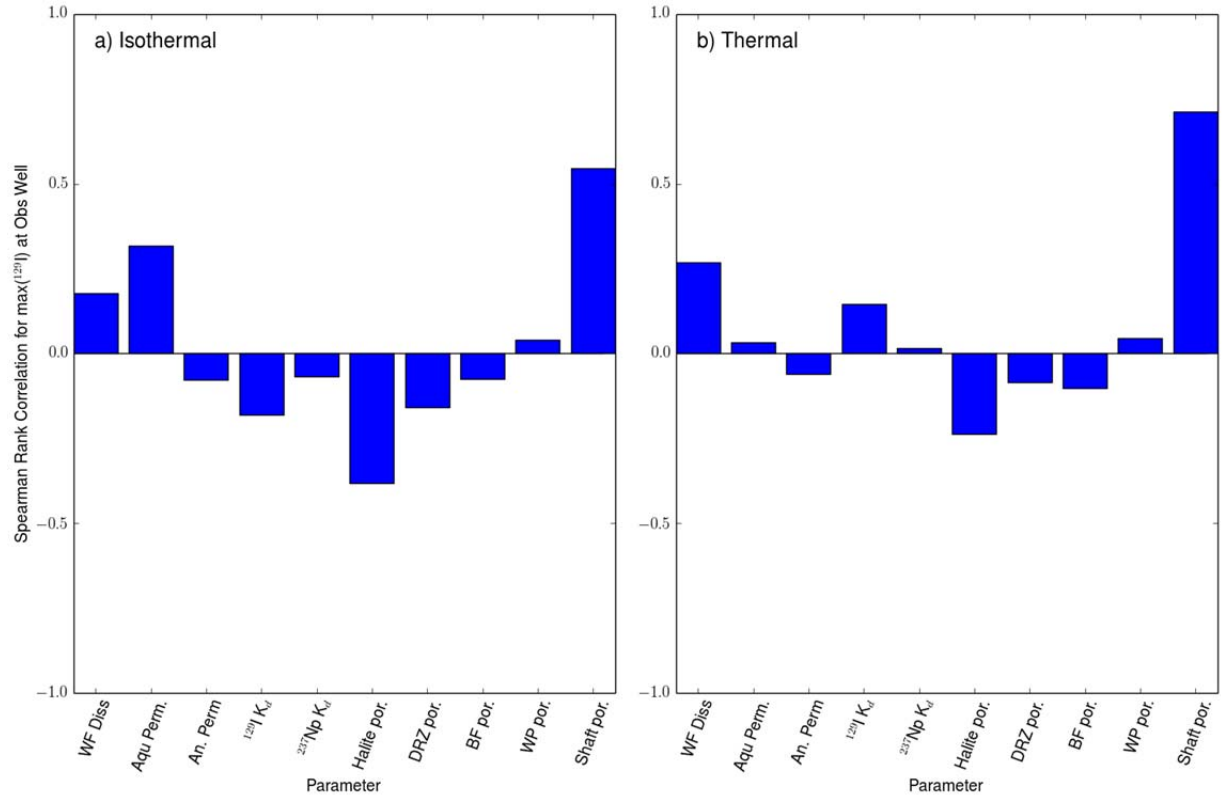

Figure 4-47. Comparison of rank correlation coefficients for the a) isothermal and b) thermal multi-drift pair simulations.

Comparison of Single-Drift Pair and Multi-Drift Pair Simulations

The single-drift pair and multi-drift pair model domains result in two different numerical models of a repository. Single-drift pair simulations represent an infinite number of drift pairs, each with its own access shaft. Thus, single-drift pair simulations are likely produce higher releases than what might be expected from a full 84-drift pair repository with a finite number of shafts. Multi-drift pair simulations represent a smaller repository (10 drift pairs), but how releases from this repository might compare to a larger (84-drift) repository is not obvious, as present results indicate that releases may be related to the ratio of the number of shafts to the number of drift pairs or to the volume available for lateral diffusion of radionuclides.

Probabilistic ^{129}I breakthrough curves (well observation location) for thermal single-drift pair (Sevougian et al. 2014) and thermal multi-drift pair simulations are compared in Figure 4-48. The single-drift pair simulations resulted in higher concentrations and broader ranges in maximum concentrations ($[^{129}I] = 10^{-14}$ to 10^{-9} mol/L) than the multi-drift pair simulations ($[^{129}I] = 10^{-14}$ to 10^{-12} mol/L). Lateral diffusion (in the y direction) of ^{129}I can be seen in the deterministic multi-drift pair simulation (Figure 4-24), and may contribute to lower ^{129}I concentrations at the well observation location. However, in these simulations diffusion up the shaft is an important means of ^{129}I transport out of the repository, so that fewer shafts per drift pair may also contribute to lower concentrations at the well observation location.

Rank correlation coefficients at the well observation location are compared in Figure 4-49. In the multi-drift pair simulations, ^{129}I concentration is most strongly correlated with shaft porosity. In the single-drift pair simulations, shaft porosity (positively correlated) and halite porosity (negatively correlated) equally influence ^{129}I concentration.

Differences between single-drift pair and multi-drift pair results imply that accurate representation of a system is necessary both for accurate prediction and for accurate understanding of system behavior. Repository design (for instance, shaft to drift ratio) may influence radionuclide release. In order to assess the influence of repository design (with the eventual goal of optimizing it) on radionuclide releases, larger repositories of varying layout (for instance, shaft to drift ratio) will be simulated in the future. When a site is chosen, simulation of potential repository designs should be a part of the planning process.

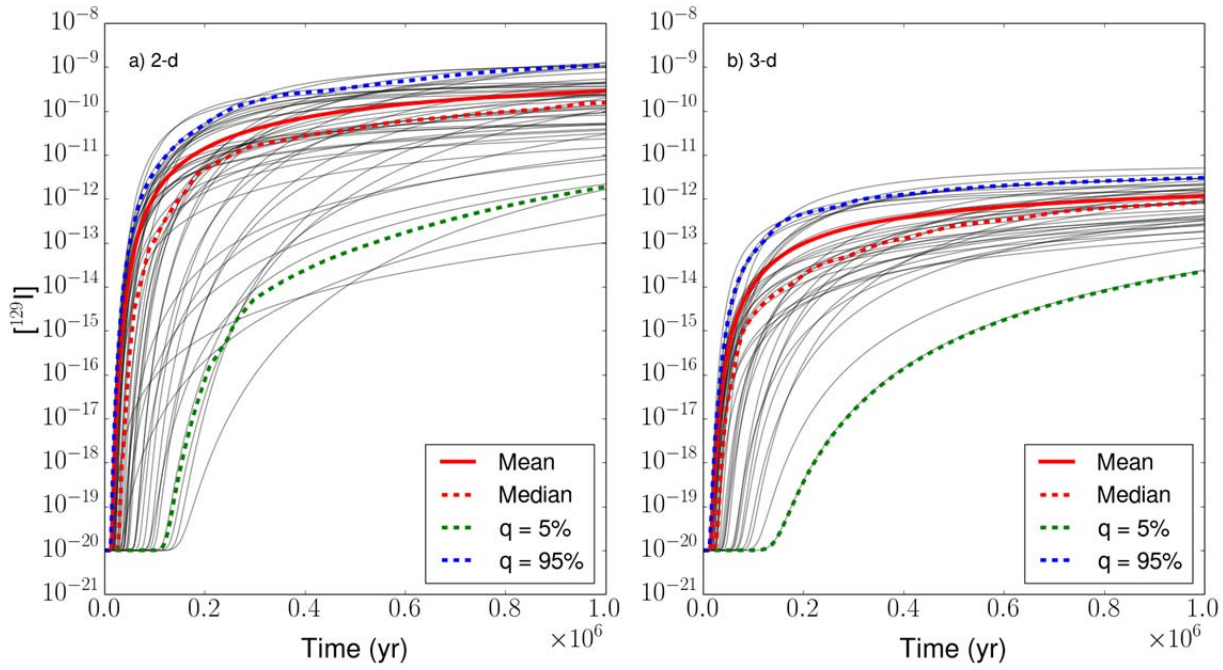

Figure 4-48. Comparison of probabilistic ^{129}I breakthrough curves at the well observation location for the a) single-drift pair simulations (Sevougian et al. 2014) and b) multi-drift pair simulations.

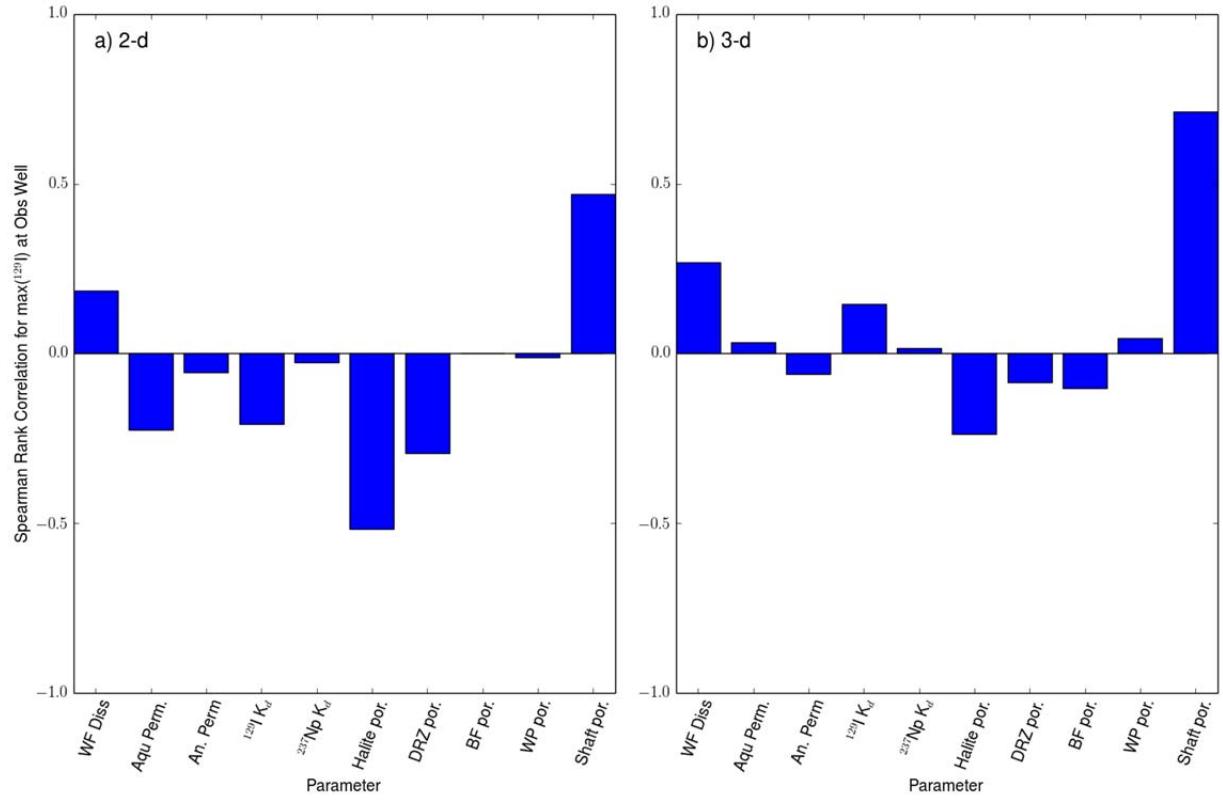

Figure 4-49. Comparison of rank correlation coefficients for the a) single-drift pair simulations (Sevougian et al. 2014) and b) multi-drift pair simulations.

4.2 Salt Reference Case for Defense HLW Glass

A reference case was developed for disposal of DOE-managed high-level radioactive waste (HLW) in a salt repository. This case shares much with the salt reference case for UNF. A thermal deterministic simulation was run using the same model domain and grid as used for the multi-drift pair salt UNF simulations. The HLW case differs in the waste form (vitrified HLW), and it introduces a new model for waste degradation appropriate for vitrified waste (Section 3.2.2). It also differs slightly in the specifics of initial and boundary conditions. Properties unique to the HLW case are described below.

4.2.1 Waste Inventory

DOE-managed HLW inventory includes waste at the Hanford Site (HS), Savannah River Site (SRS), and Idaho National Laboratory (INL) (Carter et al. 2013; SNL 2014). A portion of the SRS waste has been vitrified, HS liquid waste will be vitrified in the future, and INL calcine waste may be vitrified (Carter et al. 2013). In total, approximately 23,000 canisters of vitrified waste are expected to be produced. This iteration of the HLW repository case considers only the radionuclide inventory for projected vitrified waste from the Hanford Site (Carter et al. 2013, Table F-1), which will be distributed among an estimated 11,079 canisters, resulting in the radionuclide inventory per vitrified waste canister (in 2017) listed in Table 4-11. The HLW reference case assumes disposal in 2047. Initial radionuclide inventories in 2047 as well as inventories at later times and heat of decay over time were calculated from the 2017 inventories.

Table 4-11. HS HLW radionuclide inventory in 2017.

Nuclide	Total HS inventory (Ci)[1]	Inventory per HS canister (g)	Nuclide	Total HS inventory (Ci)[1]	Inventory per HS canister (g)	Nuclide	Total HS inventory (Ci)[1]	Inventory per HS canister (g)
^{225}Ac	2.31E+00	3.59E-09	^{239}Np	1.50E+01	5.84E-09	^{222}Rn	8.97E-02	5.26E-11
^{227}Ac	1.33E+02	1.66E-04	^{231}Pa	2.72E+02	5.20E-01	^{106}Ru	1.70E-02	4.59E-10
^{228}Ac	1.36E+01	5.47E-10	^{233}Pa	1.41E+02	6.13E-07	^{125}Sb	4.18E+02	3.65E-05
^{241}Am	1.42E+05	3.73E+00	^{234}Pa	2.59E-01	1.17E-11	^{126}Sb	8.11E+01	8.76E-08
^{243}Am	1.50E+01	6.79E-03	^{234m}Pa	1.99E+02	2.62E-11	^{126m}Sb	5.79E+02	6.65E-10
^{217}At	2.31E+00	1.30E-16	^{209}Pb	2.31E+00	4.59E-11	^{79}Se	1.22E+02	1.58E-01
^{137m}Ba	2.99E+07	5.02E-06	^{210}Pb	1.75E-02	2.07E-08	^{151}Sm	3.10E+06	1.06E+01
^{210}Bi	1.75E-02	1.27E-11	^{211}Pb	1.33E+02	4.86E-10	^{126}Sn	5.79E+02	1.84E+00
^{211}Bi	1.33E+02	2.87E-11	^{212}Pb	4.95E+01	3.22E-09	^{90}Sr	3.43E+07	2.27E+01
^{212}Bi	4.95E+01	3.05E-10	^{214}Pb	8.97E-02	2.47E-13	^{99}Tc	2.97E+04	1.58E+02
^{213}Bi	2.31E+00	1.08E-11	^{210}Po	1.61E-02	3.23E-10	^{125m}Te	1.02E+02	5.11E-07
^{214}Bi	8.97E-02	1.83E-13	^{211}Po	3.66E-01	3.46E-16	^{227}Th	1.31E+02	3.85E-07
^{113}Cd	6.37E-15	1.48E-06	^{212}Po	3.17E+01	1.61E-20	^{228}Th	4.93E+01	5.43E-06
^{113m}Cd	7.30E+03	3.04E-03	^{213}Po	2.26E+00	1.62E-20	^{229}Th	2.31E+00	9.80E-04
^{243}Cm	9.28E+00	1.62E-05	^{214}Po	8.97E-02	2.52E-20	^{230}Th	1.42E-02	6.35E-05
^{244}Cm	1.60E+02	1.78E-04	^{215}Po	1.33E+02	4.07E-16	^{231}Th	9.00E+00	1.53E-09
^{60}Co	9.88E+02	7.89E-05	^{216}Po	4.95E+01	1.28E-14	^{232}Th	8.00E+00	6.59E+03
^{134}Cs	8.47E+01	5.91E-06	^{218}Po	8.97E-02	2.86E-14	^{234}Th	1.99E+02	7.76E-07
^{135}Cs	1.46E+03	1.14E+02	^{238}Pu	4.31E+03	2.27E-02	^{206}Tl	2.32E-08	9.61E-21
^{137}Cs	3.16E+07	3.28E+01	^{239}Pu	6.91E+04	1.00E+02	^{207}Tl	1.33E+02	6.30E-11
^{152}Eu	7.16E+02	3.74E-04	^{240}Pu	1.23E+04	4.87E+00	^{208}Tl	1.78E+01	5.46E-12
^{154}Eu	3.80E+04	1.27E-02	^{241}Pu	5.78E+04	5.07E-02	^{209}Tl	4.86E-02	1.07E-14
^{155}Eu	8.58E+02	1.67E-04	^{242}Pu	1.00E+00	2.36E-02	^{232}U	3.73E+01	1.57E-04
^{221}Fr	2.31E+00	1.18E-12	^{223}Ra	1.33E+02	2.34E-07	^{233}U	5.10E+02	4.75E+00
^{223}Fr	1.83E+00	4.27E-12	^{224}Ra	4.95E+01	2.81E-08	^{234}U	2.20E+02	3.18E+00
^{152}Gd	1.08E-11	4.48E-05	^{225}Ra	2.31E+00	5.32E-09	^{235}U	9.00E+00	3.76E+02
^{129}I	4.80E+01	2.45E+01	^{226}Ra	8.97E-02	8.19E-06	^{236}U	6.00E+00	8.37E+00
^{93m}Nb	3.21E+03	1.03E-03	^{228}Ra	1.36E+01	5.25E-06	^{237}U	1.38E+00	1.53E-09
^{59}Ni	1.37E+03	1.63E+00	^{106}Rh	1.70E-02	4.31E-16	^{238}U	1.99E+02	5.34E+04
^{63}Ni	1.14E+05	1.67E-01	^{219}Rn	1.33E+02	9.23E-13	^{90}Y	3.43E+07	5.69E-03
^{237}Np	1.41E+02	1.81E+01	^{220}Rn	4.95E+01	4.84E-12	^{93}Zr	4.81E+03	1.73E+02

[1] From Carter et al. (2013, Table F-1)

4.2.2 Engineered Barrier System

4.2.2.1 Waste Form

The waste form is vitrified HLW (specifically that expected to be produced at the Hanford Site), aged to 2047. Vitrified waste is poured into steel canisters 4.5 m in length and 0.61 m in diameter, and each canister is assumed to contain 1.135 m^3 of vitrified waste (SNL 2014, Table A-24, reproduced here as Table 4-12). Vitrified waste volume is input to the vitrified waste degradation model (Section 4.2.3.4).

Table 4-12. Hanford HLW canister data summary (Table A-24 in SNL 2014)

Canister Length, cm	450
Nominal Outer Diameter, cm	61
Thickness, cm	0.95
Empty Canister Weight, kg	715
Available Volume, liter	1190
Material	Stainless Steel 304 L
Nominal Fill Height, %	95
Nominal Glass Volume, liter	1135
Filled Canister Weight, kg	3735
Glass Weight, kg	3020
Glass Density, g/cm3	2.66

4.2.2.2 Waste Package

In this early iteration of the HLW repository case, the waste package is assumed to be identical to that in the salt UNF reference case, i.e., a stainless steel canister and a 5-cm thick carbon steel overpack with outer dimensions of 5 meters in length by 1.29 m in diameter (Hardin et al. 2012). Given the dimensions of the waste package and the vitrified waste canisters, three vitrified waste canisters fit in one waste package, and waste package material properties (Table 4-13) can be calculated on the basis of component material properties. Waste package porosity is the volume fraction not occupied by waste package walls, canister walls, or waste. Saturated thermal conductivity is taken to be the geometric mean of the thermal conductivities of steel, glass, and water. Heat capacity and grain density are void independent and taken to be the volume weighted averages of values for steel and glass. Permeability, tortuosity, and dispersivity are set equal to values for the waste package in the salt UNF reference case, and as in the UNF case, the conservative assumption of instant waste package failure is made.

Table 4-13. Waste package material parameters for the HLW case.

Model Region	Permeability (m^2)	Porosity	Tortuosity	Effective Diffusion Coefficient[1,3] (m^2/s)	Longitudinal Dispersivity (m)[2]	Saturated Thermal Conductivity[3] (W/m/K)	Specific Heat Capacity (J/kg/K)	Grain Density (kg/m^3)
Waste Package	1.00×10^{-13}	0.27	1.00	6.3×10^{-10}	0.5	1.5	757	3735

[1] Effective diffusion coefficient = (free water diffusion coefficient) × (tortuosity) × (porosity) × (saturation)
[2] Transverse dispersivity = 0
[3] Saturation function = Brooks-Corey for all units; however, all material regions are fully saturated, i.e., $S_w = 1$

4.2.2.3 Repository Layout

With waste package and drift dimensions (Table 4-5) assumed in this report, 23,000 canisters would fill 7667 waste packages and require a repository of 48 drift pairs (slightly greater than half the size of a repository holding 70,000 MTHM UNF).

4.2.3 Conceptual and Numerical Models

4.2.3.1 Conceptual Model

As in the salt UNF case, waste isolation occurs in a mined repository located in a deep, relatively pure, thick, bedded halite formation. The HLW case assumes the same west to east regional head gradient (-0.0013 m/m) as the salt UNF case, but differs in the assumption of a regional geothermal heat flux of 60 mW/m^2 (appropriate for midcontinent; Blackwell et al. 2011).

4.2.3.2 Initial Conditions

Initial pressure and temperature are consistent with a head gradient of -0.0013 (m/m) from west (left) to east (right), a regional heat flow of 60 mW/m^2 applied at the bottom of the domain and a constant temperature of 28°C applied at the top of the domain. Iodine-129 is the only radionuclide tracked; its initial concentration everywhere is 10^{-20} mol/L.

4.2.3.3 Boundary Conditions

Boundary conditions for the six faces of the model domain are set as follows: The west (left), east (right), and back faces are held at initial pressures and temperatures. The top face is held at the initial temperature of 28°C and assigned a pressure gradient of zero (no fluid flow). A constant heat flux of 60 mW/m^2 is applied to the bottom face, which is assigned a pressure gradient of zero (no fluid flow). The front face is a no-flow boundary (neither fluid nor heat). Where fluid enters the model domain, it enters with ^{129}I concentration set to 10^{-20} mol/L, and where it exits the model domain, it exits carrying the ambient concentration. Diffusive flux is disallowed at the outlet boundary by specifying a zero concentration gradient.

4.2.3.4 Waste Package Source Terms

Heat source: Each waste package is modeled as a transient heat source. The energy (watts per waste package) entering the model domain is updated periodically according to values in a lookup table. The initial value is that for a waste package containing three glass pour canisters of Hanford Site vitrified waste decayed to 2047. Time steps are synced with lookup table times, and between specified times, the energy input is linearly interpolated.

Radionuclide source: Waste form degradation is modeled using a temperature-dependent rate constant that results in a waste form half-life of approximately 3×10^6 years at a temperature of 50°C (with a surface exposure factor of 4; Section 3.2.2). A random number generator is used to generate a unique surface exposure factor (between 4 and 17) for each waste package, so that degradation rate varies among waste packages. As the waste form degradation model proceeds, a radionuclide is released into solution according to its fractional inventory in the waste form (Table 4-11). Decay and ingrowth of radionuclide in the waste form is accounted for by updating the fractional inventory periodically according to values in a lookup table. Initial radionuclide mass fraction inventories in the waste form are for Hanford Site vitrified waste decayed to 2047. The vitrified waste degradation model calculates the release rate of a single radionuclide from the waste form (^{129}I in this simulation). Future versions will allow calculation of multiple radionuclide source terms.

4.2.4 Salt HLW Results

The initial heat output of a waste package containing 3 HLW canisters is about 100 times less than that of a 12-PWR waste package. Temperature in the waste package cells rises about 3°C above the initial geothermal temperature, compared to an approximately 250°C rise in temperature in the UNF case. The slight increase in repository temperatures in the HLW case does not significantly disturb the fluid flow field. Fluid flow vectors at 10 years when waste package temperatures are peaking are compared to fluid flow vectors at 100,000 years in Figure 4-50 and Figure 4-51.

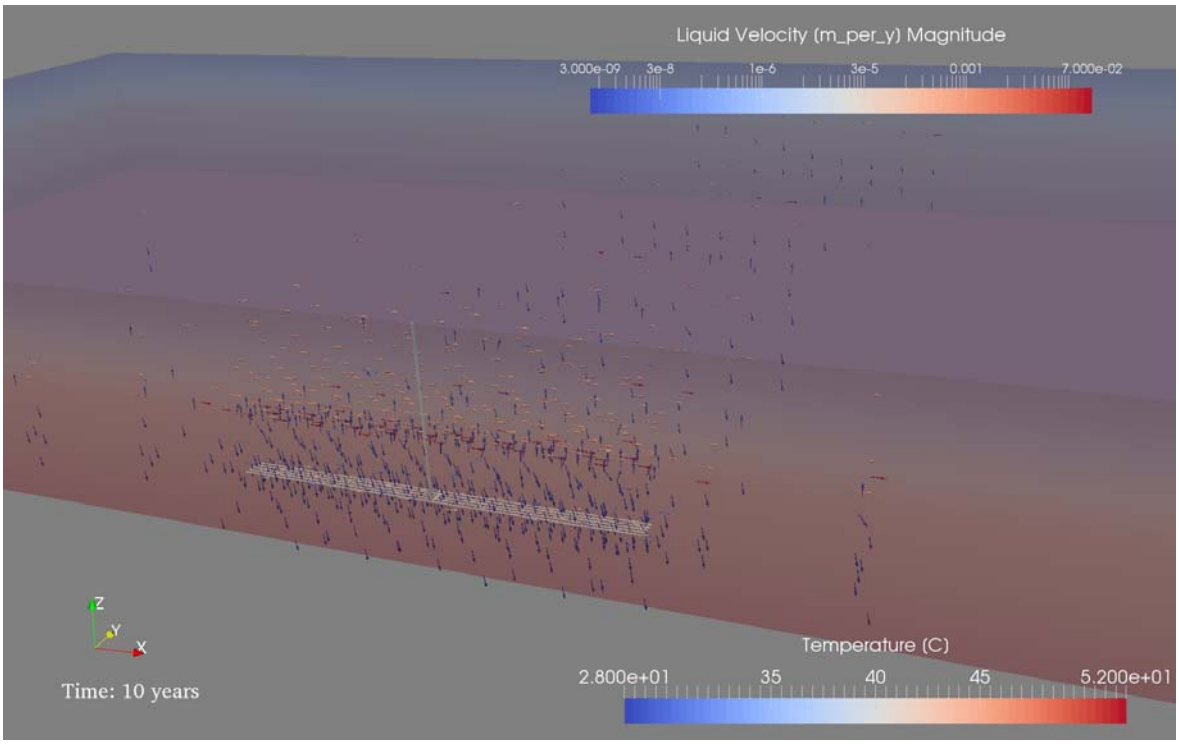

Figure 4-50. Fluid flow vectors and temperature at 10 years for the HLW simulation. Drifts and shaft are solid grey surfaces. The model domain is colored by temperature; fluid flow vectors by flow velocity.

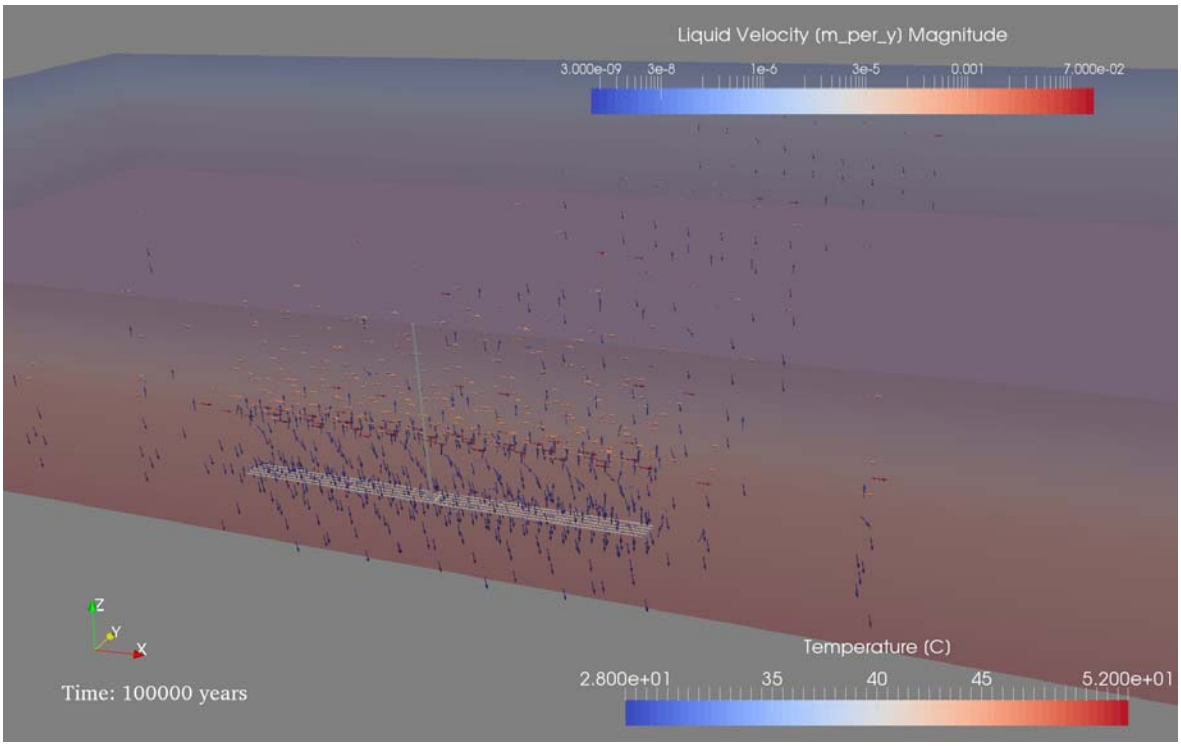

Figure 4-51. Fluid flow vectors and temperature at 100,000 years for the HLW simulation. Drifts and shaft are solid grey surfaces. The model domain is colored by temperature; fluid flow vectors by flow velocity.

Initial ^{129}I concentration in the pore fluid of the waste packages is essentially zero (instantaneous release is not included in this simulation). Over the duration of the simulation, this concentration increases variably due to variable waste form degradation rates (Figure 4-52 through Figure 4-54). At 1000 years, ^{129}I is still confined to the immediate vicinity of the repository (Figure 4-55). By 10,000 years it has begun to diffuse up the shaft and into the anhydrite interbeds (Figure 4-56) and by 100,000 years it has reached the overlying aquifer and begun to advect eastward (in the direction of the regional flow field; Figure 4-57).

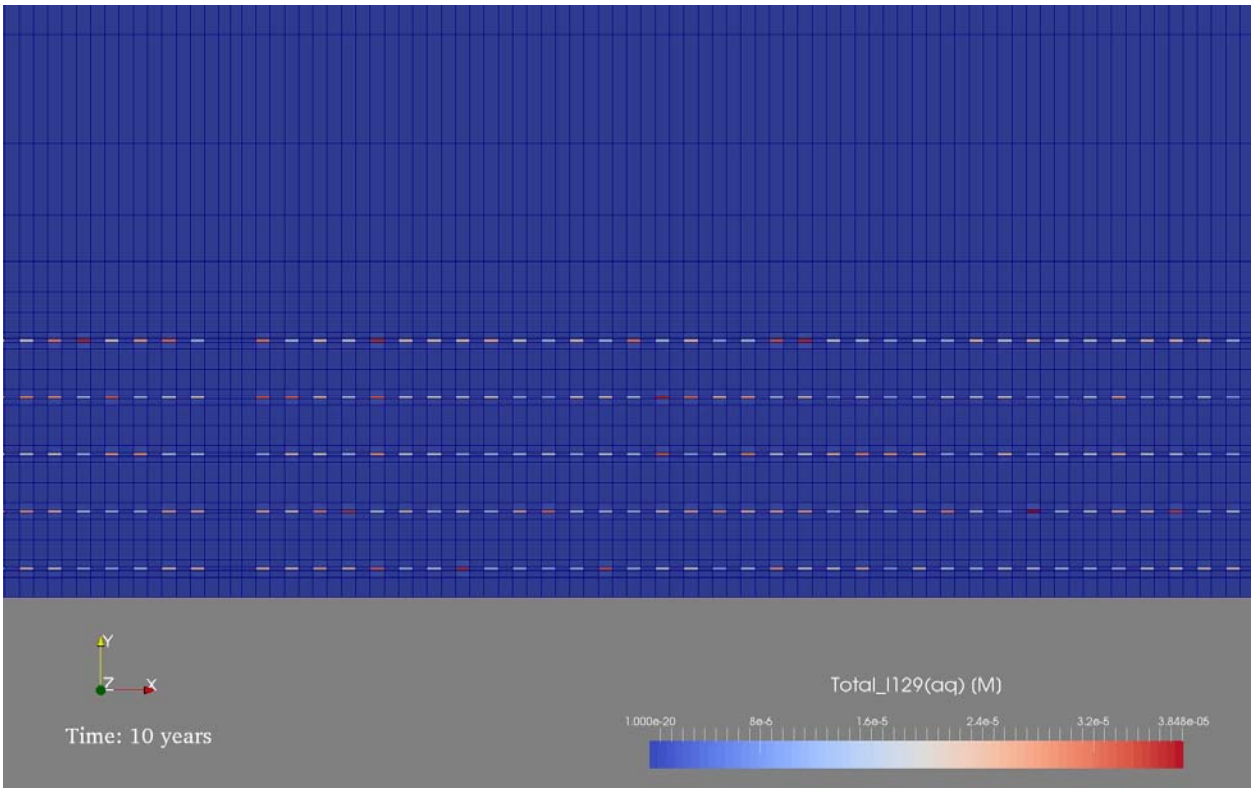

Figure 4-52. ^{129}I concentration in an x-y slice through the HLW repository at 10 years. Waste packages can be identified by their high and variable ^{129}I concentrations. The area to the left without waste packages is the access hallway.

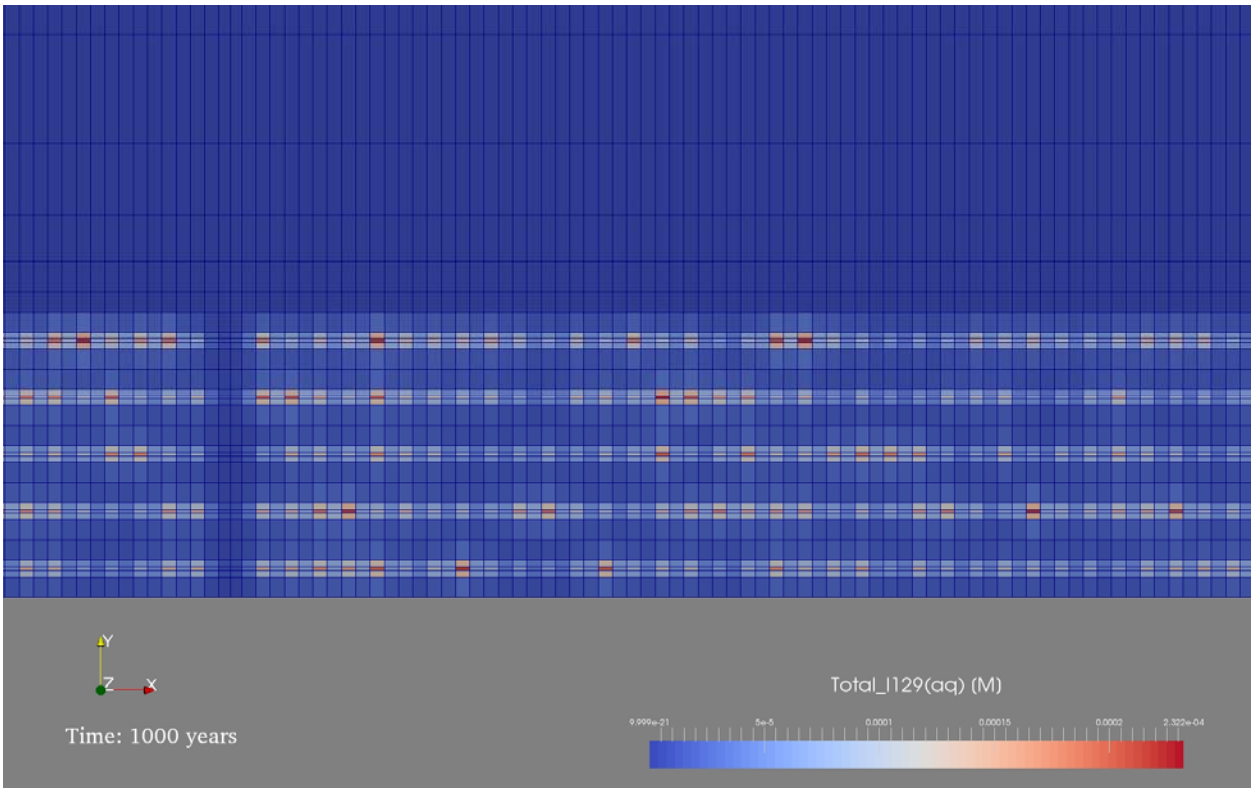

Figure 4-53. ^{129}I concentration in an x-y slice through the HLW repository at 1000 years. Maximum concentration is greater than that at 10 years (Figure 4-52).

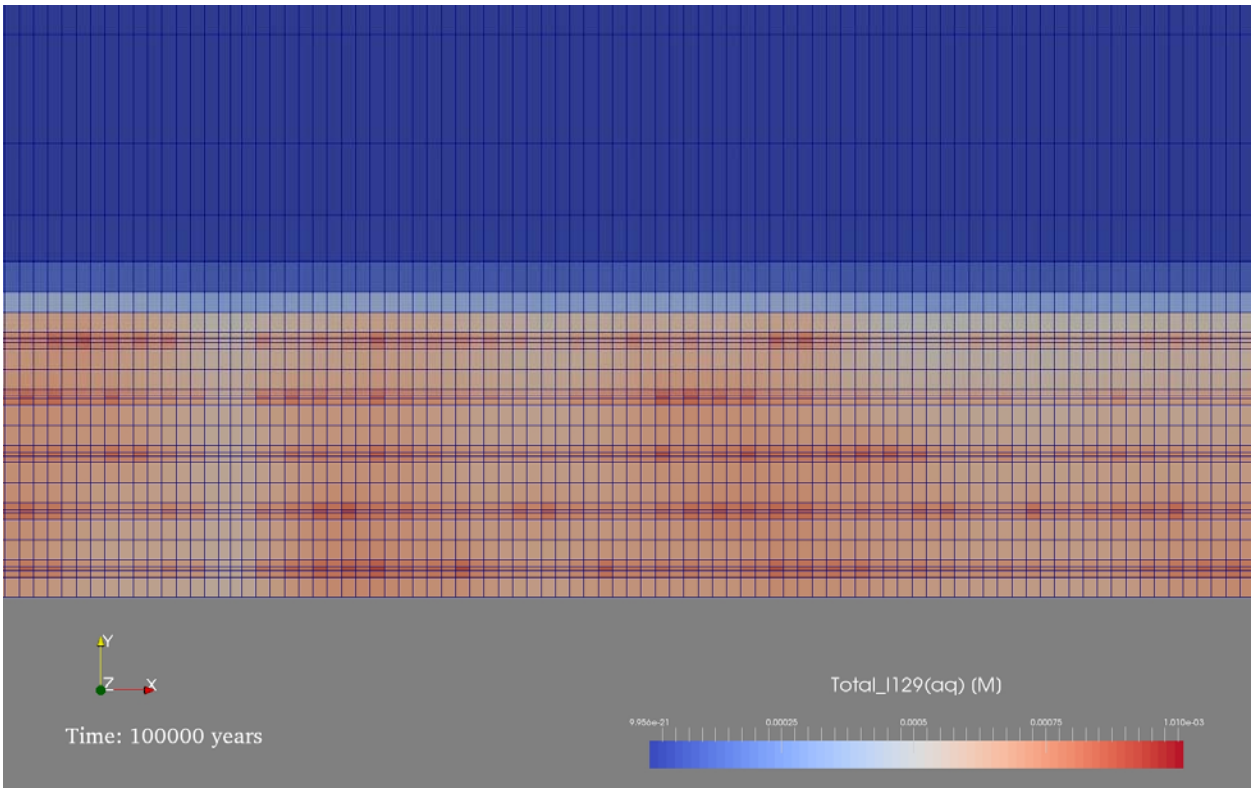

Figure 4-54. ^{129}I concentration in an x-y slice through the HLW repository at 100,000 years. Maximum concentration is greater than that at 1000 years (Figure 4-53).

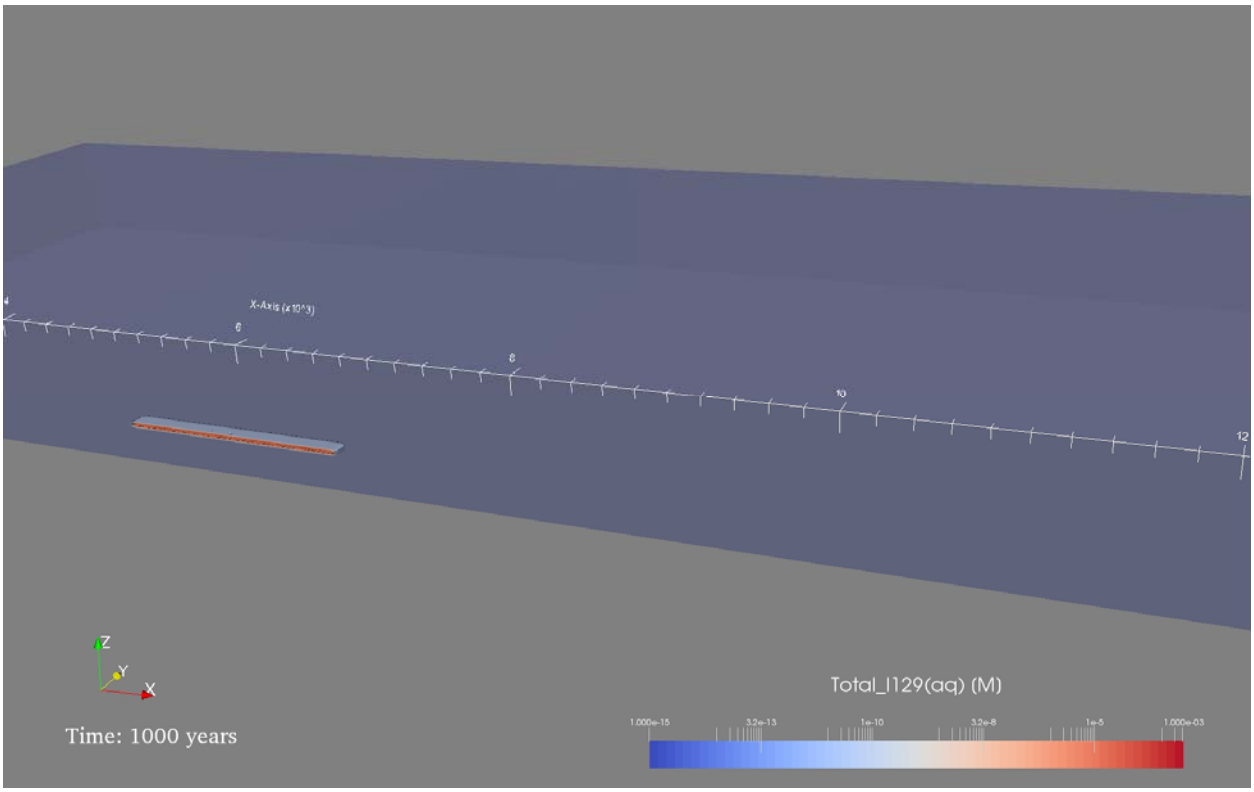

Figure 4-55. ^{129}I concentration at 1000 years for the HLW simulation. Waste packages are plotted as solid grey surfaces. Contours and the model domain are colored by ^{129}I concentration (on a log scale).

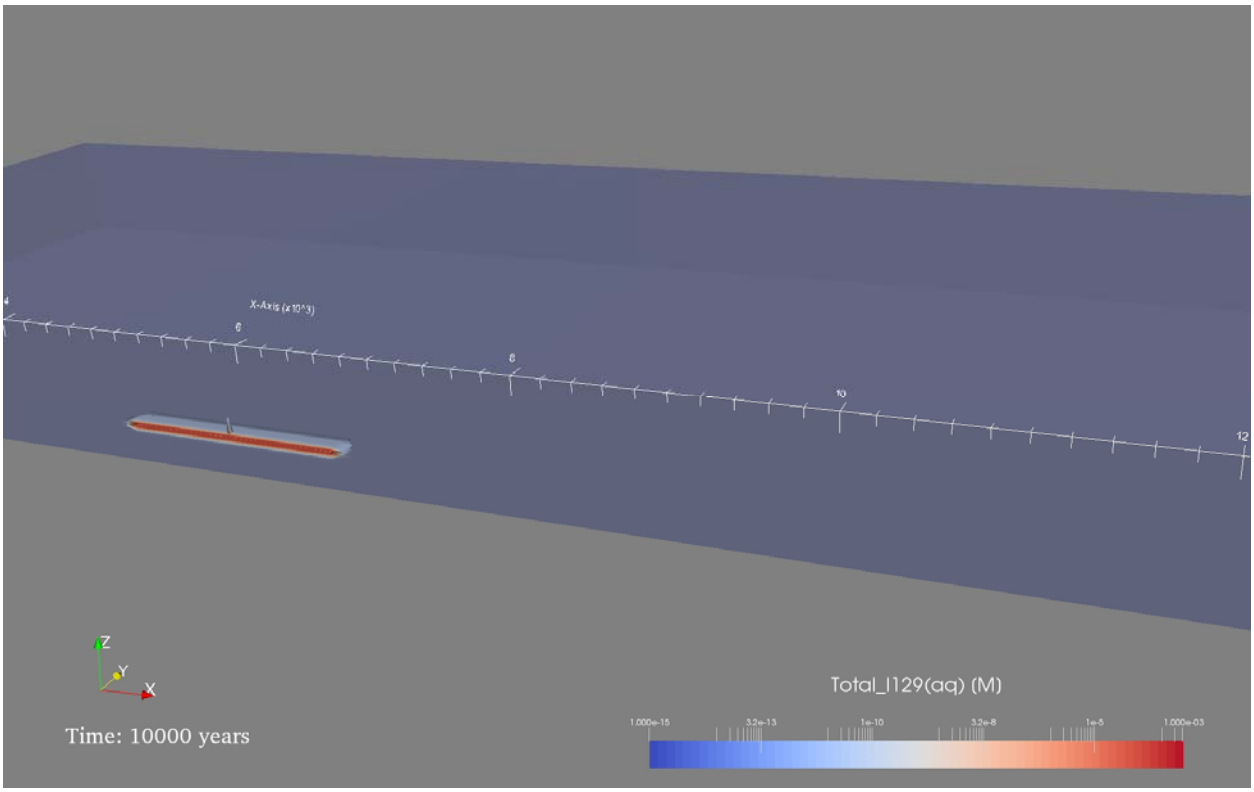

Figure 4-56. ^{129}I concentration at 10,000 years for the HLW simulation. Contours and the model domain are colored by ^{129}I concentration (on a log scale).

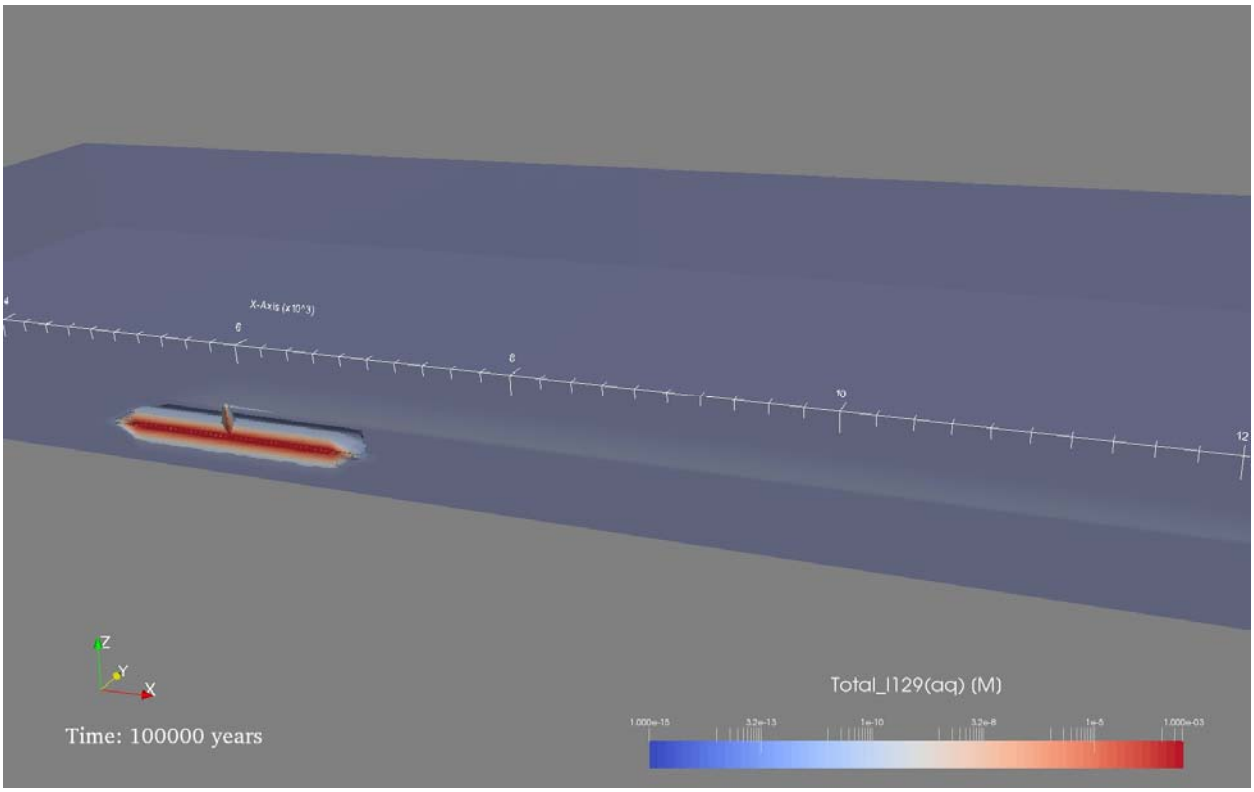

Figure 4-57. ^{129}I concentration at 100,000 years for the HLW simulation. Contours and the model domain are colored by ^{129}I concentration (on a log scale).

4.3 Clay Reference Case for UNF

Clay-rich sedimentary strata have been considered a potential medium for disposal of radioactive waste in the United States since the forerunner to the DOE introduced a program to develop radioactive waste disposal technology in 1976 (Shurr 1977, Gonzales and Johnson 1985). Clay-rich formations are an attractive disposal medium due to their low permeability, high sorption capacity, typically reducing porewaters (which limit radionuclide solubility), and (if not indurated) ability to deform plastically, which promotes self-healing of fractures.

The clay reference case draws upon the recent work of Hansen et al. (2010), Clayton et al. (2011), and Freeze et al. (2013b) for conceptualization of a mined geologic repository in shale, and upon Jove Colon et al. (2014) for the details of drift-emplacement and the engineered barrier system.

The U.S. hosts several marine sedimentary sequences containing thick beds of clay-rich sediments potentially suitable for deep geologic disposal of radioactive waste (Gonzales and Johnson 1985; Perry et al. 2014). Of these, the Pierre Shale in the northern Great Plains was considered for radioactive waste isolation by Shurr (1977), who lists a number of criteria for assessing the suitability of a shale or similar clay-rich formation for geologic disposal of radioactive waste. The same or similar criteria are considered by later authors (Gonzales and Johnson 1985; Hansen et al. 2010; Perry et al. 2014; Jove Colon et al. 2014) and include:

- Depth – The isolation horizon should be from 300 to 900 m below surface.
- Shale thickness – Maximum thickness of the isolation medium is desired, and a minimum thickness of 150 m is preferred.

- Overburden thickness – Minimal thickness of overlying geologic units is preferred.
- Lithology and mineralogy – The repository interval should be a reasonably uniform shale or other clay-rich unit with few or no interbeds of more permeable lithology.
- Penetrations (boreholes) – Boreholes of any kind are undesirable, particularly if they penetrate to rocks below the disposal horizon. It is recognized that some holes are necessary to provide geologic information at depth.
- Structure – The disposal zone should have nearly horizontal bedding and the surrounding region should be structurally simple (e.g., no folding or faulting).
- Seismicity – Seismically inactive regions are preferred.
- Topography – Minimal topographic relief is desirable to limit the influence of topography on subsurface hydraulic gradients.
- Mineral and water resources – Regions with minimal exploitable mineral and water resources, at or below the surface, are preferred.

The generic disposal concept in clay is similar to that in salt. As in the salt case, waste disposal occurs in a mined repository located in a deep, homogeneous, thickly bedded, essentially flat-lying stratum in a geologically simple and stable environment. The repository has a waste capacity of 70,000 MTHM, the maximum allowed in the Nuclear Waste Policy Act of 1983 (Sevougian et al. 2013), and the inventory is UNF. The repository consists of excavated emplacement drifts separated by an intact clay formation. Drifts are laid out in pairs, separated by a central access hallway, and shafts are used for construction, operation, and ventilation. Waste packages are emplaced horizontally, end-to-end in each drift.

The clay reference case differs from the salt reference case in ground support methods, backfill material, and thermal considerations. Whereas a mined repository in salt requires minimal ground support, it is assumed that a mined repository in clay will require cement liners in drifts, hallways, and shaft to prevent spalling (Jove Colon et al. 2014). Unlike the salt case (in which crushed salt is used as backfill), in the clay case, waste packages are buffered and drifts, hallway, and shafts are backfilled with bentonite (a clay formed from the alteration of volcanic ash, and like other unlithified clay-rich sediments having low permeability, high sorption capacity, and the ability to deform plastically.) Disposal in clay presents greater thermal challenges than disposal in salt due to the low thermal conductivity of clay/bentonite and concern that near field temperatures above 100°C will alter properties of the bentonite buffer (Hardin et al. 2011; 2012). In order to moderate near field temperatures in this iteration of the clay reference case, we (1) assume a double-layered bentonite buffer, in which the layer in contact with the waste packages is mixed with quartz sand thereby increasing its thermal conductivity (Jove Colon et al. 2014); and (2) age the UNF to 100 years OoR. As understanding of the effects of temperature on repository performance improves, future iterations of the clay reference case may take alternate approaches to moderating near field temperatures.

The clay conceptual and numerical models are further defined as described below in Sections 4.3.1 through 4.3.4 (Waste Inventory, Natural Barrier System, Engineered Barrier System, Thermal and Chemical Environment).

4.3.1 Waste Inventory

The waste inventory for the clay reference case is identical to the UNF inventory considered in the salt reference case (i.e., 70,000 MTHM comprised entirely of PWR assemblies with a burnup of 60 GWd/MTHM and initial enrichment of 4.73 wt% ^{235}U), except that in the clay case, we assume the UNF is aged to 100 years OoR. This assumption is necessary to regulate temperature in the repository due to the low thermal conductivity of bentonite and clay/shale. Initial radionuclide inventories for the clay case

(100 yr OoR) are given in Table 4-14 (Carter et al. 2013). Heat of decay as a function of time can be read from Figure 4-2, beginning at 100 years.

Table 4-14. UNF Radionuclide inventory of selected radionuclides for the clay reference case.

Isotope	Waste inventory mass[1] (g/MTHM)	Molecular weight[2] (g/mol)	Mass fraction (g / g UNF)	Mole per gram (mol / g UNF)
^{238}U	9.10×10^{5}	238.05	6.32×10^{-1}	2.65×10^{-3}
^{237}Np	1.40×10^{3}	237.05	9.72×10^{-4}	4.10×10^{-6}
^{241}Am	1.46×10^{3}	241.06	1.01×10^{-3}	4.21×10^{-6}
^{242}Pu	8.17×10^{2}	242.06	5.67×10^{-4}	2.34×10^{-6}
^{129}I	3.13×10^{2}	129.00	2.17×10^{-4}	1.68×10^{-6}
^{234}U	5.11×10^{2}	234.04	3.55×10^{-4}	1.52×10^{-6}
^{230}Th	1.04×10^{-1}	230.03	7.22×10^{-8}	3.14×10^{-10}
^{233}U	4.33×10^{-2}	233.04	3.01×10^{-8}	1.29×10^{-10}
^{229}Th	1.48×10^{-5}	229.03	1.03×10^{-11}	4.49×10^{-14}
^{226}Ra	3.99×10^{-5}	226.03	2.77×10^{-11}	1.23×10^{-13}

[1] from Carter et al. (2013, Table C-2)

[2] from Sevougian et al. (2013, Table 1)

4.3.2 Natural Barrier System

The natural barrier system (NBS) comprises the clay formation hosting the repository, the disturbed rock zone (DRZ) adjacent to the repository, and geological formations above and below the host formation. On the basis of stratigraphic sequences observed in sedimentary basins throughout the U.S. (Gonzales and Johnson 1985; Perry et al. 2014), the NBS is conceptualized as a thick (on the order of thousands of meters) marine depositional sequence created by transgression and regression of inland seas, and consisting of thick layers of low permeability sediments such as shales and marls alternating with thinner layers of high permeability sediments such as limestones and sandstones. Specifically, the NBS includes (Figure 4-59), a 500-m thick shale formation containing a homeogeneous repository horizon and two thin high-permeability interbeds (such as limestone); two 50-m thick sandstone aquifers above and below the shale; 200 m of generic (unlithified) sediments above the upper aquifer; and a 100-m thick low-permeability confining layer (such as another shale formation) below the lower aquifer. Layer thicknesses and material properties are loosely based on the regional stratigraphy surrounding the Cretaceous Pierre Shale and Dakota Sandstone (e.g., Shurr 1977; Bredehoeft et al. 1983), and are consistent with those used in previous models of generic clay repositories (Hansen et al. 2010; Bianchi et al. 2015) and within the range of those found in other marine depositional sequences in the U.S. (Gonzales and Johnson 1985; Perry et al. 2014).

Deterministic parameter values used to define the material properties of the components of the NBS are summarized in Table 4-15, and likely ranges of values are discussed in Sections 4.3.2.1 through 4.3.2.6.

Table 4-15. Key deterministic parameters for the clay reference case NBS.

Model Region	Permeability (m^2)	Porosity	Tortuosity[1]	Effective Diffusion Coefficient[2,7] (m^2/s)	Longitudinal Dispersivity (m)[3]	Saturated Thermal Conductivity[4,7] (W/m/K)	Heat Capacity[5] (J/kg/K)	Grain Density[6] (kg/m^3)
DRZ	3.16×10^{-19}	0.25	0.25	6.25×10^{-11}	0.0	1.7	830	2700
Shale	3.16×10^{-20}	0.25	0.25	6.25×10^{-11}	0.0	1.7	830	2700
Interbed	1.00×10^{-16}	0.20	0.20	4.00×10^{-11}	50.0	2.5	830	2700
Aquifer	3.16×10^{-15}	0.20	0.20	4.00×10^{-11}	50.0	3.0	830	2700
Sediment	1.00×10^{-15}	0.20	0.20	4.00×10^{-11}	50.0	1.7	830	2700
Confining Layer	3.16×10^{-20}	0.20	0.20	4.00×10^{-11}	50.0	1.7	830	2700

[1] Tortuosity calculated using Archie's law with n = 2 (Boudreau, 1996)
[2] Effective diffusion coefficient = (free water diffusion coefficient) × (tortuosity) × (porosity) × (saturation), where the free water diffusion coefficient is 10^{-9} m^2/s, appropriate for porewater similar to seawater (Li and Gregory, 1974)
[3] Transverse dispersivity = 0
[4] Estimated from Robertson (1988)
[5] Representative value based on values for calcite, quartz, feldspar, and clay (Robie and Hemingway, 1995)
[6] Representative value based on values for calcite, quartz, feldspar, and clay (Klein and Hurlbut, 1993)
[7] Saturation function = Brooks-Corey for all units; however, all material regions are fully saturated, i.e., $S_w = 1$

4.3.2.1 Disturbed Rock Zone

The disturbed rock zone (DRZ) is the volume of the host rock (shale) in which material properties are altered by the process of mining the repository. The DRZ encompasses the entire volume of the pillars that separate the drifts and extends about 9 m (twice the drift diameter) into the host rock surrounding the repository. Within the DRZ, loss of confining pressure due to drift excavation may cause expansion and fracturing, potentially increasing porosity and permeability. In deterministic model simulations, the porosity of the DRZ is held equal to that of the host shale and the permeability is set one order of magnitude larger than that of the host shale. In probabilistic simulations, the one order of magnitude increase in permeability is maintained and DRZ porosity is varied from 0.1 to 0.4 with a uniform uncertain distribution.

4.3.2.2 Repository Horizon (Shale)

The repository horizon is a 500-m thick clay-rich formation, for convenience referred to as shale. Clay-rich formations suitable for isolation of radioactive waste span a range of rock types, varying in degree of foliation and degree of consolidation and induration, from unconsolidated mud (such as the Boom Clay) to argillite (such as the Callovo-Oxfordian argillite) (Hansen et al. 2010). Porosity of such formations varies from <0.05 to >0.4, while permeability varies from on the order of 10^{-22} m^2 to 10^{-17} m^2 (Jove Colon et al. 2014; Hansen et al. 2010). The clay reference case uses deterministic values for porosity and permeability from the middle of this range. In probabilistic simulations shale porosity is varied between 0.1 and 0.4 with a uniform uncertain distribution.

4.3.2.3 High-Permeability Interbeds

In the clay reference case, the repository is centered in a 150-m thickness of homogeneous shale. Five-meter-thick high-permeability interbeds are placed 125 m above and below the repository. Their hydraulic properties are loosely based on those of limestone aquifers (Freeze and Cherry 1979). The interbeds are a potential conduit for fluid advection, and probabilistic simulations sample on interbed permeability using a log-uniform uncertain distribution, where log k (m^2) = -18 to -14.

4.3.2.4 Aquifers

Fifty-meter-thick aquifers are placed above and below the shale horizon. Material properties are based on sandstone (Freeze and Cherry 1979; Bredehoeft et al. 1983). In probabilistic simulations, aquifer permeability is varied using a log-uniform uncertain distribution between log k (m^2) = -16 to -13 (the range observed for sandstone; Freeze and Cherry 1979).

4.3.2.5 Upper Sediments

Material properties of the upper sediments are based on glacial till or other unlithified silty deposit (Freeze and Cherry 1979), such as might sit unconformably on top of an older stratigraphic sequence.

4.3.2.6 Lower Confining Layer

The lower confining layer is modeled as shale.

4.3.3 Engineered Barrier System

The engineered barrier system (EBS) comprises the waste form, waste package, layered buffers, shotcrete liners, and seals. Parameters used to define material properties for deterministic simulations are listed in Table 4-16. Sections 4.3.3.1 through 4.3.3.5 provide additional description of EBS components. Section 4.3.3.6 describes the repository layout.

Table 4-16. Key deterministic parameters for the clay reference case EBS.

Model Region	Permeability (m^2)	Porosity	Tortuosity[1]	Effective Diffusion Coefficient[2,8] (m^2/s)	Longitudinal Dispersivity (m)[3]	Saturated Thermal Conductivity[4,8] (W/m/K)	Heat Capacity[5] (J/kg/K)	Grain Density[6] (kg/m^3)
Waste Package[7]	1.00×10^{-13}	0.30	1.00	3.00×10^{-10}	0.5	16.7	466	5000.0
Buffer 1	1.00×10^{-16}	0.25	0.25	6.25×10^{-11}	0.0	2.5	830	2700
Buffer 2	5.00×10^{-21}	0.40	0.40	1.60×10^{-10}	0.0	2.5	830	2700
Shotcrete	1.00×10^{-17}	0.15	0.15	2.25×10^{-11}	0.0	1.7	830	2700

[1] Tortuosity calculated from Archie's law with n=2 (Boudreau, 1996), except for waste package.
[2] Effective diffusion coefficient = (free water diffusion coefficient) × (tortuosity) × (porosity) × (saturation), where the free water diffusion coefficient is 10^{-9} m^2/s, appropriate for porewater similar to seawater (Li and Gregory, 1974).
[3] Transverse dispersivity = 0.
[4] Estimated from Robertson (1988), except for waste package.
[5] Representative value based on values for calcite, quartz, feldspar, and clay (Robie and Hemingway, 1995), except for waste package.
[6] Representative value based on values for calcite, quartz, feldspar, and clay (Klein and Hurlbut, 1993), except for waste package.
[7] Freeze et al. (2013b) and Sevougian et al. (2014).
[8] Saturation function = Brooks-Corey for all units; however, all material regions are fully saturated, i.e., $S_w = 1$

4.3.3.1 Waste Form

The waste form is PWR UNF with a burnup of 60 GWd/MTHM and initial enrichment of 4.73 wt% ^{235}U, aged 100 yr OoR. As in the salt case, each PWR assembly is assumed to contain 0.435 MTHM and 1.44×10^6 g/MTHM of radioisotopes. Initial mass fractions of radionuclides (Table 4-14) differ slightly from those in the salt reference case due to the additional time OoR. The instant release fraction of ^{129}I (0.025) and the degradation rate of the waste form (4.8×10^{-8} $mol/m^2/s$, Section 4.1.5.7) and specific surface area (9.5 m^2/m^3) are identical to the values used in the salt reference case, and are defined on the basis of fuel corrosion rates in various synthetic groundwaters (Kienzler et al. 2012). As in the salt case, probabilistic simulations sample on waste form degradation rate using a log-uniform uncertain distribution.

4.3.3.2 Waste Package

The waste package is assumed to consist of a stainless steel canister containing 12 PWR UNF assemblies (5.22 MTHM) and a carbon steel overpack. The waste package is 5 meters in length and has a diameter of 1.29 m, consistent with the 12-PWR waste package described by Hardin et al. (2012) and identical to that used in the salt case. See Freeze et al. (2013b) for development of waste package model parameters (material properties). The clay reference case makes the conservative assumption that all waste packages fail instantly.

4.3.3.3 Bentonite/Quartz Buffer

The clay reference case assumes that waste packages will be emplaced in a double layer of bentonite buffers (Figure 4-58; Jove Colon et al. 2014). The buffer layer immediately surrounding the waste package will consist of a mixture of bentonite and quartz sand. The bentonite provides low permeability and high sorption capacity, while the addition of quartz sand increases the thermal conductivity of the buffer. In the current iteration of the clay reference case, the thickness of the bentonite/quartz buffer is 1.5 m (Jove Colon et al. 2014), and its thermal properties are appropriate for a mixture of 70% bentonite and 30% quartz (approximated from values in Robertson 1988). The porosity of a bentonite/quartz buffer would depend on the composition of the mixture and method of mixing and emplacing. In probabilistic simulations, porosity is varied between 0.1 and 0.4 with a uniform uncertain distribution.

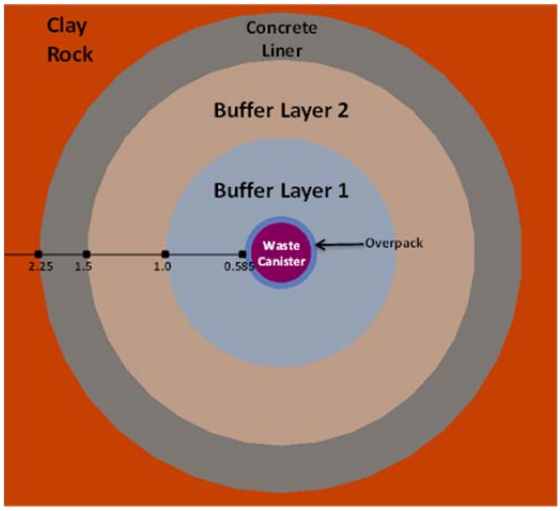

Figure 4-58. Cross section of the clay reference case disposal drift (from Jove Colon et al. (2014)). Buffer Layer 1 is bentonite/quartz. Buffer Layer 2 is bentonite.

4.3.3.4 Bentonite Buffer, Seals, and Shaft

The clay reference case assumes an additional buffer of pure bentonite between the bentonite/quartz buffer and the shotcrete lining the walls of the disposal drifts. Material properties are defined on the basis of those measured for FEBEX bentonite and MX-80 bentonite (Jove Colon et al. 2014). This iteration of the clay reference case assumes that pure bentonite is used to seal 5 meters of each drift adjacent to the access hallway, as well as to seal the access hallway itself and the shafts. Future iterations may consider more complex seals in drifts, hallway, or shaft, possibly including concrete and/or asphalt components (e.g., James and Stein 2002).

4.3.3.5 Shotcrete Liners

A mined repository in shale is expected to require the support of shotcrete (sprayed concrete). The assumed thickness in all excavations (drifts, halls, and shafts) is 0.75 m. Material properties are based on WIPP concrete and the shotcrete described in Jove Colon et al. (2014, Table 12).

4.3.3.6 Repository Layout

The repository layout is similar to that in the salt case. Pairs of disposal drifts lie at right angles to a central access hallway. Drift centers are separated by 20 m. Waste packages are emplaced horizontally, lengthwise within the drifts with a spacing of 10 m center-to-center (5-m spacing, end-to-end). Unlike the salt case, the drifts are assumed to have a circular cross-section with a diameter of 4.5 m (Jove Colon et al. 2014). Repository dimensions are listed in Table 4-17.

Hardin et al. (2011; 2012) recommend a larger drift spacing (30 m) and a smaller waste package (4 PWR) for an enclosed clay repository such as the one modeled here, in order to keep temperatures in the bentonite buffer ≤100°C as specified by international repository programs based on the findings of Bel and Bernier (2001). Jove Colon et al. (2013) note two mitigating factors: 1) that clay minerals are stable at temperatures >150°C, and 2) that future repository designs could include a "sacrificial" buffer layer in which alterations to clay mineralogy would be allowed. As research and development concerning engineered barriers continues, the clay reference case will be updated.

Table 4-17. Dimensions for the clay reference case repository.

Parameters	Value
Waste Package (WP)	
WP length (m)	5.00
WP outer diameter (m)	1.29
WP center-to-center spacing in-drift (m)	10.0
Inventory per 12-PWR WP (MTHM)	5.225
Approx. number of WPs for 70,000 MTHM	13,397.4
Emplacement Drift	
Drift diameter (m)	4.5
Drift center-to-center spacing (m)	20.0
Pillar width (m)	15.5
Number of WPs per drift	80
Drift seal length (m)	10.0
Drift length, including seals (m)	805.0
Central access hallway height (m)	4.5
Central access hallway width (m)	8.0
Approx. number of drifts needed for 70,000 MTHM	167.5
Repository	
Number of drift pairs (rounded up)	84
Repository length (m)	1,618.0
Repository width (m)	1,664.5
Repository Depth (m)	500.0
Total length of all drifts (m)	135,240

4.3.4 Thermal and Chemical Environment

Porewater of a deep, hydraulically isolated shale appropriate for radioactive waste disposal can be conceptualized as connate water (seawater) equilibrated (or partially so) with the surrounding mineral assemblage and isolated from the atmosphere. Such porewater is likely to be of moderate ionic strength, reducing, and of neutral to slightly alkaline pH, for instance the porewaters of the Callovo-Oxfordian argillite (Andra 2005) or the Opalinus Clay (Turrero et al. 2006).

4.3.4.1 Diffusion

Diffusion is expected to be a dominant means of radionuclide transport within the low permeability materials of the engineered and natural barrier systems. Effective diffusion coefficients (D_e) for each material are calculated as $D_e = \tau\phi s D_{pw}$, where τ is tortuosity, ϕ is porosity, s is saturation, and D_{pw} is the diffusion coefficient in porewater (1×10^{-9} m^2/s; Li and Gregory 1974).

In higher-permeability strata (i.e., interbeds and aquifer), fluid advection becomes a significant means of radionuclide transport and mechanical dispersion (the spreading of a solute due to variations in groundwater velocity) overwhelms diffusion. Radionuclide flux due to mechanical dispersion depends on linear fluid velocities and is proportional to material-dependent dispersivities. Relevant parameters for each material are given in Table 4-15 and Table 4-16.

4.3.4.2 Solubility

Andra (2005) calculated solubilities of radioelements in Callovo-Oxfordian porewater. Clayton et al. (2011) used these solubility values to benchmark their model for a clay generic disposal system, and we use them again here (Table 4-18). Ignoring the complexity of the near field environment (elevated temperature and the presence of introduced materials including oxygen, waste form, waste package, and bentonite buffer) and likely far field variations of porewater chemistry with depth, we assume homogeneous solubility limits throughout the model domain. Because we are tracking radioisotopes rather than elements, we convert elemental solubility to conditional isotope solubility by assuming that isotope ratios remain constant among waste form, aqueous phase, and secondary mineral phases.

Table 4-18. Element and isotope solubiity limits for clay reference case

Isotope	Element solubility limit[a]	Isotope ratio[b]	Isotope conditional solubility limit
	(mol/L)	(mol isotope / mol element)	(mol/L)
^{233}U	7.0E-07	4.7E-08	3.3E-14
^{237}Np	4.0E-09	1.00	4.0E-09
^{241}Am	4.0E-07	0.84	3.4E-07
^{129}I	infinitely soluble	0.77	infinitely soluble
^{229}Th	6.0E-07	1.2E-04	7.2E-11

[a] from Clayton et al. (2011, Table 3.3-23)

[b] calculated from 100 yr OoR, 60 GWd/MTHM inventory in Carter et al. (2013, Table C-2)

4.3.4.3 Sorption

Sorption is modeled using a linear isotherm; distribution of a solute between the aqueous and sorbed phase is characterized by the distribution coefficient K_d (Table 4-19), where the concentration in the sorbed phase is proportional to the concentration in the aqueous phase. The use of K_d is a simplification of a complex system. Distribution coefficients depend on the particular mineralogy, on the nature of the pore space, on temperature, and on pore water composition including ionic strength, pH, and eH (Miller and Wang 2012). It is expected that a site-specific PA would rely upon site-specific distribution coefficients

or other site-specific sorption parameters. For Am, Np, Th, and U, the clay reference case relies upon the range of distribution coefficients used in past models of clay repositories (McKinley and Scholtiss 1993; Hansen et al. 2010). Deterministic simulations use the midpoint of the range (determined on a log basis) for each element. This method results in deterministic values similar to or less then the values used by Andra (2005) to model sorption in the Callovo-Oxfordian argillite and by Clayton et al. (2011) to benchmark their model of a generic clay repository. Probabilistic simulations sample across the range of K_d values for neptunium (using a log uniform uncertain distribution). Iodine is often assumed to be non-sorbing (Andra 2005; Clayton et al. 2011; Bianchi et al. 2015), and the current clay reference case makes this assumption (K_d^{Iodine} = 0 mL/g) in the deterministic case. In the probabilistic case K_d^{Iodine} is varied over the same range of values as in the salt case (9.28×10^{-7} to 7.84×10^{-3} mL/g). This range is lower than that reported in McKinley and Scholtiss (1993), and on the low end of values tabulated in Miller and Wang (2012) for sorption of iodine in clay-rich sediments.

Table 4-19. Linear sorption coefficients (K_d) for clay reference case elements.

Element	K_d (mL/g)			
	Deterministic	Minimum	Maximum	Distribution
U	300	90	1000	log uniform
Np	173	30	1000	log uniform
Am	2970	300	29400	log uniform
I	0	9.28×10^{-7}	7.84×10^{-3}	log uniform
Th	1217	63	23500	log uniform

From McKinley and Scholtiss (1993) as tabulated in Hansen et al. (2010, Table 2.5-2), except for I, for which sorption is modeled identical to the salt reference case.

4.3.4.4 Temperature

Temperature in the repository depends on the background geothermal heat flux (Section 4.2.5.1) and on the heat pulse generated by radioactive decay of the waste (Figure 2). Though diffusion, solubility, and sorption are all expected to be temperature-dependent, at this time they are not modeled as such.

4.3.5 Clay Reference Case Conceptual and Numerical Models

4.3.5.1 Conceptual Model

The clay reference case conceptual model includes all of the components and processes described in Sections 4.3.1 – 4.3.4. It imagines a regional setting with no topographic relief, horizontal bedding, a regional geothermal heat flux of 60 mW/m^2 (appropriate for midcontinent; Blackwell et al. 2011), and a regional head gradient west to east of -0.0013 (m/m), similar to gradients observed in the Cretaceous aquifers of the northern Great Plains (Lobmeyer 1985; Downey and Dinwiddie 1988). The stratigraphic section is described in Section 4.3.2. The repository is placed in the middle of the shale layer, 500 m below the surface, and 5 kilometers from a hypothetical withdrawal well, at which distance radionuclide concentrations are monitored in the overlying aquifer.

Only the undisturbed scenario is considered. At repository closure (the start of the numerical simulation), the repository is assumed to be saturated with formation porewater and waste packages are assumed to have failed, resulting in an initial radionuclide concentration within each waste package calculated on the basis of initial radionuclide inventory (Section 4.3.1), initial release fraction (Section 4.3.3.1), and saturated porosity of the waste package (Table 4-16). Additional radionuclides are released as the waste form degrades (Section 4.3.3.1). Each waste package is conceptualized as a transient heat source. Energy output decreases with time and can be calculated at any time from the values in Figure 4-2 and the inventory of heavy metal in the waste package (Table 4-17). Processes include advective and conductive

heat transport, advective, diffusive, and dispersive solute transport, waste form degradation, precipitation and dissolution according to radionuclide solubility limits, sorption, and radioactive decay and ingrowth (in the aqueous phase).

4.3.5.2 Numerical Implementation

Numerical simulations of fluid flow and reactive transport for the clay reference case were performed using PFLOTRAN and a 3D, structured grid with variable spacing. Deterministic and probabilistic simulations were run isothermally, with regional fluid flow due to an east-west pressure gradient established with boundary conditions. The deterministic case was additionally run with coupled heat and fluid flow, in order to predict repository temperatures and examine the contribution of the heat of radioactive decay to fluid flow and radionuclide transport.

4.3.5.3 Model Domain

The model domain is a rectangular prism, 12,653.605 m long in the x direction, 5000 m wide in the y direction, and 900 m tall in the z direction (Figure 4-59 and Figure 4-60). The modeled repository (consisting of 5 drift pairs, a total of 800 waste packages, a central access hallway, and a shaft) sits at the front of the model domain (y = 0 m), 500 m below the surface, and approximately centered in the x direction. Due to the choice of a reflective boundary condition at y = 0 m, (see Section 4.3.5.6), this domain is equivalent to 10 drift pairs, 1600 waste packages, and 2 shafts centered in a 10,000 m wide domain. Material properties within the repository are assigned to regions representing the components of the EBS, with the exception of bentonite buffer and shotcrete liners, which were omitted for simplicity. Additionally the model domain is organized into horizontal layers corresponding to the components of the NBS with thicknesses and material properties assigned accordingly.

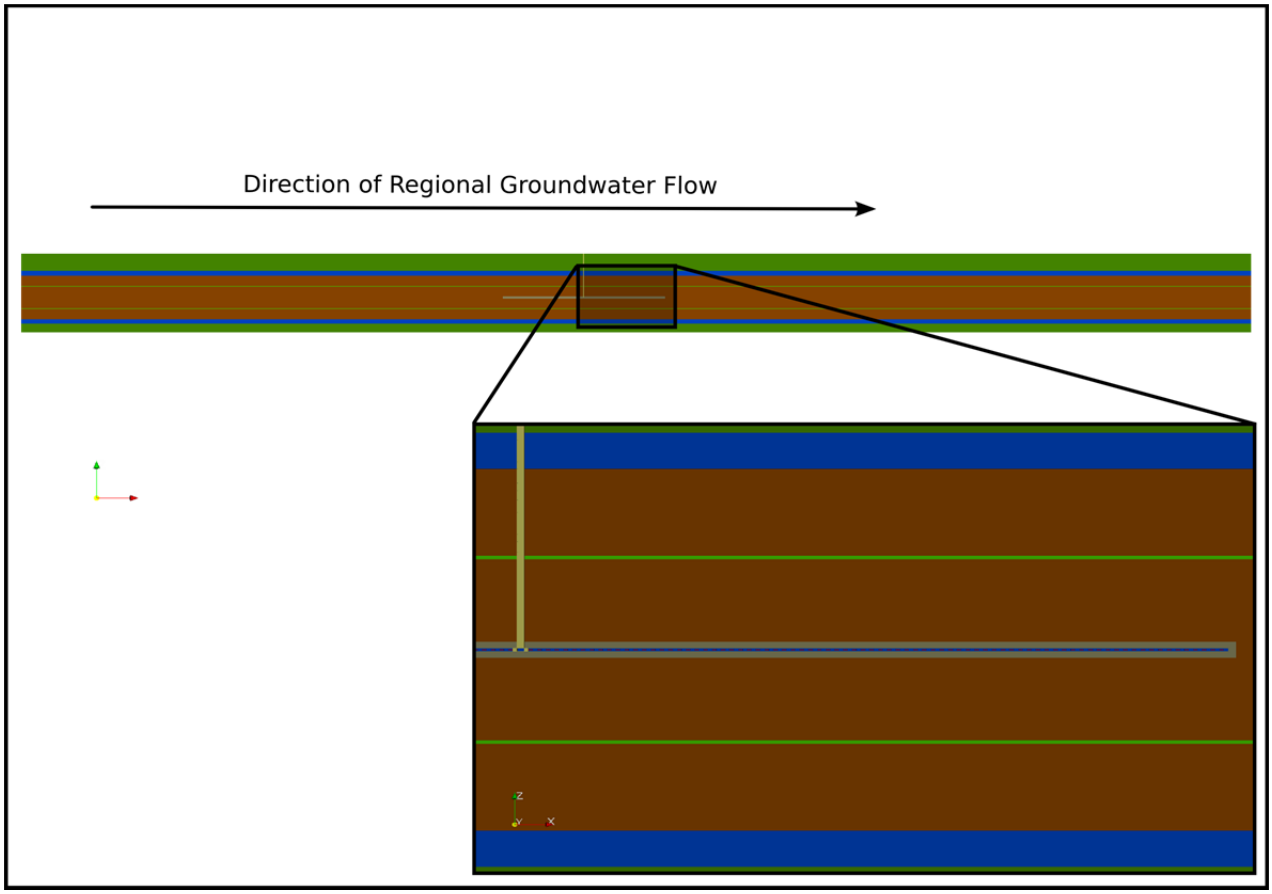

Figure 4-59. X-Z slice of the clay reference case model at the Y midpoint of the first drift pair in the repository. Clay is shown in dark brown, dark green is sediments, aquifers are shown in royal blue, grey is the DRZ, the inter beds are shown in bright green, bentonite/quartz buffer is shown in dark blue and the shaft and seals are shown in yellow.

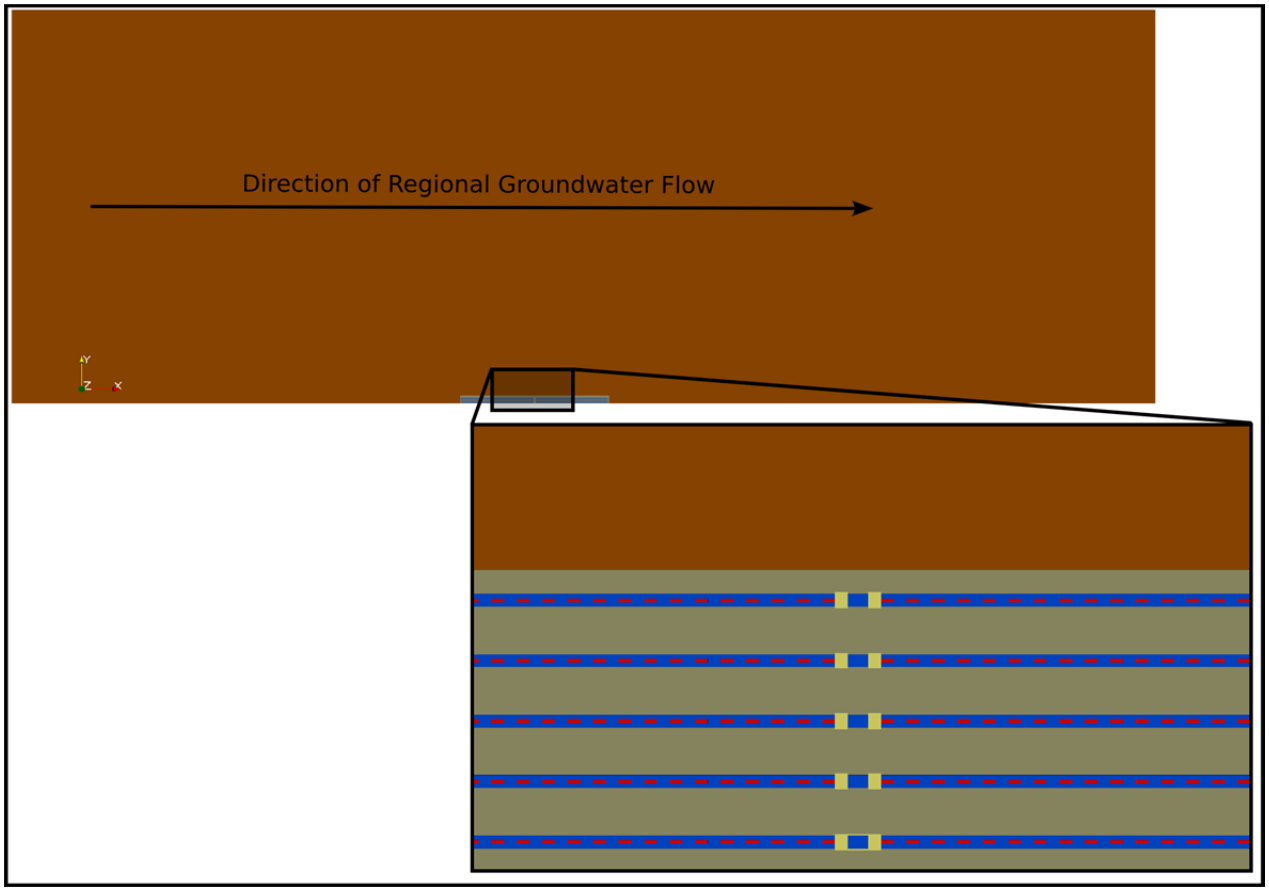

Figure 4-60. X-Y slice of the for the clay reference case model. Clay is brown, DRZ is grey, seals are yellow, bentonite/quartz buffer is dark blue and waste packages are shown in red.

4.3.5.4 Grid Spacing

Grid spacing is finest in the repository, where it is on the order of 1 m and dependent upon the dimensions of the various EBS components. Each waste package is a single grid cell, 5 by 1.29 by 1.014 m (resulting in a volume equal to that of the cylindrical waste package described in Section 4.3.3.2). With distance from the repository, grid spacing increases in the x and y directions. It decreases in the x direction as it approaches the east withdrawal boundary, providing a precise location at which to monitor radionuclide concentrations, and then increases to the end of the model domain. Grid spacing varies in the z direction in order to accommodate the repository, DRZ, interbeds, and aquifers. The maximum grid spacing is 227.6 m in the x direction, 1749 m in the y direction, and 40.5 m in the z direction. The total number of cells is 748 in x, 59 in y, 89 in z, and 3,927,748 in the entire model domain.

4.3.5.5 Initial Conditions

Isothermal simulations: Initial conditions specified are fluid pressure and radionuclide concentrations. Initial pressure throughout the model domain produces a hydrostatic gradient in the vertical direction, and a head gradient of -0.0013 (m/m) from west (left) to east (right). Simulations track 5 radionuclides: ^{241}Am, ^{237}Np, ^{233}U, ^{229}Th, and ^{129}I. Initial radionuclide concentrations in all cells except the waste package cells are 10^{-20} of mol/L, an approximation of 0 mol/L on a log basis. In the waste package cells, initial concentrations of ^{241}Am, ^{237}Np, ^{233}U, and ^{229}Th are set to 10^{-20} mol/L and initial concentrations of ^{129}I are 7.25×10^{-4} mol/L to account for the instant release of ^{129}I from the waste form.

Thermal simulations: In addition to initial fluid pressure and radionuclide concentrations, initial temperature is specified. Initial pressure and temperature are consistent with a head gradient of -0.0013 (m/m) from west (left) to east (right), a regional heat flow of 60 mW/m^2 applied at the bottom of the domain and a constant temperature of 10°C applied at the top of the domain. Initial radionuclide concentrations are identical to those in the isothermal simulations.

4.3.5.6 Boundary Conditions

Isothermal simulations: Boundary conditions must be set for the six faces of the model domain. The west (left), east (right), and back faces are held at initial pressures in order to maintain the west to east head gradient throughout the simulation time. Radionuclide concentrations at these faces are held such that any fluid entering the model domain contains 10^{-20} mol/L of each radionuclide, while fluid exiting the model domain is allowed to carry with it ambient concentrations. Diffusive flux is disallowed at the outlet boundary by specifying a zero concentration gradient. Top, bottom, and front faces of the domain are no-flow boundaries (constant head and concentration gradients of zero).

Thermal simulations: Boundary conditions for the six faces of the model domain are set as follows: The west (left), east (right), and back faces are held at initial pressures and temperatures. The top face is held at the initial temperature of 10°C and assigned a head gradient of zero (no fluid flow). A constant heat flux of 60 mW/m^2 is applied to the bottom face, which is assigned a head gradient of zero (no fluid flow). The front face is a no-flow boundary (neither fluid nor heat). As in the isothermal case, where fluid enters the model domain, it enters with all radionuclide concentrations set to 10^{-20} mol/L, and where it exits the model domain, it exits carrying ambient concentrations.

4.3.5.7 Waste Package Source Terms

Heat source: Each waste package is modeled as a transient heat source. The energy (watts per waste package) entering the model domain is updated periodically according to values in a lookup table. The initial value is that for PWR UNF 100 yr OoR. Time steps are synced with lookup table times, and between specified times, the energy input is linearly interpolated.

Radionuclide source: The degrading waste form is modeled as a far-from-equilibrium mineral, dissolving according to a zero-order rate law consistent with the degradation rate given in Section 4.3.3.1.

4.3.5.8 Solubility Limits

Radionuclide solubility limits are set by introducing fictious solid phases (one for each solubility-controlled radionuclide) with conditional solubilities (in terms of total aqueous concentration) equal to those in Table 4-18. Solid phases precipitate and dissolve at rates fast enough to maintain equilibrium between the solid and aqueous phases.

4.3.6 Clay Reference Case Results

Due to the conservative nature of ^{129}I (long half-life, unlimited solubility, and non-sorbing character), simulation results are discussed in terms of ^{129}I concentration.

4.3.6.1 Deterministic Isothermal Results

Iodine-129 concentrations in the model domain at various times are shown in Figure 4-61 through Figure 4-65. Because the bentonite shaft seal and the surrounding host shale have similar material properties, preferential diffusion up the shaft does not occur as it does in the salt case. At early times, while aqueous ^{129}I is confined to the repository, DRZ, and surrounding shale formation, transport is primarily by diffusion, as can be seen by the symmetrical nature of the 3D ^{129}I contours in Figure 4-61 through Figure 4-63. When ^{129}I reaches the aquifers above and below the shale, advective/dispersive transport becomes

important and the ^{129}I plume spreads out in the direction of regional groundwater flow (positive x, or to the east; Figure 4-64 and Figure 4-65). At 10^6 years (Figure 4-65), the 3D contour at the well observation location (x = 11,621 m) represents $[^{129}I] = 5 \times 10^{-11}$ mol/L. This concentration is approximately one order of magnitude less than the limit set by the World Health Organization for ^{129}I in drinking water (WHO 2011).

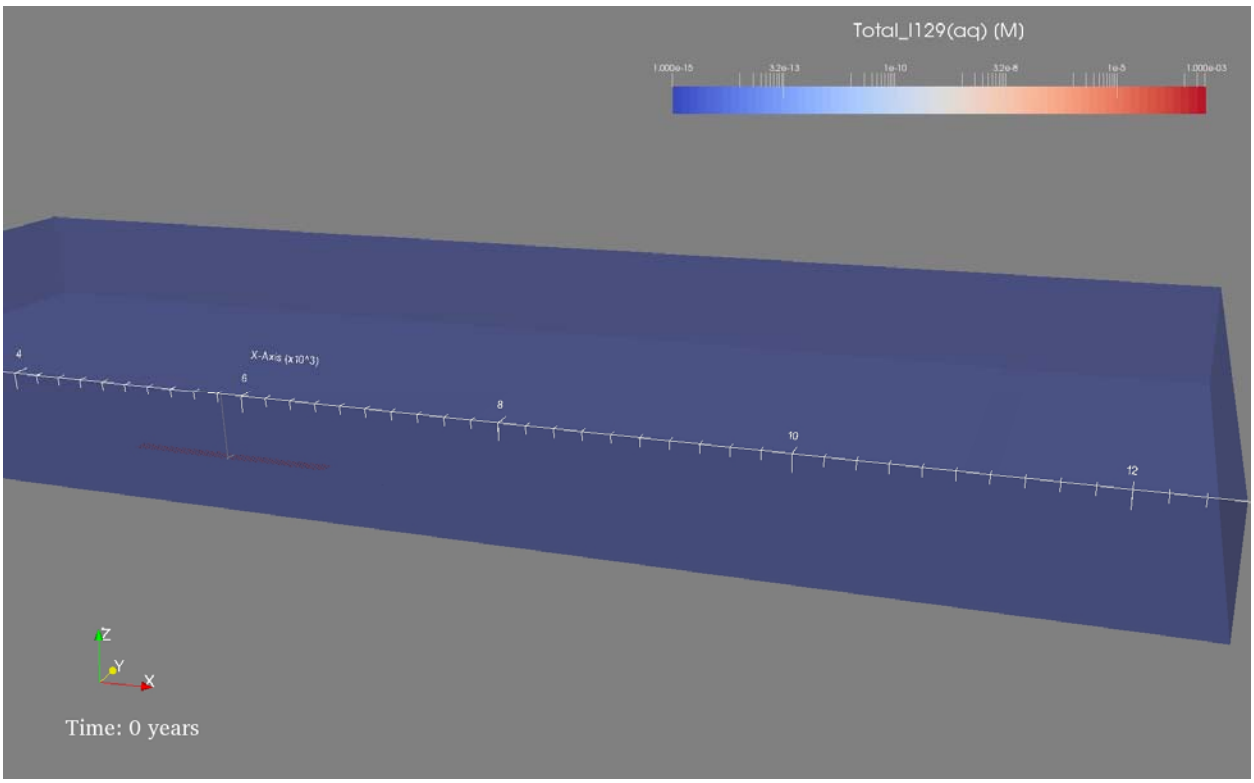

Figure 4-61. Initial ^{129}I concentration for the clay isothermal deterministic simulation. The red contours (5×10^{-5} mol/L) show the location of the waste packages in the repository. In this and the following figures, the volume of the model domain and the 3D contours are colored according to $[^{129}I]$. The shaft, hallway, and waste packages (obscured by the $[^{129}I]$ contours at early times) are represented as solid grey surfaces.

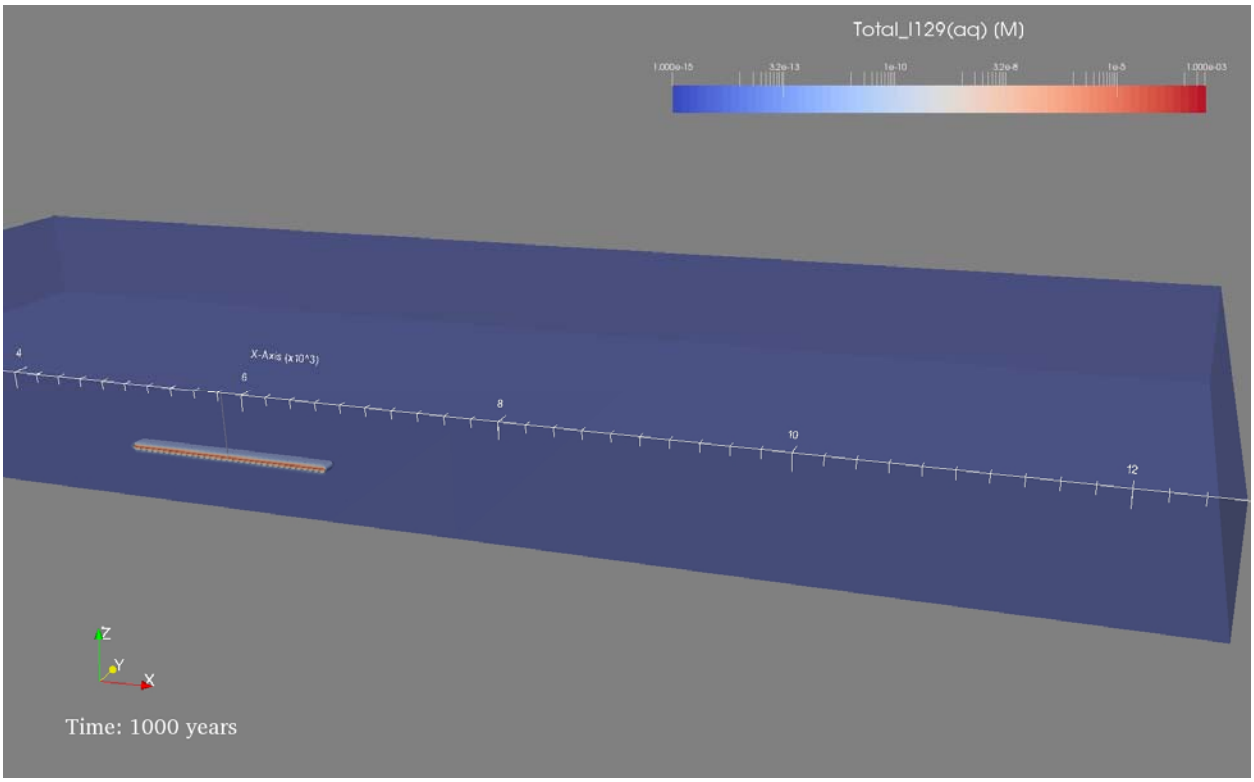

Figure 4-62. ^{129}I concentration at 1000 years. The shaft, hallway, and waste packages (obscured by the [^{129}I] contours at early times) are represented as solid grey surfaces.

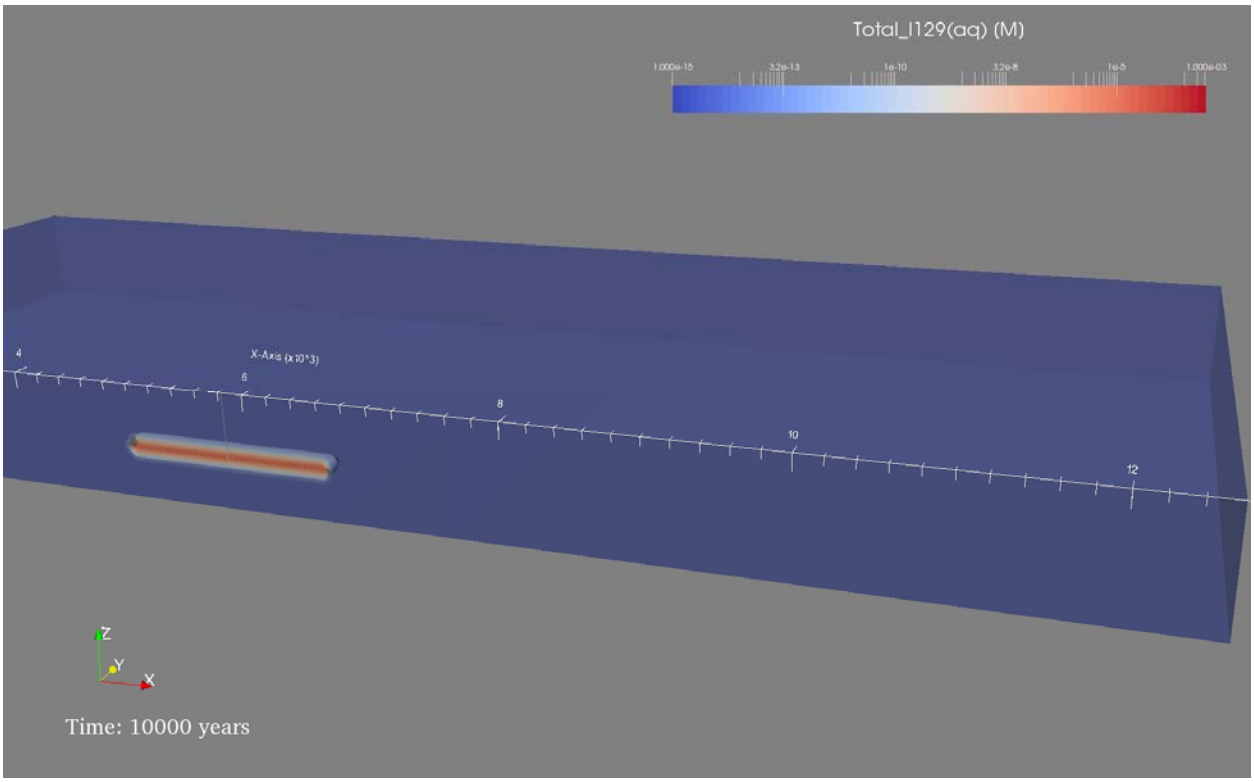

Figure 4-63. ^{129}I concentration at 10,000 years. The shaft, hallway, and waste packages (obscured by the [^{129}I] contours at early times) are represented as solid grey surfaces.

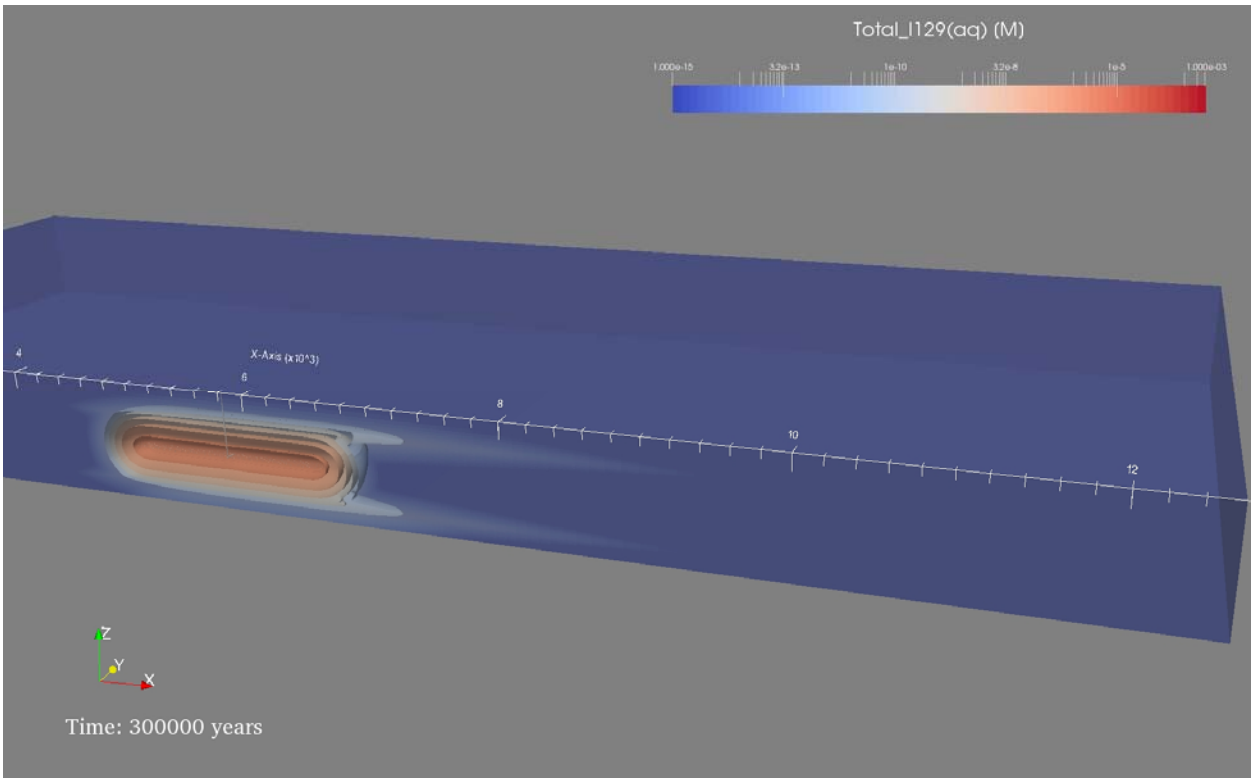

Figure 4-64. ^{129}I concentration at 300,000 years. The shaft, hallway, and waste packages are represented as solid grey surfaces.

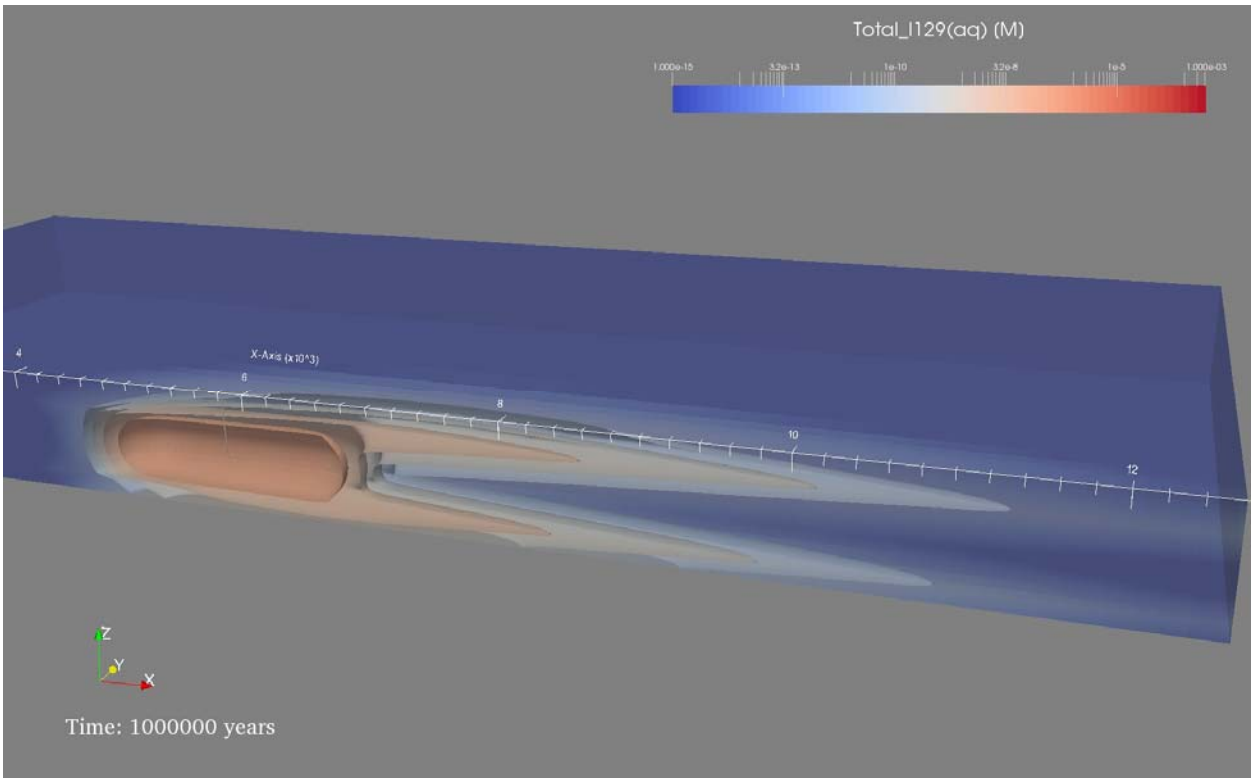

Figure 4-65. ^{129}I concentration at 1,000,000 years. The [^{129}I] = 5 × 10^{-11} mol/L contour falls just short of the well observation location at x = 11,621 m.

4.3.6.2 Probabilistic Isothermal Results

Selected parameters were sampled using the Dakota uncertainty quantification and sampling software system. The sampled parameters and their distributions are described in Sections 4.3.2 through 4.3.4 and summarized in Table 4-20. Radionuclide breakthrough (^{129}I) was monitored in 10 locations, all of which lie on the midline of the first drift pair (y = 10 m; Figure 4-66).

Table 4-20. Clay reference case probabilistic parameters.

Model Parameter	Deterministic Value	Probability Range	Distribution Type
Waste form degradation rate constant (mol/m^2/s)	4.8 × 10^{-8}	10^{-10} – 10^{-7}	Log uniform
^{129}I K_d (ml/g)	0.0	9.28 × 10^{-7} – 7.84 × 10^{-3}	Log uniform
^{237}Np K_d (ml/g)	173	30 – 1000	Log uniform
Bentonite/Quartz Buffer Porosity	0.25	0.1 – 0.4	Uniform
Shaft Porosity	0.4	0.1 – 0.4	Uniform
DRZ Porosity	0.25	0.1 – 0.4	Uniform
Shale Porosity	0.25	0.1 – 0.4	Uniform
Interbed Permeability (m^2)	1.0 × 10^{-16}	10^{-18} – 10^{-14}	Log uniform
Aquifer Permeability (m^2)	3.2 × 10^{-15}	10^{-16} – 10^{-13}	Log uniform

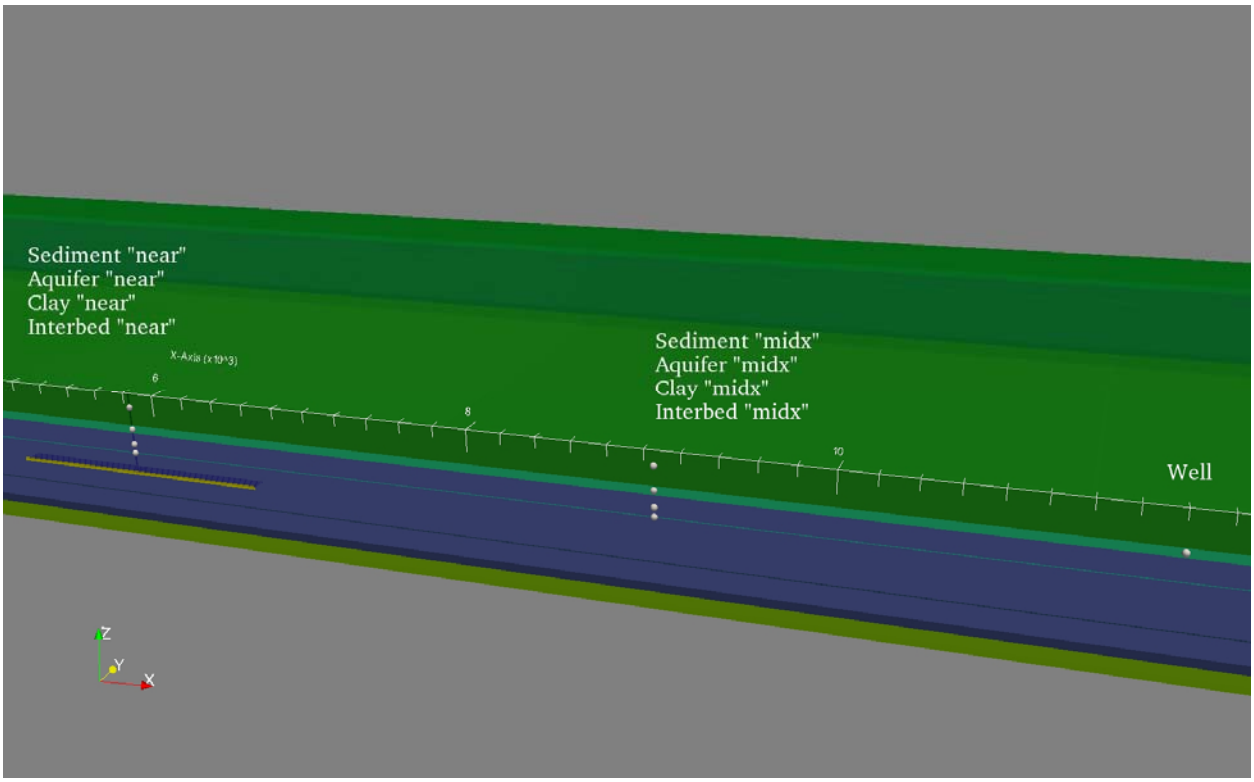

Figure 4-66. Locations of observation points for sensitivity analysis of probabilistic simulations. "Near" observation points are 7 m east of shaft. All observation points are located at y = 10 m (inside the model domain).

Figure 4-67 through Figure 4-75 show ^{129}I breakthrough curves for each of the observation points, and Figure 4-76 through Figure 4-84 show Spearman rank correlation coefficients relating maximum ^{129}I concentration to the sampled parameters. At the two observation points closest to the repository maximum ^{129}I concentrations vary by about one order of magnitude between simulations (Figure 4-67 and Figure 4-68), and depend predominately on waste form degradation rate (positive correlation) and shale porosity (negative correlation) (Figure 4-76 and Figure 4-77). At all other observation points, maximum ^{129}I concentrations vary by three orders of magnitude or more (as much as 11 orders of magnitude at the well observation location). At these observation points a strong dependence of maximum concentration on aquifer permeability (negative near the source, and positive farther from the source) is observed.

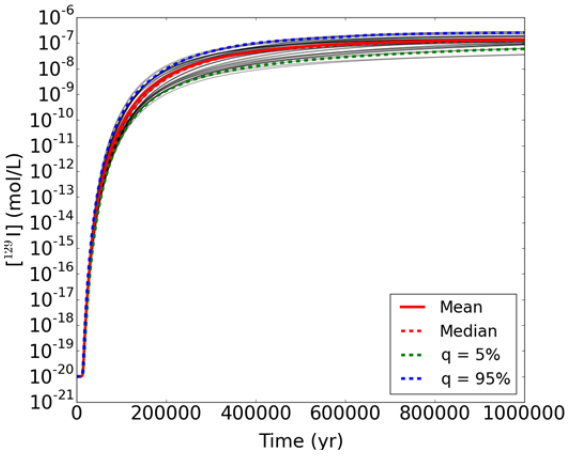

Figure 4-67. [^{129}I] versus time, clay "near".

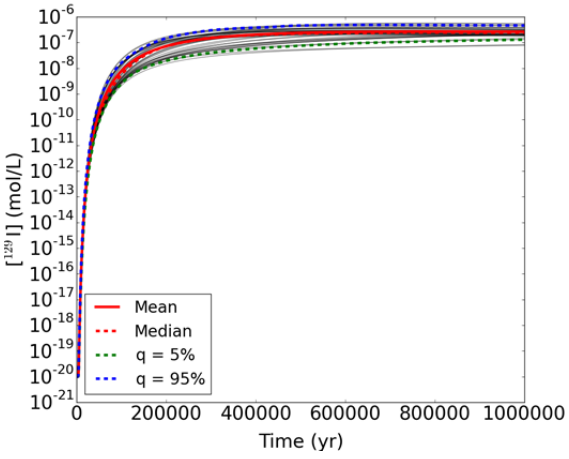

Figure 4-68. [^{129}I] versus time, interbed "near".

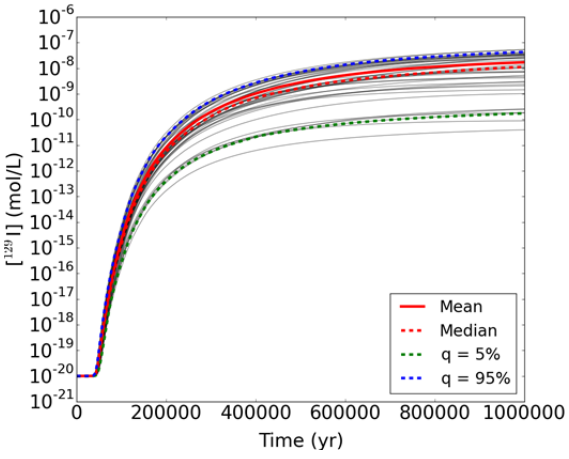

Figure 4-69. [^{129}I] versus time, aquifer "near"

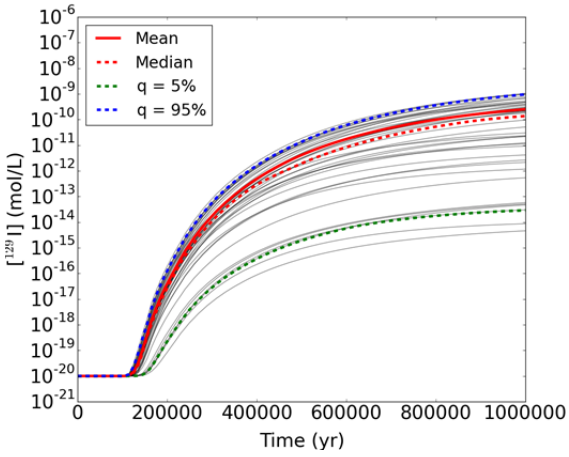

Figure 4-70. [^{129}I] versus time, sediment "near"

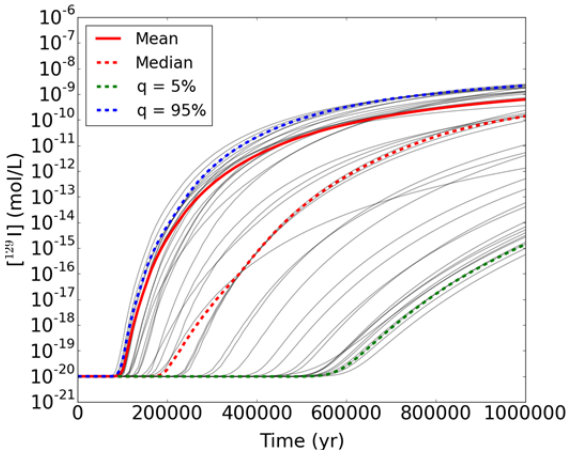

Figure 4-71. [^{129}I] versus time, clay "midx"

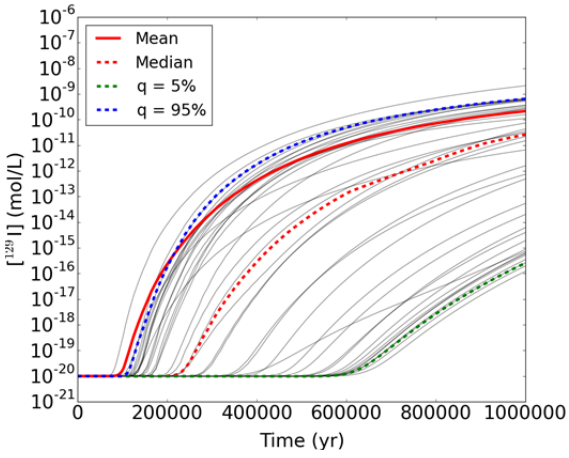

Figure 4-72. [^{129}I] versus time, interbed "midx

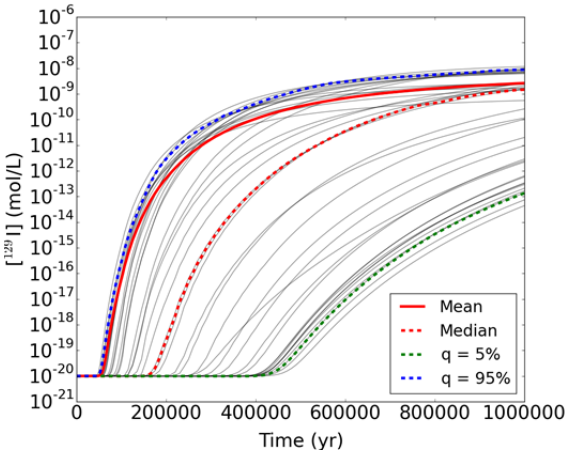

Figure 4-73. [^{129}I] versus time, aquifer "midx"

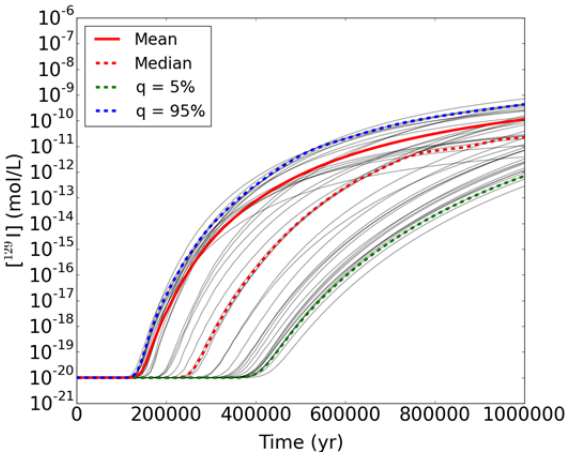

Figure 4-74. [^{129}I] versus time, sediment "midx"

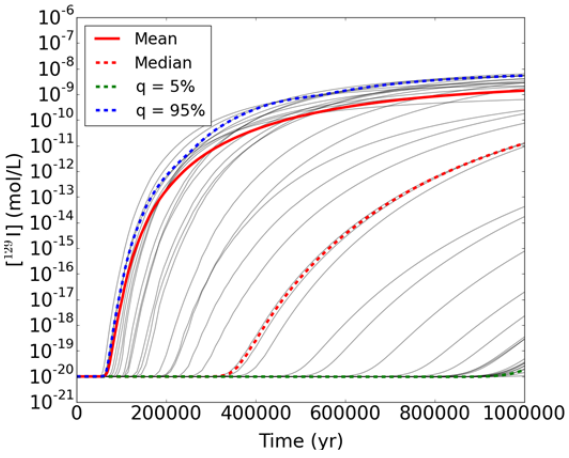

Figure 4-75. [^{129}I] versus time, well location

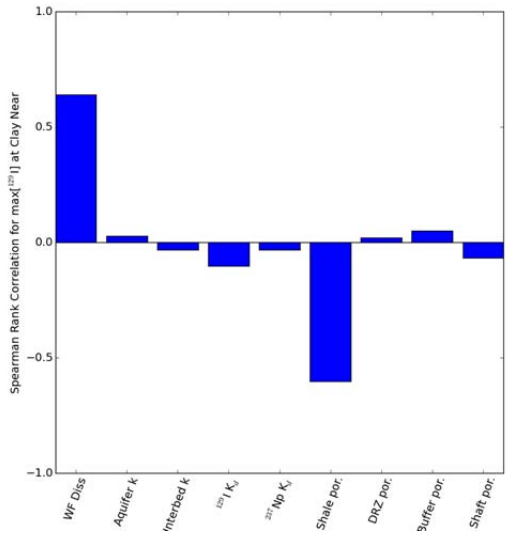

Figure 4-76. Rank correlations, clay "near"

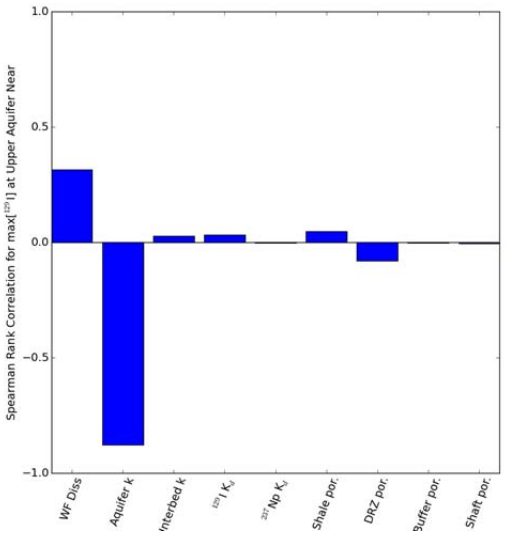

Figure 4-78. Rank correlations, aquifer "near"

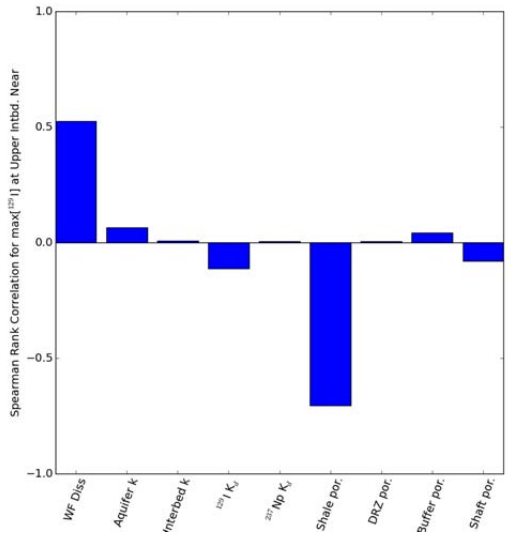

Figure 4-77. Rank correlations, interbed "near"

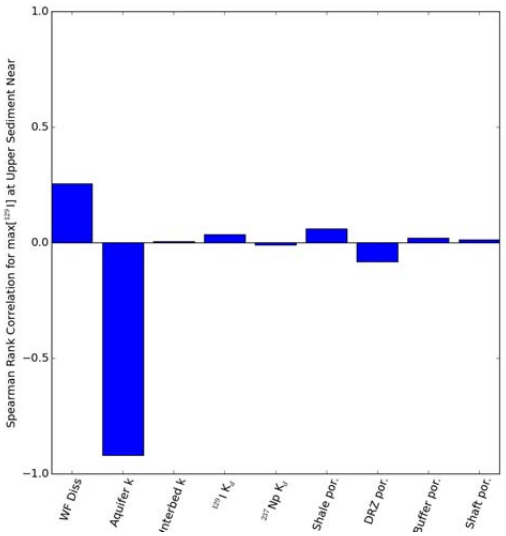

Figure 4-79. Rank correlation, sediment "near"

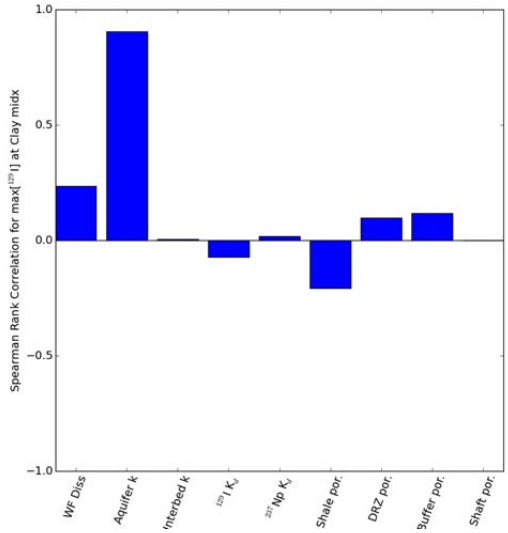

Figure 4-80. Rank correlations, clay "midx"

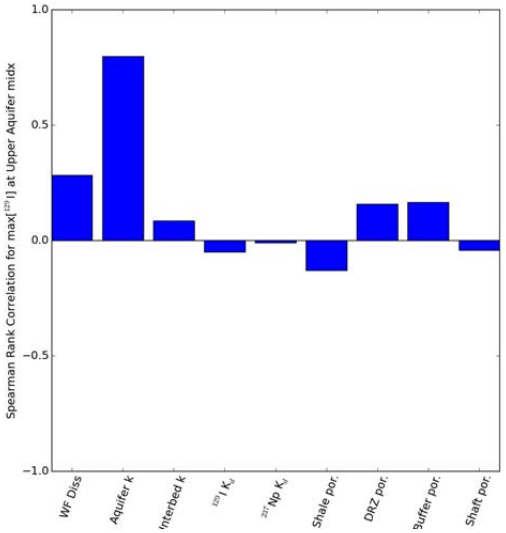

Figure 4-82. Rank correlations, aquifer "midx"

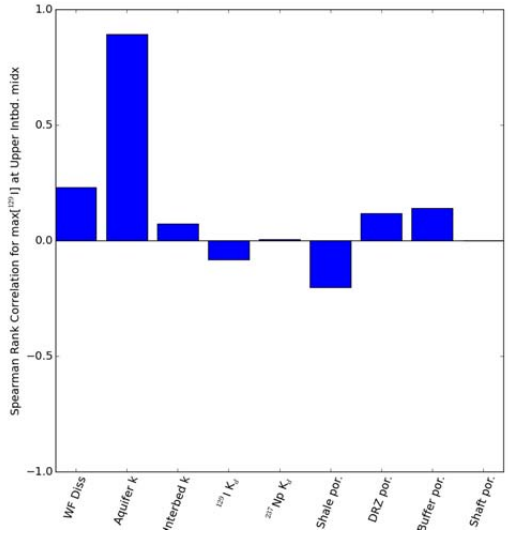

Figure 4-81. Rank correlations, interbed "midx"

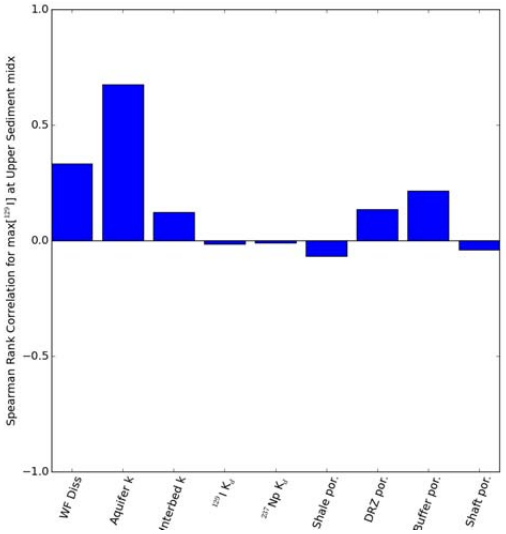

Figure 4-83. Rank correlations, sediment "midx"

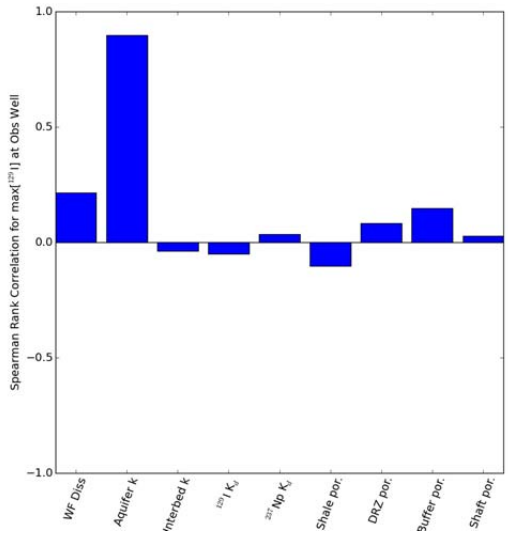

Figure 4-84. Rank correlations, well location

4.3.6.3 Deterministic Thermal Results

Whereas fluid flow in the isothermal simulations is due solely to the imposed regional head gradient, the clay deterministic thermal simulation includes coupled heat and fluid flow. Heat generated by radioactive decay in the waste form drives fluid flow in and around the repository. Temperatures and flow patterns in the near field at various times are summarized in Figure 4-85 through Figure 4-91. At a simulation time of 0 years (prior to repository heating), a background geothermal temperature gradient (generated by a basal heat flux of 60 mW/m^2) and a regional fluid flow field are established (Figure 4-85). As repository temperatures rise, a corresponding increase in fluid pressure drives fluid flow out of the repository (Figure 4-86). Maximum repository temperatures are reached around 100 years (Figure 4-87), but fluid flow continues out of the repository for several thousand years (Figure 4-88). By 10,000 years, fluid pressure in the cooling repository has dropped enough that fluid begins to flow back into the repository (Figure 4-89). The repository continues to cool and the flow field to approach that due to background head gradients throughout the remainder of the simulation time (Figure 4-90 and Figure 4-91).

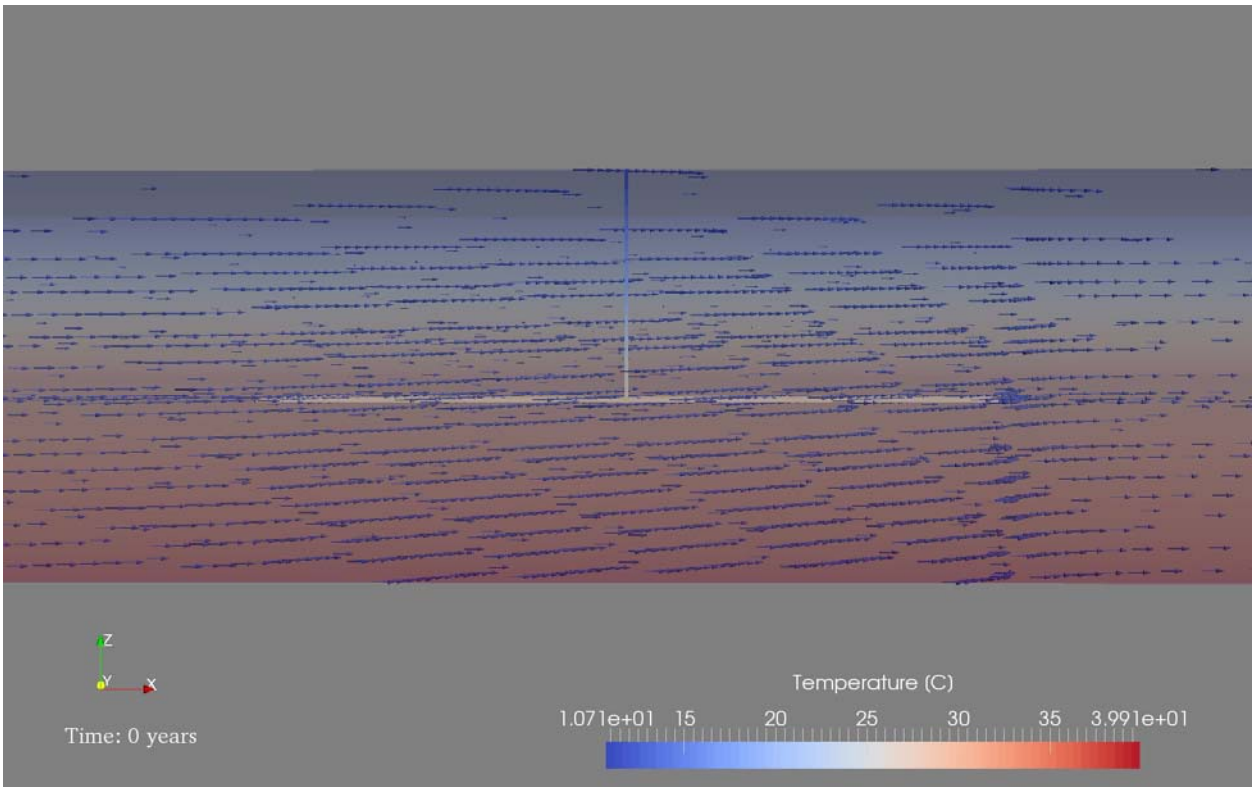

Figure 4-85. Initial background geothermal temperature gradient and regional flow field for the clay thermal deterministic simulation. The view is from the front of the model domain, looking slightly down on to the repository, whose drifts and shaft are plotted as a solid surface colored by temperature. The 3D model domain (truncated in the x direction) is transparent and also colored by temperature. Blue arrows indicate the direction of the regional flow field established by applying a head gradient of -0.0013 m/m from west (left) to east (right). Notice that the maximum temperature on the color scale of 39.9°C in this figure is less than the maximum of 170°C in the figures following.

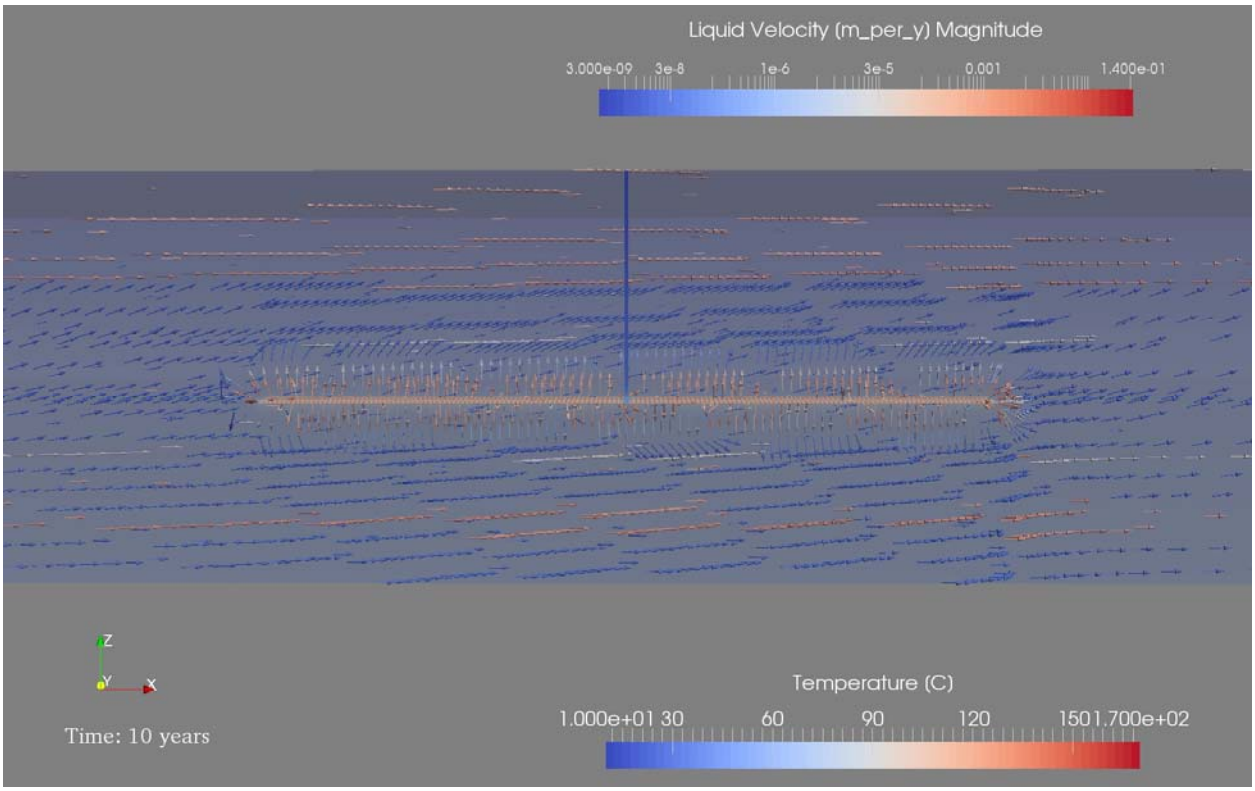

Figure 4-86. Near field temperature and fluid flow field at 10 years for the clay thermal deterministic simulation. As the repository heats, rising fluid pressures drive fluid out of the repository.

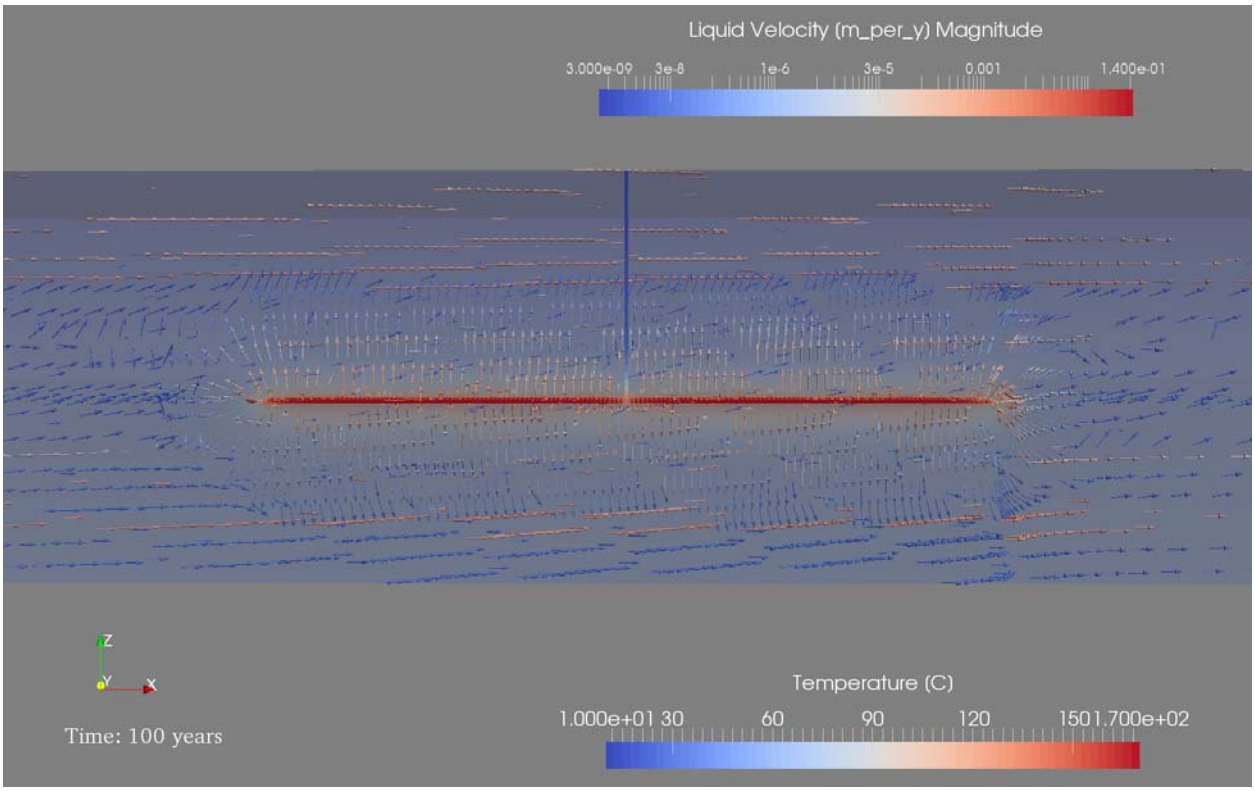

Figure 4-87. Near field temperature and fluid flow field at 100 years for the clay thermal deterministic simulation. Repository temperatures are peaking.

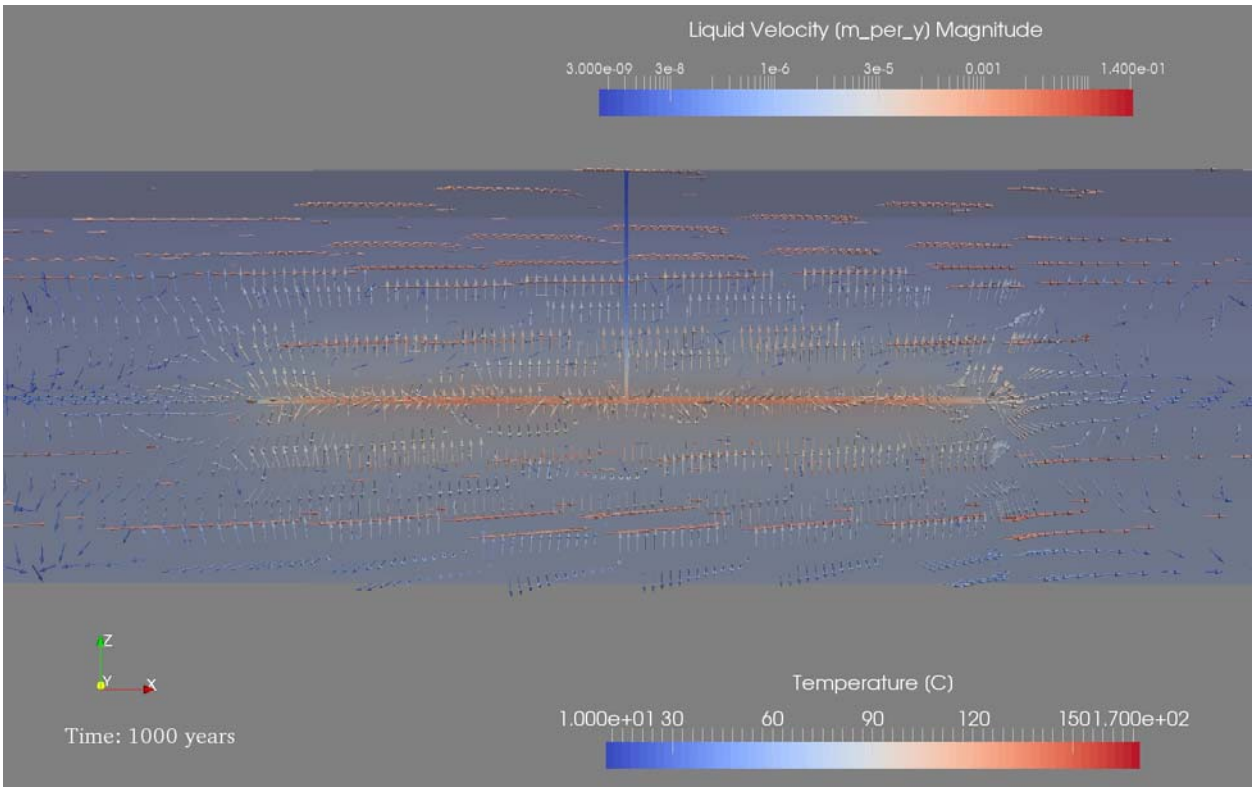

Figure 4-88. Near field temperature and fluid flow field at 1000 years for the clay thermal deterministic simulation. Fluid flow is still out of the repository.

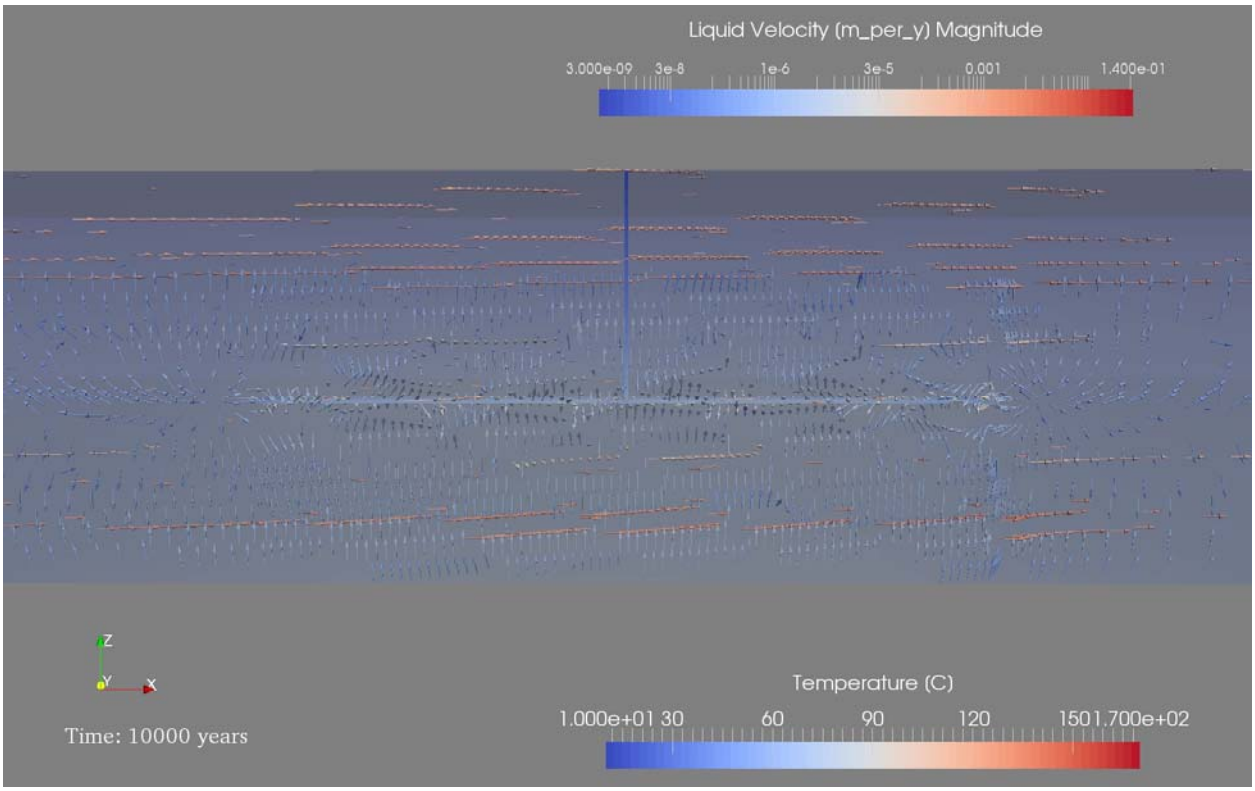

Figure 4-89. Near field temperature and fluid flow field at 10,000 years for the clay thermal deterministic simulation. By 10,000 years, fluid has begun to flow back into the cooling repository.

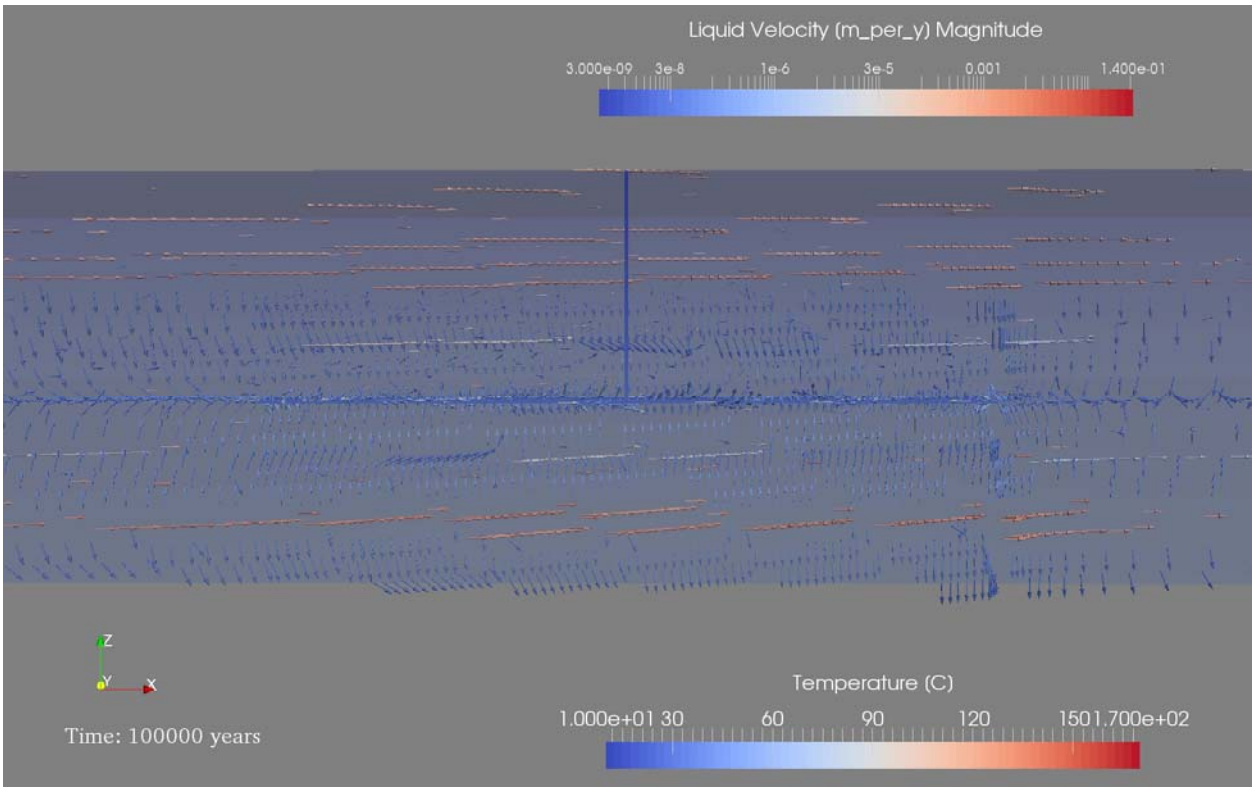

Figure 4-90. Near field temperature and fluid flow field at 100,000 years for the clay thermal deterministic simulation.

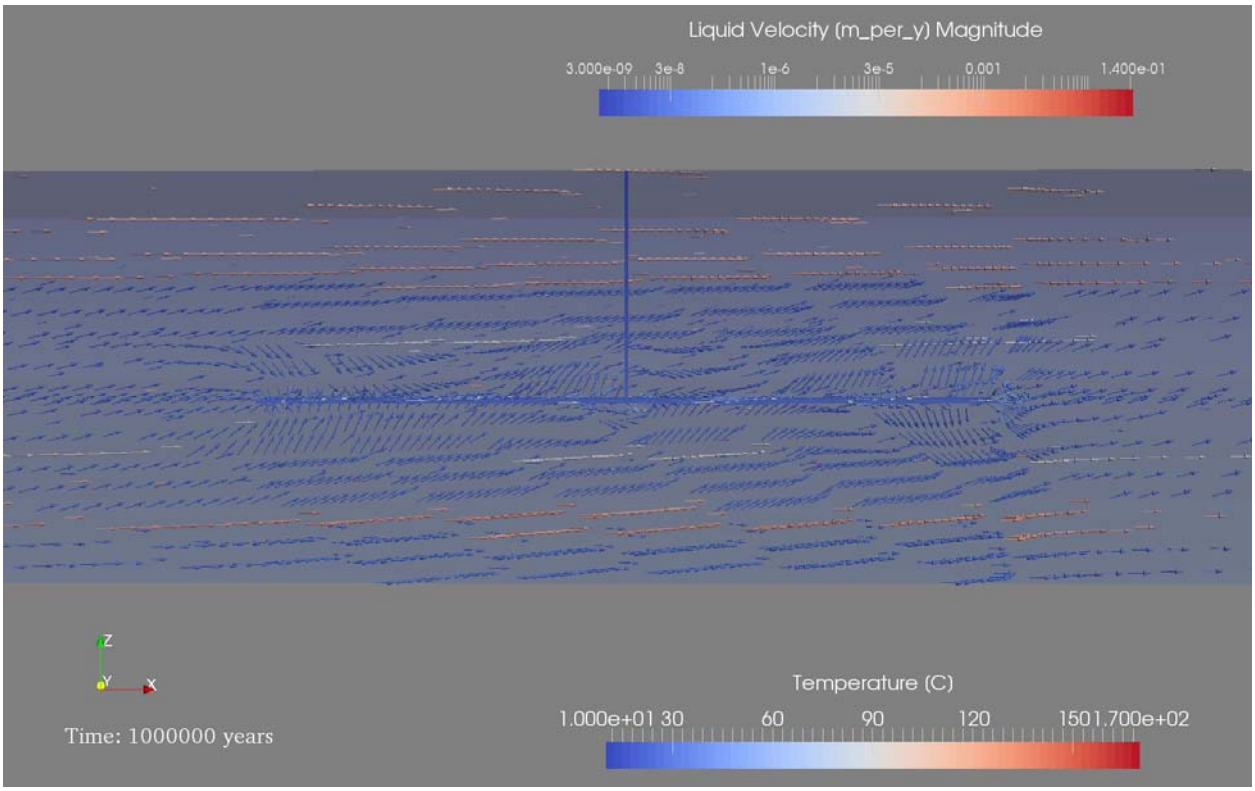

Figure 4-91. Near field temperature and fluid flow field at 10^6 years for the clay thermal deterministic simulation. Regional fluid flow is still disturbed by the repository.

In the thermal simulation, the cooling repository has the effect of drawing fluid inward, and therefore inhibits radionuclide transport outward and decreases ^{129}I concentrations in the far field by about an order of magnitude compared to concentrations predicted by the isothermal simulation. The difference can be seen in a comparison of ^{129}I breakthrough curves at the well observation location (Figure 4-92) and in the 3D contours of ^{129}I concentration at various times (Figure 4-93 through Figure 4-97). In contrast to the isothermal simulation, the thermal simulation predicts that at 10^6 years, the 5×10^{-11} mol/L concentration contour will fall approximately 1 km short of the well observation location (x = 11,621 m). The difference in predicted system behavior brought about by adding the mechanism of coupled heat and fluid flow to the simulation highlights the importance of multi-physics, mechanistic models for obtaining accurate model predictions. Within the constraints of computational feasibility and data availability, mechanistic models should be used whenever possible.

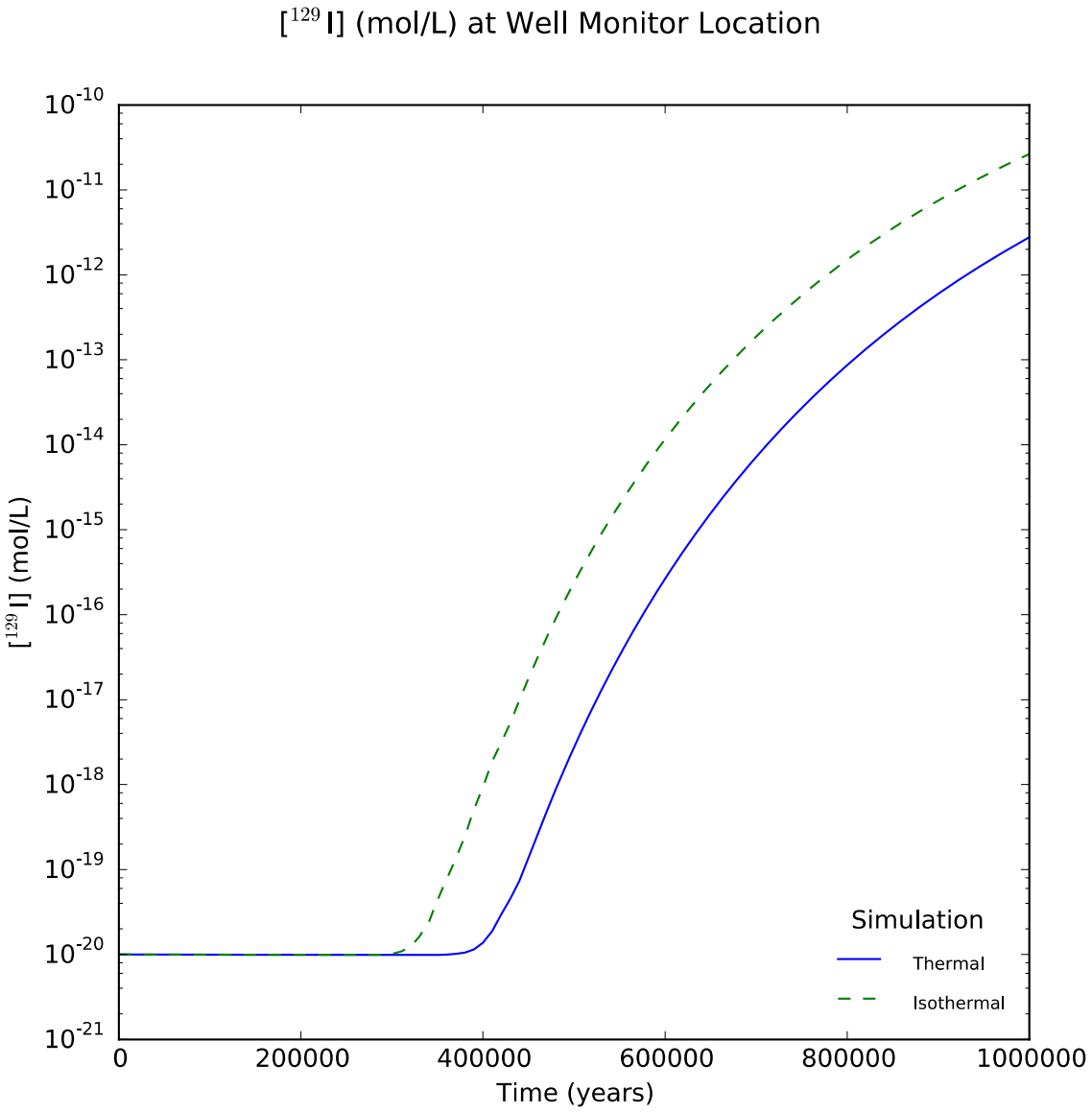

Figure 4-92. ^{129}I concentration versus time at the well observation point for the clay thermal and isothermal deterministic simulations.

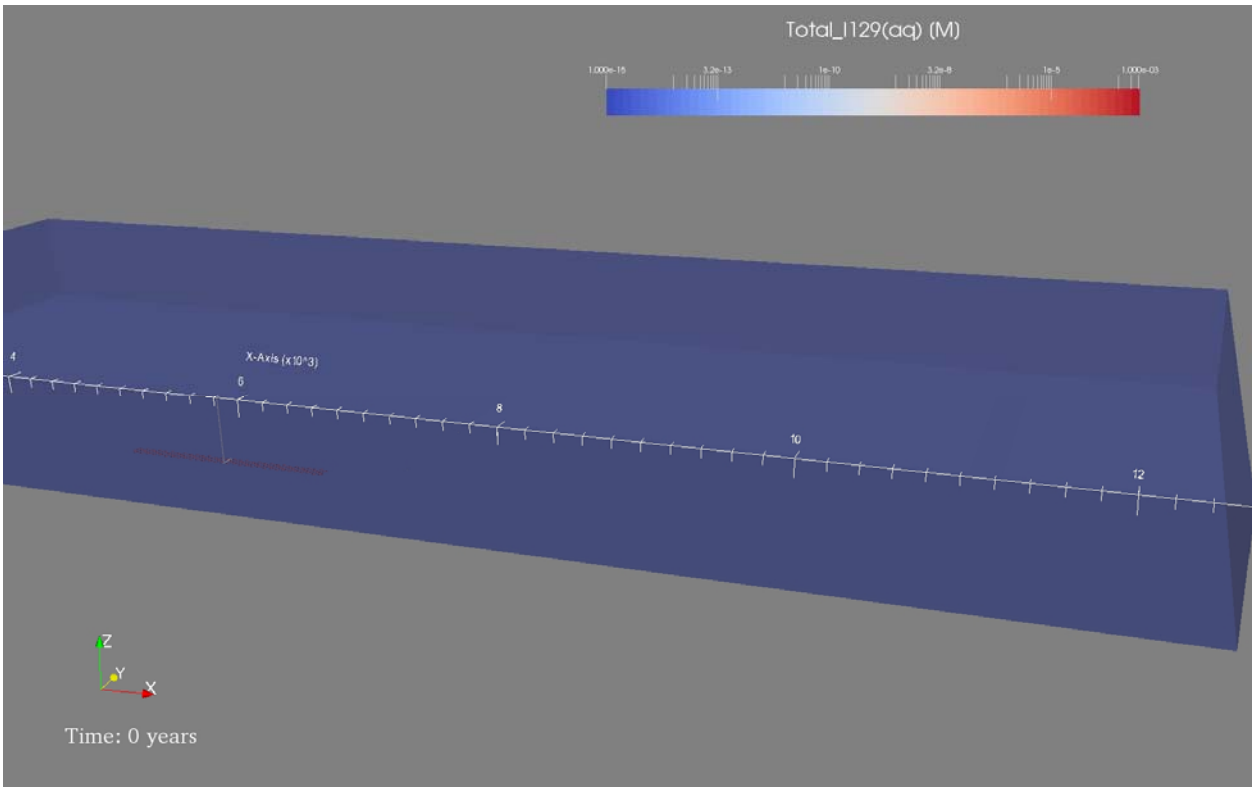

Figure 4-93. Initial ^{129}I concentration for the clay thermal deterministic simulation. The red contours (5×10^{-5} mol/L) show the location of the waste packages in the repository. In this and following figures, the volume of the model domain and the 3D contours are colored according to [^{129}I]. The shaft, hallway, and waste packages (obscured by the [^{129}I] contours at early times) are represented as solid grey surfaces.

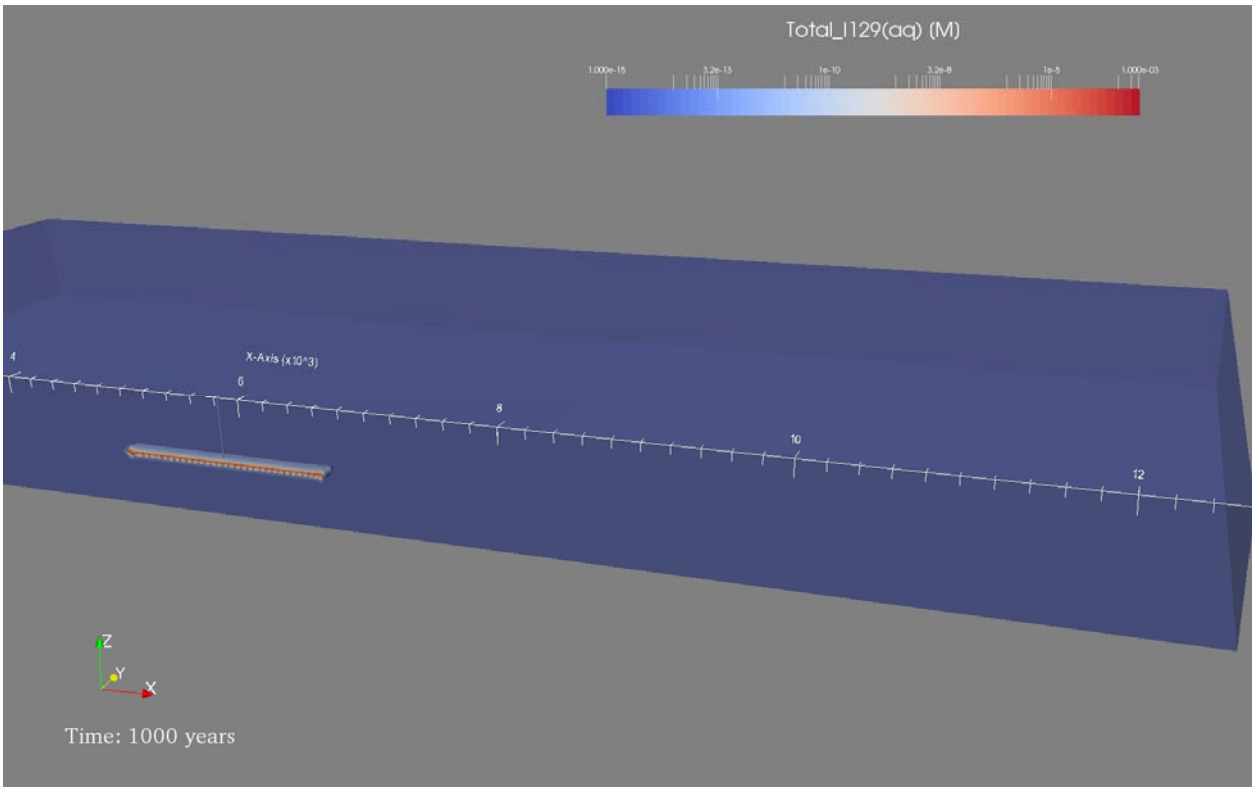

Figure 4-94. ^{129}I concentration at 1000 years for the clay thermal deterministic simulation.

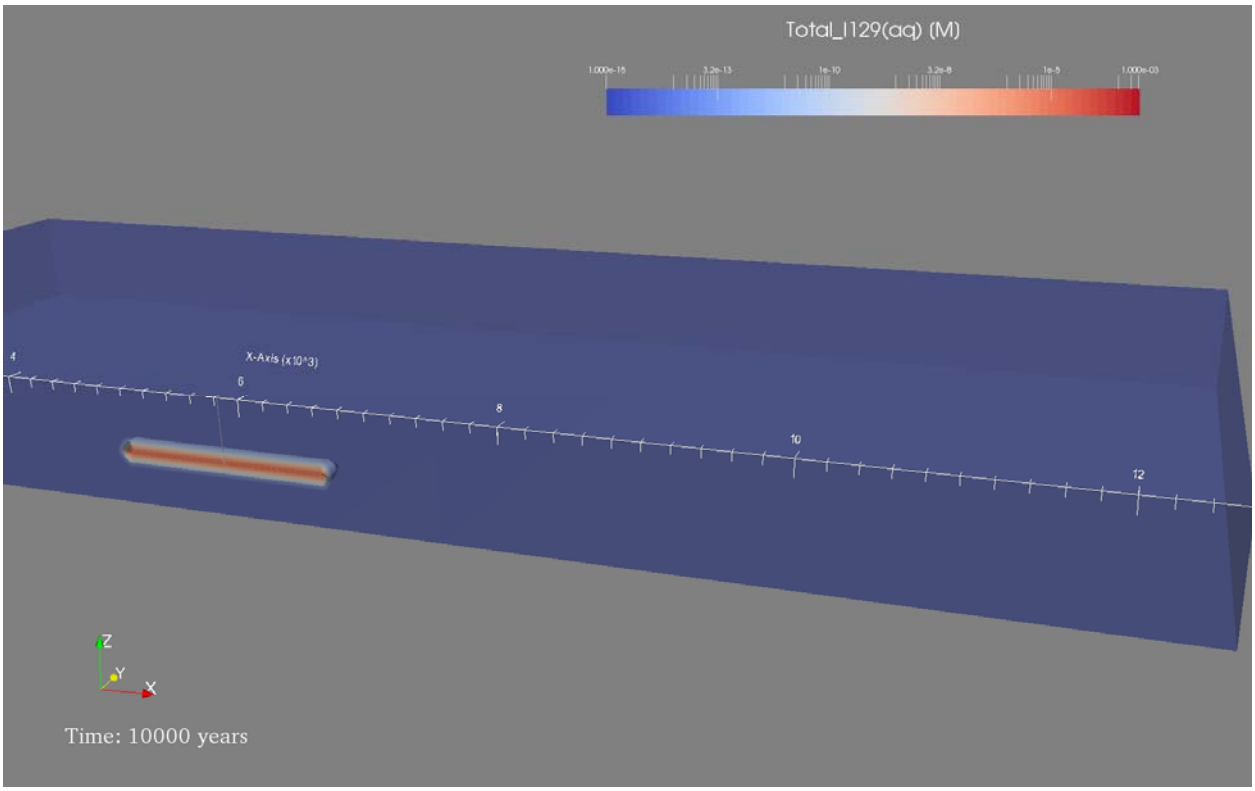

Figure 4-95. ^{129}I concentration at 10,000 years for the clay thermal deterministic simulation.

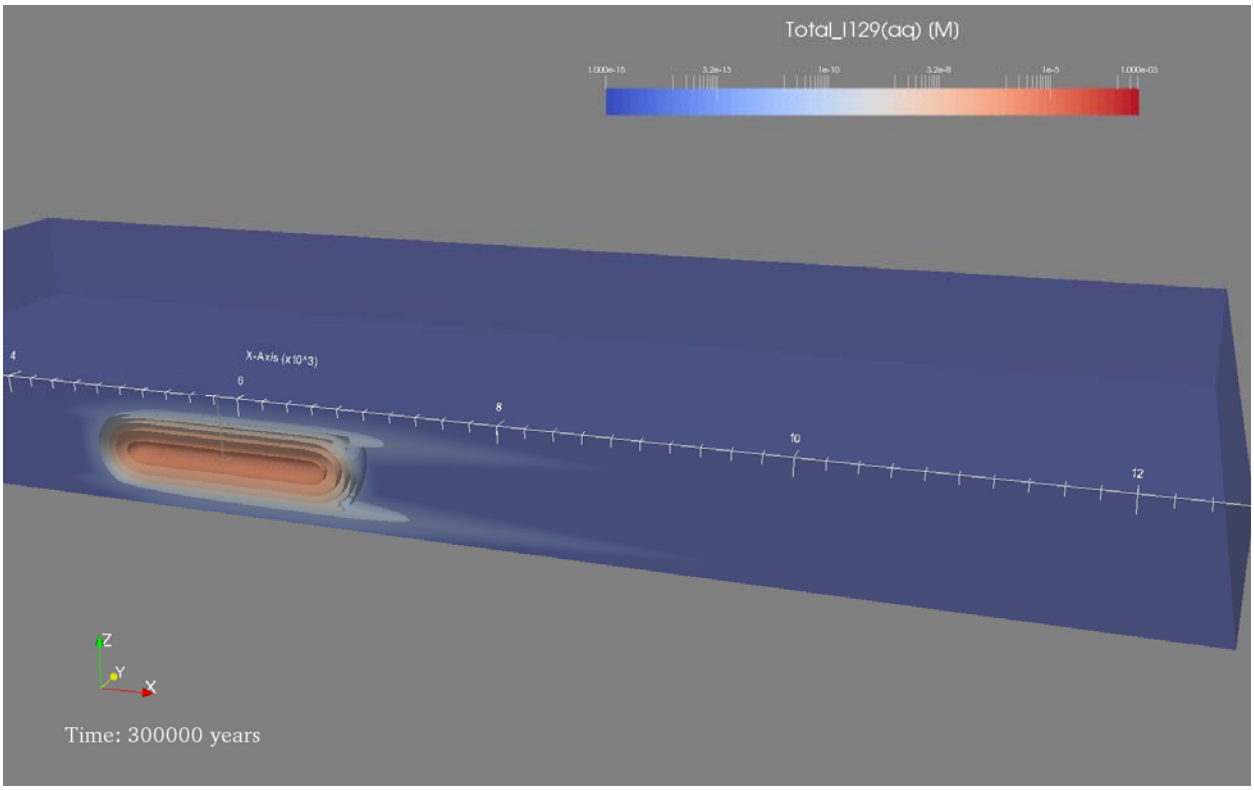

Figure 4-96. ^{129}I concentration at 300,000 years for the clay thermal deterministic simulation.

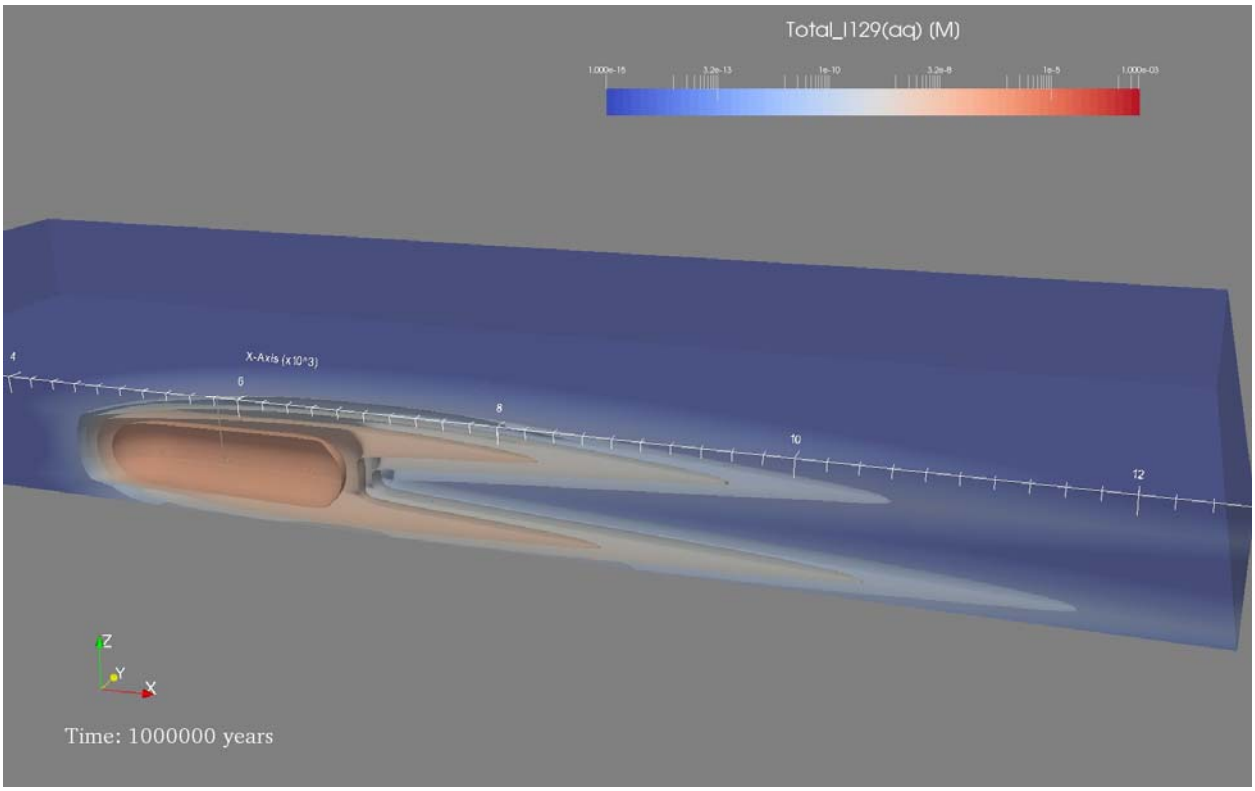

Figure 4-97. ^{129}I concentration at 10^6 years for the clay thermal deterministic simulation. [^{129}I] at the well observation point (x = 11,621 m) is about one order of magnitude less than predicted by the isothermal simulation.

5. SUMMARY AND CONCLUSIONS

This report describes specific GDSA activities in FY2015 toward the development of the enhanced disposal system modeling and analysis capability for geologic disposal of nuclear waste. Employing the HPC-capable codes PFLOTRAN and Dakota, the GDSA group added new process modeling capabilities, expanded integration with other work packages for additional process models and data, enlarged and updated the generic reference case simulation for UNF in bedded salt, simulated a new generic reference case for defense HLW glass in bedded salt, and developed and simulated a new generic reference case for UNF in clay.

The GDSA modeling advances included the addition of two source term dissolution models. One model, the Fuel Matrix Degradation Model, developed largely at Argonne National Laboratory, was directly coupled to the PFLOTRAN waste package process model. A second dissolution model, a simple HLW glass dissolution model, was built inside the PFLOTRAN waste package process model. It calculates the dissolution rate using a simple expression and accounts for changing isotopic composition over time. Additional models developed or revised for the GDSA PA capability this year include a new conceptual model for the effective simulation of canister corrosion, a revised approach for simulating isotope decay and partitioning, and a new mathematical model for simulating solid solution reactions.

A significant effort was made to integrate GDSA PA model development with UFDC work completed or underway in other work packages and other laboratories. GDSA requested formal input from the other work packages on process models and data that could be coupled or integrated with the GDSA PA model. Requested input for proposed process models included descriptions of purpose, importance, addressed FEPs, coupled parameters, implementation, and readiness. A total of 18 process model templates were received. These templates were used by management to plan work scopes for FY2016 work packages and to help prioritize GDSA integration of proposed process models over the next several years.

New generic reference case applications were developed, and the previously developed reference case for a generic UNF repository in bedded salt was expanded. Initially, the FY2014 salt repository reference case for UNF was enlarged from a thin three-dimensional vertical slice of the repository to a full three-dimensional simulation involving multiple drifts. This enlarged domain was duplicated to create the new salt reference case for defense HLW glass. Glass dissolution and radionuclide release were simulated in the defense repository reference case using the new HLW glass source dissolution model. The template of the enlarged domain was also used to build the new reference case for a generic UNF repository in clay. The new clay reference case was based on the repository design defined for the argillite reference case in Jove Colon et al. 2014.

A variety of results for the three reference cases are presented in this report, including deterministic and probabilistic results for isothermal and thermal salt UNF simulations, deterministic results for a thermal salt HLW simulation, deterministic and probabilistic results for isothermal clay UNF simulations, and deterministic results for a thermal clay UNF simulation. Also presented are the results of a preliminary grid refinement exercise and comparisons of the present multi-drift pair salt simulations to previous single-drift pair salt simulations.

Order of magnitude differences between predicted radionuclide concentrations in thermal and isothermal simulations for both the salt and the clay UNF repositories imply that multi-physics mechanistic modeling will produce a different prediction than a modeling method that relies on simplifications or abstractions of a system. Future model integration work will help to determine an efficient balance between the mechanistic modeling necessary for realism and the simplifications necessary to produce a tractable system. Parameter sensitivity analyses like those presented in this report can help guide model development and integration, data acquisition, and site selection.

Similarly large differences between single-drift pair and multi-drift pair model predictions along with differences in prediction sensitivity to input parameters imply that accurate representation of a system is necessary both for accurate prediction and for accurate understanding of system behavior, and that repository design may influence radionuclide release. In order to assess the influence of repository design (with the eventual goal of optimizing it) on radionuclide releases, larger repositories of varying layout will be simulated in the future. When a site is chosen, simulation of potential repository designs should be a part of the planning process.

The preliminary grid refinement exercise demonstrated a quantifiable effect of grid refinement on first arrival times. As GDSA modeling capabilities are expanded and refined and input parameter values updated and improved, assessing the effects of grid spacing choices will be necessary to maintain confidence in model results. The large number of simulations involved in the salt and clay probabilistic runs afforded an opportunity to refine solver tolerances in order to minimize numerical artifacts, and optimization of solver tolerances for large probabilistic simulations is an area of ongoing research.

Progress in the development of the GDSA framework continues to affirm that HPC-capable codes can be used to simulate important multi-physics couplings directly in a total system performance assessment of a geologic repository. The generic repository applications modeled to date indicate that the developing capability can simulate complex coupled processes in a multi-kilometer domain while simultaneously simulating the coupled behavior of meter-scale features, including every waste package within the domain.

6. REFERENCES

Adams, B.M., M.S. Ebeida, M.S. Eldred, J.D. Jakeman, L.P. Swiler, W.J. Bohnhoff, K.R. Dalbey, J.P. Eddy, K.T. Hu, D.M. Vigil, L.E. Baumann, and P.D. Hough 2013a. *Dakota, a Multilevel Parallel Object-Oriented Framework for Design Optimization, Parameter Estimation, Uncertainty Quantification, and Sensitivity Analysis, Version 5.3.1+ User's Manual.* SAND2010-2183, Updated May 22, 2013. Sandia National Laboratories, Albuquerque, NM. (http://dakota.sandia.gov/)

Adams, B.M., M.S. Ebeida, M.S. Eldred, J.D. Jakeman, L.P. Swiler, W.J. Bohnhoff, K.R. Dalbey, J.P. Eddy, K.T. Hu, D.M. Vigil, L.E. Baumann, and P.D. Hough 2013b. *Dakota, a Multilevel Parallel Object-Oriented Framework for Design Optimization, Parameter Estimation, Uncertainty Quantification, and Sensitivity Analysis, Version 5.3.1+ Theory Manual.* SAND2011-9106, Updated May 22, 2013. Sandia National Laboratories, Albuquerque, NM. (http://dakota.sandia.gov/)

Andra 2005. *Dossier 2005 Argile: Phenomological evolution of a geological repository*. National Radioactive Waste Management Agency, Paris, France.

Arnold. B.W., P.V. Brady, S.J. Bauer, C. Herrick, S. Pye and J. Finger 2011. *Reference Design and Operations for Deep Borehole Disposal of High-Level Radioactive Waste.* SAND2011-6749. Sandia National Laboratories, Albuquerque, NM.

Balay S., J. Brown, K. Buschelman, V. Eijkhout, W.D. Gropp, D. Kaushik, M.G. Knepley, L. Curfman McInnes, B.F. Smith and H. Zhang 2013. *PETSc Users Manual*, ANL-95/11 – Revision 3.4, Argonne National Laboratory, Argonne IL.

Bel J. and F. Bernier 2001. "Temperature criterion related to clay based backfill materials in the framework of a geological repository of heat producing radioactive waste (HLW)". *Radioactive Waste Management and Environmental Remediation*, Vol. 3, pp. 1327-1331.

Bianchi, M., H.-H. Liu, and J. T. Birkholzer 2015. "Radionuclide transport behavior in a generic geological radioactive waste repository". *Ground Water, 53*(3), 440-451. doi: 10.1111/gwat.12171

Blackwell, D. D., M. C. Richards, Z. S. Frone, J. F. Batir, M. A. Williams, A. A. Ruzo, and R. K. Dingwall 2011. "SMU Geothermal Laboratory Heat Flow Map of the Conterminous United States, 2011." Supported by Google.org. Available at http://www.smu.edu/geothermal. Retrieved August 21, 2015

Boudreau, B. P. 1996. "The diffusive tortuosity of fine-grained unlithified sediments". *Geochimica et Cosmochimica Acta, 60*(16), 3139-3142. doi: 10.1016/0016-7037(96)00158-5

Brady, P.V., B.W. Arnold, G.A. Freeze, P.N. Swift, S.J. Bauer, J.L. Kanney, R.P. Rechard, and J.S. Stein 2009. *Deep Borehole Disposal of High-Level Radioactive Waste.* SAND2009-4401. Sandia National Laboratories, Albuquerque, NM.

Bredehoeft, J. D., C. E. Neuzil, and P. C. D. Milly 1983. *Regional Flow in the Dakota Aquifer: A Study of the Role of Confining Layers*. Water-Supply Paper 2237. United States Geological Survey, Alexandria, VA.

Bruno, J. (Chair), D. Bosbach, D. Kulik, and A. Navrotsky 2007. *Chemical Thermodynamics of Solid Solutions of Interest in Nuclear Waste Management: A State-of-the-Art Report*, Chemical Thermodynamics, Vol. 10, pp. 226.

Carter, J. T., A. J. Luptak, J. Gastelum, C. Stockman, and A. Miller 2013. *Fuel Cycle Potential Waste Inventory for Disposition*. FCRD-USED-2010-000031 Rev 6. Savannah River National Laboratory, Aiken, SC.

Chen, X., H. Murakami, M. Hahn, G.E. Hammond, M.L. Rockhold, J.M. Zachara and Y. Rubin 2012. "Three-Dimensional Bayesian Geostatistical Aquifer Characterization at the Hanford 300 Area using Tracer Test Data", *Water Resources Research*, 48, doi:10.1029/2011WR010675.

Chen, X., G. Hammond, C. Murray, M. Rockhold, V. Vermeul and J. Zachara 2013. "Applications of Ensemble-based Data Assimilation Techniques for Aquifer Characterization using Tracer Data at Hanford 300 Area", *Water Resources Research*, 49, doi:10.1002/2012WR013285.

Clayton, D.J., and C.W. Gable 2009. *3-D Thermal Analyses of High-Level Waste Emplaced in a Generic Salt Repository.* AFCI-WAST-PMO-MI-DV-2009 000002. February, 2009.

Clayton, D., G. Freeze, T. Hadgu, E. Hardin, J. Lee, J. Prouty, R. Rogers, W. M. Nutt, J. Birkholzer, H. H. Liu, L. Zheng, and S. Chu 2011. *Generic Disposal System Modeling - Fiscal Year 2011 Progress Report*. SAND 2011-5828P; FCRD-USED-2011-000184. Sandia National Laboratories, Albuquerque, NM.

Cook, P. and A.L. Herczeg 2000. *Environmental Tracers in Subsurface Hydrology*, Kluwer Academic Publishers, Norwell, MA.

DOE (U.S. Department of Energy) 2008. *Yucca Mountain Repository License Application Safety Analysis Report.* DOE/RW-0573, Revision 1. U.S. Department of Energy, Washington, DC. (http://www.nrc.gov/waste/hlw-disposal/yucca-lic-app/yucca-lic-app-safety-report.html#1)

DOE (U.S. Department of Energy) 2009. *Title 40 CFR Part 191 Subparts B and C Compliance Recertification Application for the Waste Isolation Pilot Plant*. DOE/WIPP 09-3424. U.S. Department of Energy, Carlsbad Area Office, Carlsbad, NM.

DOE (U.S. Department of Energy) 2011. *Used Fuel Disposition Campaign Disposal Research and Development Roadmap*. FCRD-USED-2011-000065 REV 0. U.S. Department of Energy, Office of Nuclear Energy, Fuel Cycle Technologies, Washington, DC.

DOE (U.S. Department of Energy). 2013. *Strategy for the Management and Disposal of Used Nuclear Fuel and High-Level Radioactive Waste*, January 2013. http://energy.gov/downloads/strategy-management-and-disposal-used-nuclear-fuel-and-high-level-radioactive-waste

Downey, J. S. and G. A. Dinwiddie 1988. *The Regional Aquifer System Underlying the Northern Great Plains in Parts of Montana, North Dakota, South Dakota, and Wyoming - Summary*. Professional Paper 1402-A. United States Geological Survey, Washington, D. C.

Ebert, W., T. Todd, J. Vienna, and K. Gray 2015. *Waste Form Performance Model Development*. Presented at Used Fuel Disposition Working Group Meeting, Las Vegas, NV, June 9-11, 2015.

Fluor (Fluor Technology Inc.) 1985. *Waste Package/Repository Impact Study: Final Report*. Battelle Memorial Institute, Office of Nuclear Waste Isolation, Columbus, OH. BMI/ONWI/C-312. September, 1985.

Fluor (Fluor Technology Inc.) 1986. *Site Characterization Plan Conceptual Design Report for a High-Level Nuclear Waste Repository in Salt, Vertical Emplacement Mode*. U.S. Department of Energy, Office of Civilian Radioactive Waste Management, Salt Repository Office. September, 1986.

Fox, B. 2008. *Parameter Summary Report for CRA-2009, Revision 0*, WIPP:1.2.5:PA:QA-L:547488, Sandia National Laboratories, Carlsbad, NM.

Freeze, G., P.E. Mariner, J.A. Blink, F.A. Caporuscio, J.E. Houseworth, and J.C. Cunnane 2011. *Disposal System Features, Events, and Processes (FEPs): FY11 Progress Report.* FCRD-USED-2011-000254. SAND2011-6059P. Sandia National Laboratories, Albuquerque, NM.

Freeze, G. and P. Vaughn 2012. *Development of an Advanced Performance Assessment Modeling Capability for Geologic Disposal of Nuclear Waste: Methodology and Requirements.* SAND2012-10208. Sandia National Laboratories, Albuquerque, NM.

Freeze, G., M. Voegele, P. Vaughn, J. Prouty, W.M. Nutt, E. Hardin, and S.D. Sevougian 2013a. *Generic Deep Geologic Disposal Safety Case.* FCRD-UFD-2012-000146 Rev. 1, SAND2013-0974P. Sandia National Laboratories, Albuquerque, NM.

Freeze, G., W. P. Gardner, P. Vaughn, S. D. Sevougian, P. Mariner, V. Mousseau, and G. Hammond 2013b. *Enhancements to the Generic Disposal System Modeling Capabilities*. SAND2013-10532P; FCRD-UFD-2014-000062. Sandia National Laboratories, Albuquerque, NM.

Freeze, G., P. Gardner, P. Vaughn, S.D. Sevougian, P.E. Mariner, and V. Mousseau 2013c. *Evaluation of Advanced Performance Assessment Modeling Frameworks: Annotated Outline.* FCRD-UFD-2013-000218. SAND2013-6913P. Sandia National Laboratories, Albuquerque, NM.

Freeze, R. A. and J. A. Cherry 1979. *Groundwater*. Englewood Cliffs, NJ: Prentice Hall.

Gonzales, S. and K. S. Johnson 1985. *Shales and Other Argillaceous Strata in the United States*. ORNL/Sub/84-64794/1. Oak Ridge National Laboratory, Oak Ridge, TN.

Hammond, G., P. Lichtner, and C. Lu 2007. "Subsurface multiphase flow and multicomponent reactive transport modeling using high performance computing", in *Journal of Physics: Conference Series 78*, pp. 1-10.

Hammond, G.E., P.C. Lichtner, R.T. Mills, and C. Lu 2008. "Toward petascale computing in geosciences: application to the Hanford 300 Area", in *Journal of Physics Conference Series*, 125, 012051 doi:10.1088/1742-6596/125/1/012051.

Hammond, G.E. and P.C. Lichtner 2010. "Field-Scale Modeling for the Natural Attenuation of Uranium at the Hanford 300 Area using High Performance Computing", *Water Resources Research,* 46, W09527, doi:10.1029/2009WR008819.

Hammond, G.E., P.C. Lichtner, C. Lu, and R.T. Mills. 2011a. "PFLOTRAN: Reactive Flow and Transport Code for Use on Laptops to Leadership-Class Supercomputers", in F. Zhang, G.T. Yeh, and J. Parker (ed.) *Groundwater Reactive Transport Models,* Bentham Science Publishers.

Hammond, G.E., P.C. Lichtner and M.L. Rockhold 2011b. "Stochastic Simulation of Uranium Migration at the Hanford 300 Area", *Journal of Contaminant Hydrology*, v120-121, pp. 115-128, doi:10.1016/j.jconhyd.2010.04.005.

Hansen, F. D., E. L. Hardin, R. P. Rechard, G. A. Freeze, D. C. Sassani, P. V. Brady, C. M. Stone, M. J. Martinez, J. F. Holland, T. Dewers, K. N. Gaither, S. R. Sobolik, and R. T. Cygan 2010. *Shale Disposal of U. S. High-Level Radioactive Waste*. SAND2010-2843. Sandia National Laboratories, Albuquerque, NM.

Hansen F. D., S. J. Bauer, S. T. Broome, and G. D. Callahan 2012. *Coupled Thermal-Hydrological-Mechanical Processes in Salt: Hot Granular Salt Consolidation, Constitutive Model and*

Micromechanics. FCRD-USED-2012-000422, SAND2012-9893P. Sandia National Laboratories, Albuquerque, NM.

Hardin, E., J. Blink, H. Greenberg, M. Sutton, M. Fratoni, J. Carter, M. Dupont, and R. Howard 2011. *Generic Repository Design Concepts and Thermal Analysis (FY11)*. FCRD-USED-2011-000143 Rev. 2. Sandia National Laboratories, Albuquerque, NM.

Hardin, E., T. Hadgu, D. Clayton, R. Howard, H. Greenberg, J. Blink, M. Sharma, M. Sutton, J. Carter, M. Dupont, and P. Rodwell 2012. *Repository Reference Disposal Concepts and Thermal Load Management Analysis.* FCRD-UFD-2012-000219 Rev. 2. U.S. Department of Energy, Office of Used Nuclear Fuel Disposition, Washington, DC.

Hart, D.B., R.L. Beauheim, and S.A. McKenna 2009. *Analysis Report for Task 7 of AP-114: Calibration of Culebra Transmissivity Fields*. WIPP:1.4.1.1:TD:QA-L:RECERT:541153, Sandia National Laboratories, Carlsbad, NM.

IAEA (International Atomic Energy Association) 2003. *"Reference Biospheres" for solid radioactive waste disposal*. IAEA-BIOMASS-6, IAEA, Vienna, Austria

James S. and J. Stein 2002. *Analysis Plan for the Development of a Simplified Shaft Seal Model for the WIPP Performance Assessment*, AP-094 Rev. 0, December 11, 2002. Sandia National Laboratories, Carlsbad NM.

Jerden, J., K.E. Frey, J.M. Copple, and W. Ebert 2014. *ANL Mixed Potential Model For Used Fuel Degradation: Application to Argillite and Crystalline Rock Environments*. FCRD-UFD-2014-000490. U.S. Department of Energy, Office of Used Nuclear Fuel Disposition, Washington, DC.

Jerden, J., G. Hammond, J.M. Copple, T. Cruse, and W. Ebert 2015a. *Fuel Matrix Degradation Model: Integration with Performance Assessment and Canister Corrosion Model Development*. FCRD-UFD-2015- 000550. U.S. Department of Energy, Office of Used Nuclear Fuel Disposition, Washington, DC.

Jerden, J., J.M. Copple, K.E. Frey, and W. Ebert 2015b. *Mixed Potential Model for Used Fuel Dissolution - Fortran Code*. FCRD-UFD-2015-000159. U.S. Department of Energy, Office of Used Nuclear Fuel Disposition, Washington, DC.

Jove Colon, C. F., J. A. Greathouse, S. Teich-McGoldrick, R. T. Cygan, P. F. Weck, G. A. Hansen, L. J. Criscenti, F. A. Caporuscio, M. Cheshire, M. S. Rearick, M. K. McCarney, H. Greenberg, T. Wolery, M. Sutton, M. Zavarin, A. B. Kersting, J. D. Begg, J. Blink, T. A. Buscheck, A. Benedicto-Cordoba, P. Zhao, J. Rutqvist, C. I. Steefel, J. Birkholzer, H. Liu, J. A. Davis, R. Tinnacher, I. Bourg, L. Zheng, and V. Vilarrasa 2013. *EBS Model Development and Evaluation Report*. SAND2013-8512P. Sandia National Laboratories, Albuquerque, NM.

Jove Colon C.F., P.F. Weck, D.H. Sassani, L. Zheng, J. Rutqvist, C.I. Steefel, K. Kim, S. Nakagawa, J. Houseworth, J. Birkholzer, F.A. Caporuscio, M. Cheshire, M.S. Rearick, M.K. McCarney, M. Zavarin, A. Benedicto, A.B. Kersting, M. Sutton, J. Jerden, K.E. Frey, J.M. Copple, and W. Ebert 2014. *Evaluation of Used Fuel Disposition in Clay-Bearing Rock*. FCRD-UFD-2014-000056, SAND2014-18303R. Sandia National Laboratories, Albuquerque, NM.

Kienzler, B., M. Altmaier, C. Bube, and V. Metz 2012. *Radionuclide Source Term for HLW Glass, Spent Nuclear Fuel, and Compacted Hulls and End Pieces (CSD-C Waste)*, KIT Scientific Publishing, Report-Nr. KIT-SR 7624, Karlsruher Institut für Technologie (KIT), Straße am Forum 2, D-76131 Karlsruhe, www.ksp.kit.edu

Klein, C. and C. S. Hurlbut, Jr. 1993. *Manual of Mineralogy*. New York: John Wiley & Sons, Inc.

Li, Y. H. and S. Gregory 1974. "Diffusion of ions in sea-water and in deep-sea sediments". *Geochimica et Cosmochimica Acta, 38*(5), 703-714.

Lichtner, P.C., G.E. Hammond, C. Lu, S. Karra, G. Bisht, B. Andre, R.T. Mills, and J. Kumar 2015. *PFLOTRAN Users Manual*. www.pflotran.org.

Lichtner, P.C. 2015. *End-Member Formulation of Solid Solutions and Reactive Transport*. SAND2015-7985, Sandia National Laboratories, Albuquerque, NM.

Lichtner, P.C. and G.E. Hammond 2012. *Quick Reference Guide: PFLOTRAN 2.0 (LA-CC-09-047) Multiphase-Multicomponent-Multiscale Massively Parallel Reactive Transport Code*. DRAFT LA-UR-06-7048. December 8, 2012. Los Alamos National Laboratory, Los Alamos, NM.

Lichtner, P.C. and W.J. Carey 2006. "Incorporating solid solutions in reactive transport equations using a kinetic discrete-composition approach," *Geochimica et Cosmochimica Acta*, Vol. 70, 1356–1378.

Lobmeyer, D. H. 1985. *Freshwater Heads and Ground-Water Temperatures in Aquifers of the Northern Great Plains in Parts of Montana, North Dakota, South Dakota, and Wyoming*. Professional Paper 1402-D. United States Geological Survey, Washington, D. C.

Lu, C. and P.C. Lichtner 2007. "High resolution numerical investigation on the effect of convective instability on long term CO2 storage in saline aquifers", *Journal of Physics Conference Series*, 78, doi:10.1088/1742-6596/78/1/012042.

Mansure, A. and M. Reiter. 1977. An accurate equilibrium temperature log in AEC No. 8 , a drill test in the vicinity of the proposed Carlsbad Disposal site. Open File Report no. 80. New Mexico Bureau of Mines and Technology.

McKinley, I. G. and A. Scholtis 1993. "A comparison of radionuclide sorption databases used in recent performance assessments". *Journal of Contaminant Hydrology, 13*(1-4), 347-363. doi: 10.1016/0169-7722(93)90070-9

Meacham, P.G., D.R. Anderson, E.J. Bonano, and M.G. Marietta 2011. *Sandia National Laboratories Performance Assessment Methodology for Long-Term Environmental Programs: The History of Nuclear Waste Management*. SAND2011-8270, Sandia National Laboratories, Albuquerque, NM.

Miller, A. W. and Y. Wang 2012. "Radionuclide Interaction with Clays in Dilute and Heavily Compacted Systems: A Critical Review". *Environmental Science & Technology, 46*(4), 1981-1994. doi: 10.1021/es203025q

Mills, R., C. Lu, P.C. Lichtner, and G. Hammond 2007. Simulating Subsurface Flow and Transport on Ultrascale Computers using PFLOTRAN, *Journal of Physics Conference Series*, 78, 012051 doi:10.1088/1742-6596/78/1/012051.

Navarre-Sitchler, A., R.M. Maxwell, E.R. Siirila, G.E. Hammond and P.C. Lichtner 2013. "Elucidating geochemical response of shallow heterogeneous aquifers to CO_2 leakage using high-performance computing: implications for monitoring CO_2 sequestration", *Advances in Water Resources*, v53, pp. 45-55, doi:10.1016/j.advwatres.2012.10.005.

Nuclear Waste Policy Act 1983. Public Law 97-425; 96 Stat. 2201, as amended by P.L. 100-203. C.F.R.

Perry, F. V., R. E. Kelley, P. F. Dobson, and J. E. Houseworth 2014. *Regional Geology: A GIS Database for Alternative Host Rocks and Potential Siting Guidelines*. LA-UR-14-20368, FCRD-UFD-2014-000068. Los Alamos National Laboratory, Los Alamos, NM.

Rechard R.P., ed. 1995. *Performance assessment of the direct disposal in unsaturated tuff of spent nuclear fuel and high-level waste owned by US Department of Energy*. Volumes 1, 2, and 3. SAND94-2563/1,2,3, Sandia National Laboratories, Albuquerque, NM.

Rechard R.P. 2002. "General approach used in the performance assessment for the Waste Isolation Pilot Plant." In: *Scientific Basis for Nuclear Waste Management XXV*, November 26-29, 2001, Boston, MA, Materials Research Society, Warrendale, PA.

Rechard R.P., and M.S. Tierney 2005. "Assignment of probability distributions for parameters in the 1996 performance assessment for the Waste Isolation Pilot Plant, Part 1: Description of process." *Reliability Engineering and System Safety*, 88(1):1-32.

Rechard, R.P., and C.T. Stockman 2014. "Waste degradation and mobilization in performance assessments of the Yucca Mountain disposal system for spent nuclear fuel and high-level radioactive waste." *Reliability Engineering and System Safety*, 122(2):165-188.

Robertson, E. C. 1988. *Thermal Properties of Rocks*. 88-441. United States Geological Survey, Reston, VA.

Robie, R. A. and B. S. Hemingway 1995. *Thermodynamic Properties of Minerals and Related Substances at 298.15 K and 1 Bar (105 Pascals) Pressure and at Higher Temperatures*. Bulletin 2131. United States Geological Survey, Washington, D.C.

Sack, R.O. and P.C. Lichtner 2009. "Constraining compositions of hydrothermal fluids in equilibrium with polymetallic ore-forming sulfide assemblages," *Economic Geology*, Vol. 104, pp. 1249–1264.

Sassani, D.C., C.F. Jové Colón, P. Weck, J.L. Jerden Jr., K.E. Frey, T. Cruse, W.L. Ebert, E.C. Buck, and R.S. Wittman 2013. *Used Fuel Degradation: Experimental and Modeling Report*. FCRD-UFD-2013-000404. U.S. Department of Energy, Office of Used Nuclear Fuel Disposition, Washington, DC.

Sevougian, S.D., G.A. Freeze, M.B. Gross, J. Lee, C.D. Leigh, P. Mariner, R.J. MacKinnon, and P. Vaughn 2012. *TSPA Model Development and Sensitivity Analysis of Processes Affecting Performance of a Salt Repository for Disposal of Heat-Generating Nuclear Waste*. FCRD-UFD-2012-000320 Rev. 0, U.S. Department of Energy, Office of Used Nuclear Fuel Disposition, Washington, DC.

Sevougian, S. D., G. A. Freeze, W. P. Gardner, G. E. Hammond, and P. Mariner 2014. *Performance Assessment Modeling and Sensitivity Analyses of Generic Disposal System Concepts*. SAND2014-17658; FCRD-UFD-2014-000320. Sandia National Laboratories, Albuquerque, NM.

Sevougian, S. D., G. A. Freeze, W. P. Gardner, G. E. Hammond, P. Mariner, and R. J. MacKinnon. (2015). "Performance Assessment Modeling of a Generic SNF/HLW Repository in Salt with Coupled Thermal-Hydrologic Effects - 15423." Paper presented at the *2015 International Waste Management Symposia*, Phoenix, Arizona.

Sevougian, S.D., G.A. Freeze, P. Vaughn, P. Mariner, and W.P. Gardner 2013. *Update to the Salt R&D Reference Case*. FCRD-UFD-2013-000368, SAND2013-8255P. Sandia National Laboratories, Albuquerque, NM.

Shurr, G. W. 1977. *The Pierre Shale, Northern Great Plains: A Potential Isolation Medium for Radioactive Waste*. Open-File Report 77-776. United States Geological Survey, Reston, VA.

Smyth, J.R., B. M. Crowe, P. M. Halleck and A. W. Reed 1979. *A Preliminary Evaluation of the Radioactive Waste Isolation Potential of the Alluvium-Filled Valleys of the Great Basin*. Los Alamos National Laboratory. LA-7962-MS.

SNL (Sandia National Laboratories) 2008. *Total System Performance Assessment Model/Analysis for the License Application*, MDL-WIS-PA-000005 REV 00 ADD 01. Las Vegas, Nevada: Sandia National Laboratories.

SNL (Sandia National Laboratories) 2014. *Evaluation of Options for Permanent Geologic Disposal of Spent Nuclear Fuel and High-Level Radioactive Waste*. SAND2014-0187P; FCRD-UFD-2013-000371, Rev. 1. Sandia National Laboratories, Albuquerque, NM.

Turrero, M. J., A. M. Fernandez, J. Pena, M. D. Sanchez, P. Wersin, P. Bossart, M. Sanchez, A. Melon, A. Garralon, A. Yllera, P. Gomez, and P. Hernan 2006. "Pore water chemistry of a Paleogene continental mudrock in Spain and a Jurassic marine mudrock in Switzerland: Sampling methods and geochemical interpretation". *Journal of Iberian Geology, 32*(2), 233-258.

Vaughn, P., G. Freeze, J. Lee, S. Chu, K.D. Huff, W.M. Nutt, T. Hadgu, R. Rogers, J. Prouty, E. Hardin, B. Arnold, E. Kalinina, W.P. Gardner, M. Bianchi, H.H. Liu, and J. Birkholzer 2013. *Generic Disposal System Model: Architecture, Implementation, and Demonstration.* FCRD-UFD-2012-000430 Rev. 1, SAND2013-1539P. Sandia National Laboratories, Albuquerque, NM.

WHO 2011. *Guidelines for Drinking-water Quality, Fourth Edition*. World Health Organization, Geneva, Switzerland.

Wollenberg, H.A., S. Flexser, and L. Andersson 1982. “Radiogeological assessment of candidate sites for nuclear waste repositories, exemplified by studies of the Stripa Pluton, Sweden.” *Proceedings of the Fourth International Symposium on the Scientific Basis for Nuclear Waste Management*, Boston, MA, November 16-19, 1981, pp. 279-86.

APPENDIX A: COMPLETED MODEL INTEGRATION TEMPLATES

This appendix documents twenty-one completed Model Integration Templates (see Table 3-1) filled out by process modelers to describe a proposed integration method with the GDSA-PFLOTRAN framework. These templates are presented in the same order as the models listed in the Model Integration Table, Table 3-2, although for some of the models in Table 3-2 a Model Integration Template was not received.

Table A-1. Fuel Matrix Degradation Model (FMDM)

1. Name of Model:

Fuel Matrix Degradation Model (FMDM)

2. Principal Investigator(s) and Affiliation:

Jim Jerden (ANL), Rick Wittman (PNNL), Glenn Hammond (SNL)

3. Brief Model Description:

- Describe the processes and/or events considered in the model, as well as the applicable feature (e.g., waste form, DRZ, etc.), i.e., include a description of the FEP or FEPs addressed by this model.

The FMDM calculates the dissolution rate of used fuel based on the redox reaction currents of electrochemical reactions at the fuel/solution interface (most importantly the anodic reaction releasing uranyl species into solution) and chemical dissolution. The corrosion potential and dissolution rate calculated by the FMDM accounts for oxidation of the fuel by (primarily) radiolytic H_2O_2, the concentration of which is calculated in the FMDM based on the fuel burnup/dose rate using an analytical form of the radiolysis model, and dissolved oxygen. The FMDM also quantifies the effect of H_2 oxidation, which counteracts the oxidative reactions that promote dissolution of the fuel. The H_2 concentration can be calculated within the FMDM based on the anoxic corrosion of a steel surface, such as hardware in the waste package (to be developed). The FMDM accurately reproduces the experimental observation that relatively low concentrations of dissolved H_2 at the fuel/solution interface (~0.1mM) can completely inhibit the oxidative dissolution of the fuel. In that case, only the chemical dissolution rate of the fuel contributes to the calculated value; chemical dissolution is approximately 4 orders of magnitude slower than oxidative dissolution. The H_2 oxidation reaction is catalyzed by the noble metal particles (NMPs) distributed throughout the fuel. The FMDM accounts for the surface area of the NMPs and the effects of inhibitors (such as bromide and sulfide) on the catalytic efficiency (to be developed).

The associated FEPs is 2.1.02.01 (see below – after UFD Roadmap spreadsheet/tables). Other related FEPs are: 2.1.03.01 (waste packaging; early Failure of Waste Packages), 2.1.03.02 (waste packaging; general Corrosion of Waste Packages), 2.1.03.07 (waste packaging; internal Corrosion of Waste Packages Prior to Breach), 2.1.03.08 (waste packaging; evolution of Flow Pathways in Waste Packages), 2.1.09.02 (Chemical Characteristics of Water in Waste Packages), 2.1.09.13 (Radionuclide Speciation and Solubility in EBS). FEPs 2.1.03.07 and 2.1.03.08 are partially captured in 2.1.03.02. Also, 2.1.11.06 (Thermal-Mechanical Effects on Waste Form and In-Package EBS Components).

Objective	Feature	Process (Issue)		
		UFD FEP ID	UFD FEP Title	Process/Issue Description
Containment, Limited Release Engineered Barriers	Waste Form	2.1.02.01	SNF (Commercial, DOE) Degradation - Alteration / Phase Separation - Dissolution / Leaching - Radionuclide Release	Degradation is dependent on: - Composition of fuel and groundwater - Geometry / Structure - Enrichment / Burn-up - Surface Area of fuel - Gap and Grain Fraction - Damaged Area - THC Conditions [see also Mechanical Impact in 2.1.07.06 and Thermal-Mechanical Effects in 2.1.11.06]

4. R&D Issue(s) and Safety Case Objectives Addressed by This Model:

- What are the R&D issues? The R&D issues are SNF degradation rates, degradation products, resulting effects to the geochemistry, and effects to the RN source term and the EBS. Specific technical issues that dramatically affect the fuel degradation rates calculated by the FMDM are: (1) the coupling of the

migration of a radiolytic redox front caused by oxidants diffusing away from the fuel surface with the corrosion of steel components within the canister. The steel corrosion rate determines the generation rate of H_2, which diffuses towards the fuel where it can inhibit oxidative fuel dissolution. The in-package redox fronts also determine mobility of redox sensitive radionuclides (e.g., isotopes of U, Pu, Np, I). (2) The possible poisoning of the catalytic properties of the noble metal particles (NMP) that are responsible for the H_2 effect. The NPM-H_2 reaction is responsible for the 4 order of magnitude decrease in fuel dissolution rate; therefore, poisoning the NMP could greatly reduce this mitigating effect and increase the radionuclide source term used in PA. (3) The evolution of the reactive surface area of the fuel during degradation due to preferred dissolution at grain boundaries. These effects are taken into account in the FMDM.

- How will the modeled FEP(s) affect repository performance (especially biosphere dose) in a meaningful way? The importance of SNF degradation to the safety case is that the performance of the fuel itself is the initial and primary barrier in a multiple-barrier waste isolation system (for argillite and crystalline) to be represented in a safety analysis. The fuel degradation rate is used directly to calculate radionuclide source term values used in the reactive-transport model. High confidence in the performance of the sequential barriers used in the safety case requires an accurate representation of the source term due to fuel degradation and coupling with EBS and near-field components of repository-scale transport models. The impact of waste form degradation on the safety analysis could depend on the geologic environment owing to the expected interactions during the relevant performance period and importance of the ground water composition on the fuel dissolution rate (dissolved oxygen and hydrogen, ligands affecting dissolved concentration limits, secondary phase, etc.).
- Why is it important from a regulatory perspective? As cited from the UFD Roadmap report: "The importance of SNF [degradation] to this process and decision point [licensing] is **high** because having defensible models to represent SNF degradation processes is required." Models for SNF degradation and radionuclide release are part of ongoing R&D. To the best of our knowledge, degradation models for mixed oxide and advanced reactor fuels don't exist at present, which makes the SNF model key for supporting a licensing decision.

Describe the current "state of the art" knowledge regarding the issue(s) addressed and why this particular model advances the state of the art in an important way. Although there are number of studies on uranium dioxide degradation under particular environmental conditions, there is limited information on matrix degradation under the range of redox conditions pertinent to argillite and crystalline systems. The rates of reactions contributing to fuel matrix dissolution calculated for specific solution conditions are important to the overall fuel dissolution rate. In addition, the rapid release of radionuclide inventories from gap and grain boundaries (e.g., instant release fraction) is added to the matrix dissolution rate to calculate the total release. The release from grain boundaries increases the surface area of the fuel matrix and the overall source terms. The FMDM quantifies key reactions and processes that contribute to the fuel degradation rate: the effects of fuel burn-up on radiolysis; the radiolytic generation of H_2O_2 and other radiolysis products; the generation of H_2 during steel corrosion; the effects H_2O_2, O_2, and H_2 on the dissolution rate of the fuel; the effects of ligands (e.g., CO_3^{2-}) and other species (e.g., Fe^{2+}) present in the groundwater on dissolved concentration limits; the effects of secondary phase formation on dissolved concentration limits and radiolysis efficiency; the role of NMP catalysis and the mitigating effect of oxidation; the effects of NMP surface area (relative to the fuel surface area)and the possible poisoning effects of groundwater constituents. Quantifying these processes in the FMDM is required to make accurate and defensible long-term predictions of the fuel degradation rate and RN source terms for disposal systems of interest.

-

5. Proposed method for coupling this model to the PA model[1]

- Direct coupling or abstraction? Direct coupling of the FMDM is underway and appears to be feasible. The figure below summarizes the key processes accounted for in the FMDM and the nature of the direct coupling to PA.
- Time scale of transient modeled processes (10 years, 100 years…. 1,000,000 years?). Applied to the relevant performance period based on the anticipated or likely environmental conditions for the process to occur. For example, the period where water contacts fuel in breached waste packages.
- Degree of abstraction: reduced dimensionality; simplified representation; response surface. N/A
- Key environmental inputs required from the PA model (and its coupled submodels) and key outputs delivered by this model. Inputs: temperature, fuel burnup, groundwater composition (O_2, H_2, CO_3^{2-}, and Fe^{2+}, Br^-, SO_4^-), time when container breached, time step. Outputs: fuel dissolution rate in mass (fuel or radionuclide) per unit fuel surface area per time, mass fuel dissolved.

Are there other models you are aware of that are not being developed, which are needed for your model or for PA? The FMDM was designed to incorporate modules for key processes as they were developed to replace place-holder values being used during model development. (1) Most importantly, a model describing the direct coupling between fuel dissolution and steel corrosion within the package must be completed. This direct coupling is based on the following conceptual model: radiolysis near the fuel surface generates oxidants (H_2O_2, O_2) which diffuse to a steel surface causing corrosion and the release of H_2 and Fe^{2+}, these species diffuse towards a fuel surface thus affecting the fuel dissolution rate and radionuclide release. Early versions of the MPM were set-up to quantify this coupling, but the current model uses constant values. Further development of the steel corrosion model is required to provide representative H_2 and Fe^{2+} concentrations to quantify the H_2 effect on the fuel degradation rate. (2) A separate module that calculates the evolution of the used fuel surface area is needed to account for significant increases due to preferential grain boundary corrosion and smaller decreases due to dissolving grains. The radionuclide source terms will be determined as fractional release rates by multiplying the fuel degradation rate provided by the FMDM by the specific surface area of the fuel. (3) The EDZ damage model for argillite is currently under development but it's not integrated to PA.

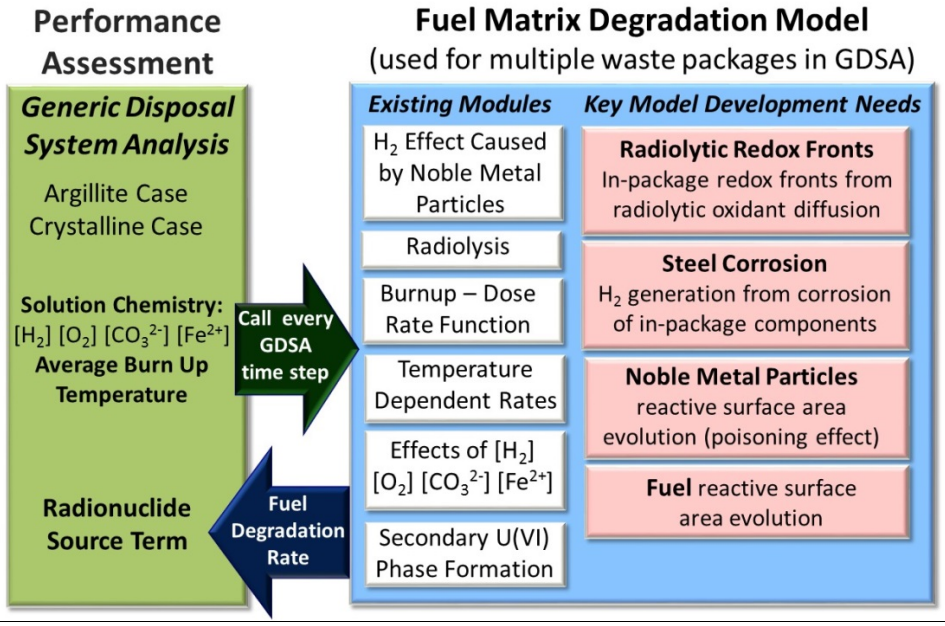

6. Real time integration horizon: estimate how long before the proposed model is ready for integration with PA and how long the integration activities might take?

- Are there intermediate steps or degrees of coupling with PA, e.g., can you couple a certain version of your model in an expedited fashion and then go to the next more detailed version—please describe how.

The current version of the FMDM includes modules for fuel matrix degradation due to reactions with radiolysis products, H_2 and Fe^{2+} due to steel corrosion, and simulated groundwater for argillite and crystalline disposal systems, and diffusion through (and homogeneous reactions with) groundwater near the fuel surface has been developed for the last couple of years. This version identifies the input and output variables to be coupled with the GDSA and time steps for fuel corrosion to be coordinated, and is currently being integrated/coupled to the PA platform (PFLOTRAN). The latter has taken a few months already.

Table A-2. Colloid-Facilitated Transport Model

1. Name of Model:
Colloid-Facilitated Transport Model

2. Principal Investigator(s) and Affiliation:
Reimus, LANL ?
Someone working on PFLOTRAN?

3. Brief Model Description:

- Describe the processes and/or events considered in the model, as well as the applicable feature (e.g., waste form, DRZ, etc.), i.e., include a description of the FEP or FEPs addressed by this model.

This model describes the colloid-facilitated transport of strongly-adsorbing and (typically) low-solubility radionuclides that become strongly associated with colloids. As such, it must also accurately describe the transport of colloids that radionuclides become strongly associated with (including the transport of intrinsic colloids that radionuclides are effectively irreversibly associated with). Although certain aspects of the model can be effectively simulated using the RELAP model, it is not expected (nor desired) that RELAP would be coupled to the PA model. It should be possible for the PA model to efficiently incorporate all the features of the model into the existing PA architecture as long as one or more species are designated as colloids and these species are assigned transport properties consistent with colloids. The key will be to assign these properties accurately and to allow solute species to interact with the colloid species in ways that are consistent with experimental observations and thermodynamic/kinetic constraints (another key is making appropriate experimental observations that can be defensibly extrapolated to relevant time and distance scales). Interactions of colloids with immobile surfaces and of radionuclides with colloids will require more sophisticated descriptions than simple Kd-type expressions. These interactions will likely have to be described by multiple species in the case of colloids and also multiple reaction sites with different adsorption and desorption rates for both colloids interacting with surfaces and radionuclides interacting with colloids and with immobile surfaces.

FEPS:
2.1.09.55 Formation of Colloids in the EBS
2.1.09.56 Stability of Colloids in the EBS
2.1.09.57 Advection of Colloids in the EBS
2.1.09.59 Sorption of Colloids in the EBS
2.1.09.61 Filtration of Colloids in the EBS
2.1.09.63 Radionuclide Release from the EBS (Colloidal)
2.2.09.60 Colloidal Transport in the Host Rock
2.2.09.61 Colloidal Transport in Other Geologic Units (Non-Host-Rock)
2.2.09.64 Radionuclide Release from the Host Rock (Colloidal)
2.2.09.65 Radionuclide Release from Other Geologic Units (Non-Host-Rock) (Colloidal)

4. R&D Issue(s) and Safety Case Objectives Addressed by This Model:

- How will the modeled FEP(s) affect repository performance (especially biosphere dose) in a meaningful way?
- Why is it important from a regulatory perspective?
- Describe the current "state of the art" knowledge regarding the issue(s) addressed and why this particular model advances the state of the art in an important way.

The modeled FEPs may be important for repository performance for long-lived, strongly-sorbing and low-solubility radionuclides because such radionuclides will really have no other plausible way of contributing to offsite dose other than by colloid-facilitated transport (except under disruptive event scenarios). This does not mean that they WILL contribute significantly to dose, but if a PA model does not consider colloid-facilitated transport of radionuclides such as Pu and Am, for instance, it will almost certainly be considered flawed or incomplete.

The current state of the art probably is this model or some other close variation of it. There are models that treat radionuclide interactions with colloids as fast, equilibrium processes, but these models will almost certainly underpredict colloid-facilitated transport because radionuclides must stay associated with colloids for long times (slow kinetics of desorption) to contribute to offsite dose.

5. Proposed method for coupling this model to the PA model[1]

- Direct coupling or abstraction?
- Time scale of transient modeled processes (10 years, 100 years…. 1,000,000 years?).
- Degree of abstraction: reduced dimensionality; simplified representation; response surface.
- Key environmental inputs required from the PA model (and its coupled submodels) and key outputs delivered by this model.
- Are there other models you are aware of that are not being developed, which are needed for your model or for PA?

Direct coupling. Time scale could be up to 1M years. Degree of abstraction is simplified representation, although some response surfaces may have to be incorporated to capture effects of varying geochemistry and heterogeneity.

Key environmental inputs: Colloid mineralogy, size distribution, and concentrations. Intrinsic colloid properties. Solution chemistry, including pH, alkalinity, and major dissolved species concentrations, temperature (for EBS and near field at short times), and, to a lesser degree, major mineralogy present, including alteration minerals in the EBS and near field.

6. Real time integration horizon: estimate how long before the proposed model is ready for integration with PA and how long the integration activities might take?

- Are there intermediate steps or degrees of coupling with PA, e.g., can you couple a certain version of your model in an expedited fashion and then go to the next more detailed version—please describe how

The current version of the model could be incorporated into the PA model in a matter of a few months (although this is a guess that would require discussion with PA modelers to refine). The bigger challenge of implementing the model will not be in coupling to PA but rather in accurately parameterizing the model to make it a practical predictive tool.

Table A-3. Radionuclide Transport As Pseudocolloids

1. Name of Model:

Radionuclide transport as pseudocolloids

2. Principal Investigator(s) and Affiliation:

James Begg (LLNL), Pihong Zhao (LLNL), Claudia Joseph (LLNL), Mavrik Zavarin (LLNL)

3. Brief Model Description:

Pseudocolloids may exist in high-level nuclear waste and could affect the transport of various radionuclides (e.g., Pu, U) in the near as well as far field of a high-level nuclear waste repository. The relative stability of the pseudocolloids will control their transport rates – this experimental program is intended to determine the stability of radionuclides associated with mineral colloids. The desorption rate or radionuclides from pseudocolloids is being measured across a range of oxide minerals. This model is intending to establish the rates of radionuclide desorption from mineral colloids.

2.2.09.01, 2.2.09.02, 2.2.09.03, 2.2.09.04, 2.2.09.05, 2.2.09.06, 2.2.09.13, 2.2.09.51, 2.2.09.59, 2.2.09.60

4. R&D Issue(s) and Safety Case Objectives Addressed by This Model:

- **R&D issues:** radionuclide desorption rates from mineral colloids
- **How will the modeled FEP(s) affect repository performance (especially biosphere dose) in a meaningful way?** Mineral colloids are expected to be an important transport mechanism for backfill materials and host rocks.
- **Why is it important from a regulatory perspective?** Radionuclide desorption rates from mineral colloids limit the colloid-facilitated migration of radionuclides into the biosphere.
- **Describe the current "state of the art" knowledge regarding the issue(s) addressed and why this particular model advances the state of the art in an important way.** Desorption rates of Pu from mineral colloids are currently not well constrained.

5. Proposed method for coupling this model to the PA model[1]

- **Direct coupling or abstraction?** abstraction
- **Time scale of transient modeled processes (10 years, 100 years…. 1,000,000 years?).** 10 to 100 years post-canister failure, equal to 10000 to 100000 years post-closure
- **Degree of abstraction: reduced dimensionality; simplified representation; response surface.** Simplified representation based on half-lives
- **Key environmental inputs required from the PA model (and its coupled submodels) and key outputs delivered by this model.** Input: Pu concentration, colloid load, pH, ionic strength, redox conditions; output: Pu concentrations associated with colloids
- **Are there other models you are aware of that are not being developed, which are needed for your model or for PA?** N/A

6. Real time integration horizon: estimate how long before the proposed model is ready for integration with PA and how long the integration activities might take?

Basic model has been developed in the last couple of years and will be improved upon (redox effect) in the next 3 years.

Table A-4. Non-Darcy Flow in Low Permeability Media

1. Name of Model:

Non-Darcy Flow in Low Permeability Media

2. Principal Investigator(s) and Affiliation:

Yifeng Wang (SNL) and Liange Zheng (LBNL)

3. Brief Model Description:

- Describe the processes and/or events considered in the model, as well as the applicable feature (e.g., waste form, DRZ, etc.), i.e., include a description of the FEP or FEPs addressed by this model.

Water flow in clay media is an important process for geological disposal of high-level nuclear wastes. Clay/shale formations have been considered as potential host rock for geological disposal of high-level radioactive waste because of their low permeability, low diffusion coefficient, high retention capacity for radionuclides, and ability to self-seal fractures. In geologic repositories for radioactive waste disposal, compacted expansive clay soils (bentonites) are also often considered as buffer materials within an engineered barrier system, to be placed in the repository tunnels between the radioactive waste and the host rock. The bentonite is usually compacted at low water content, and then progressively wetted by water from the surrounding host formation. Accurately modeling both saturated and unsaturated flow in such clay materials is critical for assessing the performance of both clay rock and buffer materials for isolating radioactive wastes at a disposal site. Non-Darcian flow behavior is characterized by non-linear relationships between water flux and hydraulic gradient.

Objective	Feature	Process (Issue)		
		UFD FEP ID	UFD FEP Title	Process/Issue Description
Containment, Limited Release Engineered Barriers	Buffer materials	2.2.01.01	Evolution of EDZ	- Advective flow - Radionuclide transport - Hydration of buffers

4. R&D Issue(s) and Safety Case Objectives Addressed by This Model:

One of the most important technical questions for the performance of a shale/clay repository is the relative importance of advection versus diffusion in the damage zone near underground tunnels/drifts. Under normal conditions (under which there are no intersections between tunnels/drifts and conductive geological structures, such as faults), the water flow velocity in the damage zone, as a result of non-Darcian flow behavior, is extremely small such that solute transport is dominated by diffusion, rather than advection. This is desirable because diffusion is a much slower transport mechanism for radionuclides.

5. Proposed method for coupling this model to the PA model[1]

- Direct coupling or abstraction? Directly implement the model in in PFLOTRAN.
- Time scale of transient modeled processes (10 years, 100 years…. 1,000,000 years?). Applied to the entire performance period.
- Degree of abstraction: reduced dimensionality; simplified representation; response surface. The model is represented by a set of algebraic equations and should be easily implemented in PFLOTRAN. No model abstraction or simplification is needed..
- Key environmental inputs required from the PA model (and its coupled submodels) and key outputs delivered by this model. Inputs: temperature, permeability (pore size). Outputs: threshold hydraulic gradient, advective flow velocity.
- Are there other models you are aware of that are not being developed, which are needed for your model or for PA? LBNL has incorporated non-darcy flow in TOUGH2 and is working on developing THM model to evaluate its importance of flow in clay and EBS bentonite.

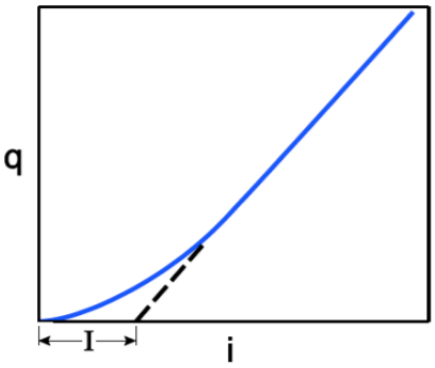

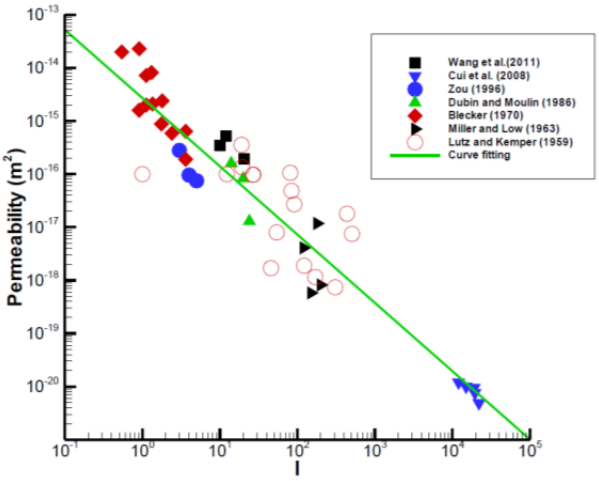

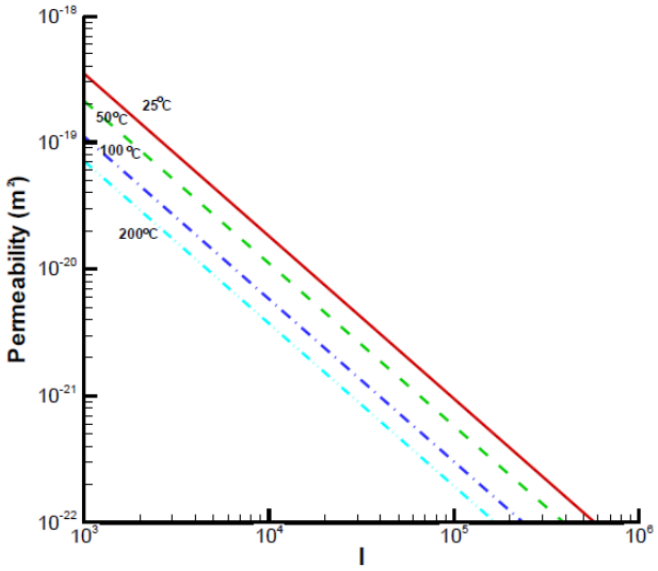

6. Real time integration horizon: estimate how long before the proposed model is ready for integration with PA and how long the integration activities might take?

- Are there intermediate steps or degrees of coupling with PA, e.g., can you couple a certain version of your model in an expedited fashion and then go to the next more detailed version—please describe how.

The model is ready for integration.

Table A-5. Discrete Fracture Network (DFN) Model

1. Name of Model:
Discrete Fracture Network (DFN) Model

2. Principal Investigator(s) and Affiliation:
Hari Viswanathan - LANL

3. Brief Model Description:

- Describe the processes and/or events considered in the model, as well as the applicable feature (e.g., waste form, DRZ, etc.), i.e., include a description of the FEP or FEPs addressed by this model.

DFNWorks is a parallelized computational suite to generate three-dimensional discrete fracture networks (DFN) and simulate flow and transport. Developed at Los Alamos National Laboratory over the past five years, it has been used to study flow and transport in fractured media at scales ranging from millimeters to kilometers. The networks are created and meshed using dfnGen, which combines FRAM (the feature rejection algorithm for meshing) methodology to stochastically generate three-dimensional DFNs on the basis of site specific data with the LaGriT meshing toolbox to create a high-quality computational mesh representation, specifically a conforming Delaunay triangulation suitable for high performance computing finite volume solvers, of the DFN in an intrinsically parallel fashion. Flow through the network is simulated in dfnFlow, which utilizes the massively parallel subsurface fow and reactive transport finite volume code PFLOTRAN a code developed at multiple national labs. A Lagrangian approach to simulating transport through the DFN is adopted within dfnTrans, developed at Los Alamos National Lab, which is an extension of the of the walkabout particle tracking method to determine pathlines through the DFN. Example applications of this suite in the areas of nuclear waste disposal under UFD include the Forsmark site in Sweden and the Swedish BRIE experiment. The next application will involve simulating problems of interest to the Swedish Task Force that DOE has now joined.

Saftey case issues addressed by this model have been captured in the UFD Roadmap Appendix B. In Table 1, the top 5 priortized FEPs that DFN can address for crystalline rock are listed.

Table 1. Specific FEPs the DFN model can address

2.2.02.01 Stratigraphy and properties of the host rock – Granite/Crystalline
2.2.09.51 Advection of dissolved radionuclides in host rock – Granite-crystalline
2.2.05.01 Fractures – Granite/Crystalline
2.2.08.01 Flow through host rock – Granite/Crystalline
2.2.08.02 Flow through EDZ – Granite/Crystalline

4. R&D Issue(s) and Safety Case Objectives Addressed by This Model:

- How will the modeled FEP(s) affect repository performance (especially biosphere dose) in a meaningful way?

Numerical models play an important role in the support and development of the safety case. Such models facilitate evaluating scenarios and hypotheses, and demonstrate our understanding of flow and transport in fractured crystalline rock. Simulations are key to predicting the longer time scales that lab and field tests cannot directly address.

- **Why is it important from a regulatory perspective?**

Demonstrating that we can simulate processes in the near and far field will build confidence in the longer term performance of crystalline disposal sites where fracture dominated flow is expected. The DFNs take into account the geometry of the fracture network which is necessary for simulating crystalline systems.

- **Describe the current "state of the art" knowledge regarding the issue(s) addressed and why this particular model advances the state of the art in an important way.**

Numerous research groups have utilized DFN models. DFNworks state of the art capabilities include a high performance platform that allows for much larger DFN fracture networks to be simulate. In addition, since the flow and transport simulator has reactive transport and multiphase flow capabilities, detailed mechanistic models of radionuclide transport within high fidelity fracture networks are possible.

5. Proposed method for coupling this model to the PA model[1]

Used to derive upscaled parameters for PA flow and transport and for benchmarking/ validation

- Time scale of transient modeled processes (10 years, 100 years…. 1,000,000 years?).

The DFN model can be used to simulate the Swedish task force experiments to validate the model. These simulations are on the order of days to a year. When simulating a field disposal site the time scale can greatly increase to 1000s to 1000000 years.

- Degree of abstraction: reduced dimensionality; simplified representation; response surface.

Direct simulation could be quite time consuming and not necessary if DFN is only used for deriving upscaled properties. However model abstraction to an emulator could be undertaken to reduce run times while capturing system behavior.

- Key environmental inputs required from the PA model (and its coupled submodels) and key outputs delivered by this model.

Fracture properties, flow field parameters, bulk rock properties.

- Are there other models you are aware of that are not being developed, which are needed for your model or for PA?

No

6. Real time integration horizon: estimate how long before the proposed model is ready for integration with PA and how long the integration activities might take?

It depends on whether DFN is only used to provide upscaled parameters or whether an abstracted DFN model is needed. Perhaps the Sandia FCM could be an abstracted version of DFN that could be used by TSPA?

- Are there intermediate steps or degrees of coupling with PA, e.g., can you couple a certain version of your model in an expedited fashion and then go to the next more detailed version—please describe how

The direct simulations are useful for test design and confidence building before a repository is built, and in the PA could be used as initial conditions before full coupling is achieved.

Table A-6. Coupled Thermal Hydrological and Chemical (THC) processes

1. Name of Model:
Coupled Thermal Hydrological and Chemical (THC) processes.

2. Principal Investigator(s) and Affiliation:
Philip Stauffer - LANL

3. Brief Model Description:

- Describe the processes and/or events considered in the model, as well as the applicable feature (e.g., waste form, DRZ, etc.), i.e., include a description of the FEP or FEPs addressed by this model.

A coupled THC model has been created for DOE within the LANL FEHM simulation code. The model includes thermal transport of both liquid and vapor and can operate in boiling salt conditions. Many new capabilities have been added to FEHM to enable the tightly coupled THC processes of fluid transport in heated salt, including (Stauffer et al., 2013): porosity change from the precipitation/dissolution of salt, with salt solubility as a function of temperature; permeability as a function of variable porosity; thermal conductivity of salt as a function of porosity and temperature; vapor pressure of water as a function of concentration and temperature; water vapor diffusion coefficient as a function of saturation, porosity, pressure, and temperature; and dehydration of hydrous minerals in impure salt. Simulations have been tested against recent and historical experimental data to develop and improve the salt material model.

Saftey case issues addressed by this model have been captured during an SNL workshop in 2013. The following table highlights the safety case issues related to the model as numbered in this workshop. Some examples of mapping these issues to UFD FEPS is included in the table.

Table 1. All High-Priority Safety Case Issues as Numbered in Sevougian et al.(2013)

3. Changes in physical-chemical properties of crushed salt backfill after waste emplacement (FEP 2.1.04.01 --- Evolution and Degradation of Backfill/buffer; 2.1.08.03 --- Flow in Backfill)
7. Brine and vapor movement in the backfill and emplacement drift, including evaporation and condensation (FEP 1.3.2 1.4)
9. Mechanical and chemical degradation of the waste forms (FEP 1.2.0)
11. Changes in chemical characteristics of brine around the waste packages (FEP 2.2.08.07 --- Mineralogic Dehydration Salt; 2.1.04.01 --- Evolution and Degradation of Backfill/buffer ; 2.2.09.01 --- Chemical Characteristics of Groundwater in Host Rock --- Salt)
15. Changes in physical-chemical properties of host rock due to thermal, hydrological, and chemical effects (FEP 2.2.02.01---Stratigraphy and Properties of Host Rock---- Salt; FEP 2.2.08.07 --- Mineralogic Dehydration Salt)
17. The formation and evolution of the DRZ (DRZ = EDZ) (FEP 2.2.08.06 ---- Flow Through EDZ --- Salt; 2.2.09.61 --- Radionuclide Transport Through EDZ --- Salt)
18. Brine and vapor movement through the host rock and DRZ, including evaporation and condensation (FEP 2.2.09.51 --- Advection of Dissolved Radionuclides in Host Rock --- Salt)
23. Thermal response of EBS and geosphere (heat transfer from waste and waste packages into the EBS and geosphere) (FEP 2.2.08.07 --- Mineralogic Dehydration Salt)
*25. Gas generation and potential physical impacts to backfill, DRZ, and host rock (FEP 2.1.03.04 ---

Localized Corrosion of Waste Packages, 2.2.12.03 --- Gas Transport In Geosphere --- Salt)
27. Colloid formation and transport in the waste package, EBS, and host rock (including DRZ) (FEP 2.2.08.01 --- Flow Through the Host Rock --- Salt)
28. Performance of seal system
31. Appropriate constitutive models (e.g., darcy flow, effective stress)
32. Appropriate representation of coupled processes in process models
33. Appropriate representation of coupled processes in total system performance assessment (TSPA) models
34. Appropriate inclusion and scaling/representation of spatially and temporally varying processes and features in process and TSPA models
37. (Modeling) verification and validation
38. (Modeling) data and results management
39. Development of accurate instrumentation and methods for in-situ testing and characterization
40. In situ demonstration and verification of repository design, with respect to impact on the host rock and the ability to comply with pre-closure and post-closure safety requirements
41. Demonstrate under representative conditions the integrated design functions of the waste package, backfill, host rock, and ventilation
42. Provide a full-scale benchmark for understanding coupled THMC processes and comparing measured system responses with model predictions and assumptions
43. (Confidence-building) Develop generic safety case
44. (Confidence-building) Comparisons to natural and anthropogenic analogs
*45. (Confidence-building) International collaboration
46. (Confidence-building) In-situ testing and demonstrations
47. (Confidence-building) Verification, validation, transparency, and traceability

4. R&D Issue(s) and Safety Case Objectives Addressed by This Model:

- How will the modeled FEP(s) affect repository performance (especially biosphere dose) in a meaningful way?

Numerical models play an important role in the support and development of the safety case (**Error! Reference source not found.**). Such models facilitate evaluating scenarios and hypotheses, and demonstrate our understanding of the physical-chemical system. Development and application of THMC models to support test planning is an integral part of development of field-scale testing and allows the rapid analysis of alternative test designs including scale effects, heating and cooling rates, boundary conditions, and coupled effects.

Pre-closure investigations must consider the duration of waste emplacement within drifts prior to backfilling and sealing those drifts. Processes occurring within this pre-closure period will modify the initial conditions of the post-closure period. Representing post-closure evolution accurately is facilitated by a robust understanding of the effects of heating and ventilation during pre-closure. Pre-closure conditions are likewise dependent on and tied to the development of the distributed rock zone during initial excavation of mined openings in the repository.

The full range of thermal perturbation should be evaluated to assess processes that occur predominantly at the higher expected temperatures. For example, thermally driven changes for common minerals in salt deposits that may be relevant to the safety case are: (1) generation of HCl vapors (Krumhansl et al., 1991) from reaction of magnesium chloride salts (e.g., $MgCl_2 \cdot 4H_2O$), and (2) dehydration of clays (and other phases), which begins at temperatures as low as 75°C (Caporuscio et al., 2013). Although these minerals tend to be minor in salt deposits, their variable distribution may have effects on geochemical conditions

potentially relevant to repository performance.

- **Why is it important from a regulatory perspective?**

Demonstrating that we can simulate processes in the near field will build confidence in the longer term performance of the simulations. These modeling efforts have led to new ideas about what may impact the initial state of the repository which can be important for evolution of drift closure. Confidence building can also help in the public review component of the regulatory process.

- **Describe the current "state of the art" knowledge regarding the issue(s) addressed and why this particular model advances the state of the art in an important way.**

Several porous flow simulators that can perform multiphase transport and reactive chemistry are available (TOUGH, CODE-BRIGHT, FEHM, PFLOTRAN); however few have as many salt specific coupled processes as are included in FEHM. CODE-BRIGHT, which has many salt specific code additions, has been used to simulate precipitation dissolution with thermal effects in salt but not at the drift scale or at boiling conditions (to our knowledge). FEHM is able to converge on boiling transitions with high thermal gradients. We can also expand the current work to include more complex chemistry because FEHM has built in multicomponent reactive chemistry developed by DOE for previous PA simulations. The FEHM team also has extensive experience simulating multiphase environmental isotopic tracers for use in PA model validation.

5. Proposed method for coupling this model to the PA model[1]

- Direct coupling or abstraction?

Direct simulation would be idea and is discussed below.

- Time scale of transient modeled processes (10 years, 100 years…. 1,000,000 years?).

Our simulated run times are on the order of several years as the initial water in the system is driven off by the thermal pulse of high level waste. The simulations take on the order of 8-20 hours to run on a single processor. This points to the need for parallel solver technology if the calculations are deemed necessary for full coupling to the PA.

- Degree of abstraction: reduced dimensionality; simplified representation; response surface.

Direct simulation could be quite time consuming. However model abstraction to an emulator could be undertaken to reduce run times while capturing system behavior.

- Key environmental inputs required from the PA model (and its coupled submodels) and key outputs delivered by this model.

Our simulations require estimation of variability in potential water sources in salt including fracture flow into the backfill, hydrous minerals, and interstitial water. We also need initial permeability structure of the DRZ and backfill. Initial thermal state, ventilation (rate and composition), and brine composition are needed. The model then predicts short term evolution of temperatures and saturations in the drift region. The output of our model has implications for mechanical deformation, gas generation, and waste package corrosion (e.g. chemical composition of brine and how much brine is in contact with waste for how long.

- Are there other models you are aware of that are not being developed, which are needed for your model or for PA?

We have not coupled FEHM to a large scale deformation code, and it would be prudent to

consider PFLOTRAN development to include both deformation and salt THC processes.

6. Real time integration horizon: estimate how long before the proposed model is ready for integration with PA and how long the integration activities might take?

We envision that the current coupled processes could be added to PFLOTRAN in the next years to allow our numerical techniques to be performed in massive parallel on a UFD standard code. This could allow full coupling with the PA as the work evolves. The work would involve FEHM developers working with PFLTORAN developers to extract the necessary code and then integrating. This could take several years to fully port the algorithms.

- Are there intermediate steps or degrees of coupling with PA, e.g., can you couple a certain version of your model in an expedited fashion and then go to the next more detailed version—please describe how

The direct simulations are useful for test design and confidence building before a repository is built, and in the PA could be used as initial conditions before full coupling is achieved. THC simulations tied to small scale experiments done before construction of drift scale tests or a full repository will likely yield data that will reduce long-term costs and highlight areas where more focus is needed.

Table A-7. Waste Canister Corrosion Model

1. Name of Model:

Waste canister corrosion model.

2. Principal Investigator(s) and Affiliation:

Jim Jerden (ANL), Carlos F. Jove Colon (SNL), Paul Mariner (SNL)

3. Brief Model Description:

- Describe the processes and/or events considered in the model, as well as the applicable feature (e.g., waste form, DRZ, etc.), i.e., include a description of the FEP or FEPs addressed by this model.

The quantification of the long-term corrosion behavior of steels in relevant environmental conditions is central to developing a science-based performance assessment of nuclear waste repositories. The waste canister corrosion model will the quantify processes that are essential for calculating the containment life times of steel waste packages and the chemical and electrochemical effects of steel corrosion on waste form degradation and radionuclide release: (1) selection of passive or active corrosion mechanisms depending on the calculated corrosion potential, (2) the generation of H_2 during anoxic corrosion, which has been shown to inhibit the dissolution of used fuel and can lead to alloy embrittlement, (3) production of radiolytic oxidants within and outside of waste packages, which can determine whether a steel corrodes by aerobic or anaerobic processes, (4) interactions with porewaters to form iron silicate colloids and surface coatings such as Fe-saponite, (5) sorption of radionuclides to colloidal and fixed steel corrosion products. The model layout and context are shown in the figures at the end of this document.

The model will have a one-dimensional reaction diffusion layout continuous with the existing Fuel Matrix Degradation Model (FMDM). As with the FMDM, the canister corrosion model will use mixed potential theory to determine the corrosion rate based on the kinetic balance of all relevant interfacial redox reactions. Homogeneous reactions and diffusion processes that determine the supply of reactants to the steel surface and alteration phase saturation indexes will be taken into account.

The FEP that is directly addressed by this model is: 2.1.03.02 (General Corrosion of Waste Packages). Other directly affected FEPs are: 2.1.09.02 (Chemical Characteristics of Water in Waste Packages), 2.1.09.05 (Chemical Interaction of Water with Corrosion Products), 2.1.12.01 (Gas Generation in EBS), 2.1.13.01 (Radiolysis - In Waste Package), 2.1.02.01 (SNF (Commercial, DOE) Degradation), 2.1.02.06 (SNF Cladding Degradation and Failure), 2.1.03.08 (waste packaging; evolution of Flow Pathways in Waste Packages).

Objective	Feature	Process (Issue)		
		UFD FEP ID	UFD FEP Title	Process/Issue Description
Containment, Limited Release Engineered Barriers	Waste Packaging	2.1.03.02	General Corrosion of Waste Packages	- Dry-air oxidation - Humid-air corrosion - Aqueous phase corrosion - Passive film formation and stability

4. R&D Issue(s) and Safety Case Objectives Addressed by This Model:

- What are the R&D issues? Steel corrosion rates in the presence of radiolytic oxidants, bentonite porewaters and evolving chemical conditions within the EBS due to waste form degradation. Hydrogen production rates and associated interfacial hydrogen reactions that either promote or inhibit corrosion. Sorption of radionuclides to colloidal and fixed steel corrosion products.
- How will the modeled FEP(s) affect repository performance (especially biosphere dose) in a meaningful way? The canister is a primary waste isolation barrier in argillite and crystalline repositories and, as such, will be a central focus any repository safety analysis. Although more experimental work is

needed, the level of understanding of steel corrosion and current modeling capabilities make a mechanistic canister corrosion rate model feasible. Integration into the GDSA will be facilitated by using the FMDM template for the model layout.

- Why is it important from a regulatory perspective? As cited from the UFD Roadmap report: "The importance of the waste container at this decision point [licensing] is high because having defensible models to represent waste container degradation processes is required. The current information is deemed insufficient to support this decision." The ongoing R&D work for canister corrosion in dry storage that is focused on oxidizing surface storage environments and breaches, but corrosion in the anoxic disposal environment involves different processes and dependencies. In addition, dissolved and solid corrosion products are key modeling requirements for disposal systems in addition to penetrations.
- Describe the current "state of the art" knowledge regarding the issue(s) addressed and why this particular model advances the state of the art in an important way. The corrosion behavior of iron and steels has been an important topic of global interest for around two thousand years. However, there remain important information gaps regarding the long-term corrosion behavior of steels under anaerobic conditions in which radiolytic oxidants may be present. Current models are based on empirical probabilistic failure models. The proposed mechanistic steel corrosion model would represent a new, state of the art tool for quantifying canister corrosion rates based on repository environments such as groundwater composition and fuel burn-up. The model would provide a quantitative framework into which new experimental observations could be incorporated and applied to site-specific repository performance assessments.

5. Proposed method for coupling this model to the PA model[1]

- Direct coupling or abstraction? Direct coupling with PFLOTRAN using the FMDM one dimensional reaction/diffusion model layout that has already been used for integration as a prototype for waste form degradation.
- Time scale of transient modeled processes (10 years, 100 years…. 1,000,000 years?). Applied to the relevant performance period based on the anticipated environmental conditions under which the process occurs.
- Degree of abstraction: reduced dimensionality; simplified representation; response surface. One dimensional reaction/diffusion model focusing on the rate-determining interfacial reactions rather than geometry specific aspects or stochastics.
- Key environmental inputs required from the PA model (and its coupled submodels) and key outputs delivered by this model. Inputs: time, temperature, solution chemistry. Primary output: steel degradation rate (mass per area per time or penetration rate e.g., micrometers per year). Other important outputs are the generation rate of hydrogen, concentrations of key redox species that determine Eh, dissolved concentrations and the masses of steel corrosion products.
- Are there other models you are aware of that are not being developed, which are needed for your model or for PA?. Waste form degradation models are needed for all high-level wastes (e.g., glass, alloy waste forms etc.). These models describe chemistry that may have important feedbacks with the canister corrosion model in terms of radolysis, pH evolution, complexation etc.

6. Real time integration horizon: estimate how long before the proposed model is ready for integration with PA and how long the integration activities might take?

- Are there intermediate steps or degrees of coupling with PA, e.g., can you couple a certain version of your model in an expedited fashion and then go to the next more detailed version—please describe how.

The conceptual layout for the canister corrosion rate model already exists as a module developed with the FMDM (see bottom Figure below). The steel corrosion model can be incorporated into the FMDM or included in PA as a stand-alone model. Since it would use the same spatial, temporal and mathematic structure as the FMDM, coupling with PA could be achieved in an expedited fashion.

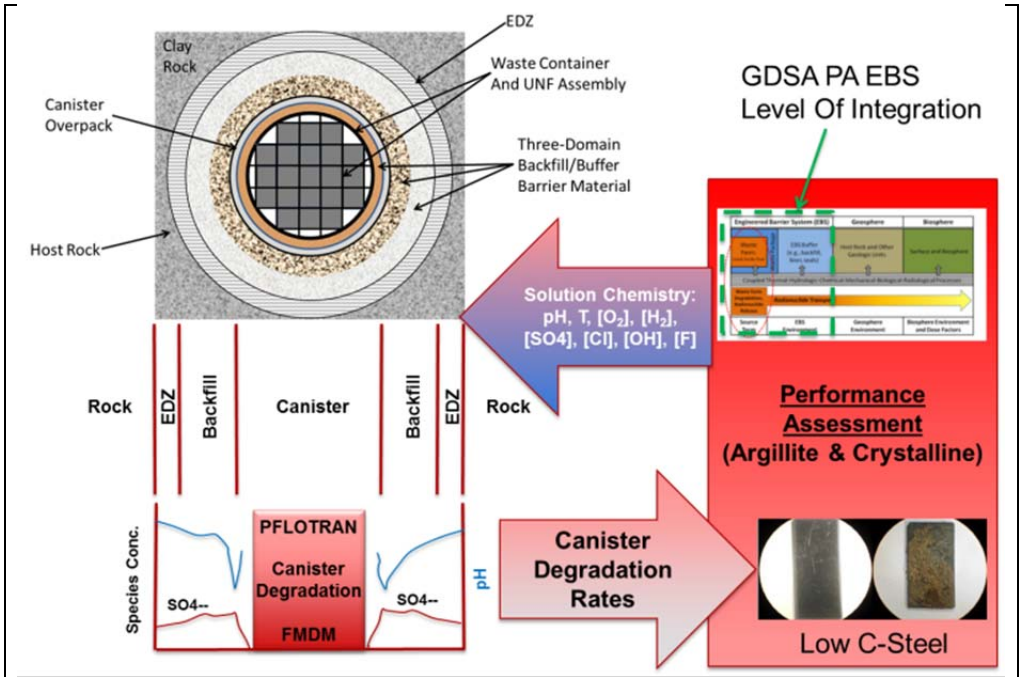

Schematic layout of the canister corrosion rate model showing relationship with the fuel matrix degradation model *(only key interfacial reactions shown)*

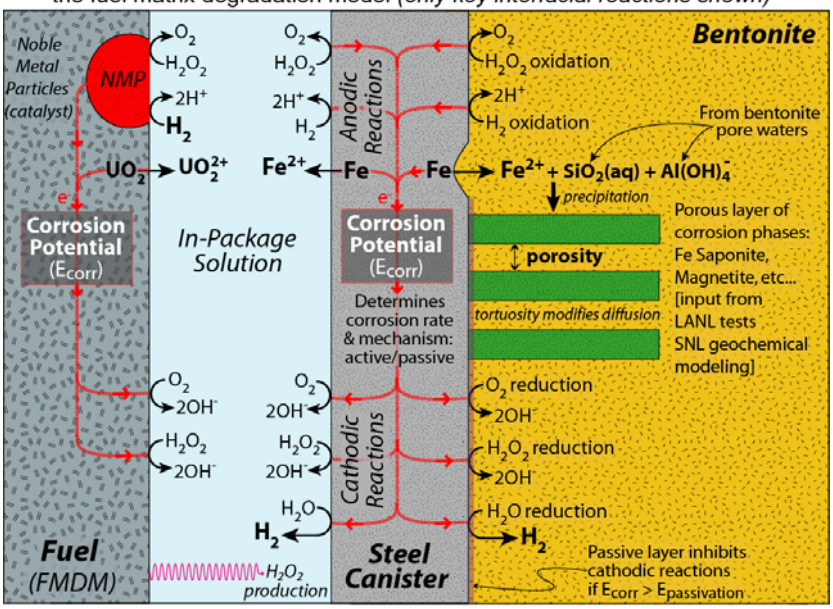

Width of irradiated zone depends on burn up, age of fuel

Table A-8. Decay in Precipitate Phase

1. Name of Model:
Decay in Precipitate Phase

2. Principal Investigator(s) and Affiliation:
P. Mariner

3. Brief Model Description:

- Describe the processes and/or events considered in the model, as well as the applicable feature (e.g., waste form, DRZ, etc.), i.e., include a description of the FEP or FEPs addressed by this model.

This model calculates decay in precipitated solid phases in each cell (i.e., the process circled in red in the Figure 1 schematic). The model is designed to release the daughter product to the cell so that it can be distributed between aqueous, solid, adsorbed, and gas phases by a partitioning model such as the Equilibrium Isotope Partitioning model (described in a separate model integration template). As is the case for decay in aqueous and adsorbed phases, decay in precipitate phases is to also be calculated in the Newton Solve step of the PFLOTRAN calculations.

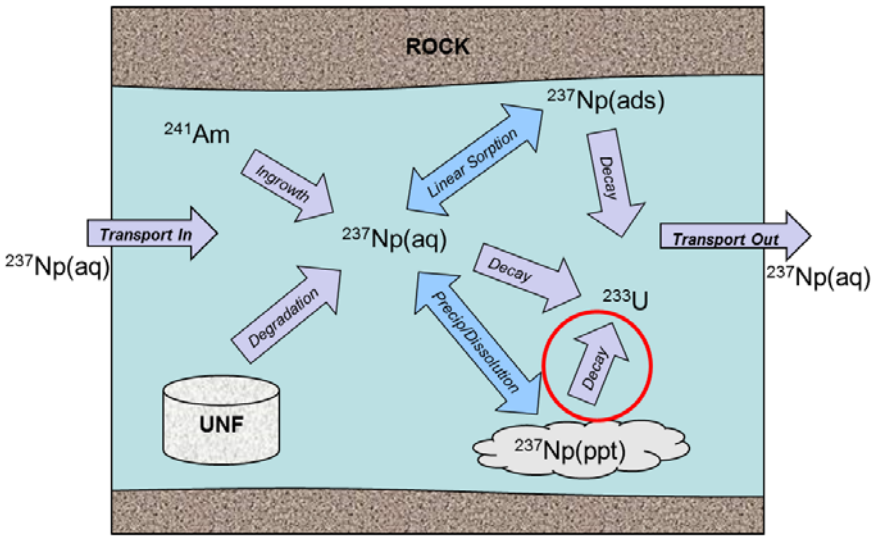

Figure 1. Schematic diagram of processes affecting concentrations ^{237}Np in aqueous, adsorbed, and precipitate phases within a single cell.

FEPs: 2.1.01.02, 2.1.09.xx, 2.2.09.xx, 2.3.09.xx

4. R&D Issue(s) and Safety Case Objectives Addressed by This Model:

- How will the modeled FEP(s) affect repository performance (especially biosphere dose) in a meaningful way?
- Why is it important from a regulatory perspective?
- Describe the current "state of the art" knowledge regarding the issue(s) addressed and why this particular model advances the state of the art in an important way.

PFLOTRAN does not currently have the capability of decaying precipitated radionuclides. This causes precipitated radionuclides to have an infinite half-life when in precipitate form and causes concentrations of daughter products to be underrepresented in the simulations. Because this treatment is incorrect and leads to underestimated release and transport of radioactivity, it needs to be corrected. The proposed model will allow precipitated radionuclides to decay and will release the daughters to the cell where they will be available for transport as dictated by partitioning constraints.

5. Proposed method for coupling this model to the PA model[1]

- Direct coupling or abstraction?

Direct coupling via PFLOTRAN sandbox

- Time scale of transient modeled processes (10 years, 100 years…. 1,000,000 years?).

Full TSPA modeling period

- Degree of abstraction: reduced dimensionality; simplified representation; response surface.

No abstraction. Direct analytical calculation.

- Key environmental inputs required from the PA model (and its coupled submodels) and key outputs delivered by this model.

Time step duration, amounts of precipitated phases, amounts of radionuclides in precipitate phases

- Are there other models you are aware of that are not being developed, which are needed for your model or for PA?

No. However, it is possible that a portion of the daughter products will be trapped within the precipitate and will not be released for potential transport. A model could be developed to estimate the fraction of various daughter products are released from the precipitate at the time they are produced and over time as a result of other processes (diffusion through precipitate, dissolution of precipitate, etc.)

6. Real time integration horizon: estimate how long before the proposed model is ready for integration with PA and how long the integration activities might take?

- Are there intermediate steps or degrees of coupling with PA, e.g., can you couple a certain version of your model in an expedited fashion and then go to the next more detailed version—please describe how

This capability would take no more than a couple of weeks to implement. This would be a fairly ordinary PFLOTRAN sandbox routine.

Table A-9. Equilibrium Isotope Partitioning (named "Effective Solubility Model for Isotopes" in Table 3-2).

1. Name of Model:
Equilibrium Isotope Partitioning

2. Principal Investigator(s) and Affiliation:
P. Mariner

3. Brief Model Description:

- Describe the processes and/or events considered in the model, as well as the applicable feature (e.g., waste form, DRZ, etc.), i.e., include a description of the FEP or FEPs addressed by this model.

This model partitions isotopes between aqueous, solid, and adsorbed phases according to imposed equilibrium constraints (e.g., elemental solubility, sorption distribution coefficients). It is designed to be performed after the Newton Solve, as shown in Figure 1. It could be easily expanded to include equilibrium gas phase partitioning.

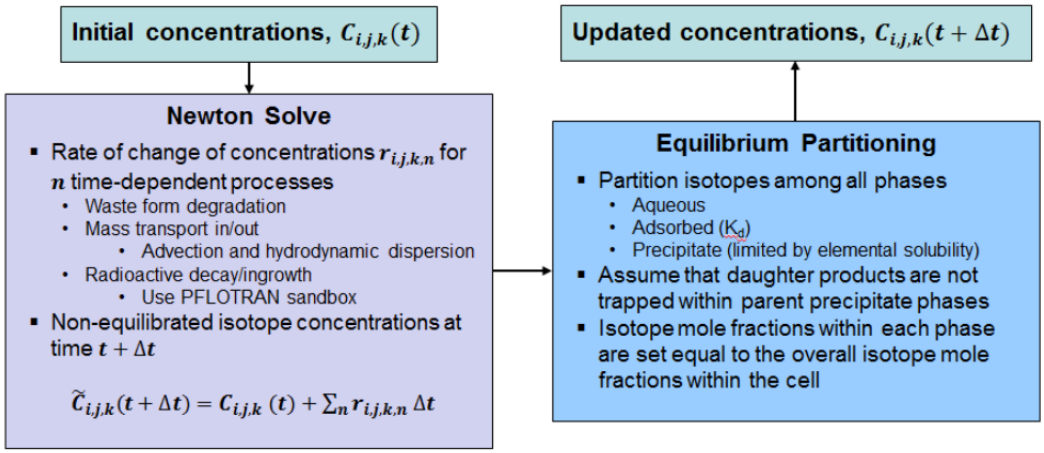

Figure 1. Flow diagram for updating isotope concentrations in PFLOTRAN using a new reaction sandbox routine for decay and ingrowth (left side) and a new process model for equilibrium partitioning (right side). (Subscripts i, j, and k denote isotope, element, and phase, respectively.)

FEPs: 2.1.09.xx, 2.2.09.xx, 2.3.09.xx

4. R&D Issue(s) and Safety Case Objectives Addressed by This Model:

- How will the modeled FEP(s) affect repository performance (especially biosphere dose) in a meaningful way?
- Why is it important from a regulatory perspective?
- Describe the current "state of the art" knowledge regarding the issue(s) addressed and why this particular model advances the state of the art in an important way.

PFLOTRAN does not currently have the capability for calculating effective solubilities for isotopes. Thus, PFLOTRAN cannot simply account for reduced solubility when multiple isotopes of the same element are present. This can lead to considerable overestimates in radionuclide mobility. This model distributes all isotopes of each element among aqueous and sorbed phases and precipitates excess isotopes when aqueous elemental concentrations exceed elemental solubilities.

5. Proposed method for coupling this model to the PA model[1]

- Direct coupling or abstraction?

Direct coding in PFLOTRAN

- Time scale of transient modeled processes (10 years, 100 years…. 1,000,000 years?).

Full TSPA modeling period

- Degree of abstraction: reduced dimensionality; simplified representation; response surface.

No abstraction. Direct calculation.

- Key environmental inputs required from the PA model (and its coupled submodels) and key outputs delivered by this model.

Amounts of all isotopes in cell, elemental solubilties, mass of sorbent, volume of water

- Are there other models you are aware of that are not being developed, which are needed for your model or for PA?

This model could be easily expanded to include a gas phase as a fourth phase for partitioning.

6. Real time integration horizon: estimate how long before the proposed model is ready for integration with PA and how long the integration activities might take?

- Are there intermediate steps or degrees of coupling with PA, e.g., can you couple a certain version of your model in an expedited fashion and then go to the next more detailed version—please describe how

This capability would take a couple of weeks or so to implement. The algorithm has been developed and tested in Mathcad.

Table A-10. Waste Package Degradation Module, Version 1.0, (non-mechanistic)

1. Name of Model:
Waste Package Degradation Module, Version 1.0

2. Principal Investigator(s) and Affiliation:
P. Mariner

3. Brief Model Description:

- Describe the processes and/or events considered in the model, as well as the applicable feature (e.g., waste form, DRZ, etc.), i.e., include a description of the FEP or FEPs addressed by this model.

This module determines the following for an individual WP: the time of initial WP breach, the extent of initial breach, and the rate of growth of the breach. In the initial implementation, general corrosion, localized corrosion, SCC-initiated corrosion, and non-detected defects are included. Outputs are sampled from distributions specific to canister materials and local conditions.

FEPs: 2.1.03.0x

4. R&D Issue(s) and Safety Case Objectives Addressed by This Model:

- How will the modeled FEP(s) affect repository performance (especially biosphere dose) in a meaningful way?
- Why is it important from a regulatory perspective?
- Describe the current "state of the art" knowledge regarding the issue(s) addressed and why this particular model advances the state of the art in an important way.

Because the waste package canister is a significant barrier to WP water intrusion, WF degradation, and radionuclide release, waste package degradation is highly important to radionuclide release to the geosphere.

Version 1.0 is a placeholder designed to represent plausible probabilities and distributions for time of initial WP breach, extent of initial breach, and rate of breach growth for various degradation processes. This version would allow GDSA to evaluate the effects of such degradation on total system performance. Future versions of this module may include state-of-the-art process models, either built into the module or coupled to it.

5. Proposed method for coupling this model to the PA model[1]

- Direct coupling or abstraction?

Direct coupling

- Time scale of transient modeled processes (10 years, 100 years…. 1,000,000 years?).

Full TSPA modeling period

- Degree of abstraction: reduced dimensionality; simplified representation; response surface.

Version 1.0 is simple. It samples degradations rates and times of breach from predefined distributions.

- Key environmental inputs required from the PA model (and its coupled submodels) and key outputs delivered by this model.

Material type and thickness, temperature, chemical environment

- Are there other models you are aware of that are not being developed, which are needed for your model or for PA?

Various process models are needed for general corrosion, localized corrosion, SSC-initiated corrosion, microbially-induced corrosion, breach growth, etc.

6. Real time integration horizon: estimate how long before the proposed model is ready for integration with PA and how long the integration activities might take?

- Are there intermediate steps or degrees of coupling with PA, e.g., can you couple a certain version of your model in an expedited fashion and then go to the next more detailed version—please describe how

Version 1.0 would take several weeks to implement. Although it is not mechanistic, it would provide the framework for adding mechanistic process models in the future. Until process models are developed for implementation, Version 1.0 would provide a means for simulating plausible WP barrier behavior and WP-to-WP variability in GDSA simulations.

Table A-11. Flow Properties of Reconsolidated and Damaged Salt

1. Name of Model:
Flow properties of reconsolidated and damaged salt

2. Principal Investigator(s) and Affiliation:
Cliff Howard, Kris Kuhlman & Tom Dewers, SNL

3. Brief Model Description:

- Describe the processes and/or events considered in the model, as well as the applicable feature (e.g., waste form, DRZ, etc.), i.e., include a description of the FEP or FEPs addressed by this model.

The investigation will help parametrize multiphase movement of brine through reconsolidating crushed (run-of-mine) salt and in damaged (but otherwise intact) salt from the DRZ.

Data parametrization capillary pressure vs. saturation, as a function of porosity are being developed. Two-phase relative permeability (air and brine) are being developed as a function of porosity, too.

UFD FEP Numbers:
2.1.08.01 (Flow through the EBS),
2.1.08.03 (Flow in backfill),
2.1.08.04 (Flow through seals),
2.1.08.06 (Alteration and Evolution of EBS Flow Pathways),
2.1.08.08 (Capillary Effects in EBS),
2.1.08.09 (Influx/Seepage into the EBS)

4. R&D Issue(s) and Safety Case Objectives Addressed by This Model:

- How will the modeled FEP(s) affect repository performance (especially biosphere dose) in a meaningful way?
- Why is it important from a regulatory perspective?
- Describe the current "state of the art" knowledge regarding the issue(s) addressed and why this particular model advances the state of the art in an important way.

Simulation of the hydrologic (coupled with thermal and mechanical) behavior in a salt repository in process models or PA models requires parameters and constitutive models to represent the capillary pressure relationship and the relative permeability relationship. Currently these models use analogs from low-permeability oil reservoir rocks, since there is very little salt-specific data available. Salt is well-known to be a highly reactive medium for flow, so quartz sand or carbonate reservoirs may not make good analogs for salt, especially considering the significant amount of creep and pressure dissolution that occurs during crushed salt reconsolidation.

This data can affect the evolution of the brine in a repository, the amount of brine which flows into a repository from the host rock, and the efficacy of any seals or backfill constructed from crushed salt.

5. Proposed method for coupling this model to the PA model[1]

- Direct coupling or abstraction?
- Time scale of transient modeled processes (10 years, 100 years…. 1,000,000 years?).
- Degree of abstraction: reduced dimensionality; simplified representation; response surface.
- Key environmental inputs required from the PA model (and its coupled submodels) and key outputs delivered by this model.
- Are there other models you are aware of that are not being developed, which are needed for your model or for PA?

These data will be used to parametrize PA models and constitutive models used in PA directly.

6. Real time integration horizon: estimate how long before the proposed model is ready for integration with PA and how long the integration activities might take?

- Are there intermediate steps or degrees of coupling with PA, e.g., can you couple a certain version of your model in an expedited fashion and then go to the next more detailed version—please describe how

Since this is data, its integration should be straightforward and rapid.

Table A-12. TOUGH-RBSN

1. Name of Model: TOUGH-RBSN

2. Principal Investigator(s) and Affiliation: Kunhwi Kim (LBNL), Jonny Rutqvist (LBNL), Jim Houseworth (LBNL), Jens Birkholzer (LBNL)

3. Brief Model Description:

- Describe the processes and/or events considered in the model, as well as the applicable feature (e.g., waste form, DRZ, etc.), i.e., include a description of the FEP or FEPs addressed by this model.

TOUGH-RBSN is a coupled Thermal-Mechanical-Hydrological (THM) fracture-damage model which combines the thermal hydrological capabilities of TOUGH2 with the geomechanical and fracture-damage capabilities of the Rigid-Body-Spring-Network (RBSN) model. It is similar to TOUGH-FLAC except that the RBSN geomechanical model focuses on discrete fracture damage instead of continuum geomechanical behavior emphasized by FLAC. TOUGH-RBSN uses THM processes to determine where and how discrete fractures form and integrates the developing discrete fracture system into both the thermal-hydrological and geomechanical responses. It is capable of developing and treating complex three-dimensional fracture systems both in terms of opening of fractures by excessive shear and tensile stress and closing of fractures by normal stresses.

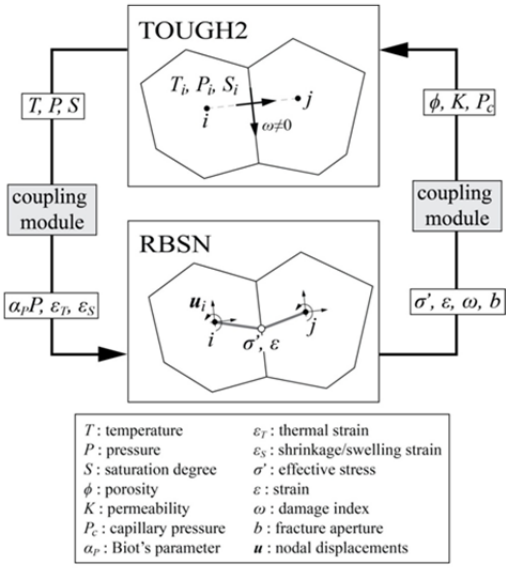

The most closely associated FEP is 2.2.01.01 (see below – from the UFD Roadmap spreadsheet/tables). Related FEPs are 2.1.08.09 (Influx/Seepage Into the EBS), Open Boreholes (1.1.01.01), Thermal Effects on Flow in EBS (2.1.11.10), Flow Through Host Rock (2.2.08.01), Effects of Excavation on Flow (2.2.08.04), and Mechanical Effects from Preclosure Operations (1.01.02.02).

Objective	Feature	Process (Issue)		
		UFD FEP ID	UFD FEP Title	Process/Issue Description
Limited Release – Natural Barriers	Natural System - Geosphere	2.2.01.01	Evolution of EDZ	- Lateral extent, heterogeneities - Physical properties - Flow pathways - Chemical characteristics of groundwater in EDZ - Radionuclide speciation and solubility in EDZ - Thermal-mechanical effects - Thermal-chemical alteration

4. R&D Issue(s) and Safety Case Objectives Addressed by This Model:

- How will the modeled FEP(s) affect repository performance (especially biosphere dose) in a meaningful way?

TOUGH-RBSN has been developed mainly for an argillite repository environment where the low permeability of the natural argillite rock system is a key attribute for repository performance. A strong repository performance relies on maintenance of the rock system low permeability attribute over the performance period. One of the few ways in which this attribute can degrade significantly is through the formation of fractures in the excavation disturbed zone around waste emplacement drifts. Observations in URLs in argillite rock show that fracturing in the near-tunnel zones should be expected and have also been shown to significant increases in the rock permeability locally. This is the main area of application of the TOUGH-RBSN model for a nominal performance assessment case (no disruptive scenarios).

- Why is it important from a regulatory perspective?

As cited from the UFD Roadmap report: "The importance of excavation disturbance or damage to the Site Suitability and Licensing decision point varies by rock type. For this decision point, improved representation of excavation disturbance and damage, particularly reduced uncertainty, and how these processes impact and are affected by the developing design would need to be demonstrated. For repository systems developed in clay or shale, the understanding of the EDZ is of **high** importance and the available information is insufficient."

- Describe the current "state of the art" knowledge regarding the issue(s) addressed and why this particular model advances the state of the art in an important way.

There are few, if any, other methods available for computing complex fracture network growth and attenuation on a fundamental basis coupled with THM processes.

5. Proposed method for coupling this model to the PA model[1]

- Direct coupling or abstraction?

Abstraction would be needed because of computational burden associated with the calculation.

- Time scale of transient modeled processes (10 years, 100 years…. 1,000,000 years?).

This initial style of implementation could be used at selected time intervals and locations to estimate evolving fracture conditions that would then be passed on to other models in the PA. The time resolution would follow the change in stress, temperature, and hydraulic pressure in the near field, with more frequent use of RBSN in the early period when conditions are changing more quickly.

- Degree of abstraction: reduced dimensionality; simplified representation; response surface.

Suggest for initial use that the two-dimensional, quasi-static, RBSN model be used as a stand-alone method to assign fracture properties (porosity, permeability, spacing) within the EDZ for the near-field flow and transport models used in the PA.

- Key environmental inputs required from the PA model (and its coupled submodels) and key outputs delivered by this model.

The model would require inputs from a near-field process model, e.g., TOUGH-FLAC (or TOUGHREACT-FLAC), for temperature, fluid pressure, and mechanical stress. The advantage of TOUGH-FLAC as the coupled process model (instead of TOUGH-RBSN) is a better representation of geomechanics for clays and bentonite (and inclusion of chemical couplings if TOUGHREACT-FLAC is used). The development of fractures in the RBSN model would be translated into effective fracture properties for use in TOUGH-FLAC as a continuum fracture field. Essentially, this would be a coarse coupling (in time) of TOUGH-FLAC with RBSN to periodically to account for fracture generation/attenuation. These continuum fracture properties would also be used by PFLOTRAN or other PA models for fluid flow and radionuclide transport in the near-field environment.

- Are there other models you are aware of that are not being developed, which are needed for your model or for PA? No.

6. Real time integration horizon: estimate how long before the proposed model is ready for integration with PA and how long the integration activities might take?

- Are there intermediate steps or degrees of coupling with PA, e.g., can you couple a certain version of your model in an expedited fashion and then go to the next more detailed version—please describe how

There hasn't been any work directly towards integration of the TOUGH-RBSN model with PA up to this point. The idea proposed in item 5 would need a few months of dedicated effort to complete.

Table A-13. Coupled THMC Model for EBS Bentonite (called "THMC processes in EBS" in Table 3-2)

1. Name of Model:

Coupled THMC model for EBS bentonite

2. Principal Investigator(s) and Affiliation:

Liange Zheng (LBNL) and Jonny Rutqvist

3. Brief Model Description:

- Describe the processes and/or events considered in the model, as well as the applicable feature (e.g., waste form, DRZ, etc.), i.e., include a description of the FEP or FEPs addressed by this model.

During the lifespan of a geologic repository, the performance of the EBS is affected by complex thermal, hydrogeological, mechanical, chemical and biological processes, such as heat release due to radionuclide decay, multiphase flow (including gas release due to canister corrosion), swelling of buffer materials, radionuclide diffusive transport, waste dissolution, and chemical reactions. All these processes are related to each other. An in-depth understanding of these coupled processes is critical for the performance assessment (PA) of an EBS and the entire repository. Coupled thermal-hydrological-mechanical-chemical (THMC) models were developed for EBS bentonite using TOUGHREACT-FLAC3d. While these models obviously consider each individual THMC processes, they also take into account the HM, TM, HC, TC and MC coupling. Currently the focus of these models is the long term chemical alteration (mainly illitization) and its effect on the swelling stress.

These models address FEP 2.1.04.01, Buffer/Backfill; Related FEPs are 2.1.07.02, 03, 04, 09, 10 Mechanical Processes; FEPs 2.1.08.01, 03, 06, 07, 08, Hydrologic Processes; FEPs 2.1.11.04, 08 Thermal Processes, by studying coupled processes in the EBS; and FEPs 2.1.09.06, 52, 53, 54, Chemical Processes—Transport.

Objective	Feature	Process (Issue)		
		UFD FEP ID	UFD FEP Title	Process/Issue Description
Containment, Limited Release Engineered Barriers	Backfill/buffer	2.1.04.01	Evolution and Degradation of Backfill/ buffer	- Alteration - Thermal expansion / Degradation - Swelling/Compaction - Erosion/Dissolution - Evolution of backfill flow pathways

4. R&D Issue(s) and Safety Case Objectives Addressed by This Model:

- How will the modeled FEP(s) affect repository performance (especially biosphere dose) in a meaningful way?

Smectite is the major mineral phase of EBS bentonite and an essential component for EBS to provide some safety functions such as limiting transport in the near field, reducing microbial activity, damping rock-shear movement, preventing canister sinking and limiting pressure on canister, etc. The alteration of smectite, including structural change (e.g. Na-smectite to Ca-smectite) and more importantly the illitization (transformation of smectite to illite via several intermediate phase changes), will compromise the function of EBS be reducing the swelling capacity of EBS and sorption capacity, which are directly related to the corrosion of canister and the transport of radioactive nuclides. The coupled THMC models provide a quantification of such changes.

- Why is it important from a regulatory perspective?

From regulatory point of view, We not only construct EBS with bentonite that has the desired permeability, swelling capacity and sorption capability, but also have to make sure these importance properties can be maintained or at least acceptably compromised over the lifespan of a geological repository. As cited from the UFD Roadmap report: "The importance of the other engineered barrier system materials at this decision point is **high** because having defensible models to represent their degradation, impacts on other processes within the engineered barrier system, and impacts on radionuclide transport is required. The current information is deemed **insufficient** to support this decision."

- Describe the current "state of the art" knowledge regarding the issue(s) addressed and why this particular model advances the state of the art in an important way.

These coupled THMC models advanced the state of art in two ways. First, they enhance our understanding of the

illitization and its effect of mechanical behavior. Although illitization is widely evidenced in geological formations (which is why illitization becomes an issue for EBS bentonite), it was not confirmed by experiments because duration of these experiments was not long enough and conditions under which experiments were conducted deviated from the in situ conditions of a repository, and more importantly some coupled processes were neglected. The coupled THMC models overcome these limitations and provide quantitative evaluation of illitization and its effect of mechanical behavior. Second, the development of TOUGHREACT-FLAC3D improved the ability of simulating coupled processes. Although several codes claimed to have the capability of simulating coupled THMC. The THMC model conducted in UFD is the first of this kind model reported.

5. Proposed method for coupling this model to the PA model[1]

- Direct coupling or abstraction?
  Abstraction is needed for the model to be used by PFLOTRAN.

- Time scale of transient modeled processes (10 years, 100 years…. 1,000,000 years?).
  Applied to the entire performance period.

- Degree of abstraction: reduced dimensionality; simplified representation; response surface.
  Response surface is probably a more feasible way to incorporate this model to PA model. Response surface, for example, illitization as a function of key flow, chemical parameters and time, can be established based on coupled THMC model and integrated to the PA model.

- Key environmental inputs required from the PA model (and its coupled submodels) and key outputs delivered by this model.
  Inputs: heat release function, thermal conductivity, permeability, porosity, pore water composition, mineralogical composition, sorption capacity, mechanical properties.
  Outputs: Evolution of permeability, porosity, abundance of smectite, sorption capacity and swelling stress over time.
- Are there other models you are aware of that are not being developed, which are needed for your model or for PA?
  The chemical model for bentonite still needs a lot of improvement: the chemical reactions taking place need to be better understood and reactions rates need to be better constrained. The mechanical model for bentonite is relatively mature but key parameters need to be calibrated against long term data.

6. Real time integration horizon: estimate how long before the proposed model is ready for integration with PA and how long the integration activities might take?

- Are there intermediate steps or degrees of coupling with PA, e.g., can you couple a certain version of your model in an expedited fashion and then go to the next more detailed version—please describe how.

While the chemical and mechanical model still need to be improved and the coupling between chemical and mechanical processes needs to be refined, “temporary” abstracted models (e.g. response surface) can be derived and integrated with PA model. The abstracted models can be updated when process models are improved.

Table A-14. TOUGH-FLAC and TOUGHREACT-FLAC including BBM (called "THM model of buffer materials (unsaturated)" in Table 3-2)

1. Name of Model: TOUGH-FLAC and TOUGHREACT-FLAC including BBM

2. **Principal Investigator(s) and Affiliation:** Jonny Rutqvist (LBNL), Jens Birkholzer (LBNL)

3. Brief Model Description:

- Describe the processes and/or events considered in the model, as well as the applicable feature (e.g., waste form, DRZ, etc.), i.e., include a description of the FEP or FEPs addressed by this model.

In nuclear waste isolation, TOUGH-FLAC provides a model framework for modeling coupled THM processes in the EBS and host rock and their interactions using state-of-the-art macroscopic constitutive models for bentonite, crushed rock salt backfill, clay, salt and crystalline host rocks. For rigorous modeling of the THM behavior of bentonite-based (swelling) buffer and back-fill materials, the BBM (Barcelona Basic Model) and BExM (Barcelona Expansive Model) models have been implemented into TOUGH-FLAC.

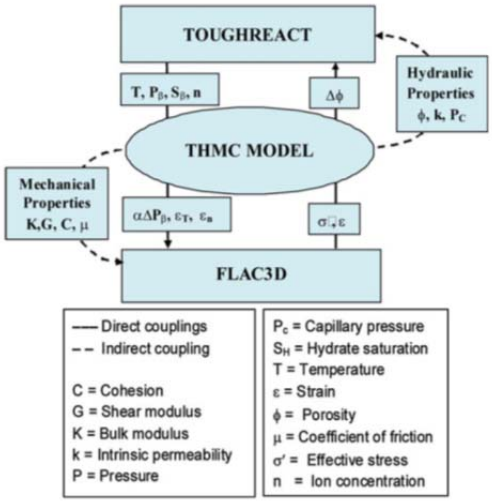

The most closely associated FEP is 2.1.04.01 (see below – from the UFD Roadmap spreadsheet/tables). Related FEPs are 2. Flow Through the EBS (2.1.08.01), 2.1.08.03 (Flow through Backfill), 2.1.08.06 (Alteration and Evolution of EBS Flow Pathways), 2.1.08.09 (Influx/Seepage Into the EBS), Open Boreholes (1.1.01.01), Thermal Effects on Flow in EBS (2.1.11.10),), 2.2.01.01 (Evolution of EDZ) , Flow Through Host Rock (2.2.08.01), Effects of Excavation on Flow (2.2.08.04), Mechanical Effects from Preclosure Operations (1.01.02.02), Degradation of Liner/Rock Reinforcement Materials in EBS (2.1.06.01), Heat Generation in EBS (2.1.11.01), Effects of Backfill on EBS Thermal Environment (2.1.11.03), Effects of Drift Collapse on EBS Thermal Environment (2.1.11.04), Effects of Influx (Seepage) on Thermal Environment (2.1.11.05), Thermal-Mechanical Effects on Backfill (2.1.11.08), Thermally-Driven Buoyant Flow / Heat Pipes in EBS (2.1.11.12), Effects of Gas on Flow Through the EBS (2.1.12.02), Gas Transport in EBS (2.1.12.03), Thermal-Mechanical Effects on Geosphere (2.2.11.06),

Objective	Feature	Process (Issue)		
		UFD FEP ID	UFD FEP Title	Process/Issue Description
Containment Limited Release – Engineered Barriers	Backfill/Buffer	2.1.04.01	Evolution and degradation of backfill/buffer	- Alteration - Thermal expansion / Degradation - Swelling/Compaction - Erosion/Dissolution - Evolution of backfill flow pathways

4. R&D Issue(s) and Safety Case Objectives Addressed by This Model:

- How will the modeled FEP(s) affect repository performance (especially biosphere dose) in a meaningful way?
- Why is it important from a regulatory perspective?
- Describe the current "state of the art" knowledge regarding the issue(s) addressed and why this particular model advances the state of the art in an important way.

In context of geologic nuclear waste disposal, coupled THM processes are relatively short-lived from safety assessment perspective, but could potentially give rise to permanent changes, such as the formation of a damaged zone around excavations that could provide a path for transport of radionuclides if released from a waste package. The mechanical evolution and swelling of the protective buffer are imperative to its functions, such as to provide long-term mechanical support to seal the excavation damage zone and to prevent further damage during the thermal peak. At the same time, the mechanical evolution of the buffer is governed by complex coupled interactions with temperature and hydraulics, between micro and macro clay structures, as well as with the host rock.

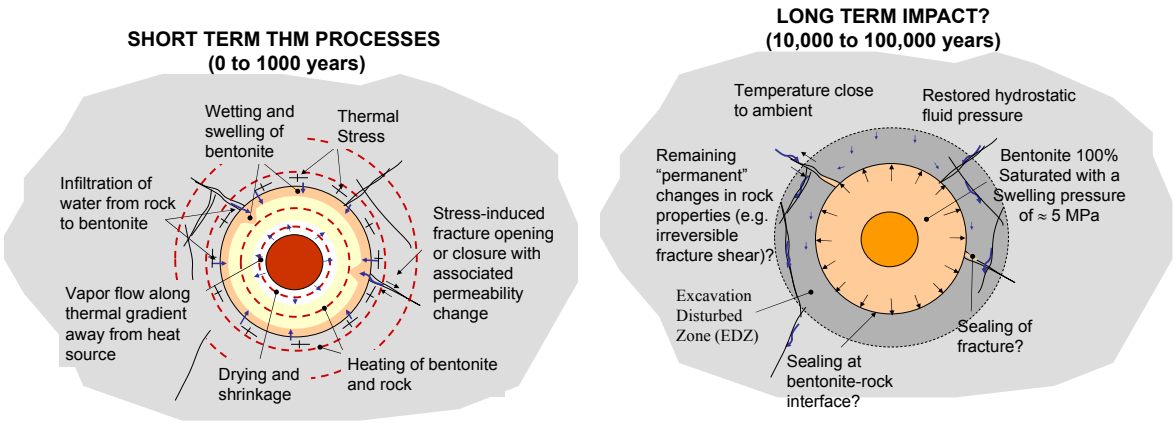

BBM is well established and tested for the modeling of unsaturated-saturated soils, including bentonite. It is the most common model of its kind, although other similar constitutive models have been developed at a number of academic institutions in Europe. The input parameters for different types of bentonite (e.g. compacted bentonite blocks, pellets, sand-bentonite mixtures) are being established through laboratory experiments and large scale field experiments. BExM can in addition to BBM be used for modeling the underlying dual-structural behavior, which is important to consider in swelling clay for accurate and mechanistically correct modeling of the resaturation, swelling, and permeability evolution of the buffer. BExM and dual-structural models is at the forefront of research and further testing, validations against experiments and applications are needed to gain experience and confidence in using such advanced model. There is only one other code worldwide having such model implemented in a THM code; CodeBright developed at University of Cataluña, Barcelona. The dual-structure model can also provide the necessary link between mechanical and chemical processes, for the investigation of effects of chemical changes on the long-term stability of a buffer, and through the coupling of TOUGHREACT and FLAC3D. Such THMC coupling is described under argillite models. It is the only one of its kind. For calculating changes in the DRZ (or EDZ), constitutive models will be different in Crystalline and other rock types, such as Argillaceous rocks. However, the analysis of EDZ evolution must be conducted using a model that includes both the EBS and host rock and their interactions, meaning that the evolution of the host rock or the evolution of the EBS cannot be analyzed independently. The TOUGH-FLAC model framework with BBM and BExM provides such a model, and the extension to TOUGHREACT-FLAC clearly advances the state-of-the-art and will be important for evaluating potential chemical effects on the long-term stability of the EBS.

From a regulatory perspective, the UFD Roadmap report states: "The importance of the other engineered barrier system materials at this decision point is **high** because having defensible models to represent their degradation, impacts on other processes within the engineered barrier system, and impacts on radionuclide transport is required. The current information is deemed **insufficient** to support this decision."

5. Proposed method for coupling this model to the PA model[1]

- Direct coupling or abstraction?
- Time scale of transient modeled processes (10 years, 100 years…. 1,000,000 years?).
- Degree of abstraction: reduced dimensionality; simplified representation; response surface.
- Key environmental inputs required from the PA model (and its coupled submodels) and key outputs delivered by this model.
- Are there other models you are aware of that are not being developed, which are needed for your model or for PA?

The TOUGH-FLAC with BBM and BExM constitutive THM models provides a tool for calculating the evolution of the EBS and the host rock, including the disturbed rock zone (DRZ) from just after emplacement to over 100,000 years. The analysis for coupling to the PA model might be conducted in a 2D cross-section of one emplacement drift or alternative a 3D model focused on the near field of an emplacement tunnel or a few emplacement tunnels in different parts of a repository and for different FEPs such as nominal case or such as for cases of extensive gas generation. The input required is the geometry, heat source, THM properties of buffer and host rock, initial THM conditions (such as in situ stress). The output to the PA model would be the changes in flow properties (e.g. permeability and porosity) in the EBS and near-field including the buffer and DRZ and also to inform PA related to local flow created by coupled THM processes.

6. Real time integration horizon: estimate how long before the proposed model is ready for integration with PA and how long the integration activities might take?

- Are there intermediate steps or degrees of coupling with PA, e.g., can you couple a certain version of your model in an expedited fashion and then go to the next more detailed version—please describe how

The calculation of the THM evolution of the EBS and host rock over a 100,000 year time frame for a 2D cross-section of an emplacement tunnel has already been demonstrated and published. The current TOUGH-FLAC framework with currently implemented constitutive models for such model geometry could be used for provided output to PA today. Modeling these processes in 3D has also been demonstrated associated with modeling of large-scale field tests over tens of years and could be extended to 100,000 years if considering multiple tunnels in parts of a repository. For any site, there will be a need to develop and study rock behavior in situ, such as the evolution of DRZ which will depend on the rock type and site specific properties. An appropriate model for the evolution of the DRZ properties should be developed, calibrated, and validated against such in situ experiments (i.e. drift scale test and niche excavation experiments at Yucca Mountain). For larger models including 3D of multiple emplacement tunnels and shafts to be included in this kind of THM model, more efficient calculations would be necessary, which could be solved with future porting of TOUGH-FLAC for high performance computing. Such porting of the FLAC3D code planned to be conducted within the next few years.

Table A-15. TOUGH-FLAC for Salt Coupled THM Processes

1. Name of Model: TOUGH-FLAC for salt coupled THM processes

2. Principal Investigator(s) and Affiliation: Jonny Rutqvist (LBNL), Laura Blanco Martin (LBNL), Jens Birkholzer (LBNL)

3. Brief Model Description:

- Describe the processes and/or events considered in the model, as well as the applicable feature (e.g., waste form, DRZ, etc.), i.e., include a description of the FEP or FEPs addressed by this model.

In nuclear waste isolation, TOUGH-FLAC provides a framework for modeling coupled THM processes in the EBS and host rock and their interactions using state of-the-art macroscopic constitutive models for bentonite, crushed rock salt backfill, clay, salt and crystalline host rocks. For rigorous modeling of the THM behavior of salt host rocks (bedded and domal salt), and crushed salt backfill, state-of-the-art constitutive models have been implemented, including the Lux-Wolters model for the analysis of damage induce permeability changes, sealing and healing. TOUGH-FLAC has been extended to model coupled THM processes under large strain associated with reconsolidation of emplacement tunnels backfilled with crust salt.

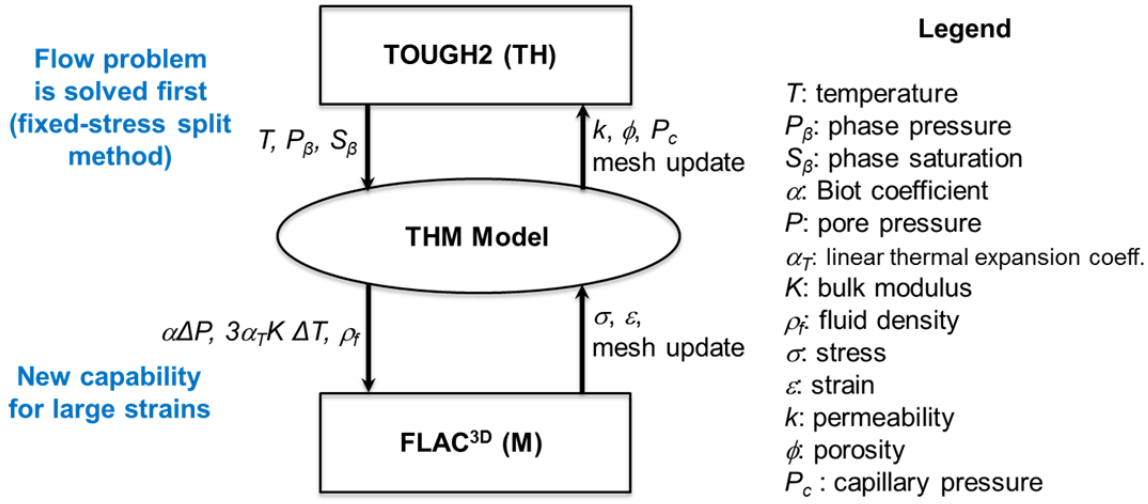

The most closely associated FEP is 2.1.01.01 (see below – from the UFD Roadmap spreadsheet/tables). Related FEPs are 2. Flow Through the EBS (2.1.08.01), 2.1.08.03 (Flow through Backfill), 2.1.08.06 (Alteration and Evolution of EBS Flow Pathways), 2.1.08.09 (Influx/Seepage Into the EBS), Open Boreholes (1.1.01.01), Thermal Effects on Flow in EBS (2.1.11.10), 2.2.01.01 (Evolution of EDZ) , Flow Through Host Rock (2.2.08.01), Effects of Excavation on Flow (2.2.08.04), Mechanical Effects from Preclosure Operations (1.01.02.02), Heat Generation in EBS (2.1.11.01), Effects of Backfill on EBS Thermal Environment (2.1.11.03), Effects of Drift Collapse on EBS Thermal Environment (2.1.11.04), Effects of Influx (Seepage) on Thermal Environment (2.1.11.05), Thermal-Mechanical Effects on Backfill (2.1.11.08), Thermally-Driven Buoyant Flow / Heat Pipes in EBS (2.1.11.12), Effects of Gas on Flow Through the EBS (2.1.12.02), Gas Transport in EBS (2.1.12.03), Thermal-Mechanical Effects on Geosphere (2.2.11.06)

Objective	Feature	Process (Issue)		
		UFD FEP ID	UFD FEP Title	Process/Issue Description
Limited Release – Natural Barriers	Natural System - Geosphere	2.2.01.01	Evolution of EDZ	- Lateral extent, heterogeneities - Physical properties - Flow pathways - Chemical characteristics of groundwater in EDZ - Radionuclide speciation and solubility in EDZ - Thermal-mechanical effects - Thermal-chemical alteration

4. R&D Issue(s) and Safety Case Objectives Addressed by This Model:

- How will the modeled FEP(s) affect repository performance (especially biosphere dose) in a meaningful way?
- Why is it important from a regulatory perspective?
- Describe the current "state of the art" knowledge regarding the issue(s) addressed and why this particular model advances the state of the art in an important way.

In context of geologic nuclear waste disposal, coupled THM processes are relatively short-lived from safety assessment perspective, but could potentially give rise to permanent changes, such as the formation of a damaged zone around excavations that could provide a path for transport of radionuclides if released from a waste package. As for the natural salt, it is well known that its initial tightness could be affected by processes that take place at different stages during the lifetime of a repository. First, the development of an excavation damaged zone (EDZ) around the mined openings represents a potential risk because preferential flow pathways could be created. Thermo-mechanical damage occurs if the dilatancy boundary is exceeded. Second, a pore pressure-driven percolation process (fluid infiltration) can take place if the pore pressure locally exceeds the minimum compressive principal stress. Several factors can result in fluid permeation: thermal pressurization within the rock (due to thermal expansion of pore fluids that cannot escape in a very low-permeability medium – this is particularly true when the pore space is mostly occupied by low compressibility fluids, such as water or brine), convergence-induced pore pressure increase, and gas generation from the waste packages, among others. Should thermo-mechanical damage or fluid infiltration occur, the initial, near-zero permeability of the host rock would be superseded by an increased, secondary permeability. These perturbations, however, are generally not persistent in a plastic medium such as rock salt. Once the stress regime becomes favorable, healing takes place. Healing processes consist in the development of cohesion between former crack planes (in extension of pore space closure). They decrease damage by helping bond fracture surfaces and close micro-fractures, i.e., salt damage is reversible. Additionally, local widening of grain boundaries caused by percolation of pore fluids ceases as the pore pressure decreases below the minimum compressive principal stress. Damage, healing and percolation processes within natural salt have been thoroughly studied at the laboratory scale and have been included in advanced, validated constitutive relationships. Damage and healing have also been observed in various field studies. The Lux-Waters constitutive model, is the most comprehensive model for salt THM behavior, including damage, sealing and healing, although similar constitutive models have been developed at other academic institutions is Germany. For modeling salt and consolidation of the EBS, coupling under large stain has been developed and tests for TOUGH-FLAC, and creep is also included and linked through the Lux-Wolters model. In a salt repository, the analysis of EDZ evolution must be conducted using a model that includes both the EBS and host rock and their interactions, meaning that the evolution of the host rock or the evolution of the EBS cannot be analyzed independently.

From a regulatory perspective, the UFD Roadmap report states: "The importance of the other engineered barrier system materials at this decision point is **high** because having defensible models to represent their degradation, impacts on other processes within the engineered barrier system, and impacts on radionuclide transport is required. The current information is deemed **insufficient** to support this decision."

5. Proposed method for coupling this model to the PA model[1]

- Direct coupling or abstraction?
- Time scale of transient modeled processes (10 years, 100 years…. 1,000,000 years?).
- Degree of abstraction: reduced dimensionality; simplified representation; response surface.
- Key environmental inputs required from the PA model (and its coupled submodels) and key outputs delivered by this model.
- Are there other models you are aware of that are not being developed, which are needed for your model or for PA?

The TOUGH-FLAC with salt constitutive THM models provides a tool for calculating the evolution of the crushed salt backfill and the host rock, including the disturbed rock zone (DRZ) from just after emplacement to over 100,000 years. The analysis for coupling to the PA model might be conducted in a 2D cross-section of one emplacement drift or alternative a 3D model focused on the near field of an emplacement tunnel or a few emplacement tunnels in different parts of a repository and for different FEPs such as nominal case or such as for cases of extensive gas generation. The input required is the geometry, heat source, THM properties of buffer and host rock, initial THM conditions (such as in situ stress). The output to the PA model would be the changes in flow properties (e.g. permeability and porosity) in the EBS and near-field including the buffer and DRZ and also to inform PA related to local flow created by coupled THM processes.

6. Real time integration horizon: estimate how long before the proposed model is ready for integration with PA and how long the integration activities might take?

- Are there intermediate steps or degrees of coupling with PA, e.g., can you couple a certain version of your model in an expedited fashion and then go to the next more detailed version—please describe how

The calculation of the THM evolution of the EBS and host rock over a 100,000 year time frame for a 2D cross-section of an emplacement tunnel has already been demonstrated and published. The current TOUGH-FLAC framework with currently implemented constitutive models could be used for provided output to PA today. Modeling these processes in 3D has also been demonstrated associated with modeling of large-scale field tests over tens of years and could be extended to 100,000 years if considering multiple tunnels in parts of a repository. For larger models including 3D of multiple emplacement tunnels and shafts to be included in this kind of model, more efficient calculations would be necessary, which could be solved with future porting of TOUGH-FLAC for high performance computing. Such porting of the FLAC3D code is planned to be conducted within the next few years.

Table A-16. TPHM-FLAC3D for clay formation (called "Two-Part Hooke's Model (saturated)" in Table 3-2)

1. Name of Model:

TPHM-FLAC3D for clay formation

2. Principal Investigator(s) and Affiliation:

Liange Zheng (LBNL) and James Houseworth (LBNL)

3. Brief Model Description:

- Describe the processes and/or events considered in the model, as well as the applicable feature (e.g., waste form, DRZ, etc.), i.e., include a description of the FEP or FEPs addressed by this model.

The two-part Hooke's model (TPHM) is a stress–strain relationship that conceptualizes a rock body into two distinct parts: a "hard part" that only experiences small deformation and a "soft part" that experiences large deformation. The two parts follows the different forms of Hooke's Law. According to traditional Hooke's law, for elastic material, the proportionality in the stress-strain relationship should be constant. However, this proportionality is in fact not always constant in many cases, but rather stress-dependent. TPHM extends the traditional Hooke's law and provided a more accurate description of the elastic stress–strain relationship for clay formation than the traditional Hooke's law. TPHM has been implemented in FLAC3D to simulate the stress evolution in clay formation after excavation.

This model is primarily related to FEP 2.2.01.01, Evolution of EDZ (here pertaining to a clay/shale rock environment); A related FEP is 2.2.07.01, Mechanical effects on host rock.

Objective	Feature	Process (Issue)		
		UFD FEP ID	UFD FEP Title	Process/Issue Description
Limited Release – Natural Barriers	Natural System - Geosphere	2.2.01.01	Evolution of EDZ	- Lateral extent, heterogeneities - Physical properties - Flow pathways - Chemical characteristics of groundwater in EDZ - Radionuclide speciation and solubility in EDZ - Thermal-mechanical effects - Thermal-chemical alteration

4. R&D Issue(s) and Safety Case Objectives Addressed by This Model:

- How will the modeled FEP(s) affect repository performance (especially biosphere dose) in a meaningful way?

This model affects the mechanical behavior of host rock such as sealing of EDZ and the evolution of permeability as a function of stress, and therefore the flow and transport in host clay formation.

- Why is it important from a regulatory perspective?

As cited from the UFD Roadmap report: "The importance of excavation disturbance or damage to the Site Suitability and Licensing decision point varies by rock type. For this decision point, improved representation of excavation disturbance and damage, particularly reduced uncertainty, and how these processes impact and are affected by the developing design would need to be demonstrated. For repository systems developed in clay or shale, the understanding of the EDZ is of **high** importance and the available information is insufficient."

- Describe the current "state of the art" knowledge regarding the issue(s) addressed and why this particular model advances the state of the art in an important way.

This model overcomes the limitation of traditional single part Hooke's law and offers more accurate mathematical description of the stress–strain relationship for elastic mechanical processes. The concept then can also be extended to other constitutive relationships such as permeability-stress, porosity-stress relationships.

5. Proposed method for coupling this model to the PA model[1]

- Direct coupling or abstraction?
  Abstraction is needed for the model to be used by PFLOTRAN.

- Time scale of transient modeled processes (10 years, 100 years…. 1,000,000 years?).
  Applied to the entire performance period.

- Degree of abstraction: reduced dimensionality; simplified representation; response surface.
  Response surface is probably a more feasible way to incorporate this model to PA model.

- Key environmental inputs required from the PA model (and its coupled submodels) and key outputs delivered by this model.
  Inputs: mechanical properties
  Outputs: Evolution of stress, permeability, porosity over time.

- Are there other models you are aware of that are not being developed, which are needed for your model or for PA?
  TPHM has been implemented in FLAC3D and tested with the field data, but it has not been incorporated in the THM/THMC model. The effect of TPHM on the overall hydrological and mechanical evolution of clay formation needs to be studied with a THM model that employs TPHM.

6. Real time integration horizon: estimate how long before the proposed model is ready for integration with PA and how long the integration activities might take?

- Are there intermediate steps or degrees of coupling with PA, e.g., can you couple a certain version of your model in an expedited fashion and then go to the next more detailed version—please describe how.

TPHM affects the fundamental stress-strain relationship and is relevant for stress changes in clay formation, but THM model that utilize TPHM has to be developed to understand its effect on hydrological and mechanical evolution of clay formation.

Table A-17. PBNP RD

1. Name of Model: PBNP RD

2. **Principal Investigator(s) and Affiliation:** Carl Steefel (LBNL)

3. Brief Model Description:

- Describe the processes and/or events considered in the model, as well as the applicable feature (e.g., waste form, DRZ, etc.), i.e., include a description of the FEP or FEPs addressed by this model.

The long-term management of nuclear waste repositories requires reliable predictions of diffusion through waste-containment barriers, such as compacted bentonite and clay-bearing rock formations. For clays, cation diffusion processes are influenced by the electrical charge of the diffusing solute, pore geometry, and the electrical double-layer structure at the clay/water interface. Most currently available diffusion models do not specifically include the expected changes in metal-diffusion rates due to these variations. The Poisson-Boltzmann Nernst-Plank radionuclide diffusion (PBNP RD) model for diffusion through clays accounts for these interactions by integrating microscopic characterization of the electric double layer (EDL) and incorporating the integrated EDL effects into a continuum modeling method.

The most closely associated FEPs are 2.1.09.052 and 2.2.09.53 (see below – from the UFD Roadmap spreadsheet/tables). Related FEPs are Radionuclide Transport through EDZ (2.2.09.61), Radionuclide Release from the EBS (2.1.09.63), Radionuclide Transport through Liners and Seals (2.1.09.62), and Advection of Dissolved Radionuclides in Host Rock (matrix diffusion) (2.2.09.51).

Objective	Feature	Process (Issue)		
		UFD FEP ID	UFD FEP Title	Process/Issue Description
Limited Release – Engineered Barriers	Engineered Barriers	2.1.09.52	Diffusion of Dissolved Radionuclides in EBS - In Waste Form - In Waste Package - In Backfill - In Tunnel	- Gradients (concentration, chemical potential) - Diffusive properties (diffusion coefficients) - Flow pathways and velocity - Saturation
Limited Release – Natural Barriers, Dispersion and Dilution	Natural System – Geosphere	2.2.09.53	Diffusion of Dissolved Radionuclides in Host Rock	- Gradients (concentration, chemical potential) - Diffusive properties (diffusion coefficients) - Flow pathways and velocity - Saturation

4. R&D Issue(s) and Safety Case Objectives Addressed by This Model:

- How will the modeled FEP(s) affect repository performance (especially biosphere dose) in a meaningful way?

For crystalline and argillite disposal systems, the rate of diffusion through the EBS and near field host rock could be a key attribute affecting repository performance and biosphere dose.

- Why is it important from a regulatory perspective?

As cited from the UFD Roadmap report: “The importance of engineered barrier system radionuclide transport processes at this decision point is **high** for the transport of dissolved radionuclides and **medium** for colloid-facilitated transport processes. Defensible models to represent radionuclide transport processes are required. Information is available to represent radionuclide transport processes, but would have to be applied to specific environments, media, and design concepts. R&D would lead to improved methods and approaches. Thus, the adequacy of information is deemed **partially sufficient** to support this decision.” Also, “For repository systems developed in crystalline rock, the understanding of natural system radionuclide transport processes and properties is of **high** importance and the available information is **partially sufficient** with respect to the decision.” and “For repository systems developed in clay or shale, the understanding of natural system radionuclide transport processes and properties is of **high** importance and the available information is **partially sufficient** with respect to the decision.”

- Describe the current “state of the art” knowledge regarding the issue(s) addressed and why this particular model advances the state of the art in an important way.

Most currently available diffusion models do not specifically include the expected changes in metal-diffusion rates due to electrochemical effects. In nano-porous materials such as clays, these effects can significantly alter diffusion rates of radionuclides. The current models including electrochemicals effects are CrunchEDL and PHREEQC.

5. Proposed method for coupling this model to the PA model[1]

- Direct coupling or abstraction?

The PBNP RD model would be implemented through a combination of direct implementation in PFLOWTRAN and an abstraction for the electrochemical potential driving force – see "Degreee of abstraction" below.

- Time scale of transient modeled processes (10 years, 100 years…. 1,000,000 years?).

Given the implementation in PFLOWTRAN, the time resolution for changes in diffusion would be defined by the computation of near-field environment chemical and temperature conditions.

- Degree of abstraction: reduced dimensionality; simplified representation; response surface.

Suggest developing a response surface for estimating the gradient in electrical potential as a function of composition and temperature and combine this with the modified diffusion constitutive relationship including electrochemical diffusion effects (see FCRD-UFD-2014-000493) for computing diffusive flux in PFLOTRAN.

- Key environmental inputs required from the PA model (and its coupled submodels) and key outputs delivered by this model.

The model would require inputs from a near-field process model, e.g., TOUGHREACT-FLAC, for temperature, chemical composition, and pore compaction in clay materials.

- Are there other models you are aware of that are not being developed, which are needed for your model or for PA? No.

6. Real time integration horizon: estimate how long before the proposed model is ready for integration with PA and how long the integration activities might take?

- Are there intermediate steps or degrees of coupling with PA, e.g., can you couple a certain version of your model in an expedited fashion and then go to the next more detailed version—please describe how

There hasn't been any work directly towards integration of the PBNP RD model with PA up to this point. The idea proposed in item 5 would need a few months of dedicated effort to complete.

Table A-18. Kinetic Multiple Site Sorption-Desorption Model

1. Name of Model:
Kinetic Multiple Site Sorption-Desorption Model

2. Principal Investigator(s) and Affiliation:
Reimus, LANL ?
Someone working on PFLOTRAN?

3. Brief Model Description:

- Describe the processes and/or events considered in the model, as well as the applicable feature (e.g., waste form, DRZ, etc.), i.e., include a description of the FEP or FEPs addressed by this model.

This 'model' is intended to describe radionuclide adsorption and desorption using a relatively simple alternative to a Kd model in which adsorption is considered to take place onto multiple sites with different site densities and different sorption and desorption rate constants (the ratio of sorption to desorption rate constant is effectively a Kd value for a given site). The model was developed in conjunction with the development of an experimental method designed to interrogate the slow desorption kinetics of sparse sites, which are very difficult to interrogate by conventional methods, yet they have a large influence on transport predictions over long time and distance scales. The parameterization of the model by the experimental method is considered valid for a given heterogeneous experimental mineral assemblage and water chemistry, but the intent is that the parameterization can be adjusted for minor to moderate deviations in these variables using well-established geochemical principles (for example, knowledge of the dependence of surface complexation reactions on pH and complexing ligands in solution or the dependence of ion exchange reactions on abundance of competing ions). Major variations in these variables may require additional experiments for accurate parameterization. The integration of this model into a PA model implemented using the PFLOTRAN platform should be relatively straightforward, as it represents a simplification of an equilibrium geochemical speciation model that is fully coupled to a transport model (one of the advertised features of PFLOTRAN). In fact, the multi-site, multi-rate adsorption-desorption model can be thought of as an abstraction of the full coupling of a geochemical code like PHREEQC or EQ3/6 to a transport code like PFLOTRAN to allow more efficient computation.
FEPS:
2.1.09.53 Sorption of Dissolved Radionuclides in the EBS
2.2.05.55 Sorption of Dissolved Radionuclides in Host Rock
2.2.05.56 Sorption of Dissolved Radionuclides in Other Geologic Units (Non-Host-Rock)

4. R&D Issue(s) and Safety Case Objectives Addressed by This Model:

- How will the modeled FEP(s) affect repository performance (especially biosphere dose) in a meaningful way?
- Why is it important from a regulatory perspective?
- Describe the current "state of the art" knowledge regarding the issue(s) addressed and why this particular model advances the state of the art in an important way.

The modeled FEPs will likely be important for repository performance only for certain radionuclides and in certain scenarios. The model will have the greatest impact on weakly or moderately adsorbing radionuclides with long half-lives and high dose conversion factors (e.g., uranium and neptunium in oxidizing environments or oxidizing scenarios, although other nuclides are possible in various scenarios/environments). For such nuclides, the predicted dose (regulatory impact) will be inversely correlated with the degree of adsorption in the EBS and host rock. The model is expected to be less important for strongly adsorbing radionuclides because less sophisticated models (e.g., simple Kd models with large bounding Kd values) will likely be sufficient to demonstrate that performance and regulatory objectives can be met. However, for strongly adsorbing radionuclides, a similar model abstraction may be beneficial to describe radionuclide associations with mobile colloids.
The current state of the art has two end members: (1) simple Kd models, and (2) full geochemical models that account for all reactions that can affect adsorption (and many that don't), including solution-phase complexation and speciation reactions, and surface reactions on different minerals and different sites on different minerals. The Kd models clearly have limitations (not easily extended to different water chemistries or other potentially varying conditions), and the latter models have

generally been recognized as being intractable from the standpoint of being accurately parameterized in complex heterogeneous systems. Some attempts have been made to strike a balance between these two model extremes (e.g., generalized composite surface complexation models, component additivity models), and the model suggested here would fall into this category but on the low end of complexity and the high end of computational efficiency.

5. Proposed method for coupling this model to the PA model[1]

- Direct coupling or abstraction?
- Time scale of transient modeled processes (10 years, 100 years…. 1,000,000 years?).
- Degree of abstraction: reduced dimensionality; simplified representation; response surface.
- Key environmental inputs required from the PA model (and its coupled submodels) and key outputs delivered by this model.
- Are there other models you are aware of that are not being developed, which are needed for your model or for PA?

Direct coupling, although it will ultimately be direct coupling of an abstraction. Time scale could be up to 1M years. Degree of abstraction is simplified representation, although some response surfaces may have to be incorporated to capture effects of varying geochemistry and heterogeneity.
Key environmental inputs: Solution chemistry, including pH, alkalinity, and major dissolved species concentrations, temperature (for EBS and near field at short times), and major mineralogy present, including alteration minerals in the EBS and near field.

6. Real time integration horizon: estimate how long before the proposed model is ready for integration with PA and how long the integration activities might take?

- Are there intermediate steps or degrees of coupling with PA, e.g., can you couple a certain version of your model in an expedited fashion and then go to the next more detailed version—please describe how

The current version of the model could be readily coupled to the PA model and would not take long to implement. The challenge of implementing the model will not be in coupling to PA but rather in accurately parameterizing the model to make it a practical predictive tool.

Table A-19. Colloid Stability Model

1. Name of Model:

Colloid stability model

2. Principal Investigator(s) and Affiliation:

Pihong Zhao (LLNL), Mavrik Zavarin (LLNL)

3. Brief Model Description:

Intrinsic Pu colloids may exist in high-level nuclear waste and could affect the transport of Pu in the near as well as far field of a high-level nuclear waste repository. The relative stability of the intrinsic colloids will control their transport rates – this experimental program is intended to determine the stability of intrinsic colloids relative to pseudocolloids at room and at elevated temperatures. The dissolution rate of intrinsic colloids is measured at different temperatures. This model is intending to establish the conditions and rates of intrinsic colloids dissolution.

2.2.09.01, 2.2.09.02, 2.2.09.03, 2.2.09.04, 2.2.09.05, 2.2.09.06, 2.2.09.13, 2.2.09.51, 2.2.09.59, 2.2.09.60

4. R&D Issue(s) and Safety Case Objectives Addressed by This Model:

- **R&D issues:** intrinsic colloid dissolution rates as a function of temperature
- **How will the modeled FEP(s) affect repository performance (especially biosphere dose) in a meaningful way?** Stability of intrinsic colloids will control Pu transport rates.
- **Why is it important from a regulatory perspective?** Pu transport rates will directly impact the long-term repository performance.
- **Describe the current "state of the art" knowledge regarding the issue(s) addressed and why this particular model advances the state of the art in an important way.** Solubilities of Pu oxides are known but their rates of dissolution are not.

5. Proposed method for coupling this model to the PA model[1]

- **Direct coupling or abstraction?** abstraction
- **Time scale of transient modeled processes (10 years, 100 years…. 1,000,000 years?).** months to 1000 of years
- **Degree of abstraction: reduced dimensionality; simplified representation; response surface.** N/A
- **Key environmental inputs required from the PA model (and its coupled submodels) and key outputs delivered by this model.** Input: temperature, Pu release rates, redox conditions; output: intrinsic colloids dissolution rates
- **Are there other models you are aware of that are not being developed, which are needed for your model or for PA?** N/A

6. Real time integration horizon: estimate how long before the proposed model is ready for integration with PA and how long the integration activities might take?

N/A, discussions with PA modelers are needed

Table A-20. Diffusion of Actinides through Bentonite

1. Name of Model:

Diffusion of actinides through bentonite

2. Principal Investigator(s) and Affiliation:

Claudia Joseph (LLNL), Mavrik Zavarin (LLNL)

3. Brief Model Description:

Actinides with long half-lives (e.g., ^{238}U, ^{237}Np) will primarily contribute to the long-term radiotoxicity of high-level nuclear waste in a repository. If actinides are released from the waste they will interact with the potential repository backfill material bentonite. Under ideal compacted conditions, molecular diffusion is expected to be the main transport process to the surrounding of the repository. The experimental and modeling program is intended to determine the actinide speciation in solution based on the state of knowledge collected in thermodynamic databases and spectroscopic analysis. In addition, the actinides' sorption and migration parameters on and through the buffer shall be determined by experiments and subsequently modeling of the results for a wide range of conditions (temperature, pCO_2, and pO_2).

2.1.09.13, 2.1.09.52, 2.1.09.53, 2.1.09.54, 2.1.09.58, 2.1.09.59, 2.1.09.61

4. R&D Issue(s) and Safety Case Objectives Addressed by This Model:

- **R&D issues:** speciation, sorption and diffusion parameters as a function of temperature, pCO_2, and pO_2
- **How will the modeled FEP(s) affect repository performance (especially biosphere dose) in a meaningful way?** The effective estimation about the retardation quality of the backfill material and the expected breakthrough of the actinides through the buffer barrier will be possible.
- **Why is it important from a regulatory perspective?** The actinides diffusion and sorption parameters will directly impact the long-term repository performance.
- **Describe the current "state of the art" knowledge regarding the issue(s) addressed and why this particular model advances the state of the art in an important way.** Transport and sorption parameters are often determined by simple experimental set-ups under aerobic conditions, room temperature and in inert background electrolytes which are not reflect realistic repository conditions.

5. Proposed method for coupling this model to the PA model[1]

- **Direct coupling or abstraction?** abstraction
- **Time scale of transient modeled processes (10 years, 100 years…. 1,000,000 years?).** 10 to 100 years post-container failure
- **Degree of abstraction: reduced dimensionality; simplified representation; response surface.** Reduced dimensionality (1D and 2D instead of 3D), simplified representation
- **Key environmental inputs required from the PA model (and its coupled submodels) and key outputs delivered by this model.** Input: temperature, pH, salinity, redox potential, water diffusion coefficient, specific surface area, density; output: effective diffusion coefficient, distribution coefficient, speciation
- **Are there other models you are aware of that are not being developed, which are needed for your model or for PA?** no

6. Real time integration horizon: estimate how long before the proposed model is ready for integration with PA and how long the integration activities might take?

The model is ready for implementation, the diffusion data is missing. Long-term experiments are necessary (6 months to 6 years).

Table A-21. Thermodynamic Database Development and Surface Complexation/Ion Exchange Model Development

1. Name of Model:

Thermodynamic database development and surface complexation/ion exchange model development

2. Principal Investigator(s) and Affiliation:

Mavrik Zavarin (LLNL), Claudia Joseph (LLNL), Cindy Atkins Duffin (LLNL), Tom Wolery* -retired

3. Brief Model Description:

Evolution of the nuclear waste repository geochemical conditions and the transport behavior of radionuclides necessitate the development of thermodynamic databases for the prediction of the evolution of groundwater composition and mineralogy. Similarly, surface complexation and ion exchange databases are needed to predict the sorption of radionuclides as they migrate through the repository and into the host rock.

This effort includes international collaborations focused on the development of state of the art thermodynamic and sorption databases (e.g., NEA, HZDR) for use in performance assessment of nuclear waste repositories.

2.2.09.01, 2.2.09.02, 2.2.09.03, 2.2.09.04, 2.2.09.05, 2.2.09.06, 2.2.09.13, 2.2.09.51, 2.2.09.59, 2.2.09.60, 2.1.09.13, 2.1.02.01, 2.2.09.55, 2.2.09.56, 2.2.09.57, 2.2.09.58, 2.2.09.61, 2.2.09.64, 2.2.09.65, 2.1.09.53, 2.1.09.02, 2.1.09.01

4. R&D Issue(s) and Safety Case Objectives Addressed by This Model:

- **R&D issues:** Thermodynamic database development necessitates continued support to update and upgrade data. Comprehensive surface complexation/ion exchange databases do not exist and next generation PA model will need to move away from earlier K_d approaches.
- **How will the modeled FEP(s) affect repository performance (especially biosphere dose) in a meaningful way?** Development of both thermodynamic and sorption databases in a more defensible manner will allow a reduction of orders of magnitude (?) in the conservative estimates imposed by the simplifications in earlier PA modeling efforts. These upgrades will likely substantially reduce dose estimates.
- **Why is it important from a regulatory perspective?** Regulatory requirements will likely impose the use of state of the art methodologies to describe the geochemical environments within the repository and the host rock and the resulting transport behavior of radionuclides. As such, the UFD program will need to support the development of both thermodynamic databases and surface complexation/ion exchange databases to support nuclear waste repository performance calculations.
- **Describe the current "state of the art" knowledge regarding the issue(s) addressed and why this particular model advances the state of the art in an important way.** NEA is the premier international institution developing thermodynamic databases for use in nuclear waste repository science. Support for this endeavor comes from a variety of national nuclear waste repository research programs. Development of comprehensive surface complexation/ion exchange databases has been identified as a long-term need for the nuclear waste repository PA modeling internationally. Database development appears to be a primary stumbling block in the development of more robust radionuclide transport modeling capabilities.

5. Proposed method for coupling this model to the PA model[1]

- **Direct coupling or abstraction?** abstraction
- **Time scale of transient modeled processes (10 years, 100 years…. 1,000,000 years?).** all times
- **Degree of abstraction: reduced dimensionality; simplified representation; response surface.** Simplified representation will likely be used as thermodynamic and surface complexation/ion exchange models will be too complex to effectively include in PA models directly.
- **Key environmental inputs required from the PA model (and its coupled submodels) and key outputs delivered by this model.** Input: THC conditions in repository and host rock as a function of time; output: mineral dissolution/precipitation, speciation, radionuclide sorption
- **Are there other models you are aware of that are not being developed, which are needed for your model or for PA?** N/A

6. Real time integration horizon: estimate how long before the proposed model is ready for integration with PA and how long the integration activities might take?

Working thermodynamic databases are available now but must be updated with new data as it becomes available. Comprehensive surface complexation/ion exchange databases are not available at this time and would require ~ 3 years of sustained funding to become operational (rudimentary databases are available now).